



# **Development of an engineered wetland system for sustainable landfill leachate treatment**

**THIS THESIS IS SUBMITTED IN PARTIAL FULFILMENT OF  
THE REQUIREMENTS FOR THE DEGREE OF  
DOCTOR OF PHILOSOPHY (PhD)**

**By**

**Alya Aqeel Mohammed**

**B.Sc., M.Sc.**

**School of Engineering - Cardiff University**

**UK**

**2017**

# DECLARATION AND STATEMENTS

## **DECLARATION**

This work has not been submitted in substance for any other degree or award at this or any other university or place of learning, nor is being submitted concurrently in candidature for any degree or other award.

Signed ..... (candidate) Date.....

## **STATEMENT 1**

This thesis is being submitted in partial fulfilment of the requirements for the degree of Doctor of Philosophy (PhD).

Signed ..... (candidate) Date.....

## **STATEMENT 2**

This thesis is the result of my own independent work/investigation, except where otherwise stated, and the thesis has not been edited by a third party beyond what is permitted by Cardiff University's Policy on the Use of Third Party Editors by Research Degree Students. Other sources are acknowledged by explicit references. The views expressed are my own.

Signed ..... (candidate) Date.....

## **STATEMENT 3**

I hereby give consent for my thesis, if accepted, to be available online in the University's Open Access repository and for inter-library loan, and for the title and summary to be made available to outside organisations.

Signed ..... (candidate) Date.....

# ABSTRACT

Sustainable and effective treatment of landfill leachate has become one of the most important environmental problems due to the fluctuating composition and quantity, as well as its high concentrations of pollutants. High-tech solutions applied for the leachate treatment are expensive and energy consuming, and in addition they are not suitable at many landfill sites, especially those in rural areas. Hence there is need to develop novel and sustainable low-energy systems for the effective treatment of landfill leachates.

Constructed wetlands (CWs) are inexpensive simple to operate and they have the potential to remove not only organic carbon and nitrogen compounds, but heavy metals. This study focussed on the design, development and experimental investigation of a novel CWs for the treatment of landfill leachate. The CWs employed dewatered ferric waterworks sludge (DFWS) as the main substrate. The overall aim of the study was to design and assess the novel configuration of the CWs, whilst also contributing to advancing the understanding of pollutant removal from the landfill leachate in the CWs, through the development of models to explain the internal processes and predict performance.

The key design and operational variables investigated were: the primary media used, i.e. the DFWS, and the wetting and drying regimes. The CWs was configured as 4-stages in series which was operated for 220 days. Thereafter, an additional unit was added due to clogging and the CWs was operated for 185 days in this second period. Results and experimental observations indicate that the chemical treatment processes (adsorption and precipitation) contributed to the clogging.

The DFWS used served as adsorbent for heavy metals removal in the system. Results of heavy metals, organic matter (COD), ammonia and total nitrogen removal indicate average removals of 99%, 62%, 83% and 81%, respectively in first period; and 100%, 86%, 90% and 82% in second period, with an average heavy metals loading rate  $0.76 \text{ g m}^{-2} \text{ day}^{-1}$ , organic loading rate  $1070 \text{ g m}^{-2} \text{ day}^{-1}$ , ammonia loading rate of  $178 \text{ g m}^{-2} \text{ day}^{-1}$  and total nitrogen loading rate  $192 \text{ g m}^{-2} \text{ day}^{-1}$ . Results were supported through mathematical analysis using STELLA model for heavy metals transformation in CWs and numerical modelling using HYDRUS CW2D, which enhanced understanding of the internal processes for organic matter and nitrogen

removal. The result from STELLA modelling showed that up to 90% of the removal of heavy metals was through adsorption, which is highly significant. While HYDRUS CW2D results showed that the main path of nitrogen removal was through simultaneous nitrification and denitrification.

Overall, results have shown that CWs design has great potential for reduction of metals and nutrients in landfill leachate. Results of this study can contribute to future CW research and design for landfill leachate treatment, through the increased understanding of long-term pollutant removal in these systems. In time, this may result in the wider application of CWs for landfill leachate treatment to better protect the environment.

# DEDICATION

This thesis work is dedicated to my loved country, Iraq and my family who has been a constant source of support and encouragement during the preparation of this research.

# ACKNOWLEDGEMENTS

I want to take this opportunity to express my immeasurable appreciation and deepest gratitude for the help and support extended to me by all those who gave me the chance to accomplish this thesis.

My sincere gratitude is to my supervisor, Dr Akintunde Babatunde is more than I can express in words. It has been an honour to be his PhD. student. I appreciate his support, suggestions, valuable discussions and continuous provisions that benefited me much in completion and success of this study. Without his support, I could not have finished my dissertation successfully.

I would like also to express my gratitude to my co-supervisor Dr. Peter Cleall who has been always helpful. I am deeply grateful to him for valuable discussions we had during my research project.

Further gratitude and appreciation is expressed to my loved country, Iraq represented by Ministry of Higher Education and Scientific Research for funding my study and giving me this opportunity.

I would like to thank Cardiff University technical staff, who helped me during my PhD journey. In particular, I would like to thank Harry, and Steffan from the soil lab for their services in constructing and completing my experimental setup. Also, I would like to thank Jeffrey Rowlands and Marco Santonastaso for their help in the laboratory work by analysing the heavy metals.

Special thanks go to my friend Benjamin for his help in my column system setup and for his supported.

Warm and special thanks are expressed to my mother, brothers, sisters and all my family for their support during the period of this research.

Finally, special thanks go to my friends, especially my flat met Sally and to my friend Muna, Samia and Aseel and my office members especially Talib who supported me.

Alya Mohammed

# LIST OF PUBLICATIONS

## Papers

1. A. Mohammed; T. Al-Tahmazi; A.O. Babatunde, Attenuation of metal contamination in landfill leachate by dewatered waterworks sludges, (2016) J. Ecological Engineering, 94, 656-667.
2. 1. A. Mohammed; A.O. Babatunde, Modelling heavy metals transformation in vertical flow constructed wetlands, (2017), Journal of Ecological Modelling, 345, 62- 71.

## Conference

1. A. Mohammed; A. Babatunde, Understanding Integrated Removal of Heavy Metals, Organic Matter and Nitrogen in a Constructed Wetland System Receiving Simulated Landfill Leachate, International Journal of Environmental, Chemical, Ecological, Geological and Geophysical Engineering, Presented at the Conference on ICWTWQ 2017, Dubai, Volume 11, Issue 4, April 2017, 279- 285. (Published and oral presentation). **This paper was selected as the best paper in the conference.**
2. A. Mohammed; A. Babatunde, Influence of heavy metals on organic matter and ammonia removal from landfill leachate in a constructed wetland system, Presented at the Conference on Inaugural International Conference on Natural and Constructed Wetlands: Interaction between Scientists and Engineers, Galway, Ireland, 21 – 22 June, 2016. (Oral presentation).

# TABLE OF CONTENTS

Contents	
<b>DECLARATION AND STATEMENTS</b> .....	2
<b>ABSTRACT</b> .....	3
<b>DEDICATION</b> .....	5
<b>ACKNOWLEDGEMENTS</b> .....	6
<b>TABLE OF CONTENTS</b> .....	8
<b>LIST OF FIGURES</b> .....	15
Chapter 1 .....	1
Introduction .....	1
1.1 Overview .....	2
1.1.1 Landfill leachate treatment.....	2
1.1.2 Constructed wetland system for landfill leachate treatment .....	3
1.1.3 Aims and Objectives.....	5
1.2 Outline of thesis.....	6
.....	7
Chapter 2 .....	8
Literature Review: Constructed wetlands for landfill leachate treatment .....	8
2.1 Introduction.....	9
2.2 Landfill leachate.....	9
2.2.1 Landfill Leachate treatment- systems and limits.....	11
2.3 CWs definition .....	13
2.3.1 Free water surface constructed wetlands.....	13

2.3.2	Horizontal subsurface-flow constructed wetlands .....	14
2.3.2.1	Vertical subsurface-flow constructed wetlands .....	15
2.3.2.2	Tidal flow CWs .....	16
2.4	Pollutant removal mechanisms in constructed wetlands .....	18
2.4.1	Development of CWs for organic matter removal.....	19
2.4.2	Development CWs in nitrogen removal.....	20
2.4.2.1	Nitrification .....	21
2.4.2.2	Denitrification .....	21
2.4.2.3	Other N removal pathways.....	22
2.4.3	Development of CWs for HM removal.....	23
2.4.3.1	HM adsorption in CWs .....	23
2.4.3.2	Precipitation and co-precipitation of HM in CWs.....	25
2.4.3.3	Plant uptake .....	26
2.4.3.4	Filtration and sedimentation .....	27
2.5	The problem of bed clogging in CWs .....	28
2.5.1	Clogging Mechanism and contributing factors .....	28
2.6	Modelling VF CWs.....	29
2.6.1	HYDRUS- CW2D model .....	31
2.6.2	STELLA model .....	31
2.7	Chapter summary .....	32
Chapter 3 .....		34
Characterization and Metals Adsorption by DWSs .....		34
3.1	Introduction.....	35
3.2	Materials and Methods .....	35
3.2.1	General physicochemical characterization.....	35
3.2.1.1	pH.....	36
3.2.1.2	Point of zero charge (PZC).....	36

3.2.1.3	Determination of Specific surface area (SSA) .....	37
3.2.1.4	Aluminium and iron oxalate .....	38
3.2.2	Adsorption study - Kinetic and Equilibrium tests .....	38
3.2.2.1	Kinetics of heavy metals adsorption by DWSs .....	38
3.2.2.1.1	Synthetic metal solution .....	38
3.2.2.1.2	Optimum dosage and time experiment .....	39
3.2.2.1.3	Kinetic models .....	39
3.2.2.1.4	Validation of the kinetic models .....	40
3.2.2.2	Adsorption isotherm .....	41
3.2.2.2.1	Effect of initial pH solution .....	41
3.2.2.2.2	Adsorption models .....	41
3.2.3	Statistical analysis .....	43
3.3	Results and Discussion .....	43
3.3.1	General physicochemical characterization .....	43
3.3.2	Optimization of factors influencing metals uptake .....	47
3.3.2.1	Effect of adsorbent dosage .....	47
3.3.2.2	Effect of contact time .....	47
3.3.2.3	Initial pH effect .....	48
3.3.3	Adsorption study .....	51
3.3.3.1	Adsorption kinetics modelling .....	51
3.3.3.2	Adsorption isotherm modelling .....	54
3.3.3.2.1	Langmuir isotherm model .....	54
3.3.3.2.2	Freundlich isotherm model .....	55
3.3.3.2.3	Temkin isotherm model .....	57
3.3.3.2.4	Frumkin isotherm model .....	59
3.3.3.2.5	Harkins- Jura isotherm model .....	60
3.3.3.3	Fe removal .....	61
3.3.4	Differences in heavy metals removal by DWSs .....	61
3.4	Conclusion .....	62
Chapter 4	.....	63
Mechanistic study of Pb, Cr and Cd uptake by DWSs	.....	63

4.1	Introduction.....	64
4.2	Material and Methods .....	65
4.2.1	Total extraction carbon (TEC).....	65
4.2.2	Sequential extraction of Pb, Cr and Cd sorbed by DWSs .....	65
4.2.3	FTIR spectroscopy .....	66
4.2.4	Statistical analysis .....	66
4.2.4.1	Principal component analyses.....	67
4.2.4.2	Canonical correlation analysis.....	67
4.3	Results and Discussions.....	67
4.3.1	Sequential extraction .....	67
4.3.1.1	Sequential extraction before total extraction carbon.....	67
4.3.1.2	Sequential extraction after total extraction carbon.....	69
4.3.2	FTIR spectroscopy .....	73
4.3.2.1	FTIR spectroscopy before total extracted carbon.....	73
4.3.2.2	FTIR spectroscopy after total extracted carbon.....	74
4.3.3	Statistical analysis .....	76
4.3.3.1	Principal component analysis.....	76
4.3.3.2	Canonical component analysis.....	76
4.4	Conclusion.....	80
Chapter 5.....		81
General performance and design of a novel engineered wetland system for landfill leachate treatment .....		81
5.1	Introduction.....	82
5.2	Materials and Methods .....	83
5.2.1	System configuration .....	83
5.2.1.1	Perspex columns .....	84
5.2.1.2	Media and plants.....	85

5.2.2	Synthetic wastewater.....	86
5.2.3	System operation.....	86
5.2.4	Sampling and process .....	87
5.3	Results and Discussion .....	89
5.3.1	Overall performance of CWs.....	89
5.3.2	Heavy metals removal in CWs.....	94
5.3.2.1	Iron removal.....	97
5.3.2.2	Lead removal .....	98
5.3.2.3	Chromium removal.....	98
5.3.2.4	Cadmium removal.....	98
5.3.3	Clogging Phenomena in stage C .....	99
5.3.4	Organic matter removal in CWs.....	100
5.3.5	Nitrogen removal in CWs.....	103
5.3.5.1	NH <sub>4</sub> -N removal.....	105
5.3.5.2	Total nitrogen removal .....	106
5.4	Conclusions.....	108
Chapter 6 .....		109
Modelling organic matter and nitrogen removal in CWs treating landfill leachate using HYDRUS CW2D.....		109
6.1	Introduction.....	110
6.2	HYDRUS .....	110
6.2.1	Water transport in HYDRUS .....	111
6.2.2	The unsaturated soil hydraulic properties .....	111
6.2.3	Solute transport in HYDRUS.....	112
6.2.4	Numerical solution to governing flow and solute Equations .....	113

6.2.5	CW2D solute transport: components and processes .....	113
6.3	Materials and Methods .....	114
6.3.1	Physical models.....	114
6.3.2	Initial modelling considerations .....	114
6.3.2.1	Soil laboratory tests and hydraulic properties .....	115
6.3.2.2	Influent pollutant concentrations .....	116
6.3.2.3	Ammonia adsorption isotherm .....	117
6.3.3	HYDRUS modelling .....	118
6.4	Results and Discussions .....	120
6.4.1	Results of soil laboratory tests.....	120
6.4.2	Hydraulic properties.....	121
6.4.3	Freundlich isotherm model for ammonia adsorption .....	122
6.4.4	HYDRUS modelling result .....	123
6.4.4.1	Water flow .....	123
6.4.4.2	Simulation result for one cycle .....	124
6.4.4.2.1	Column C CWs Simulation result .....	124
6.4.4.2.2	Column D CWs Simulation result .....	126
6.4.4.2.3	Column E CWs Simulation result.....	127
6.4.4.3	Simulation result for first and second periods .....	129
6.4.4.3.1	Column C CWs simulation result .....	129
6.4.4.3.2	Column D CWs simulation result .....	130
6.4.4.3.3	Column E CWs simulation result .....	131
6.5	Conclusion.....	138
Chapter 7 .....		139
Modelling heavy metals transformation in CWs treating landfill leachate....		139
7.1	Introduction.....	140
7.2	Material and Method .....	141
7.2.1	Setup of HH sludge dewatered sludge VFCW .....	141

7.2.2	Description of the model .....	142
7.2.3	Michaelis- Menten equation for plant uptake and growth .....	144
7.2.3.1	Plant germination and HM uptake .....	144
7.2.3.2	Analysis of HM in <i>Phragmites australis</i> plants .....	145
7.2.3.3	Michaelis- Menten equation for plant uptake .....	146
7.2.3.4	Plant growth .....	147
7.2.3.5	Michaelis- Menten equation for plant growth .....	147
7.2.3.6	Adsorption of HM by dewatered ferric sludge .....	148
7.2.3.7	Impact of HM on plant growth .....	149
7.2.3.8	Plant uptake .....	149
7.2.3.9	Plant mortality .....	150
7.2.4	Calibration and sensitivity analysis .....	150
7.3	Results and Discussion .....	153
7.3.1	Simulation of heavy metals using STELLA software .....	153
7.3.2	Sensitivity analysis .....	160
7.3.3	Fate of heavy metals in VFCW .....	163
7.4	Conclusion.....	164
Chapter 8	.....	166
Conclusion and Recommendations	.....	166
8.1	Conclusion.....	167
8.2	Recommendations for further work.....	169
Appendix A	.....	193
Figures of physicochemical characterisation of DWSs and removal efficiency of HM by DWSs	.....	193
Appendix B	.....	206

# LIST OF FIGURES

Figure 2. 1 Typical arrangement of a FWS CW (adapted from Kadlec and Wallace 2008) .....	14
Figure 2. 2 Typical arrangement of a HF CWs (adapted from Cooper et al. 1996)..	15
Figure 2. 3 Typical arrangement of a VF CWs (adapted from Kadlec and Wallace, 2008) .....	16
Figure 2. 4 Organic matter transformation and removal process in VF CWs (adapted from Stefanakis <i>et al.</i> 2014) .....	19
Figure 2. 5 Nitrogen transformation and removal process in VF CWs (adapted from Stefanakis <i>et al.</i> , 2014) .....	20
Figure 3. 1 Point of zero charge (PZC) of HH sludge.....	37
Figure 3. 2 XRD patterns of the DWS (figure shown pattern for the HH sludge used as an example).....	44
Figure 3. 3 Removal efficiency of heavy metals by HH sludge at different contact time and three different sludge dosages.....	49
Figure 3. 4 Sorption kinetics of heavy metals onto HH sludge using: a) first order, b) second order and c) intraparticle diffusion model (secondary axis in Figures b and c, represent the data for Fe).....	53
Figure 3. 5 Sorption isotherm of heavy metals onto DWS using Langmuir isotherm model at different pHs (data refers to the HH sludge used as an example).....	55
Figure 3. 6 Sorption isotherm of heavy metals onto DWS using Freundlich isotherm model at different pHs (data refers to the HH sludge used as an example).....	56
Figure 3. 7 Sorption isotherm of heavy metals onto DWS using Temkin isotherm model at different pHs (data refers to the HH sludge used as an example).....	58
Figure 3. 8 Sorption isotherm of heavy metals onto DWS using Frumkin isotherm model at different pHs (data refers to the HH sludge used as an example).....	59
Figure 3. 9 Sorption isotherm of heavy metals onto DWS using Harkins- Jura model at different pHs (data refers to the HH sludge used as an example).....	60
Figure 4. 1 Percentage distribution of lead between various fractions determined by the sequence extraction test (a) before total extraction carbon (b) after total extraction carbon.....	70
Figure 4. 2 Percentage distribution of chromium between various fractions determined by the sequence extraction test (a) before total extraction carbon (b) after total extraction carbon.....	71

Figure 4. 3 Percentage distribution of cadmium between various fractions determined by the sequence extraction test (a) before total extraction carbon (b) after total extraction carbon. ....	72
Figure 4. 4 FTIR spectra of HH dewatered waterworks sludge (a) before and (b) after total carbon extraction loaded and not loaded with Pb, Cr and Cd at pH 4.....	75
Figure 5. 1 Constructed wetland system showing: (1) first period of operation on the left, and (2) second period of operation on the right.....	84
Figure 5. 2 Schematic of a single Stage CWs for the landfill leachate treatment....	85
Figure 5. 3 Schematic of CWs in first period (0-220 days) .....	89
Figure 5. 4 Schematic of CWs in second period (220-405 days).....	89
Figure 5. 5 Dynamics of HM concentrations in the influent and effluent and HM removal in CWs during period 1 to the left and period 2 to the right. ....	91
Figure 5. 6 Dynamics of pollutant concentrations in the influent and effluent and pollutant removal in CWs during period 1 (left) and period 2 (right).....	92
Figure 5. 7 HM concentrations in each stage and removal efficiency (Mean $\pm$ SD) for period 1 .....	94
Figure 5. 8 Vertical DO distribution (Mean $\pm$ SD) at different depth (from top layer to bottom) in all stages of CWs .....	95
Figure 5. 9 HM concentrations in each stage and removal efficiency (Mean $\pm$ SD) for period 2 .....	97
Figure 5. 10 COD removal in stage C in first period .....	100
Figure 5. 11 Variation and removal efficiency of COD in the four stages of CWs during period 1.....	102
Figure 5. 12 Variation and removal efficiency of COD in the four stages of CWs during period 2.....	103
Figure 5. 13 NH <sub>4</sub> -N, NO <sub>x</sub> -N and TN-N profile and removal efficiency of NH <sub>4</sub> -N and TN-N across the four stages of the CWs in period 1 .....	104
Figure 5. 14 NH <sub>4</sub> -N, NO <sub>x</sub> -N and TN-N profile and removal efficiency of NH <sub>4</sub> -N and TN-N across the five stages of the CWs in period 2.....	105
Figure 6. 1 Finite element mesh as displayed in HYDRUS.....	119
Figure 6. 2 Soil water characteristic curve.....	122
Figure 6. 3 Freundlich plot for ammonia adsorption .....	123
Figure 6. 4 Flux effluent results of measured data and HYDRUS model output, per calibrated parameter for column C and D. ....	124
Figure 6. 5 Flux effluent results of measured data and HYDRUS model output, per calibrated parameter for column E. ....	124

Figure 6. 6 Simulated time series for DO within two main layers for two consecutive loadings for column C .....	125
Figure 6. 7 Simulated and measured effluent concentration of COD for two consecutive loadings for column C .....	126
Figure 6. 8 Simulated and measured effluent concentration of NH <sub>4</sub> -N for two consecutive loadings for column D .....	126
Figure 6. 9 Simulated and measured effluent concentration of NO <sub>3</sub> -N for two consecutive loadings for column D .....	127
Figure 6. 10 Simulated time series for DO within two main layers for two consecutive loadings for column E .....	128
Figure 6. 11 Simulated and measured effluent concentration of NH <sub>4</sub> -N for two consecutive loadings for column E.....	128
Figure 6. 12 Simulated and measured effluent concentration of NO <sub>3</sub> -N for two consecutive loadings for column E.....	129
Figure 6. 13 Measured and simulated data of effluent COD for Column C at 215 days for period 1.....	132
Figure 6. 14 Measured and simulated data of effluent COD for Column C at 185 days for period 2.....	133
Figure 6. 15 Measured and simulated data of effluent NH <sub>4</sub> -N for Column D at 215 days for period 1.....	134
Figure 6. 16 Measured and simulated data of effluent NH <sub>4</sub> -N for Column D at 185 days for period 2.....	135
Figure 6. 17 Measured and simulated data of effluent NO <sub>3</sub> -N for Column E at 215 days for period 1.....	136
Figure 6. 18 Measured and simulated data of effluent NO <sub>3</sub> -N for Column E at 185 days for period 2.....	137
Figure 7. 1 STELLA diagram for the Pb model.....	143
Figure 7. 2 STELLA diagram for the Cr model.....	143
Figure 7. 3 STELLA diagram for the Cd model.....	144
Figure 7. 4 <i>Phragmites australis</i> after ten days of growth.....	145
Figure 7. 5 The linear regression of $C_0/v_u$ vs. $C_0$ for $K_u$ and $U_m$ determination for Pb, Cr and Cd.....	146
Figure 7. 6 The linear regression of $C_0/v_G$ vs. $C_0$ for $K_r$ and $G_m$ determination for Pb, Cr and Cd Process equations .....	148
Figure 7. 7 Model calibration and validation for (a) Pb, (b) Cr and (c) Cd removal in mg L <sup>-1</sup> in the CWs using column A.....	156

Figure 7. 8 Comparison of model predicted and field measured of Pb, Cr and Cd removal in $\mu\text{g L}^{-1}$ in the CWs using column A during model calibration. ....	157
Figure 7. 9 Comparison of model predicted and field measured of Pb, Cr and Cd removal in $\mu\text{g L}^{-1}$ in the CWs using column A during model validation. ....	158
Figure 7. 10 Model validation for (a) Pb, (b) Cr and (c) Cd removal in $\text{mg L}^{-1}$ in the CWs using column B. ....	159
Figure 7. 11 Comparison of model predicted and field measured of Pb, Cr and Cd removal in $\mu\text{g L}^{-1}$ in the CWs using column B during model validation.....	160
Figure A. 1 Point of zero charge (PZC) determination of aluminium- based sludges.....	194
Figure A. 2 Point of zero charge (PZC) determination of ferric- based sludges. ....	195
Figure A. 3 XRD patterns of aluminum-based sludges.....	196
Figure A. 4 XRD patterns of ferric-based sludges. ....	197
Figure A. 5 Removal efficiency of lead by aluminum- based sludges at different contact time and three different sludge dosages.....	198
Figure A. 6 Removal efficiency of lead by ferric- based sludges at different contact time and three different sludge dosages. ....	199
Figure A. 7 Removal efficiency of chromium by aluminium- based sludges at different contact time and three different sludge dosages. ....	200
Figure A. 8 Removal efficiency of chromium by ferric- based sludges at different contact time and three different sludge dosages.....	201
Figure A. 9 Removal efficiency of cadmium by aluminium- based sludges at different contact time and three different sludge dosages.....	202
Figure A. 10 Removal efficiency of cadmium by ferric- based sludges at different contact time and three different sludge dosages.....	203
Figure A. 11 Removal efficiency of iron by aluminium- based sludges at different contact time and three different sludge dosages.....	204
Figure A. 12 Removal efficiency of iron by ferric- based sludges at different contact time and three different sludge dosages. ....	205

# LIST OF TABLES

Table 2. 1 Summary of the characteristics of landfill leachate in different countries.....	10
Table 2. 2 Treatment performance of CWs in OM and N removal.....	18
Table 2. 3 Maximum HM adsorption capacity of different industrial by-products .....	25
Table 2. 4 Review of main model development in CWs. ....	30
Table 3. 1 Adsorption isotherm model equations and corresponding linear forms.....	42
Table 3. 2 Physicochemical properties of the aluminium- based sludges (n=3).....	45
Table 3. 3 Physicochemical properties of ferric- based sludges (n=3).....	46
Table 3. 4 Optimum values of key adsorption parameters used in heavy metals removal.....	50
Table 4. 1 Correlation matrix for the physicochemical characterization of the DWSs.....	78
Table 4. 2 Principal component analysis of physicochemical characterisation of DWSs (n=14).....	79
Table 4. 3 Varimax rotated loadings for the dewatered waterworks sludges .....	80
Table 5. 1 Operating scheme for the first period constructed wetland system.....	83
Table 5. 2 Operating scheme for the second period constructed wetland system. ...	83
Table 5. 3 Characteristics of influent and effluent of the CWs for the four stages (Mean $\pm$ SD) .....	93
Table 5. 4 Characteristics of influent and effluent of the CWs for the five stages (Mean $\pm$ SD) .....	93
Table 6. 1 Components simulated in CW2D multi-component solute transport (Langergraber and Šimůnek 2005).....	113
Table 6. 2 Processes simulated in CW2D multi-component solute transport (Langergraber and Šimůnek 2006). ....	114
Table 6. 3 CW2D solute transport component input concentrations for period 1. ...	117
Table 6. 4 CW2D solute transport component input concentrations for period 2. ...	117
Table 6. 5 CW2D solute transport component input concentrations for one cycle. ...	117
Table 6. 6 Gravimetric and volumetric moisture content for HH sludge. ....	120
Table 6. 7 Measured and predicted values of volumetric water content at different section. ....	121
Table 6. 8 Van Genuchten – Mualem soil hydraulic parameters for column C, D and E.....	122

Table 7. 1 Summary of the state variables, processes, parameters and their associated units in the model development for Pb.....	151
Table 7. 2 Summary of the state variables, processes, parameters and their associated units in the model development for Cr.....	152
Table 7. 3 Summary of the state variables, processes, parameters and their associated units in the model development for Cd. ....	153
Table 7. 4 Sensitivity analysis for the selected parameters included in the model.	162
Table B. 1 Adsorption rate constant and correlation coefficients for first order model for adsorption of heavy metals on DWSs.....	207
Table B. 2 Adsorption rate constant and correlation coefficients for second order model for adsorption of heavy metals on DWSs.....	209
Table B. 3 Adsorption rate constant and correlation coefficients for Intraparticle diffusion model for adsorption of heavy metals on DWss. ....	211
Table B. 4 Kinetic model parameters by liner regression method for pseudo first order model for the sorption of heavy metals by DWSs.....	213
Table B. 5 Kinetic model parameters by liner regression method for pseudo second order model for the sorption of heavy metals by DWSs.....	215
Table B. 6 Constant parameters, adsorption capacity and correlation coefficient for lead calculated for the five-adsorption models at different pHs. ....	217
Table B. 7 Constant parameters, adsorption capacity and correlation coefficient for chromium calculated for the five-adsorption models at different pHs.....	222
Table B. 8 Constant parameters, adsorption capacity and correlation coefficient for cadmium calculated for the five-adsorption models at different pHs.....	227
Table B. 9 Constant parameters, adsorption capacity and correlation coefficient for iron calculated for the five-adsorption models at pH 2.....	232

# **Chapter 1**

## **Introduction**

## 1.1 Overview

### 1.1.1 Landfill leachate treatment

All municipal landfills are susceptible to infiltration by precipitation and runoff. As the water infiltrates the landfill, substances leach from the waste including oxygen demanding organic compounds, suspended solids, nitrogen compounds, phosphorus, metals and toxic organics. Consequently, landfill leachate is often characterized as hazardous and highly polluted. The composition of landfill leachate varies widely depending on a variety of parameters including type of landfill waste, climatic conditions, landfill age and mode of operation (Kjeldsen et al. 2002).

Landfill leachates are capable of causing severe environmental impacts especially in water bodies such as aquifers and surface waters. These effects may include eutrophication or toxic effects on aquatic organisms resulting from ammonium nitrogen ( $\text{NH}_4\text{-N}$ ), heavy metals (HM) or organic matter (OM).  $\text{NH}_4\text{-N}$  concentrations often present more of a long-term problem than the leaching of degradable organic substances such as volatile fatty acids. It is generally recognised that mature leachates contain relatively low concentrations of degradable organic material but high levels of  $\text{NH}_4\text{-N}$ , up to  $5000 \text{ mg L}^{-1}$  (Li *et al.*, 1999). Such high  $\text{NH}_4\text{-N}$  levels, together with the enormous quantities of leachates have posed serious pollution threat to the water environment. Therefore, the removal of  $\text{NH}_4\text{-N}$  has become a critical issue in leachate treatment.

On the other hand, HM which are commonly found in high concentrations in landfill leachate include iron, manganese, zinc, chromium, lead, copper and cadmium. They are a potential source of pollution if the leachate migrates into ground water, surface water and reservoirs.

Collected leachate must either be treated on-site to meet discharge permits or transported to a treatment facility off-site. The high variability of leachate characteristics makes the design and operation of treatment facilities difficult. Treatment of the leachate frequently requires a combination of physical, chemical, and biological treatment processes. Many municipal wastewater treatment plants will require pre-treatment of leachates to reduce high contaminant concentrations or remove toxic substances before they can accept them. Hauling and pre-treatment is usually an expensive option for leachate management, and it may create potential

hazards during transportation. Construction and operation of conventional wastewater treatment facilities on-site are also expensive. One reason for the expense is due to the need for continuous management by trained personnel during the many years of post-closure leachate collection and treatment.

### **1.1.2 Constructed wetland system for landfill leachate treatment**

Constructed wetland system (CWs) are engineered treatment systems that make use of the same contaminant removal mechanisms that function in natural wetlands. They have been found to provide treatment for a wide range of pollutant compositions and for highly variable flow rates. One reason for this is the diverse environments CWs provide, including both aerobic and anaerobic microsites.

CWs have low capital costs, low maintenance requirements, and they can be integrated into an urban resource management plan (Inamori et al. 2007; Tomenko et al. 2007; Vymazal 2007; Babatunde et al. 2008; Vymazal 2011). They provide wildlife habitats, green space and recreational opportunities in addition to their treatment function. These types of systems have been used for treatment of municipal wastewater, acid mine drainage, urban stormwater runoff, agricultural runoff, animal wastes and industrial wastewater. A more recently explored application is the treatment of landfill leachate in these systems.

CWs are generally categorized into surface flow and subsurface flow wetlands. Subsurface flow wetlands are the most common CWs type in Europe; such systems have been consistently effective in the removal of biochemical oxygen demand, suspended solids, and pathogenic organisms (Garcia et al. 2003; Akrotos and Tsihrintzis 2006). However, nutrient removal is generally limited because of a lack of the oxygen content that is necessary to oxidize ammonium, and the low adsorption capacities of the common substrates used for phosphorus and HM retention (Tanner et al. 2002). Therefore, intensified CWs such as artificially aerated and tidal-flow CWs were developed to improve oxygen transfer in CWs (Saeed et al. 2012). Artificially aerated CWs can increase oxygen transfer rate to  $160 \text{ g m}^{-2} \text{ day}^{-1}$  by compressing air from the atmosphere into the wetland bed with the use of a blower (Kadlce and Wallace 2008). Consequently, nutrient removal is intensified and the required area is reduced. However, such technology is not widespread because aeration process consumes a great deal of energy. Also, the fouling of air diffusers within CWs must

be considered, as well as the provisions for replacing or chemically cleaning diffuser assemblies.

Tidal flow constructed wetland system (TF CWs) are a relatively new technology that utilizes a novel oxygen transfer method (Wu et al. 2011). TF CWs are regularly filled with wastewater and then drained, and TF CWs act as passive pumps that expel and draw air from the atmosphere into pore spaces (Zhao *et al.*, 2004a). In this way, the oxygen transfer rate reaches  $350 \text{ g m}^{-2} \text{ day}^{-1}$  (Wu et al. 2011), and the ammonium and organics treatment capacities are consequently improved significantly (Hu et al. 2012). However, denitrifier growth and activity is inhibited by either high oxygen content or inadequate electron donor sources, thus resulting in increase in effluent nitrate content in these systems (Zhao *et al.*, 2004b). Therefore, modification of the original TF CWs configuration is necessary in order to achieve satisfactory Total nitrogen (TN) removal performance. To enhance TN removal anoxic condition can be developed by fixing the retention time in the tidal flow operational strategy.

Various media such as soil, gravel, sand and limestone have been used in CWs. However, the novelty of the CW being proposed in this thesis lies in the use of dewatered waterworks sludge (DWS) as a substrate for pollutant removal from wastewater. DWS are waste by products generated by certain drinking-water treatment processes, for which limited sustainable application has been found to date, resulting in their disposal predominantly by landfilling (Wang et al. 1993). These materials are primarily composed of amorphous masses of iron and aluminium hydroxides, and they also contain sediment and humic substances removed from the raw water and traces of coagulating agents used in the water treatment process (Chu 2001). DWS have a large surface area and are highly reactive, this makes them a potential adsorbent for pollutants (Ippolito et al. 2011).

Extensive laboratory scale studies on the novel reuse of alum sludge in CWs have been conducted to treat various types of wastewater (Babatunde *et al.*, 2009; Zhao *et al.*, 2009; Zhao *et al.*, 2011; Hu *et al.*, 2012). However, the use of DWS to treat high-strength wastewater, such as landfill leachate with high concentration of pollutants has not been investigated by researchers till date.

This project presents for the first time, the use of Fe-DWS in CWs for landfill leachate treatment. The CW is designed to enhance  $\text{NH}_4\text{-N}$  removal, and achieve higher TN removal integrated with removal of OM and HM. The performance of the CW in

removing a range of landfill leachate priority pollutants (including heavy metals and nutrients) is investigated to determine the overall effectiveness of the system.

### **1.1.3 Aims and Objectives**

The main aim of the study is to contribute to a better understanding of the use of CWs for sustainable landfill leachate treatment; and to develop a novel CWs for sustainable landfill leachate treatment, using a novel by-product, dewatered water sludge as the main substrate.

The objectives of the study are:

1. To undertake detailed physical, chemical and engineering characterization of drinking water sludges in order to determine their suitability to enhance the removal of HM, OM and TN from artificial landfill leachate during treatment in CWs.
2. Using batch kinetic and equilibrium studies, to examine the kinetics and determine the adsorption capacity of the drinking water sludges for Pb, Cr, Cd and Fe
3. To investigate and determine the mechanism of heavy metals removal from landfill leachate by the drinking water sludges, using principal component and canonical correlation analysis to evaluate the physicochemical properties of the drinking water sludges that are relevant to heavy metal attenuation; and then using sequential extraction to study the nature of the interactions established between the metal ions and the surfaces of the drinking water sludges.
4. To determine the role of the inorganic and organic fractions of the drinking water sludges in metal attenuation using FTIR spectroscopy.
5. Based on the characterization and HM adsorption tests, to select suitable drinking water sludges for the design and development of a novel CWs for landfill leachate treatment, and to assess the configuration and performance of the system in the laboratory, using >400 days of data in order to assess the effect of high pollutant loading rate, different operational conditions (anoxic condition and tidal flow strategy) and the impact of the pollutant relative concentrations on the treatment performance.
6. To use numerical simulation (HYDRUS-CW2D) to increase understanding of fundamental processes of transformation and elimination of pollutants in system, and

contribute to unravelling the black box approach of these systems, whereby, interaction (media, water, plants, microorganism) are not well known.

7. To develop a dynamic model using the Structural Thinking Experiential Learning Laboratory with Animation (STELLA) for simulating HM removal in the CWs in order to increase our understanding of the fate and transformation of HM in the systems.

## **1.2 Outline of thesis**

A literature review of constructed wetlands and their application for landfill leachate management and treatment is firstly given in chapter 2. The research presented in this thesis has been carried out through the investigation of the ability of fourteen DWSs for the adsorption of selected HM that have been found in landfill leachate. This was carried out using laboratory experiments, principally kinetic and equilibrium analysis. Characterisation of the DWSs is presented alongside the analysis of their metal adsorption characteristics in chapter 3. Not only the adsorption capacity and kinetics should be investigated, but also the way that HM are bound is necessary as it can be used to predict the heavy metals availability, mobility and toxicity. Therefore, the study of adsorption mechanism is carried out in chapter 4. From the results of chapters 3 and chapter 4, the selected DWS was used as the main media in CWs which was designed and operated in Cardiff University School of Engineering. Influent and effluent analysis was carried out over a period of 400 days to obtain a comprehensive dataset concerning the treatment performance of the CWs, and to determine the effect of the design and operation variables. Chapter 5 provides details of the experimental setup and procedure used to investigate the performance of the CWs for OM, NH<sub>4</sub>-N and HM removal. Chapter 6 explores the application of HYDRUS 2D, a software package that simulates water, heat and solute transport through variably saturated media, to enhance the understanding of the removal processes of OM and NH<sub>4</sub>-N occurring in the CWs. Modelling of HM removal in CWs is also important with regards to understanding the HM behaviour in the integrated treatment processes. The fate of HM in the CWs was investigated through the development of a mathematical model using the STELLA as presented in chapter 7. Finally, the main conclusions of the project and recommendations for further work are presented in chapter 8.

**Issues**

- CWs is focussed separately on biodegradable organic matters and nutrients on the one hand; and toxic pollutants on the other.
- Inevitable coagulants use in water treatment works generates annually more than 2 million tons in the US and 131,000 tons in the UK.
- Variable DWS characteristics can impose different behaviour for HM retention when use it as a low cost substrate in CWs.

**Aims:**

To develop a novel engineered system to contribute to a better understanding of the use of CWs for sustainable landfill leachate treatment.

**Chapter Three  
Characterization & HM  
adsorption by DWSs**

- Evaluate the physicochemical properties of different DWSs that are relevant to HM removal.
- Investigate the characteristics of Pb, Cr, Cd and Fe removal by DWSs through batch experiments investigating the equilibrium and kinetics of adsorption.
- Study the effect of pH, adsorbent dose and contact time on the removal of HM.

**Chapter Four  
Mechanistic study of Pb, Cr and  
Cd uptake by DWSs**

- Using PCA and CCA to evaluate the relationship between physicochemical properties of different DWSs and heavy metals attenuation.
- Study the nature of the interactions established between the HM and the surfaces of DWSs.
- Ascertain the role of the inorganic and organic fractions of DWSs in the HM attenuation processes.

**Chapter Five  
General performance of  
engineered wetland system**

- Overall performance of CWs-ferric- based sludge in HM, OM and TN removal and assess the impact of their relative concentrations.
- Investigation of the effect of high pollutant loading rate and different operational conditions (anoxic condition and tidal flow) on the treatment performance.

**Chapter six  
Modelling OM & N removal  
using HYDRUS CW2D**

- To develop and validate a numerical model of the constructed wetland system with emphasis on pollutant prediction.
- To increase understanding of the fundamental processes of transformation and elimination of pollutants in the system and contribute to unravelling the (black box) approach to these systems.

**Chapter seven  
Modelling HM transformation  
in VF CWs**

- To develop a dynamic model for simulating adsorption, plant uptake and growth from the VF CWs, which uses ferric dewatered sludge (HH) as main substrate.
- To calibrate the model using the available experimental data.
- Apply the model to simulate the fate of HM in the VF CWs.

**Conclusion and future work**

# **Chapter 2**

## **Literature Review: Constructed wetlands for landfill leachate treatment**

## 2.1 Introduction

This chapter provides a literature review of previously undertaken research of relevance to the field of study. In recognition of the significant opportunity offered by CWs for landfill leachate management, this review aims to provide a concise appraisal of the application of CWs for the treatment of high strength wastewater such as landfill leachates, focusing on the design, performance, retrofit issues and design guidelines. Firstly, landfill leachate and its characterization is reviewed, and the treatment in various form and associated limitation is explored. Thereafter, the review focussed on the application of CWs for landfill leachate management. The use of vertical flow CWs for high strength wastewater treatment, such as landfill is then investigated, highlighting the benefits and shortcomings that have influenced this research.

The key objectives of this review are:

- To review the development and state of the art of the application of CWs for high-strength wastewater treatment,
- To collate information on the design, performance challenges faced in the use of CWs for high strength wastewater treatment,
- To identify gaps in knowledge, research and practice for the use of CWs for landfill leachate treatment; and offer recommendations as to how to advance the uptake of CWs for such high strength wastewater treatment.

## 2.2 Landfill leachate

Landfill leachate is generated as a mixture of rainwater percolated through wastes, surface runoff, underground water infiltration water produced from the biodegradation of wastes and the inherent water of the wastes themselves (Bou-Zeid and El-Fadel 2004; Renou et al. 2008). Due to the complicated solid waste deposited in landfills, leachate contains a variety of pollutants which can be classified into four groups: (i) dissolved organic matter expressed as total organic carbon, including methane, volatile fatty acids and biorecalcitrant compounds such as fulvic and humic substances; (ii) metallic ions such as Ca, Mg, Na, K, NH<sub>3</sub>, Fe, Mn and the anions Cl<sup>-</sup>, SO<sub>4</sub><sup>2-</sup>, S<sub>2</sub><sup>-</sup>, CO<sub>3</sub><sup>2-</sup> and potentially toxic ion metals such as Cd, Cr, Pb, Ni, Cu, Zn and As; (iii) xenobiotic organic compounds, which can include a huge variety of

halogenated and phenolic compounds, alcohols, aldehydes, and ketones; and (iv) trace compounds (Kulikowska and Klimiuk 2008).

Landfill leachates are difficult to characterise because their compositions and concentrations depend on a variety of factors such as waste composition, age of landfill site, geology, temperature, moisture content and other seasonal and hydrological factors (Christensen et al. 2001; Abdul Aziz et al. 2004). Table (2.1) summarises the range of leachate constituent concentrations in different countries.

**Table 2. 1 Summary of the characteristics of landfill leachate in different countries.**

Parameter (mg L <sup>-1</sup> )	References			
	1	2	3	4
<b>BOD</b>	4- 57,700	0- 4,000	-	834.3- 1,000.7
<b>COD</b>	31- 89,520	150- 6,000	<10- 33,700*	1,105- 1,906
<b>TOC</b>	0- 28,500	-	2.8- 5,690*	-
<b>Nitrate nitrogen (as N)</b>	0- 51	< 1- 0.5	-	9.4- 21.2
<b>Ammonia nitrogen (as N)</b>	0- 1,966	5- 100	1,029- 1,977	467.5- 676.5
<b>Total phosphates</b>	0.2-130	1- 10	-	13.53- 19.93
<b>Total solids</b>	0- 59,200		-	-
<b>Total dissolved solids</b>	584-44,900	0- 42,300	-	-
<b>pH</b>	3.7- 8.8	3.7- 9	5.95- 7.65	7.66- 8.01
<b>Calcium</b>	60- 7,200	100- 1,000	62- 3,646	-
<b>Magnesium</b>	17- 15,600	16.5- 15,600	92- 555	-
<b>Sodium</b>	0- 7,700	0- 7,700	1,340- 2,039	-
<b>Chloride</b>	4.7-4,816	20- 2,500	1,965- 2,705	817.7- 3,154
<b>Sulfate</b>	10- 3,240	< 1- 300	52- 1,173	54.95- 270.4
<b>Chromium</b>	0.2- 18	< 0.01-0.5	<0.04- 0.56*	0.17- 0.78
<b>Cadmium</b>	0.3- 17	< 0.01	2.65	0.01- 0.6
<b>Copper</b>	0.005-9.9	< 0.008- 10	0.39*	0.18- 1.85
<b>Lead</b>	0.001- 2	0- 5	<0.04- 0.28*	0.23- 11.39
<b>Nickel</b>	0.2- 79	0.4-3	4.34	0.06- 0.512
<b>Iron</b>	4- 2,820	0.2- 5,500	2.2- 448	1.94- 38.67
<b>Zinc</b>	0.6-370	0- 1,350	2.25	17.21- 1,311

1- (Ray et al. 1986) In USA; 2- (Rong 2009) In Finland; 3- (Thornton et al. 2000) In UK; 4- (Zhang et al. 2013) In China. \* (Baun and Christensen 2004) In UK.

Landfill leachates can cause severe environmental impacts especially in water bodies such as aquifers and surface waters. These effects may include eutrophication or toxic effects on aquatic organisms resulting from ammonia, heavy metals or organic compounds. Ammonium nitrogen concentrations often present more of a long-term problem than the leaching of degradable organic substances such as volatile fatty acids. This is because nitrifying bacteria are autotrophic microorganisms that have a

slow respiration rate, and require a considerable amount of oxygen to function. Moreover, the presence of a large amount of carbonaceous substrates in these strong effluents often prevents oxygen being used for nitrification. It is generally recognized that landfill leachate contains relatively low concentration of degradable organic material but high levels of  $\text{NH}_4\text{-N}$ , up to  $5000 \text{ mg L}^{-1}$  (Li and Zhao 2001). Such high  $\text{NH}_4\text{-N}$  levels together with enormous quantities of leachates, poses a serious pollution threat to the water environment, and the removal of  $\text{NH}_4\text{-N}$  has become a critical issue in landfill leachate treatment.

Landfill leachates might contain among many other constituents, heavy metals in considerable concentrations. The heavy metals which are usually present in concentrations ranging from micrograms to milligrams per liter (Christensen et al. 2001), may constitute environmental problem, if the leachate migrates into surface or groundwater. Thus, in recent decades, monitoring of heavy metals in landfill leachate has been commonly been required by the authorities and routinely performed by landfill operators (Abdul Aziz et al. 2004).

Ray *et al.* (2007) found that heavy metal concentrations are generally low in the leachate formation stage and highest during the acid formation stage. However, complexation reactions with humic and other organic substances attenuate the metal concentration towards the later stages of the landfill stabilization process. Martensson *et al.* (1999) had expressed a similar view about the complexing capacity of heavy metals such as cadmium, nickel, zinc and dissolved organic carbon. In addition, an investigation by Baun (2004) into heavy metal distribution in landfill leachate showed that significant fractions of heavy metals were associated with municipal solid waste derived dissolved organic matter, suggesting that dissolved organic matter plays an important role in heavy metal speciation and migration.

### **2.2.1 Landfill leachate treatment- systems and limits**

The treatment of landfill leachate depends on its composition and characteristics (Alvarez-Vazquez *et al.*, 2004), the nature of the organic matter present as well as the age and structure of the landfill. Different technologies including biological treatments, physico-chemical treatments, as well as natural systems such as constructed wetlands (Klomjek and Nitorisavut 2005) and leachate recirculation (Reinhart 1996; Reinhart & Al-Yousfi 1996; Warith et al. 2009) have been developed in recent years,

not only to minimize the generation of toxic contaminants from leachate, but also to comply with the increasingly stringent discharge standards in different countries.

Physico-chemical treatments have been found to be suitable not only for the removal of refractory substances from stabilized leachate, but also as a refining step for biologically treated leachate. Prior to discharge, additional effluent refining using physico-chemical treatments such as chemical precipitation, activated carbon adsorption, and ion exchange can be carried out on-site. However, the drawbacks of these techniques include the high cost of operation due to the high chemical consumption, the sensitivity of the process to pH and the generation of sludge.

Biological purification processes are classified as aerobic or anaerobic depending on whether or not the biological processing medium requires an O<sub>2</sub> supply. In aerobic processing, organic pollutants are mainly transformed into CO<sub>2</sub> and solid biological products (sludge) by using the atmospheric O<sub>2</sub> transferred to the wastewater. In anaerobic treatment, organic matter is converted into biogas, comprising chiefly CO<sub>2</sub> and CH<sub>4</sub> and in a minor part into biological sludge. Biological processes have been shown to be very effective in removing organic and nitrogenous matter from immature leachates when the BOD/COD ratio has a high value (>0.5). With time, the major presence of refractory compounds (mainly humic and fulvic acids) tends to limit process's effectiveness (Lema *et al.*, 1988). Even if aerobic processes proved to be effective for the removal of organic carbon, nutrients and ammonia content, a number of drawbacks identified below have shifted the focus to other technologies (Wiszniewski *et al.* 2006):

- Relatively high capital costs.
- High energy consumption.
- Requires skilled personnel and regular monitoring.
- Susceptible to hydraulic overloads.
- The settling property of sludge is not always easy to control.
- High production of sludge that must be thickened.

On the other hand, Wiszniewski *et al.* (2006) reported the drawbacks of anaerobic treatment systems which include:

- Heavy metals which can hamper digestion.
- Ammonia toxicity from ammonia remaining in the effluent.
- Susceptibility to pH and temperature changes.

CWs treatment of landfill leachate is an attractive alternative method of water quality improvement (Loer *et al.* 1999). The use of CWs

for landfill leachate treatment began to develop in the late 1980s through to the mid of 1990s, with both subsurface flow (Trautmann et al. 1989; Staubitz et al. 1989; Birkbeck et al. 1990) and surface flow ( Trautmann et al. 1989; Martin et al. 1993).

Typical types of CWs applied in organic matter, nitrogen and HM removal include surface flow CWs and subsurface flow CWs; these can be further divided into horizontal subsurface and vertical subsurface flow systems. In recent years, new types of CWs with enhanced TN removal performance have emerged; these include tidal flow, effluent recirculation and saturated up-flow and down-flow CWs. The configuration performance (capacity and efficiency), and limitations of these CWs are summarized and discussed in the following sections.

## **2.3 CWs definition**

Constructed wetland system are engineered (man-made) wastewater treatment and purification systems that include chemical (adsorption, precipitation), physical (sedimentation, filtration), and biological (plant uptake, microbial processes) processes. These processes are similar to the processes that occur in natural wetland systems (Vymazal 2014; Song et al. 2015). The use of CWs for wastewater treatment, particularly domestic wastewater, has grown in recent years due to their very effective removal of pollutants, low energy requirements, ease of maintenance and relatively cheap construction and operating costs. CWs are applied all over the world to treat several kinds of wastewater such as storm run-off, domestic wastewater, industrial wastewater, agricultural drainage, acid mine waste and landfill leachate (Vymazal et al. 2015; Wu et al. 2015; Vymazal & Brezinova 2016).

There are three main types of CW: free water surface; horizontal subsurface-flow and vertical subsurface-flow. These designs are described in the following sections.

### **2.3.1 Free water surface constructed wetlands**

Free water surface (FWS) CWs are distinguished by an area of open water when the water slowly flows above a surface with few centimetres' column depth. Where rooted macrophytes are incorporated, they grow in soil or an alternative media at the base of the CW. Water depths are usually shallow, and this, along with the presence of vegetation helps to control the flow through the CW with the aim of creating plug-flow

conditions (Reed et al. 1995). Plug-flow conditions serve to maximise contact between the wastewater and the biological surfaces on which pollutant removal take place.

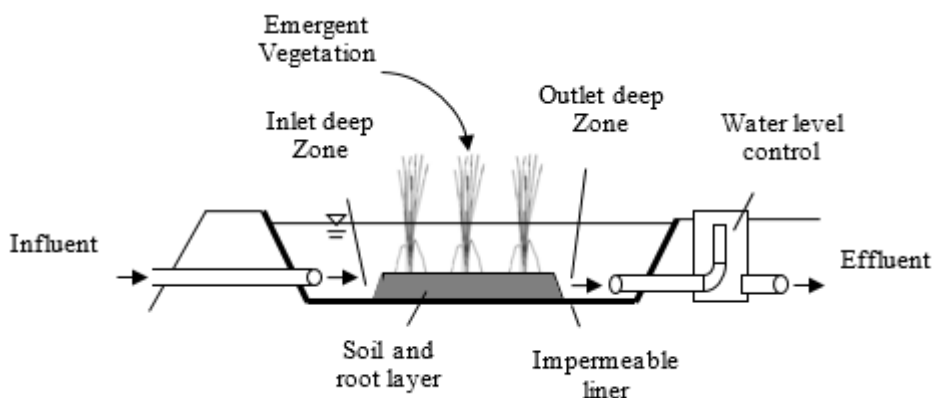


**Figure 2. 1 Typical arrangement of a FWS CW (adapted from Kadlec and Wallace 2008)**

FWS CWs are commonly used to treat less concentrated wastewaters, e.g. effluent from secondary or tertiary treatment and storm water runoff. They are also commonly used for mine water, groundwater and leachate treatment (Kadlec & Wallace 2008). Figure 2. 1 shows an example of a FWS CW with emergent vegetation.

FWS CWs is effective in removing SS and OM, but the area requirements are more stringent when it is used for reducing nutrient (Kadlec 1995).

### **2.3.2 Horizontal subsurface-flow constructed wetlands**

Subsurface-flow CWs differ from FWS CWs in that they do not feature a body of water on the surface. All flow moves through the porous substrate media. A typical horizontal subsurface-flow (HF) CW is shown in Figure 2.2.

Often referred to as “reed beds”, HF CWs are typically constructed using gravel and/or soil as substrate media (Kadlec and Wallace 2008). The bed of the CW is slightly inclined (gradient 1-3%) to promote gravitational water flow from the inlet to the outlet (Bryan et al. 2003). The wastewater is treated as it passes through various aerobic, anoxic and anaerobic zones (Cooper et al. 1996). Since the system is constantly saturated, aerobic zones are confined to the roots of the macrophytes in the CW. Thus, oxygen transfer and therefore aerobic treatment processes (e.g., nitrification) are usually low in HF CWs.

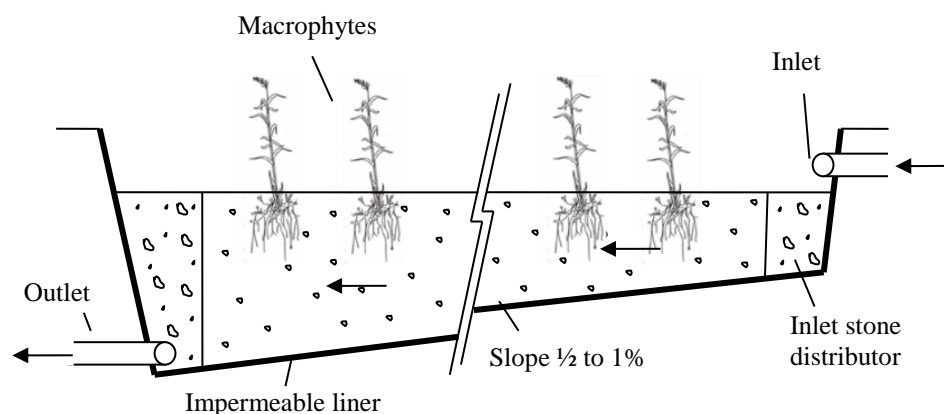


**Figure 2. 2 Typical arrangement of a HF CWs (adapted from Cooper et al. 1996)**

HF-CWs is effective in reducing suspended solids and OM (chemical oxygen demand (COD), biochemical oxygen demand (BOD)) as shown in Table 2.2. All these results indicate that oxygen transfer into HF CWs is limited and anoxic/anaerobic conditions are predominant in HF-CWs (Vymazal 2002; Kadlec & Wallace 2008; Albuquerque, Oliveira et al. 2009; Albuquerque, Arendacz et al. 2009).

### **2.3.2.1 Vertical subsurface-flow constructed wetlands**

Vertical subsurface-flow (VF) CWs receive influent wastewater in intermittent batches, thus they are not constantly saturated as in HF CWs. A typical VF CW is shown in Figure (2.3).

VF CWs typically consist of layers of gravel/sand, with the wetland vegetation planted at the top of the bed (Stefanakis et al., 2014). In most VF CWs, the influent wastewater is fed in batches onto the bed surface, flooding the surface and then travelling vertically by the gravity through the substrate media before it is collected at the bottom of the system from a gravel drainage layer. The driving force for the development of VF CWs is to achieve fully-nitrified effluents (Cooper 1999). Till now, it has become a well-established technology known as a compact treatment wetland system due to its high treatment capacity compared to FWS CWs and HF CWs (Weedon 2010).

Unlike HF CWs, the wetland medium in VF CWs is not water-saturated due to the intermittent loading, and therefore oxygen transfer is enhanced (Brix 1994b; Cooper 1999).

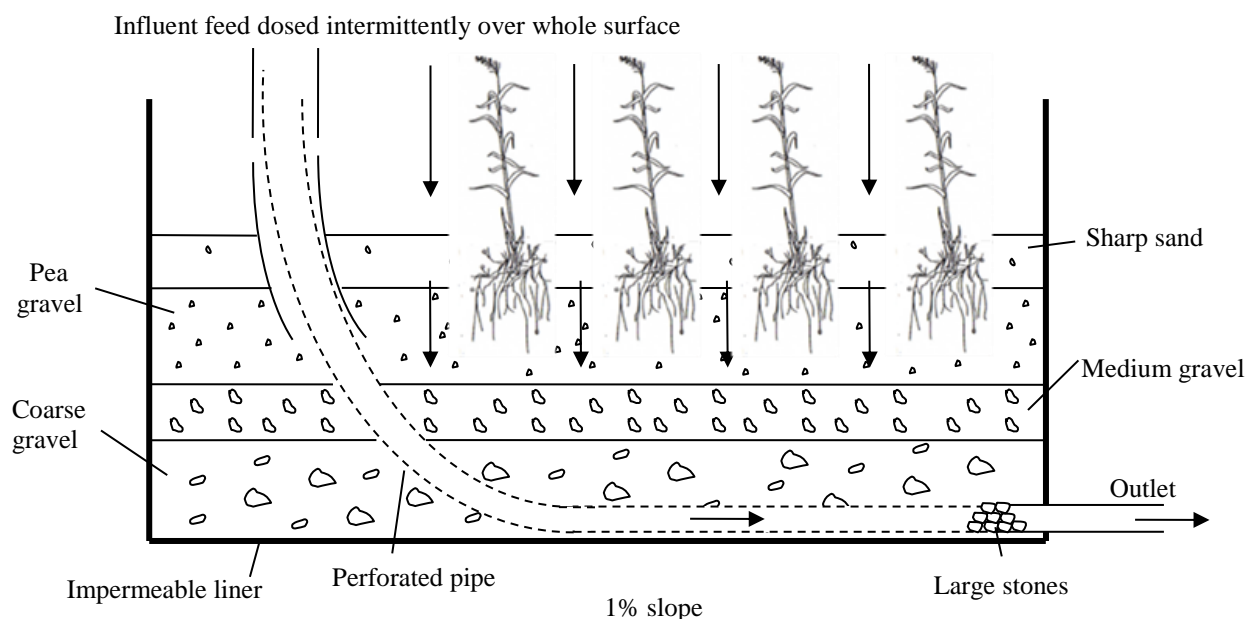


**Figure 2. 3 Typical arrangement of a VF CWs (adapted from Kadlec and Wallace, 2008)**

As a result, VF CWs has the ability to produce nitrified effluents from municipal or domestic wastewater, or even more concentrated wastewater such as landfill leachates and food processing wastewater (Kadlec & Wallace, 2008). Table 2.2 shows that VF CWs can achieve nearly complete nitrification (>90%). The general NLR adopted is below  $10 \text{ g m}^{-3}\text{d}^{-1}$ , but high loading rates above  $10 \text{ g m}^{-3}\text{d}^{-1}$  have also been applied in some cases, with effective nitrification performance (>80%) achieved. On the contrary, denitrification in VF CWs is restricted due to the predominating aerobic condition in the bed media. The TN reduction rarely exceeds 50%, consequently all these results suggest that a single stage VF CWs may not be capable of delivering tertiary effluent with regard to TN removal.

### 2.3.2.2 Tidal flow CWs

TF CWs are VF systems with alternative hydraulic operating conditions (Figure 2.4). Instead of the influent wastewater simply percolating through the CW and leaving the system in one pass, the wastewater is held in the system and then released after a set period of time. As the CW is filled, influent  $\text{NH}_4\text{-N}$  is adsorbed to the media and influent organic matter is degraded by the CW biofilm (Kadlec and Wallace 2008). Subsequently, as the water is drained from the CW, it acts as a “passive pump”, drawing air into the system (Sun et al. 2005). Atmospheric diffusion then oxidized biofilm causing the nitrification processes. As the CW is refilled, the oxidised N is

released from the media as oxidation has transformed the positive  $\text{NH}_4^+$  ion into negative nitrite ( $\text{NO}_2^-$ ) and nitrate ( $\text{NO}_3^-$ ) ions, which are repelled by the negative charge of the soil media. Influent organic matter provides a C supply for denitrification processes to occur in anoxic zones in the inner layer of the CW biofilm, where a high oxygen diffusion resistance allows heterotrophic denitrifiers to survive (Hu et al. 2014).

Due to TF treatment advantages, it has been mainly tested for high contamination loads such as agricultural wastewater (Zhao, Y.Q. et al. 2004b) and a mixture of landfill leachate and activated sludge (De Feo 2007). A positive result can be obtained when combining TF and effluent recirculation (Sun et al. 2003; Y Q Zhao et al. 2004b). Table 2.2 clearly demonstrates the greatly enhanced oxygen transfer and treatment capacity with the TF operation. Although  $\text{NH}_4\text{-N}$  reduction was incomplete in the studies with high strength wastewater, significant reduction was achieved under extremely high organic loading rate (OLR,  $\text{kg COD m}^{-3} \text{ day}^{-1}$ ) up to  $11 \text{ kg COD m}^{-3} \text{ day}^{-1}$ . When the wastewater strength was reduced to the domestic level, effective OM and  $\text{NH}_4\text{-N}$  reduction (>80%) were achieved simultaneously under OLR of  $0.2 \text{ kg m}^{-3} \text{ day}^{-1}$  and NLR of  $38 \text{ g m}^{-3} \text{ day}^{-1}$  (Wu et al. 2011). The oxygen transfer rate was estimated as high as 203 and  $473 \text{ g O}_2 \text{ m}^{-2} \text{ day}^{-1}$  based on the oxygen consumption rate in Sun *et al.* (1999,2005) respectively. In Wu *et al.*, (2011) the oxygen transfer rate was directly measured as  $350 \text{ g O}_2 \text{ m}^{-2} \text{ day}^{-1}$ . This has been demonstrated with the highly nitrified effluent and limited TN reduction in Sun et al. (1999, 2005), and Wu et al. (2011).

Table 2. 2 Treatment performance of CWs in OM and N removal

Wastewater	Influent OM (mg L <sup>-1</sup> )	Influent N (mg L <sup>-1</sup> )	Removal efficiency %			Configuration	Reference
			COD	NH <sub>4</sub> -N	TN		
Industrial Wastewater	170	32	61	22-56	-	FWS	(Chen et al. 2006)
Landfill leachate	4360	46	20	44	13	FWS	(Ogata et al. 2015)
Agricultural runoff	103- 132	7- 9	-	48- 69	55- 65	FWS	(Lu et al. 2009)
Landfill leachate	5850- 12820	144- 360	97	-	43	HF	(Chiemchaisri et al. 2009)
Landfill leachate	4770	2865	36	38	-	HF	(Yalcuk and Ugurlu 2009)
Synthetic	587	66	89	72	77	HF with step feeding	(Stefanakis et al., 2011)
Landfill leachate	1108	176	53	40	-	HF	(Nivala et al. 2007)
Landfill leachate	202	86	84	83	74	VF	(De Feo 2007)
Diluted leachate	35- 301	8-103	86	79	68	VF	(De Feo, 2007)
Gray water	270	37	84	92	-	VF CWs with recirculation	Sklarz et al., 2009
Piggery	2464	121	77	62	-	Four stages TFCWs with effluent recirculation	(Zhao et al., 2004b)
Artificial wastewater	300	60	90	55	70	TFCWs with effluent recirculation	Chang et al., 2014
Synthetic domestic	193- 366	34- 75	84	81	44	Single stage TFCW with recirculation	(Wu et al., 2011)

## 2.4 Pollutant removal mechanisms in constructed wetlands

Removal of pollutants from wastewater is essential for the protection and maintenance of receiving aquatic environments. In order to avoid depreciation of water resources, regulatory agencies are setting increasingly stringent effluent discharge standards. In an attempt to meet licensed discharge criteria, the wastewater industry realises that the use of cost-effective and environmentally friendly technologies such as constructed wetlands play an important role.

The following sections will highlight some major pollutant removal mechanisms in constructed wetlands with a focus on organic matter, nitrogen and heavy metals which are commonly found in landfill leachate.

### 2.4.1 Development of CWs for organic matter removal

Treatment wetlands may receive large amounts of external organic carbon. Degradable carbon is decomposed or transformed by a variety of reactions depending on the conditions present in the wetland (Figure 2.6).

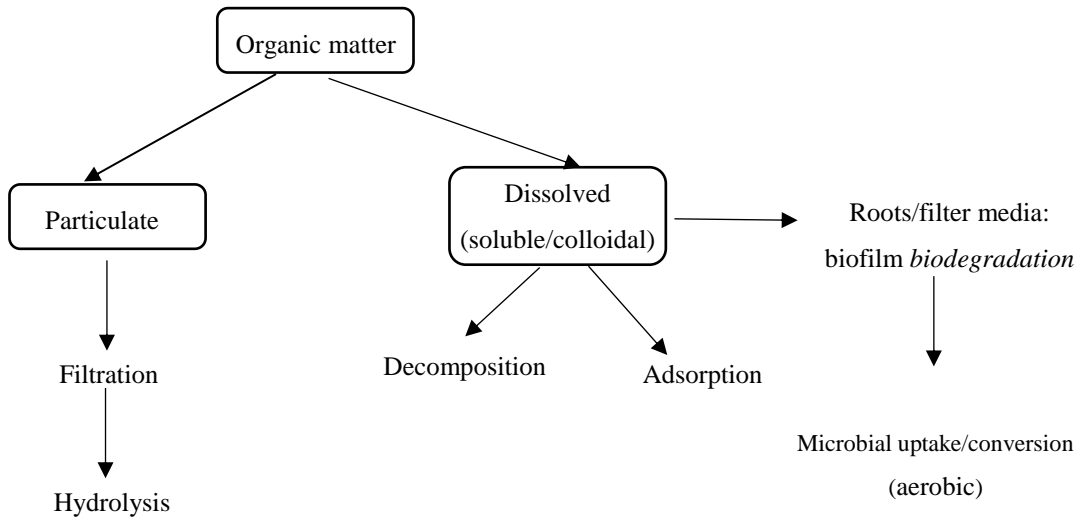


**Figure 2. 4 Organic matter transformation and removal process in VF CWs (adapted from Stefanakis et al. 2014)**

Some studies indicated that organic matter removal in constructed wetlands is mainly through aerobic, anaerobic, adsorption, filtration, and microbial metabolism (Karathanasis et al. 2003; Song et al. 2006; Stefanakis et al. 2014), and can be assessed by the change in COD and BOD concentrations in the wetlands. Furthermore, the removal of soluble organic substances is accomplished by the growth of microorganisms on the media, adhered on the rhizomes and roots of the macrophytes (Song et al., 2006). The function of constructed wetlands is largely dependent on organic matter accretion, dissipation and cycling. Organic matter accumulation in wetlands supplies energy to microorganisms for denitrification by providing a long-term source of carbon and sustainable source of nutrients. Bacteria and fungi are decomposers in CWs and through mineralization and gasification have been reported (Choudhary et al. 2011) to play the main role of organic matter elimination. Additionally, these microorganisms synthesize biomass and form organic metabolic by products. Moreover, it has been noted (Hong et al. 2001; Ma and Burken 2003) that further to phytovolatilization, some wetland plants release contaminants to

the atmosphere by absorbing them in their roots first and subsequently transpire them via their transpiration stream.

### 2.4.2 Development CWs in nitrogen removal

Nitrogen is an essential nutrient for all living organisms, being present in the form of proteins, nucleic acids, adenosine phosphates and pigments. (Hagopian and Riley 1998). Yet, nitrogen compounds are among the main pollutants of concern in wastewater because of their role in (along with other nutrients such as phosphorus) contributing to eutrophication, favouring algal blooms, and depreciation of dissolved oxygen levels in receiving water bodies. Furthermore, unionised ammonia ( $\text{NH}_3$ ) and nitrite ( $\text{NO}_2$ ) are toxic to fish and other aquatic organisms in low concentrations. In wastewater, the most important inorganic forms of nitrogen are  $\text{NH}_4$ ,  $\text{NO}_3$ ,  $\text{NO}_2$  and dissolved nitrogen gas ( $\text{N}_2$ ). N removal is usually achieved biologically by nitrification, denitrification and ammonification processes as shown in Figure 2.7

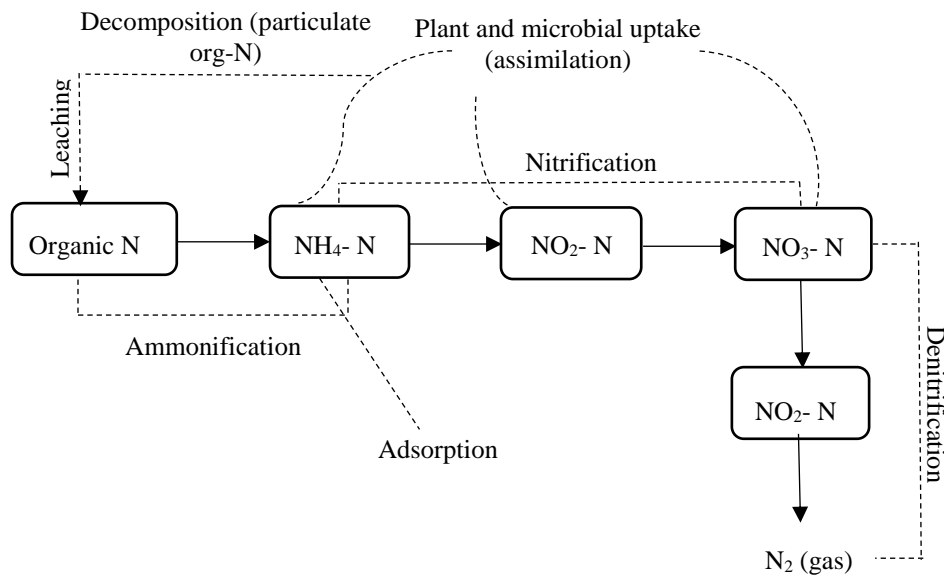


**Figure 2. 5 Nitrogen transformation and removal process in VF CWs (adapted from Stefanakis *et al.*, 2014)**

Organic nitrogen compounds in wastewaters originate from food, faeces and urine, these high molecular weight compounds (proteins, urea, amino acids) are proteolysed and deaminated to ammonia. The overall multi step biochemical process in the N transformation chain called ammonification. The organic nitrogen is converted to

ammonia by this process. The rate of ammonification is related to the oxygen- rich layer. This process is also affected by temperature, pH, C/N ratio, nutrient content and soil condition.

#### 2.4.2.1 Nitrification

Nitrification has been typically referred to as two separate strictly aerobic processes carried out by chemoautotrophic bacterial, although it is now recognised that heterotrophic nitrification (Keeney 1973) and archaeal nitrification (Wuchter et al. 2006) occur and can be of global significance. In the first step of nitrification ammonia is oxidized to nitrite by *Nitrosomonas*, *Nitrosococcus*, *Nitrosolobus* and *Nitrosospira* bacteria, and then to nitrate by *Nitrospira*, *Nitrospina*, *Nitrococcus* and *Nitrobacter* (Vymazal et al. 1998; Vymazal 2007; Kadlec and Wallace 2008; Faulwetter et al. 2009; Lee et al. 2009; Saeed and Sun 2012). In this processes CO<sub>2</sub> is utilized as carbon sources and inorganic source as energy source. The two process stages are as follows (Metcalf and Eddy 2003):



As shown in Equation (2.1), during respiratory activities of the nitrifier, two moles of H<sup>+</sup> are released into the environment lowering the pH of the water. Nitrification of ammonia to nitrate consumes approximately 4.6 mg O<sub>2</sub>, 8.64 mg HCO<sub>3</sub><sup>-</sup> for each milligram of ammonia nitrogen nitrified (Vymazal 2007; Faulwetter et al. 2009; Saeed & Sun 2012).

This process seems to be the most important ammonia removal process in VF CWs, compared to other process, due to the good aeration condition (Cooper 1999; Vymazal 2007; Faulwetter et al. 2009).

#### 2.4.2.2 Denitrification

Under anoxic conditions and when easily biodegradable carbon is available heterotrophic organisms reduce NO<sub>3</sub><sup>-</sup> → NO<sub>2</sub><sup>-</sup> → NO → N<sub>2</sub>O → N<sub>2</sub>, and acetate is used as the electron donor in this case. Denitrification requires an organic carbon source, and this is usually lacking at the end of the nitrification stage in most types of wastewater where the organic matter has already been oxidised. The carbon (energy) requirements for denitrification are 2.68 g of acetate per gram of nitrate nitrogen

(Kadlec and Wallace 2008). For methanol and glucose, the requirements are 1.90 g and 2.67 g, respectively, per gram of nitrate nitrogen (Kadlec and Wallace 2008). Bernet et al. (1996) indicated an optimum carbon level of 2.85 g COD (g NO<sub>3</sub>-N)<sup>-1</sup>.

In soils and wetlands where both aerobic and anaerobic zones coexist, nitrification and denitrification are known to occur simultaneously in a process called simultaneous nitrification and denitrification (SND). In particular, when there is organic carbon in anoxic zones of CWs where nitrate is present, it can represent a limiting factor for denitrification (Zhao et al. 1999). The addition of a commercially available carbon source to enhance denitrification can represent a critical cost to the treatment process. The opposing DO requirements for nitrification and denitrification mean that by lowering DO concentration to improve denitrification, nitrification rates are reduced. The oxygen gradient seems to be the most important factor which affected SND phenomena. According to Bakti and Dick (1992) the dissolved oxygen gradient is controlled by several factors, such as bulk dissolved oxygen level, the particle size of floc, the loading of organic substrate and aeration cycle.

### 2.4.2.3 Other N removal pathways

Other possible N transformation pathways in CWs such as plant uptake, adsorption and volatilization. NO<sub>3</sub>-N and NH<sub>4</sub>-N are the two forms of N that are absorbed by plants, with the latter being more favoured compared with the former (Stefanakis and Tsihrintzis 2012). However, plant uptake can take place during the growing season (spring and summer).

Ammonia can be adsorbed to the surface of the media in CWs, but this process mainly depends on the characteristic of the porous media used and the surface charge. In addition, in VF CWs with intermittent loading, there is relatively short contact time between wastewater and the media, and adsorbed NH<sub>4</sub>-N can nitrify during resting time (Kadlec and Wallace 2008).

With pH > 9.3, ammonia converts to NH<sub>3</sub> gas by volatilization process and losses through water surface to the atmosphere (Vymazal 2007; Saeed and Sun 2012).

Anaerobic ammonia oxidation (ANAMMOX) is a recently discovered process which is anaerobic conversion of nitrite and ammonium to nitrogen gas in the absence of organic carbon (Faulwetter et al. 2009). Because of the reduced carbon and oxygen requirements, less than half the oxygen and no carbon, as compared to conventional

routes, anammox is particularly suited to the treatment of high strength industrial wastewaters in which the ammonium content is high and the organic carbon content very low (Mulder et al. 1995). Another recent pathway of N transformation is the CANON (complete autotrophic nitrogen removal over nitrate) process. The process relies on the simultaneous interaction of aerobic and anaerobic ammonium oxidisers (Third 2003). However this process need more investigation to identify the optimal operation condition (Stefanakis et al. 2014).

### **2.4.3 Development of CWs for HM removal**

Leachate mainly consists of heavy metals, organic and inorganic matters such as ammonia, sulphate and cationic metals (Christensen et al. 1994). Constructed wetlands have been used extensively for the removal of heavy metals. Moreover, they can remove heavy metals from wastewater and leachate through different mechanisms such as physical, chemical and biological processes (Vymazal et al. 2007; Terzakis et al. 2008; Danh et al. 2009; Bang et al. 2015). According to Marchand *et al.* (2010), HM in CWs can be removed via four main mechanisms: (1) adsorption to substrate, sediments and organic matter; (2) precipitation as insoluble salts (mainly sulphides and oxyhydroxides); (3) absorption and induced changes in biogeochemical cycles by plants and bacteria; and (4) filtration and sedimentation. All these reactions which lead to accumulation of metals in the substrate of wetlands, will be summarized and discussed in the following sections.

#### **2.4.3.1 HM adsorption in CWs**

Adsorption which is the transfer of ions from a soluble phase to a solid phase, is one potential treatment process that can be used to remove metals in CWs. It may result in short-term retention or long-term stabilization. Metals are adsorbed to particles either by ion exchange, depending on factors such as the type of element and the presence of other elements competing for adsorption sites (Seo et al. 2008), or chemisorption. Sheoran and Sheoran (2006) found that of Pb, Cu, Cr, Zn, Ni and Cd retention by adsorption.

Freundlich and Langmuir models may be used to determine maximum metal immobilization and their retention capacity over time (Behnamfard and Salarirad 2009; Božić et al. 2013; Coelho et al. 2014; Tan et al. 2015; Cheng et al. 2013). In order to quantify the retention capacity of substrates over time, column experiments

may be used. Various media have been assessed as adsorbents for heavy metals, and the process could be made more attractive if the sorbent is inexpensive and does not require complicated pre-treatment or regeneration. In this regards, DWS can be a potential adsorbent for heavy metals removal from wastewater in particular landfill leachate. DWSs are low-cost and easily available worldwide; and they are generated during the drinking-water treatment process. They are primarily composed of Fe/Al hydroxides which are often amorphous species, and they contain sediment and humic substances from the raw water.

In recent year, the ability of DWS to remove HM from wastewater has been recognized (Zhou & Haynes 2011; Chiang et al. 2012; Coelho et al. 2014; Castaldi et al. 2015).

Table 2.3 lists the maximum adsorption capacity of DWSs and other active by-products to HM determined under room temperature (R.T.). As can be seen, DWSs exhibited very high HM adsorption capacity. However, HM adsorption capacity is not the only factor to be considered in selecting DWSs for CWs. The availability of this material is another key factor. The material is easily and locally available in large amount. Furthermore, there should not be any release of hazardous substances during the application. From this point of view, DWSs have some other advantages over other industrial by- products.

**Table 2. 3 Maximum HM adsorption capacity of different industrial by-products**

Materials	Study conditions	Maximum capacity	Reference
<b>DWS</b>	Particle size < 125 µm; pH 2- 9; initial Pb (207.2 mg L <sup>-1</sup> ), Cr (III) and Cr (VI) (52 mg L <sup>-1</sup> ); R.T.	Pb (53.8- 62.2 mg g <sup>-1</sup> ) Cr (III) (19.24- 26.5 mg g <sup>-1</sup> ) Cr (VI) (11- 11.44 mg g <sup>-1</sup> )	(Zhou and Haynes, 2011)
<b>DWS</b>	Particle size < 3.15 mm; pH 5.5; initial As, Cd, Pb and Zn 200 mg L <sup>-1</sup> ; R.T.	As (40 mg g <sup>-1</sup> ), Cd (9.7 mg g <sup>-1</sup> ), Pb (120 mg g <sup>-1</sup> ) and Zn (40 mg g <sup>-1</sup> )	(Chiang et al., 2012)
<b>DWS</b>	pH 4.5; initial Pb (165.76 mg L <sup>-1</sup> ) and Cu (50.8 mg L <sup>-1</sup> ); R.T.	Pb (7.67- 40.2 mg g <sup>-1</sup> ) Cu (4.13- 6.7 mg g <sup>-1</sup> )	(Castaldi et al., 2015)
<b>Cashew nut shell</b>	Particle size between 0.212 mm to 1.18 mm; pH 5- 7; initial Pb, Cr and Cd 200 mg L <sup>-1</sup> ; R.T.	Pb (28.653 mg g <sup>-1</sup> ), Cr (8.4211 mg g <sup>-1</sup> ) and Cd (11.233 mg g <sup>-1</sup> )	(Coelho et al., 2014)
<b>beech sawdust</b>	Particle size < 1 mm; pH 1.6- 5.3; initial Cu, Ni and Zn 200 mg L <sup>-1</sup> ; R.T.	Cu (4- 4.5 mg g <sup>-1</sup> ), Ni (4- 4.5 mg g <sup>-1</sup> ) and Zn (2 mg g <sup>-1</sup> )	(Bozic et al., 2013)
<b>A dried biomass wasted from biotrickling filters</b>	Particle size < 250 µm; pH 2- 5; initial Pb 200 mg L <sup>-1</sup> .	Pb (160 mg g <sup>-1</sup> )	(Cheng et al., 2013)
<b>biochar derived from municipal sewage sludge</b>	Particle size < 0.45 mm; pH 1- 6; initial Cd 200 mg L <sup>-1</sup> .	Cd (42.8 mg g <sup>-1</sup> )	(Tan et al. 2015)

### 2.4.3.2 Precipitation and co-precipitation of HM in CWs

Metals, such as Fe, Al and Mn, can form insoluble compounds through hydrolysis and/or oxidation. This leads to the formation of a range of oxides, oxyhydroxides and hydroxides (Sheoran and Sheoran, 2006). The amounts and forms of Fe in solution strongly affect metal removal. Fe (II) is soluble and dominates under reduced condition in CWs, and it represents an important bioavailable fraction. Fe(III) is the dominant form under aerobic conditions (Jönsson et al. 2006). This form of Fe can precipitate to produce oxides, hydroxides and oxyhydroxides with which other metals may coprecipitate. Fe(II) can also precipitate as oxides (Jönsson et al. 2006) or coprecipitate with other metals such as Zn, Cd, Cu or Ni (Matagi et al. 1998) However, Fe oxide is very dependent on DO variations, therefore the binding of metals with Fe oxide cannot be considered as a long- term removal mechanism. Moreover, Fe oxide has high affinity to metals that have similar size to Fe such as Zn, Cd, Cu, and Ni

(Dorman et al. 2009). However, the co-precipitation is limited when there is sufficient amount of  $SO_4$  which reduces the potential of metal removal (Sung and Morgan 1980).

Under anaerobic conditions and the presence of sufficient carbon source, sulphates can be reduced to sulphides by sulphate reducing bacteria (Sheoran and Sheoran, 2006). These can combine with various elements, i.e., As, Hg, Se, Zn and Pb to formation of highly insoluble metal sulphides (Murray-Gulde et al. 2005) as shown in equations below:



where  $CH_2O$  represents organic matter and  $M$  stands for metals.

Sulphate reduction is considered to be one of the most important processes for removal of HM in CWs (Kosolapov et al. 2004). For instance, in CWs that have received diluted landfill leachate, nearly all Pb and Cd in this leachate were present in the sediment as sulphide (Kosolapov et al. 2004).

Metals may also form metal carbonates. Although carbonates are less stable than sulphides, they can contribute to initial trapping of metals (Sheoran and Sheoran, 2006). Carbonate precipitation is especially effective for the removal of Pb and Ni (Lin 1995). According to Maine *et al.* (2006), the influent alkalinity of wastewater, carbonate and calcium concentrations favoured the metal retention in the sediment.

### 2.4.3.3 Plant uptake

CWs plants play a key role in assimilating dissolved HM from wastewater (Brix 1994a; Vymazal et al. 1998; Cheng et al. 2002; Marchand et al. 2010; Sheoran and Sheoran 2006). Compared to the other pollutants (nitrogen and phosphorus), the HM removal by plants is up to 5% of total HM removed in CWs (Stottmeister et al. 2003; Lee and Scholz 2007). HM are taken up by roots and distributed to the other parts of plants. However, a small portion is translocated to the other plant parts (e.g. shoots and leaves) (Khan et al. 2009; Bonanno and Lo Giudice 2010). Therefore, harvesting of the aboveground plant contributes only a small percent of the total HM removal in CWs (Cheng et al. 2002; Kosolapov et al. 2004; Marchand et al. 2010). Although a small portion of HM is removed by plant, studies comparing planted and unplanted systems often lead to conflicting results regarding the importance of plants (Lee and

Scholz 2007). A key point that is often overlooked is the supply of organic matter through the decay of dead plant material (Stottmeister et al. 2003). Plant-derived organic matter in wetlands over time continuously support sites for metal sorption and precipitation, as well as carbon sources for microbial population, thus promoting long-term functioning (Beining and Otte 1996; Beining and Otte 1997; Jacob and Otte 2003; Jacob and Otte 2004; Batty and Younger 2007). In addition, plants can contribute to HM removal through other processes such as filtration, sedimentation and adsorption, and through ensuring enhanced aeration of the bed (Kosolapov et al. 2004).

#### **2.4.3.4 Filtration and sedimentation**

CWs act as active filter for HM, as wastewater passes through the pores of substrate and the extensive plant root, HM becomes trapped in the system. Plants, such as *Phragmites australis*, promote the retention of precipitated metal hydroxide particles (Cooper et al. 1996; Vymazal et al. 1998). Retention times increase with increasing vegetation density, thus enabling better sedimentation. The wastewater flow velocity, the particles settling velocity, the pore volume of the bed media and wetland length, all these are factors that can affect the filtration efficiency (Sheoran and Sheoran 2006).

Sedimentation, another physical process for HM removal, follows other process such as precipitation or after floc-formation. Flocs may adsorb other types of suspended materials, including metals which can sink or trapped within media grains.

In conclusion, CWs help to treat different types of wastewater loaded with heavy metals, and thereby prevents the spread of metal contamination in surface and subsurface waters. High metal removal rates close to 100% have been reported in both natural and CWs. Understanding the basic mechanisms and processes controlling the metal removal increases the probability of success of the treatment wetland application. However, in most cases studies focused on HM removal in CWs without taking in their consideration the effect of HM on removal of other pollutant such as OM and NH<sub>4</sub>-N.

## 2.5 The problem of bed clogging in CWs

Clogging is defined as the developed process over operational time that leads to the blockage of substrate pores, and the subsequent losses in permeability because of the accumulation of solids or excessive formation of microbial biofilms, which build-up from pollutants degradation inside the pore space within the wetland substance (Knowles et al. 2011; Stefanakis et al. 2014; Song et al. 2015). However, clogging processes are complicated phenomena and no specific factors were stated to be the actual causes of the clogging in the systems. In general, clogging affected not only the efficiency but it can also reduce the useful operational lifetime.

### 2.5.1 Clogging Mechanism and contributing factors

Wetland scientists have recently reported various processes that influence the hydraulic conductivity of the wetland bed. The recognized mechanisms that contribute to clogging include: (Yao et al. 1971; Platzer and Mauch 1997; Winter and Goetz 2003; Langergraber et al. 2003; Molle et al. 2005)

- *Accumulation of organic and inorganic solid*: it has been reported that clogging developed as a result of substrate pore blockage by accumulation of both organic and inorganic matter. Suspended solids are gradually deposited onto the bed surface, leading to outer bed blockage. The other scenario is that these solids could be filtered and retained by subsurface flow via the mechanisms of transport and attachment, thus leading to inner blockage. The outer blockage limits the oxygen supply and impacts on organic solids removal where the organic can be decomposed by aerobic bacteria. Thus, the increase of outer blockage can lead to increase of the inner blockage. The use of sedimentation tank as a pre-treatment stage can remove the major portion of incoming solids. This is found to be a crucial step for the effective and long-term operation of the system.
- *Biomass production*: In subsurface CWs, most biomass forms as biofilms on the surface of the porous media grains, leading to clogging of the subsurface pores. Several studies conclude that greater biofilm development occurs at the inlet region where the nutrient content is greatest and microorganism metabolize them for their growth. Biofilm can develop webs across pore spaces and plug the pores between aggregates, as a result hydraulic conductivity is reduced. Other studies also reported that biological clogging

can be noted particularly when nutrient loadings are relatively high. In order to prevent this type of clogging, the biomass growth rate has to be in equilibrium with the decay rate.

- *Composition of clogging material:* The biodegradability of accumulated matter affect the clogging process. Organic composition of the total matter accumulated in the pores plays an important role in causing clogging, especially when CWs are applied for the treatment of high strength organic wastewater.
- *Rootzone effect:* The role of plants in subsurface CWs clogging is an on- going debate. Many researchers reported that root growth would counteract media clogging (Coleman et al. 2001; Brix 1994). However, a dense root and attached biofilm could affect the hydraulics of the flow and contribute to pore clogging. On the other hand, decomposition of the dead root parts and continuous new root development can create channels in the substrate for water movement downward (Vymazal et al. 1998).
- *Chemical processes:* Chemical treatment processes, such as adsorption and precipitation may play a role in clogging development. These processes are associated with the removal of metals, petroleum, synthetic hydrocarbons, ammonia-nitrogen and phosphorous. Chemical precipitation of heavy metals as hydroxide and sulphide may form film-like coatings on media surfaces (Sheoran and Sheoran 2006). Clogging may occur when the system treat industrial wastewater with high concentration of heavy metals (Kadlce and Wallace 2008).

## 2.6 Modelling VF CWs

CWs are still described as black box (Pastor et al. 2003; Tomenko et al. 2007) and only little effort has been made to understand the main processes leading to wastewater purification, where interaction between soils, vegetation, water and microorganisms are active in parallel and mutually influence each other (Kadlec & Wallace 2008). For the same reason, almost all the available design guidelines are based on empirical rules of thumb, such as those using the specific surface area requirements or simple first-order decay models.

The main objective of numerical and mathematical modelling is to obtain a better understanding of the processes governing the biological and chemical transformation and degradation processes occurring in CWs (Langergraber 2008).

The current status of CWs modelling focus on HYDRUS- CW2D and STELLA and are presented in sections 2.6.1 and 2.6.2, whilst Table 2.4 reviews the main model development in CWs.

**Table 2. 4 Review of main model development in CWs.**

<b>Model</b>	<b>Description</b>	<b>Comments</b>	<b>References</b>
Regression models	Mainly been focused on input-output data rather than on internal process data.	Multivariate linear regression equations were successfully employed for effluent benzene prediction in a study of benzene removal in vertical-flow CWs.	(Tang et al. 2009)
First-order models	Focus on individual wetland processes such as mass transport, volatilization, sedimentation and sorption.	This approach has been used for design and to predict almost all major pollutants such as organic matter (OM), suspended solids (SS), nitrogen (N) and RP.	(Mitchell and McNevin 2001)
Artificial neural networks	A mathematical or computational model that tries to simulate the structure and/or functional aspects of biological neural networks.	A design equation had been driven through Neural networks for the removal of TN in CWs.	(Akratos et al. 2009)
Self-Organizing Maps	Algorithm model that implements a characteristic non-linear projection from the high-dimensional space of sensory or other input signals onto a low dimensional array of neurons.	- This approach applied to predict the outlet concentration of BOD <sub>5</sub> , NH <sub>3</sub> -N and P in the integrated constructed wetlands treating farmyard runoff. - It can also be applied to predict the HM removal in CWs.	- (Zhang et al. 2008; Zhang et al. 2009). -(Lee and Scholz 2006).
FITOVERT model	Mathematical model for vertical sub-surface flow, VSSF CWs.	It has to be pointed out that most of the values were obtained for FITOVERT model based on an extended literature analysis.	(Kumar and Zhao 2011).
PHWAT software	A modular modeling tool was presented to be suitable for simulating the clogging process in 1, 2 and 3D.	This numerical model is able to simulate the effect of biomass growth on the hydraulic properties of saturated porous media, i.e. bioclogging.	(Brovelli et al. 2009).
2D mechanistic model	A two- dimensional (2D) mechanistic mathematical model.	This model applied to evaluate the relative contribution of different microbial reactions to organic matter removal (in terms of COD) in HSSF-CWs that treated urban wastewater.	(Ojeda et al. 2008)

### 2.6.1 HYDRUS- CW2D model

HYDRUS-2D was used as a starting point for the CW2D implementation. According to Langergraber and Simunek (2005), this model can simulate system receiving high pollutant load and oxygen transport through the plant root. It can also solve Richards's equation for saturated and unsaturated conditions and it includes equation for convection and dispersion of heat and mass transport. The main drawback of this model is that up until now, only dissolved pollutants are considered and the model cannot predict pollutant degradation during dry periods.

Langergraber (2003) used CW2D module to study the hydraulic behaviour of CWs. The system that he used consists of different layers of various sized gravel planted with *Arundo donax*. The result showed that the simulated and measured data exhibited close fit for the pilot scale CWs. The simulation result of Toscano *et al.* (2009) also showed close fit between the measured data when they modelled the pollutant removal in pilot scale two stage subsurface flow CWs. Morvannoua 2014 studied the fate of nitrogen through a VF CWs using gravel, treating directly domestic raw wastewater. Their results showed that  $\text{NH}_4\text{-N}$  was significantly adsorbed onto organic matter and was then converted to  $\text{NO}_3\text{-N}$ , and that heterotrophic biomass was mainly present in the sludge layer (first 20 cm). However all these study tested the hydraulic behaviour of CWs and pollutant removal using sand and gravel as main media in VF CWs.

### 2.6.2 STELLA model

STELLA is a graphical programming language developed for system dynamic study to better understand the nonlinear dynamic system in CWs. Pimpan & Jindal (2009) explained the adsorption, desorption and plant uptake in the FWS CWs planted with bulrush for cadmium removal using STELLA software. They explained the adsorption, desorption and plant uptake in clay loam soil and sand mixture. The simulated and measured average Cd removal values were in good agreement.

The model was also developed for nitrogen removal by Ouyang *et al.* (2011). The major nitrogen removal mechanism in VF CWs include: deposition and hydrolysis of organic nitrogen, nitrification and denitrification processes, leaching through substance zone and plant uptake. Kumar *et al.* (2011) employed dewatered alum sludge modelling phosphorus fate in VF CWs. Their result showed about 72% of

phosphorus was removed by adsorption, while 20% was through plant uptake. However the use of STELLA model for understanding the fate and transformation of HM in VF CWs using ferric sludge is not investigated yet.

## **2.7 Chapter summary**

As a 'green' system with lower energy consumption and low cost of construction, operation and maintenance; constructed wetlands have become a popular technical alternative worldwide for the treatment of various wastewaters over the past three decades (Brix 1999; Healy et al. 2007; Vymazal 2007; Babatunde et al. 2008; Vymazal 2011). Anaerobic and aerobic reactions in CWs were utilized to break down, immobilize or incorporate OM, TN and HM effluent (Batzias and Siontorou 2008). Therefore, CWs are effective in reducing organic components and nitrogen of landfill leachate (Chiemchaisri et al. 2009). However,  $\text{NH}_4\text{-N}$  is more difficult to remove in CWs than organic matter as nitrification bacteria are autotrophic microorganisms that have a slow respiration rate and require a considerable amount of oxygen to function. Another challenge facing researchers in CWs is the presence of large amount of carbonaceous substrates in landfill leachate which often prevents oxygen being used for nitrification in the wetland. In addition, the presence of HM at high concentrations in landfill leachate usually causes toxic effects to microbes and inhibits ammonia oxidation (Metcalf and Eddy 2003).

Tidal flow is the alternative strategy identified in literature to have excellent applicability for enhance oxygen transfer and the treatment capacity (Zhao et al. 2004a; Sun et al. 2005).

Overall, CWs is limited in oxygen transfers, and FWS and HF CWs seem less suitable for the autotrophic processes than VF CWs and TF CWs. On the other hand, partial nitrification could become the rate-limiting step for the denitrification process in these CWs due to the low oxygen transfer. Consequently, the overall nitrogen removal rate via autotrophic nitrogen conversion in CWs is still very low. On the other hand, TF CWs design does not allow for the anoxic condition required for denitrification to occur. A method that can maintain persistently low dissolved oxygen (DO) in the CWs bulk water is of great importance to achieve high rate autotrophic nitrogen removal with CWs.

No previous study has investigated the use of CWs for the tidal flow and anoxic condition to treat landfill leachate.

This thesis was examine in detail the use of tidal flow and anoxic condition by fixed retention time to improve the removal of OM and TN. In addition, DWS was used as main media in CWs to improve the removal of HM from artificial landfill leachate by adsorption process. Adsorption is a known process for metals removal in CWs, but it is not possible to ascertain whether adsorption is taking place in a CW simply from measuring influent and effluent concentrations. Therefore, HM adsorption capacity and the way the metals are bound to the DWS is necessary to investigate.

# **Chapter 3**

## **Characterization and Metals Adsorption by DWSs**

### 3.1 Introduction

This chapter investigated the ability of fourteen DWSs for the adsorption of selected heavy metals that have been found in landfill leachate i.e. lead (Pb), chromium (Cr), cadmium (Cd) and iron (Fe). Adsorption is a known process for metals removal in CWs, but it is not possible to ascertain whether adsorption is taking place in a CW simply from measuring influent and effluent concentrations. This is because metals can be removed in other ways such as sedimentation, precipitation and plant uptake. Therefore, the DWSs proposed for use in the CWs in this study were further characterised in order to determine their capacity for adsorption. The main objectives of this chapter were:

- 1) To determine the physicochemical properties of the different DWSs which are relevant to heavy metals removal,
- 2) To investigate the characteristics of Pb, Cr, Cd and Fe removal by the DWSs through batch experiments investigating the equilibrium and kinetics of adsorption,
- 3) To study the effect of pH, adsorbent dose and contact time on the removal of heavy metals by DWSs.

The chemical and physical characteristics of the sludges were determined, and this provided valuable data regarding the constituents of DWSs. It also helps to understand some of the pollutant removal patterns.

### 3.2 Materials and Methods

#### 3.2.1 General physicochemical characterization

DWSs were collected from fourteen drinking water treatment works located in the United Kingdom. The treatment plant locations were kept anonymous on request, and samples obtained were simply labelled using a sequential alphabetic code generated from the location names. The dewatered waterworks sludge samples were air-dried

---

Part of this Chapter has already been published as 'Attenuation of metal contamination in landfill leachate by dewatered waterworks sludges' ,(2016), A. Mohammed; T. Al-Tahmazi; A.O. Babatunde, J Ecological Engineering, 94, 656-667.

and ground to pass a 2-mm mesh sieve, and then used for the characterization and adsorption tests. Elemental metal composition of the sludges was determined using inductively coupled plasma optical emission spectroscopy (ICP–OES), after digestion in a microwave with 15.8M of HNO<sub>3</sub> and 11.65M of HCL (1:1 HCl: HNO<sub>3</sub>). The digested solution was then analysed for the concentrations of Al, Fe, Mn, Mg, Ca, K, Zn, Cl, P, Na and SO<sub>4</sub>. The sludges were also subjected to X-ray diffraction analysis using a Phillips PW3830 x-ray diffractometer in order to determine their mineralogy.

The chemical and physical characteristics of the sludges were determined as follows:

### **3.2.1.1 pH**

The method of heavy metals sorption in sludges are different at different sludge pH values, and the sludge's ability of to retain them depends on its resistance to any change in sludge pH.

pH value of the sludges were determined according to the standards BS ISO 10390:2005 (ISO 1994).

### **3.2.1.2 Point of zero charge (PZC)**

Determination of point of zero charge (PZC) is an important element in the characterization of adsorbents. This is mainly because the PZC defines the affinity of the adsorbent surface to the ionic species. Therefore, knowledge of PZC can help in the selection of adsorbent for removal of specific wastewater pollutants (Castaldi et al. 2014).

PZC was determined using the solid addition method (Mohan and Gandhimathi 2009) as described herewith: 45 mL of 0.1M KNO<sub>3</sub> solution was measured into series of 100 mL conical flasks. For each series of the test, the pH<sub>0</sub> (pH<sub>0</sub>= initial pH of the solution) was adjusted to 2, 4, 6, 8 and 10 by adding either HNO<sub>3</sub> or NaOH. Thereafter, the total volume of the solution in each flask was made up to 50 mL by adding KNO<sub>3</sub> solution. The pH<sub>0</sub> of the solutions were then accurately noted. 1g samples of the sludges were then added to each flask and manually agitated. The pH values of the supernatant were noted. The difference between the initial and final pH (pH<sub>f</sub>) values ( $\Delta\text{pH} = \text{pH}_0 - \text{pH}_f$ ) was plotted against the pH<sub>0</sub>. The point of intersection of the fitted line with the pH<sub>0</sub> axis gave the PZC Figure (3.1).

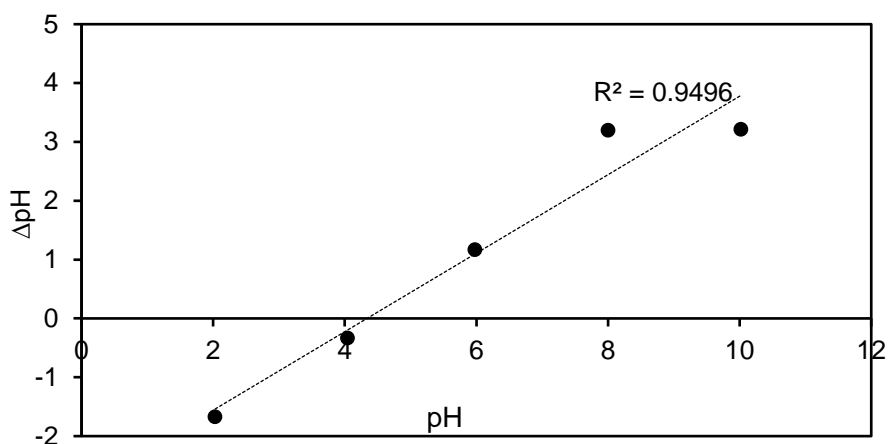


Figure 3. 1 Point of zero charge (PZC) of HH sludge.

### 3.2.1.3 Determination of Specific surface area (SSA)

Specific Surface Area (SSA) refers to the area/unit mass of sludge and is usually expressed as  $\text{m}^2 \text{g}^{-1}$ . SSA may exhibit a significant influence on controlling the fundamental behaviour of many fine-grained sludges. It varies greatly between sludges because of differences in mineralogy, organic composition and particle-size distribution (Cerato and Lutenegeger 2002).

In this study, specific surface area was determined using Ethylene Glycol Monoethyl Ether (EGME) method (Cerato and Lutenegeger 2002). DWSs which passed a #40 sieve were placed in an oven at  $60^\circ\text{C}$ . This lower temperature content need longer drying periods which set for 48 h, and check weighing have been made at 2 to 4 hour intervals to reach a constant mass to prevent oxidation of organic content. After oven drying, approximately 1 g of DWS was placed in an aluminium tare, and the mass of the sample was determine using an electronic analytical balance with an accuracy of 0.001 g. Approximately 3 mL of EGME was added to the DWS with a pipette and mixed together with a gentle hand swirling motion to create a uniform slurry. It was important to cover all sample particles with the EGME in order to obtain an accurate surface area measurement. The tare was then placed inside a standard laboratory glass sealed vacuum desiccator and was allowed to equilibrate for 20 min. The desiccators were then evacuated using a vacuum pump which provided a vacuum of 630 mm Hg (30 in). After 24 h, the tares were removed from the desiccator and weighted using analytical balance. The weight was taken again after 16 h and then after 24 h. This method was considered sufficiently accurate, since the mass did not

vary more than 0.001 g. Therefore, the specific surface area was calculated using Equation 3.1.

$$SSA = \frac{W_a}{0.000286W_s} \quad (3.1)$$

where SSA is Specific Surface Area in  $\text{m}^2 \text{g}^{-1}$ ,  $W_a$  is weight of ethylene glycol monoethylether (EGME) retained by the sample in grams (final slurry weight-  $W_s$ ), 0.000286 is the weight of EGME required to form a monomolecular layer on a square meter of surface ( $\text{g m}^{-2}$ ),  $W_s$  is weight of sample added initially (g).

#### **3.2.1.4 Aluminium and iron oxalate**

Amorphous Al and Fe oxalate of soils are often extracted by an ammonium oxalate solution. In this study, Al and Fe oxalate in sludges were determined following the method of McKeague and Day (1966). 10 mL of 0.2 M acidified ammonium oxalate were added to the DWS (250 mg) in a 15 ml tube which was stoppered tightly. Thereafter, and in order to keep the samples in darkness, the tubes were covered using aluminium foil. The tubes were then shaken on a rotary shaker at 50 rpm for 4 h and centrifuged at 1800 rpm for 20 min. An aliquot of the extract was digested with  $\text{HNO}_3$  and  $\text{H}_2\text{SO}_4$  and Fe and Al were determined.

### **3.2.2 Adsorption study - Kinetic and Equilibrium tests**

#### **3.2.2.1 Kinetics of heavy metals adsorption by DWSs**

Information on the kinetics of metals uptake by DWSs is required to select the optimum condition for full- scale batch metals removal processes. Kinetic studies were carried out in batches using synthetic metals solution, different dosage of sorbent and different time as described below:

##### **3.2.2.1.1 Synthetic metal solution**

To examine the kinetics of heavy metals adsorption by the DWSs, batch experiments were used to investigate the kinetics of the adsorption process. Initial metal concentration for individual solutions were taken as  $500 \text{ mg L}^{-1}$  for Fe,  $5 \text{ mg L}^{-1}$  for Cd,  $1 \text{ mg L}^{-1}$  for Cr and  $0.5 \text{ mg L}^{-1}$  for Pb. The concentrations of the heavy metals used

were chosen based on their typical concentration in young landfill leachate in the UK (Thornton et al. 2000; Baun and Christensen 2004). The solutions for each heavy metal was prepared in the laboratory using  $\text{FeSO}_4 \cdot 7\text{H}_2\text{O}$  salt,  $\text{CdSO}_4 \cdot \frac{8}{3}\text{H}_2\text{O}$  salt,  $\text{Cr}(\text{SO}_4)_2 \cdot 12\text{H}_2\text{O}$  salt and  $\text{PbCl}_2$  salt, respectively for Fe, Cd, Cr and Pb.

### 3.2.2.1.2 Optimum dosage and time experiment

To investigate the effect of adsorbent dosage and equilibration time, different masses of the sludge samples (0.1, 0.5 and 1.0 g) were equilibrated with 100 mL each of heavy metal solutions ( $500 \text{ mg L}^{-1}$  for Fe,  $5 \text{ mg L}^{-1}$  for Cd,  $1 \text{ mg L}^{-1}$  for Cr, and  $0.5 \text{ mg L}^{-1}$  for Pb), contained in 250 mL polyethylene bottles for 1–96 hr using a rotary shaker. The mixture at each specified time was withdrawn, filtered and analysed for each heavy metals using an Optima 210 DV ICP OES, and the uptake of those metals were determined using Equation 3.2.

$$q_e = \frac{(C_0 - C_e)}{m} v \quad (3.2)$$

2)

where  $C_0$  and  $C_e$  (both in  $\text{mg L}^{-1}$ ) are the initial ( $t=0$ ) and final heavy metals concentrations at equilibrium ( $q_e$ ), respectively ( $\text{mg g}^{-1}$ ),  $v$  is the volume of the solution (L) and  $m$  is the mass of DWSs used (g).

### 3.2.2.1.3 Kinetic models

The kinetics of the adsorption process for each metal ion by the sludges was analysed by fitting the kinetic data to the pseudo first-order equation, pseudo second-order equation, and the intraparticle diffusion models, the linear form of which are given below, respectively as Equations 3.3- 3.8 (Babatunde and Zhao 2010).

$$\frac{dq_t}{dt} = K_1 (q_e - q_t) \quad (3.3)$$

$$\frac{dq_t}{dt} = K_2 (q_e - q_t)^2 \quad (3.4)$$

$$q = k_d t^{0.5} + c \quad (3.5)$$

After integration and applying the initial conditions  $q_t=0$  at  $t = 0$ , and  $q_t = q_t$ , at  $t = t$ .

$$\log(q_e - q_t) = \log q_e - \frac{K_1}{2.303} t \quad (3.6)$$

$$\frac{t}{q_t} = \frac{1}{k_2 q_e^2} + \left( \frac{1}{q_e} \right) t \quad (3.7)$$

where  $q_t$  is the amount of adsorbate adsorbed at time  $t$  ( $\text{mg g}^{-1}$ ),  $K_1$  is the pseudo-first-order rate constant ( $\text{min}^{-1}$ ) and  $t$  the contact time (min),  $K_2$  is the pseudo-second-order rate constant ( $\text{g mg}^{-1} \text{min}^{-1}$ ),  $K_d$  and  $C$  is the rate constant for intraparticle diffusion in ( $\text{mg g}^{-1} \text{min}^{-1/2}$ ) and the intercept, respectively.

The initial rates of intraparticle diffusion can be obtained by linearization of Eq. (3.5). The values were further supported by calculating the pore diffusion coefficient  $\bar{D}$  ( $\text{cm}^2 \text{s}^{-1}$ ) using Eq. (3.8), where  $t_{1/2}$  (min) is the time for half of the adsorption and  $r$  is the average particle radius of the adsorbent particles.

$$\bar{D} = \frac{0.03r^2}{t_{1/2}} \quad (3.8)$$

Data from the kinetic adsorption experiments can be found in Appendix B (Tables B.1-B.3).

### 3.2.2.1.4 Validation of the kinetic models

The applicability of the kinetic models to describe the adsorption process, apart from the correlation coefficient ( $R^2$ ), was further investigated and validated using the normalized standard deviation (NSD), and average relative error (ARE), all of which are defined as:

$$NSD = 100 \sqrt{\frac{1}{N-1} \sum_{i=1}^N \left[ \frac{q_t^{\text{exp}} - q_t^{\text{cal}}}{q_t^{\text{exp}}} \right]^2} \quad (3.9)$$

$$ARE = \frac{100}{N} \sum_{i=1}^N \left| \frac{q_t^{\text{exp}} - q_t^{\text{cal}}}{q_t^{\text{exp}}} \right| \quad (3.10)$$

where  $q_t^{\text{exp}}$  and  $q_t^{\text{cal}}$  ( $\text{mg g}^{-1}$ ) are experimental and calculated amount of heavy metals adsorbed on the sludges at time  $t$  and  $N$  is the number of measurements made. The smaller the NSD and ARE values are, the more accurate is the estimation of  $q_t$  values (Behnamfard and Salarirad 2009).

### 3.2.2.2 Adsorption isotherm

In order to optimize the design of an adsorption system for the removal of metals, it is important to establish the most appropriate conditions. Therefore, the fit of the adsorption models was investigated at different pHs as describe below:

#### 3.2.2.2.1 Effect of initial pH solution

For the equilibrium experiments, a contact time of 48 h and an optimal dosage of 10  $\text{g L}^{-1}$  were used as predetermined from the batch experiments. To obtain equilibrium data for determining the heavy metals adsorption capacity, and to investigate the effect of solution pH, 1g of the sludges was equilibrated with 100 mL of heavy metals solution (with initial pH ranging from 2 to 9). The range of concentrations of the heavy metals used were 0.05-1  $\text{mg Pb L}^{-1}$ ; 0.05-1  $\text{mg Cr L}^{-1}$ ; 0.05-5  $\text{mg Cd L}^{-1}$  and 5 -500  $\text{mg Fe L}^{-1}$ . This wide range of heavy metals concentration was chosen to study the variability in heavy metals adsorption capacity values and its dependence on the initial concentration of the heavy metals, and to investigate the effect of low initial metal concentration on the adsorption, giving the low concentration of heavy metals typically found in UK landfill leachates (Thornton et al. 2000; Baun and Christensen 2004). A possible reason for the low concentration is that the heavy metals in landfill leachate have been found to be bound in or onto particulate matter; this, settles in the settling tank and reduces the concentration of the heavy metals in the landfill leachate (Øygaard et al. 2007). After the set equilibrium time (48 h), the mixtures were withdrawn, filtered and analysed for residual heavy metal concentration using ICP–OES. The amount of heavy metals adsorbed by the sludges from the solution at equilibrium,  $q_e$  in  $\text{mg g}^{-1}$ , was computed using Equation 3.2.

#### 3.2.2.2.2 Adsorption models

The equilibrium data was fitted with the Langmuir, Freundlich, Temkin, Frumkin and Harkins–Jura adsorption isotherm models. Data from the adsorption experiments can

be found in Appendix B (Tables B6-B9). Table 3.1 gives the adsorption isotherm equations and their corresponding linear forms used in this study. The constant parameters obtained from the regression plots of the linear forms of the equations are summarized in Appendix B (Tables B.6- B.9). These parameters are useful for estimating the maximum adsorption capacity of the adsorbent material used in this study.

**Table 3. 1 Adsorption isotherm model equations and corresponding linear forms.**

Isotherm equation	Equation	Linear plot
Langmuir	$q_e = \frac{Q_m b C_e}{1 + b C_e}$	$\frac{C_e}{q_e} = \frac{1}{Q_m} C_e + \frac{1}{b Q_m}$
Freundlich	$q_e = K_F C_e^{1/n}$	$\log q_e = \log K_F + \frac{1}{n} \log C_e$
Temkin	$q_e = \frac{RT}{b} \ln(k_T C_e)$	$q_e = B_1 \ln k_T + B_1 \ln C_e$
Frumkin	$\frac{\theta}{1-\theta} e^{-2a\theta} = K C_e$	$\log \left[ \left( \frac{\theta}{1-\theta} \right) \frac{1}{C_e} \right] = \log K + 2a\theta$
H-J	$q_e = \left( \frac{A}{B - \log C_e} \right)^{1/2}$	$\frac{1}{q_e^2} = \frac{B}{A} - \frac{1}{A} \log C_e$

Where  $q_e$  and  $C_e$  are as previously defined,  $b$  is the Langmuir adsorption constant ( $L \text{ mg}^{-1}$ ), which is related to the energy of adsorption, and  $Q_m$  signifies the adsorption capacity ( $\text{mg g}^{-1}$ ).  $K_F$  is the Freundlich constant ( $\text{g}^{-1}$ ) related to the bonding energy; and  $\frac{1}{n}$  is the heterogeneity factor, in which  $n$  is a measure of the deviation from linearity of the adsorption.  $RT/b = B_1$ ;  $R$  is the gas constant ( $8.31 \text{ J mol}^{-1} \text{ K}^{-1}$ ),  $T$  is the absolute temperature in K.  $k_T$  is the equilibrium binding constant ( $L \text{ mg}^{-1}$ ) and  $B_1$  is related to the heat of adsorption, where  $\theta$  is the fractional occupation ( $\theta = q_e/q_m$ ;  $q_e$  is the adsorption capacity in equilibrium ( $\text{mg g}^{-1}$ ),  $q_m$  the theoretical monolayer saturation capacity ( $\text{mg g}^{-1}$ ) which is determined from the Dubinin-Radushkevich isotherm equation). The parameter  $a$  is the interaction coefficient, it is positive for

attraction and negative for repulsion; its zero value indicates no interaction between the adsorbate species, in this case, the Frumkin equation coincides with Langmuir one.

### 3.2.3 Statistical analysis

Statistical analysis was carried out using the Kruskal-Wallis test. The test is a nonparametric statistical test that assesses the differences among three or more independently sampled groups on a single, non-normally distributed continuous variable. All data fitted with linearized Langmuir isotherm model at pH4 were examined using this test to compare  $Q_m$  among adsorbents at 95% significance; and to determine if there was a difference between the adsorbents.

## 3.3 Results and Discussion

### 3.3.1 General physicochemical characterization

The elemental composition of the sludges is presented in Tables 3.2 and 3.3. All Al and Fe- based sludges, with exception of HU sludge, were slightly acidic, the pH values ranging from 6.05 to 7.06 for Al-sludges and 4.09 to 6.64 for Fe-sludges. The pH values of the sludges can have an effect on their adsorption of heavy metals. As the pH of the sludges decreases, ion exchange becomes the dominant process for heavy metals retention (Elzahabi and Yong, 2001). The range of values of the  $pH_{pzc}$  were 4.76- 6.77 and 3.77- 6.95, respectively for Al- and Fe- based sludges (Tables 3.2 and 3.3). The  $pH_{pzc}$  plays a key role in the adsorption process. When the  $pH > pH_{pzc}$ , the surface of the sludges becomes dominantly negatively charged and the adsorption of metal ions will be facilitated by electrostatic attraction (Babatunde et al., 2009). The mean specific surface area (SSA) was  $327.90 \pm 115.50$  and  $184.80 \pm 95.21 \text{ m}^2 \text{ g}^{-1}$  for AL- and Fe- based sludges respectively. In comparison with other studies e.g. Babatunde et al., 2009, the SSA were found to be higher. A reason for this could be due to the fact that the total surface area was measured by the adsorption of polar liquid (EGME) (Cerato and Lutenegger, 2002), whilst other studies measured the external surface areas by the BET- $N_2$  method. The high surface area of DWSs is a positive attribute when they are being used as adsorbent. X-ray diffraction analysis (Appendix A- Figures A.3 and A.4) reveal the amorphous nature and poorly ordered particles within the DWSs. The diffraction patterns did not reveal

any sharp diffraction characteristic peak over a broad range of d-spacings ( $10-80^\circ$ ,  $2\theta$ ) for most samples of the sludges (Figures 3.2). However, some of the sludges (GU, OS, HU, BS, AR, HO, and CA) showed peaks of crystallized materials such as quartz, graphite, lithium boride and lithium phosphate (Figures A.3 and A.4); and this can have an effect on the heavy metals adsorption process. For instance, graphite which is a result of the conversion of organic matter may reduce the adsorption capacity. This is because the organic matter play important role in adsorption of heavy metals through complexation. On the other hand, the presence of quartz that develops a negative charge on the sludges can contribute to adsorption of the heavy metals through ligand complexation (Tahir and Naseem 2007). Results also reveal that 85% (mean value) of the total Al in the Al- based sludges is oxalate Al, while 53% (mean value) of the total Fe in the Fe- based sludges is oxalate Fe. This confirms the amorphous nature of the sludges (McKeague and Day, 1966).

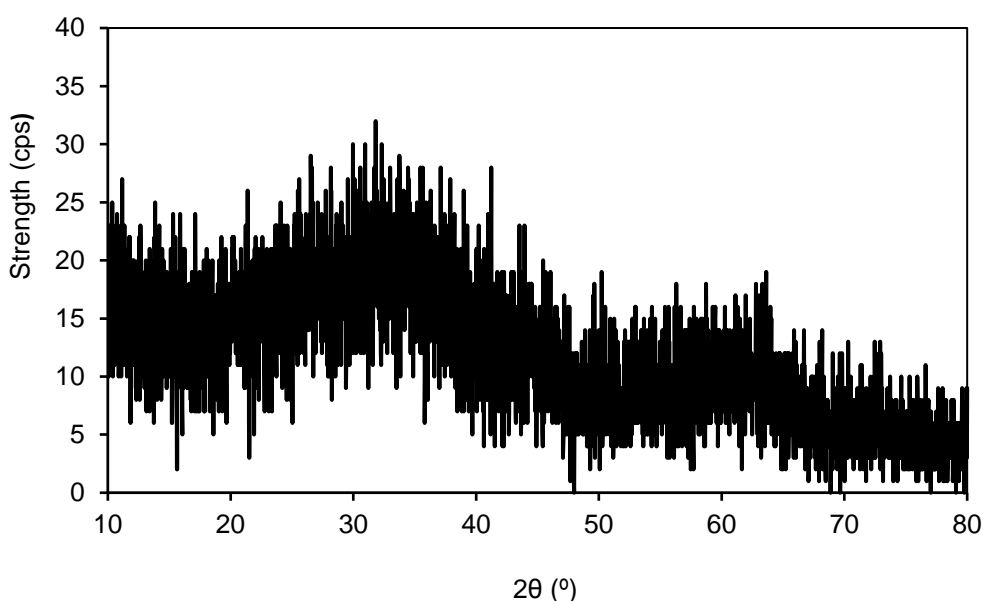


**Figure 3. 2 XRD patterns of the DWS (figure shown pattern for the HH sludge used as an example).**

Table 3. 2 Physicochemical properties of the aluminium- based sludges (n=3).

Properties		GU	WD	OS	HU	WA
Al	mg L <sup>-1</sup>	112.81	104.22	105.34	151.88	108.78
Fe		17.00	9.75	28.73	8.25	5.94
Mn		0.33	0.29	0.40	0.66	0.43
Mg		0.25	0.27	0.30	0.97	0.28
Ca		0.79	1.52	0.53	3.12	0.60
Na		0.04	0.06	0.10	0.19	0.11
K		0.47	0.36	0.72	1.47	0.43
P		0.15	0.71	0.45	4.78	0.44
Zn		0.03	0.04	0.12	0.12	0.07
Cl		0.81	1.88	1.19	2.72	0.33
SO <sub>4</sub>		0.81	1.88	1.19	2.72	0.33
TC		119.6	119.6	170.6	75.21	154.4
OC		118.9	119.1	170.1	74.2	154
Al-OXL		110.12	95.28	88.26	105.51	96.02
Fe-OXL	13.35	3.68	14.42	2.52	4.64	
SSA	m <sup>2</sup> g <sup>-1</sup>	364.1	468	206.9	390.4	210.1
pH	--	6.26	6.27	6.05	7.06	6.31
pH <sub>pcz</sub>	--	5.75	6.61	4.91	6.77	4.67

Table 3. 3 Physicochemical properties of ferric- based sludges (n=3).

Properties		BS	FO	HH	AR	MO	HO	WY	CA	BU
Al	mg L <sup>-1</sup>	4.59	21.16	5.16	5.87	3.89	65.35	4.84	6.80	5.80
Fe		298.10	241.69	193.85	277.72	257.80	143.29	287.34	255.46	212.09
Mn		0.94	2.32	0.37	0.52	0.79	0.57	1.28	0.45	0.17
Mg		0.47	0.25	0.28	0.28	0.20	0.53	0.23	0.43	0.21
Ca		6.54	2.77	2.49	22.34	1.28	1.74	0.83	3.52	2.39
Na		0.14	0.13	0.22	0.12	0.15	0.12	0.09	0.16	0.07
K		0.75	0.28	0.75	0.31	0.62	1.40	0.50	1.22	0.41
P		0.61	0.43	0.31	0.35	0.39	0.62	0.77	0.29	0.44
Zn		0.19	0.09	0.15	0.08	0.39	0.15	0.16	0.09	0.13
Cl		4.06	4.26	4.51	6.32	6.93	3.86	8.55	7.45	2.81
SO <sub>4</sub>		4.06	4.26	4.51	6.32	6.93	3.86	8.55	7.45	2.81
TC		110.8	137	161.9	88.62	117.4	105.2	113.7	115.9	154
OC		110.8	137	161.9	88.62	117.4	105.2	113.7	115.9	153.6
Al-OXL		1.14	17.36	1.36	2.99	1.85	58.63	3.46	1.02	4.67
Fe-OXL		143.08	121.33	121.38	113.63	149.52	72.41	146.37	144.48	138.48
SSA	m <sup>2</sup> g <sup>-1</sup>	203.4	120.3	131.9	97.02	186.4	414.5	132.3	219.8	157.2
pH	--	5.47	5.49	4.55	6.64	4.48	5.49	4.3	4.09	4.75
pH <sub>pcz</sub>	--	4.79	4.23	4.33	6.95	3.77	4.26	3.81	3.8	3.94

### 3.3.2 Optimization of factors influencing metals uptake

#### 3.3.2.1 Effect of adsorbent dosage

The adsorption of heavy metals by different masses of the sludges (1g, 0.5g and 0.1g) was studied as a function of contact time. Determining the optimum dosage and equilibration time is crucial for determination of the adsorption capacity and the influencing factors. Although the different sludge masses exhibited the same trends in adsorption behaviour, it is clear that increasing the adsorbent (sludge) mass increases the heavy metals removal. This is possibly due to the fact that there is more surface area available when there is increase in adsorbent mass (figure 3.3). However, beyond certain doses, the removal plateaus with no significant increase in the percentage of heavy metals removal. Accordingly, the result in Figures A.5 – A.12 (Appendix A) shows that there were no significant difference in total removal percentage of heavy metals especially for Pb, Cr and Cd, for most of the DWSs beyond 5 g L<sup>-1</sup> and 10 g L<sup>-1</sup>. Table 3.4 also shows that the optimum sludge dosage to remove more than 90% of Pb and Cr was 5 g L<sup>-1</sup> for most of the Al- and Fe-based sludges. This may be attributed to the metal-vacant sites on the sludges at 5g L<sup>-1</sup> which are available for Pb and Cr ions in solution when the concentration of these metals were low (i.e. 0.5 mg L<sup>-1</sup> and 1 mg L<sup>-1</sup> respectively). For Fe, when the concentration was 500 mg L<sup>-1</sup>, the removal percentages were 38% and 93%, respectively at the 5 g L<sup>-1</sup> and 10 g L<sup>-1</sup> doses. Moreover, the ratio of metal ions to the adsorbent is low, so the adsorption involves much higher energy site. When this ratio increases, as in Fe at 5 mg L<sup>-1</sup>, the energy sites becomes saturated and the adsorption of lower energy sites begins with a decrease in removal efficiency (Ferreira et al. 2014).

#### 3.3.2.2 Effect of contact time

The amount of metal ions adsorbed is controlled by the velocity with which the adsorbate is transported from the external surface to the internal surface of active sites on the adsorbent's particles (Makris et al. 2006; Ferreira et al. 2014). Figure A.5 – A.12 (Appendix A) indicates a sharp rise in the heavy metals removal within the first hour, indicating the instant at which the adsorption process takes place. This can be adduced to the excess of binding sites on highly accessible surfaces like particles and macropores. Over time, the curves start to plateau because the rate of removal is

much slower. This is due to the accumulation of metal ions on the binding sites until it reaches equilibrium; and thereafter sorption would be via intraparticle diffusion in meso- and micropores and/or sorption by the organic matter (Makris et al. 2006; Zhou and Haynes 2011). In general, these findings are in agreement with those reported in other similar studies using water treatment residuals for heavy metals removal such as: Zhou and Haynes (2011) who reported that about 90% of Pb and Cr removal occurred within 120 minutes, and Castaldi et al. (2015) who showed that 72% and 85% of Pb, respectively adsorbed by Fe- and Al-based sludge after 1 h. In this study, the removal of Pb, Cr, Cd, and Fe reached, respectively, 98% , 92%,18%, and 84% for Al-based sludges; and 97%, 89%, 70%, and 42%, respectively, for Fe-based sludges, within the first hour of contact for most sludges. However, the optimum time to remove more than 90% of heavy metals for both types of sludges was 48 hour as shown in Table 3.4.

### 3.3.2.3 Initial pH effect

Initial pH solution is a crucial factor in metal adsorption by adsorbents. In the lower pH ranges, the solution pH can affect the adsorption process in different ways. The  $pH_{pzc}$  of the sludges ranged from 3.8 to 7.1, while the pH ranged from 4.09 to 7.06. Thus, at pH values less than the  $pH_{pzc}$ , the sludges will have net positive charge due to the presence of the OH group (alum oxalate and iron oxalate) which are positively charged at low pH (Bradl, 2004). As the pH rises above the  $pH_{pzc}$ , the surface of sludges become predominant negatively charged (Babatunde et al., 2009). The positive charge at low pH weakens the adsorption performance for the heavy metals. In addition, at low pH there is a huge amount of H<sup>+</sup> ion competing with the metal ions and this negatively impacts the adsorption process for heavy metals (Chen et al. 2015b). The optimum pH to reach the maximum adsorption in this study was pH 4 for the removal of Pb, Cr and Cd and pH 2 for removal of Fe (Table 3.4).

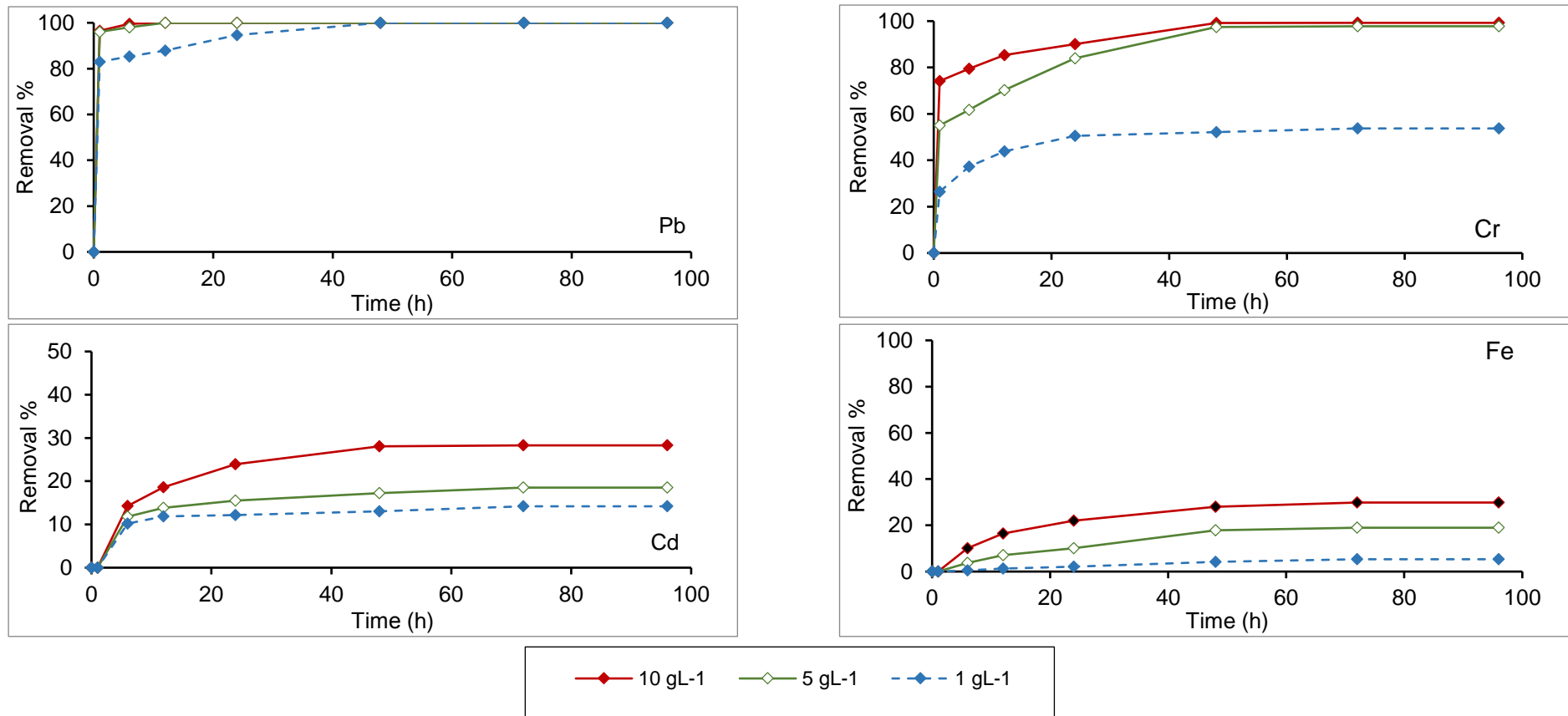


Figure 3. 3 Removal efficiency of heavy metals by HH sludge at different contact times and three different sludge dosages.

Table 3. 4 Optimum values of key adsorption parameters used in heavy metals removal.

Key adsorption parameters	Heavy metals	GU	WD	OS	HU	WA	BS	MO	HO	CA	FO	HH	AR	WY	BU	Optimum values used
Time(h) at which >90% removal	Pb	24	12	24	12	48	6	6	24	24	12	1	6	48	-	48
	Cr	24	12	24	12	48	24	12	24	48	48	48	48	48	48	48
	Cd	-	-	-	-	-	-	-	-	-	-	-	24	-	-	-
	Fe	24	24	24	24	24	-	-	48	-	-	-	-	-	-	48
Sludge dosage (g L <sup>-1</sup> ) at which >90% removal	Pb	5	5	5	5	5	1	5	5	1	5	5	1	5	-	5
	Cr	5	5	10	5	5	5	10	5	5	5	5	10	5	5	5
	Cd	-	-	-	-	-	-	-	-	-	-	-	10	-	-	10
	Fe	10	5	10	5	10	-	-	10	-	-	-	-	-	-	>10
pH at maximum uptake (Q <sub>m</sub> ) from Langmuir model	Pb	2	4	7	4	4	7	2	7	4	4	4	7	7	4	4
	Cr	4	4	4	7	4	4	2	7	4	2	2	4	2	4	4
	Cd	7	7	4	4	4	4	7	4	4	4	7	7	4	9	4
	Fe	2	2	2	2	2	2	2	2	2	2	2	2	2	2	2

### 3.3.3 Adsorption study

#### 3.3.3.1 Adsorption kinetics modelling

Studies of the kinetics of adsorption is important to understand the transference velocity of metal ions from aqueous solution to the adsorbent surface, and the time to reach the equilibrium (Božić et al. 2013). In this study, the pseudo first-order, pseudo second-order and intraparticle diffusion models were employed to fit the experimental data. From Tables B2- B5 it can be seen that the pseudo second-order model exhibited better fit for Cr for all the sludges, with the exception of WD, WA and CA sludges. The correlation coefficient, NSD and ARE of the pseudo-second order model fit ranged, respectively from 0.99%- 1%, 1.43%- 21.06% and 0.85%- 9.79%. Furthermore, the calculated  $q_e$  values through this model is close to the experimental values. This strongly suggests that the sorption kinetics of Cr onto DWSs is well described by a pseudo-second order kinetic model. It also implies that the rate-limiting step is chemisorption, which involves sharing of valence forces or electron exchange between Cr ion and the DWSs, rather than diffusion or ion exchange between the sorbent and the sorbate (Akhtar et al. 2008). Zhou and Haynes (2011) reported similar trend for Cr adsorption onto Al- based sludges and they suggested that chromium have been shown to form strong, inner sphere complexes with Al and Fe oxide surfaces by predominantly bidentate bonding.

The kinetic data for Pb was well described by pseudo first-order model with correlation coefficient, NSD and ARE ranging, respectively from 0.662%- 1%,  $7.6 \times 10^{-5}\%$ - 17.15% and  $2.6 \times 10^{-5}\%$ - 6.11%. In addition, the  $q_e$  value determined from the model is close to the experimental value (Table B1, B4 and B5). Several authors have shown that the adsorption of Pb is well fitted with the pseudo second-order model rather than the first order (Nghah and Fatinathan 2010; Zhou and Haynes 2011; Cheng et al. 2015).

Diffusion as opposed to chemical reaction can also be the rate-limiting step in the case of Cd (except for HH, AR and WY sludges) adsorption where the correlation coefficients ranged from 0.86 to 0.98, indicating a good fit of the intraparticle diffusion model with the kinetic data (Table B3). However, the plot as shown in Figure 3.4c is nonlinear, indicating that intraparticle diffusion is not the only rate-limiting step. Furthermore, this figure also reveal, that the plots did not pass through the origin, and

this implies that other mechanisms might also be involved in the kinetics of adsorption all of which could be operating simultaneously (Hameed 2008). According to Ferreira et al. (2014), the interception is related to the thickness of the limiting layer. The larger the intercept, the greater is the amplitude of the surface diffusion in the rate-limiting stage. Based on the intraparticle diffusion model, the values of pore diffusion coefficient ( $\bar{D}$ ) were determined to be between  $4.8 \times 10^{-8}$  -  $58 \times 10^{-7} \text{ cm}^2 \text{ min}^{-1}$  for Cd indicating that the process is governed by diffusion, however; pore diffusion is not the only rate limiting step.

The correlation coefficients of Fe kinetic adsorption were high (0.82- 0.99), but high NSD (27%- 1214%) and ARE (27.82%- 705.7%) confirm that the removal of Fe is by precipitation and not by adsorption as discussed in section 3.3.3.3. In addition, the  $q_e$  values obtained from fitting with the kinetic models are not close to the experimental values, with the exception of GU and HU which follow first-order model with high correlation coefficient and low NSD and ARE as shown in Tables B4 and B5.

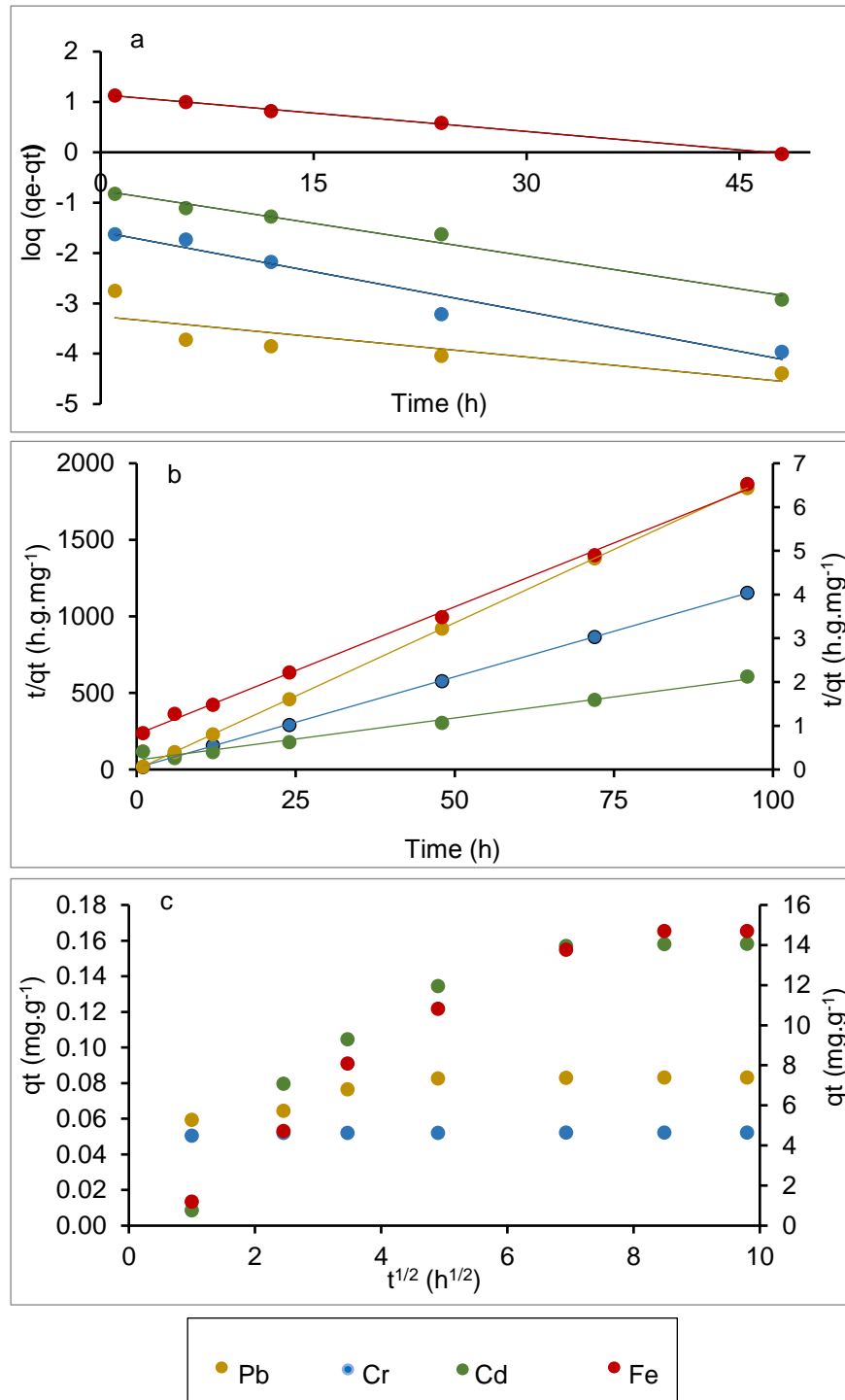


Figure 3. 4 Sorption kinetics of heavy metals onto HH sludge using: a) first order, b) second order and c) intraparticle diffusion model (secondary axis in Figures b and c, represent the data for Fe).

### 3.3.3.2 Adsorption isotherm modelling

Fourteen samples of DWSs were investigated in this study as adsorbents for heavy metals in landfill leachate. It is important to understand the adsorption process of the heavy metals (Pb, Cr, Cd, and Fe) by the sludges from various sources in order to reveal any significant influence of their physicochemical characteristics on the adsorption behaviour. Several adsorption isotherm models including Langmuir, Freundlich, Temkin, Frumkin and Harkins-Jura were used to fit the experimental data.

#### 3.3.3.2.1 Langmuir isotherm model

Langmuir model relates the coverage of molecules on a solid surface to concentration of a medium above the solid surface at a fixed temperature. This isotherm model is based on three assumptions: adsorption is limited to monolayer coverage; all surface sites are the same and can only accommodate one adsorbed atom; and the adsorbed molecule on a given site is independent of its neighboring sites occupancy.

Langmuir model was found to fit the adsorption data of Pb and Cr quite well with  $R^2 = 0.79- 0.93$  and  $0.71- 1$ , respectively, with the exception of WA and MO sludges for Pb, and GU for Cr. Results presented in Table B6 and B7 also reveal that for some sludges, the maximum adsorption capacity for Pb and Cr were at pH 4. This could be because when the  $pH > 4$ , Pb and Cr start to form hydroxides species such as  $Pb(OH)_2$ ,  $Cr(OH)_2$  or  $Cr(OH)_3$ . These hydroxides have less ability to adsorb than  $Pb^{+2}$  and  $Cr^{+3}$  (Babatunde et al., 2009; Makris et al., 2006). On the contrary, the other sludges (WD, HU, WA, MO, FO and HH) in Pb adsorption and (GU, WD, OS, WA, BS, CA, FO and AR) in Cr adsorption presented different behaviour. This may be due to the effect of  $pH_{pzc}$  as discussed in 3.3.1, where the  $pH_{pzc} > pH$  of the solution, therefore the surface of those sludges becomes dominantly positive charged. In addition, the presence of silica that develop a negative charge on the sludges can contribute to adsorption of metal cations. These characteristics can be the reason for the observed adsorption behaviour for Pb and Cr.

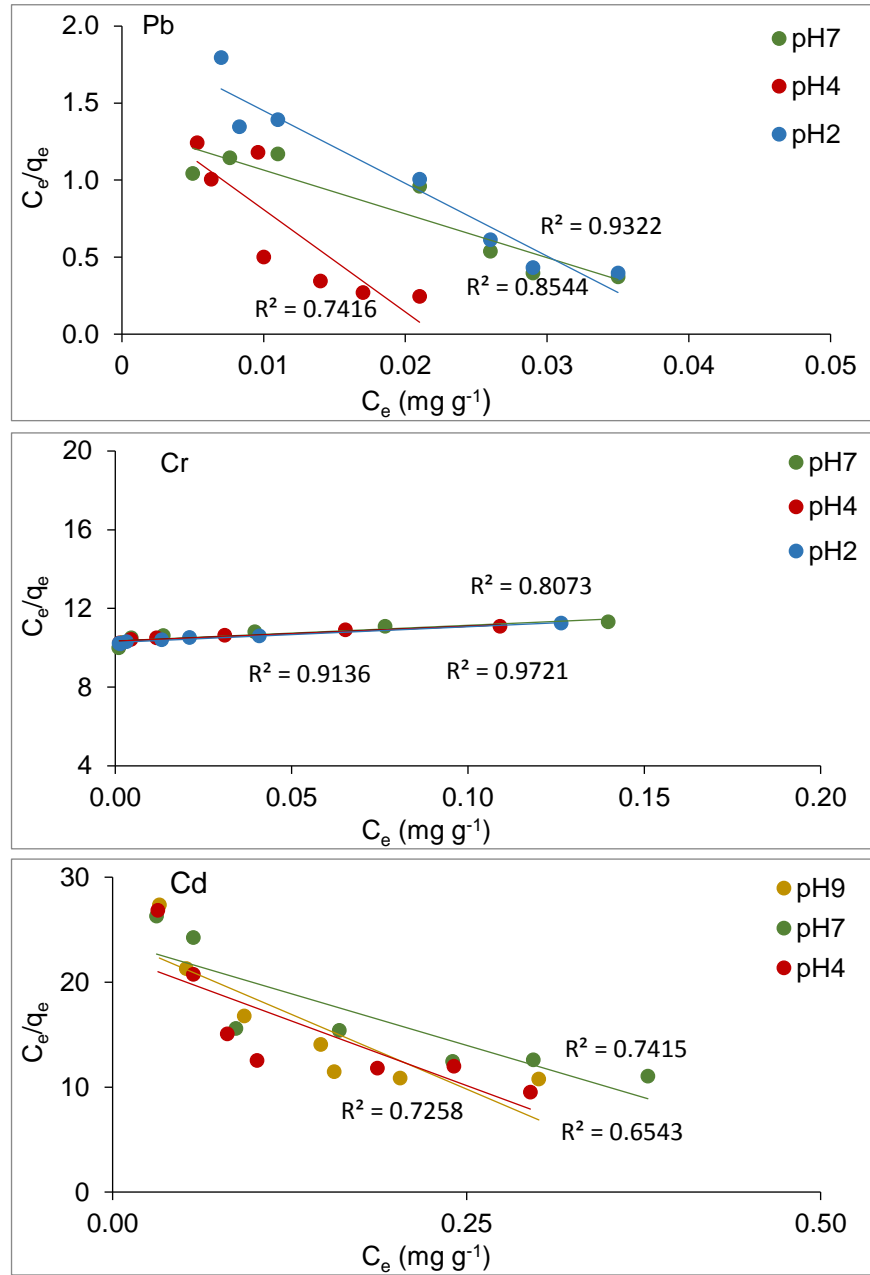


Figure 3. 5 Sorption isotherm of heavy metals onto DWS using Langmuir isotherm model at different pHs (data refers to the HH sludge used as an example).

### 3.3.3.2.2 Freundlich isotherm model

Another widely used model for describing heavy metals sorption is the Freundlich model. It is an empirical equation that is widely used for the description of adsorption equilibrium. The equation is useful for describing the adsorption of organic and inorganic compounds on a wide variety of adsorbents including DWSs.

Freundlich isotherm model was particularly well fitted to describe the multilayer formation of Cr, Cd and Pb on the heterogeneous surfaces of the DWSs (see Tables B6- B8). However, this was not the case for the adsorption of Pb onto the WA sludge as shown in Table B6. The constant  $K_f$  and  $n$  are, respectively the adsorption capacity and adsorption intensity. The  $n$  values for Cr were generally  $>1$  and ranged from 1.33-2.31, indicating favourable adsorption. Higher  $n$  value imply stronger interaction between DWSs and heavy metal ions (Hameed, 2008). However, the  $n$  values for Pb were  $<1$  for most of the sludges, this suggests that precipitation reaction may well be

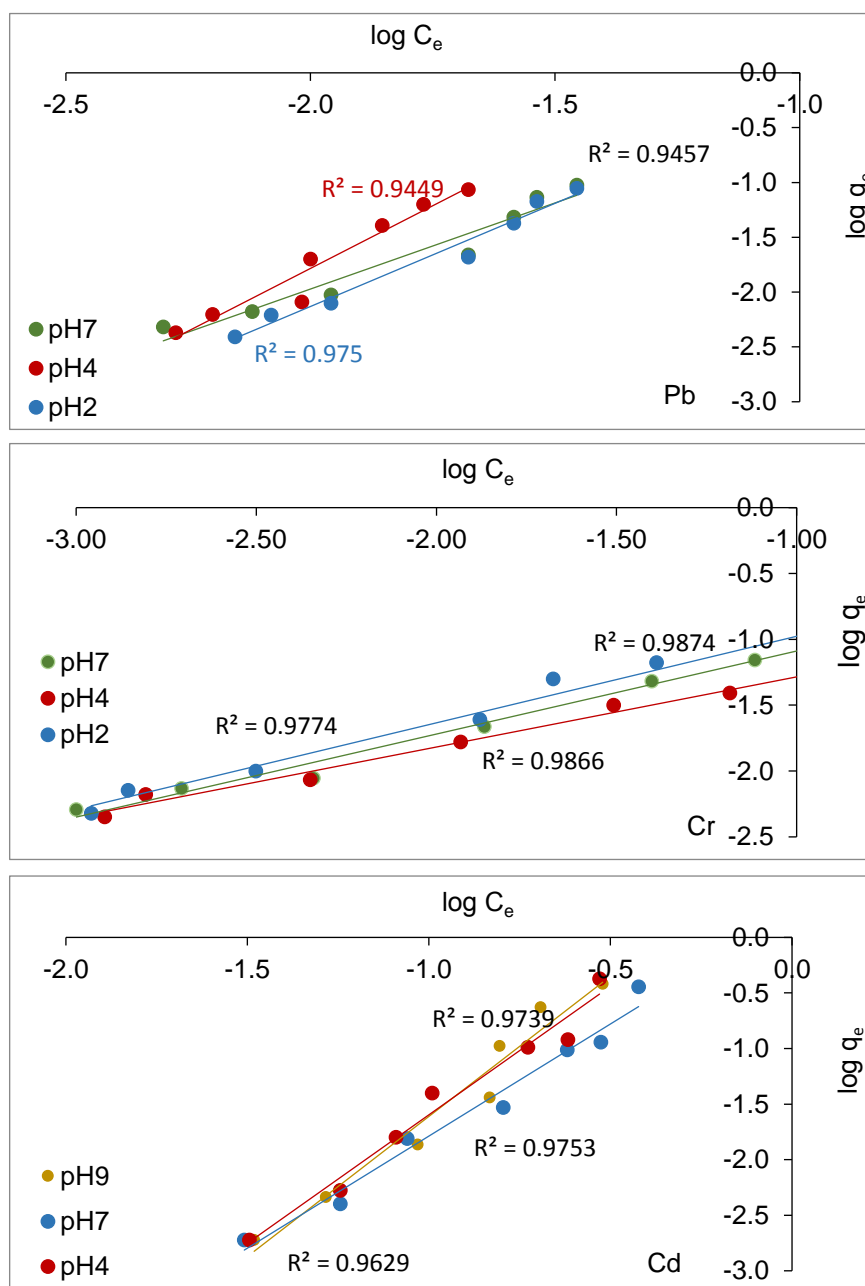


Figure 3. 6 Sorption isotherm of heavy metals onto DWS using Freundlich isotherm model at different pHs (data refers to the HH sludge used as an example).

occurring in addition to adsorption (Hua et al. 2015). The  $n$  values for Cd adsorption for some sludges were  $<1$  and ranged from 0.38- 0.97, indicating that precipitation reaction may occur in these cases, whilst for others, the  $n$  value was  $>1$  and ranged from 1.07- 1.52 indicating favourable adsorption.

### **3.3.3.2.3 Temkin isotherm model**

With the exception of Fe, the Temkin isotherm model was able to describe the adsorption data well for all the heavy metals. The derivation of the Temkin isotherm considers that the heat of adsorption of all the molecules in the layer would decrease linearly with coverage. This decrease in heat is linearly rather than logarithmically related to sorbate/sorbent interactions (Vijayaraghavan et al. 2006). The Temkin isotherm-binding constant increased with increasing pH and reached maximum values of  $334.1 \text{ L mg}^{-1}$  and  $31.72 \text{ L mg}^{-1}$ , respectively for Pb and Cd (see data in Tables B6- B8). In contrast with Cr, there was decrease in the constant  $B_1$  which is related to the heat of adsorption, and it decreased with increase in pH. This may suggest that the adsorption activity increases at low pH. However, the model was unable to describe all data, as there were some low correlation coefficients as shown in Tables B6- B8.

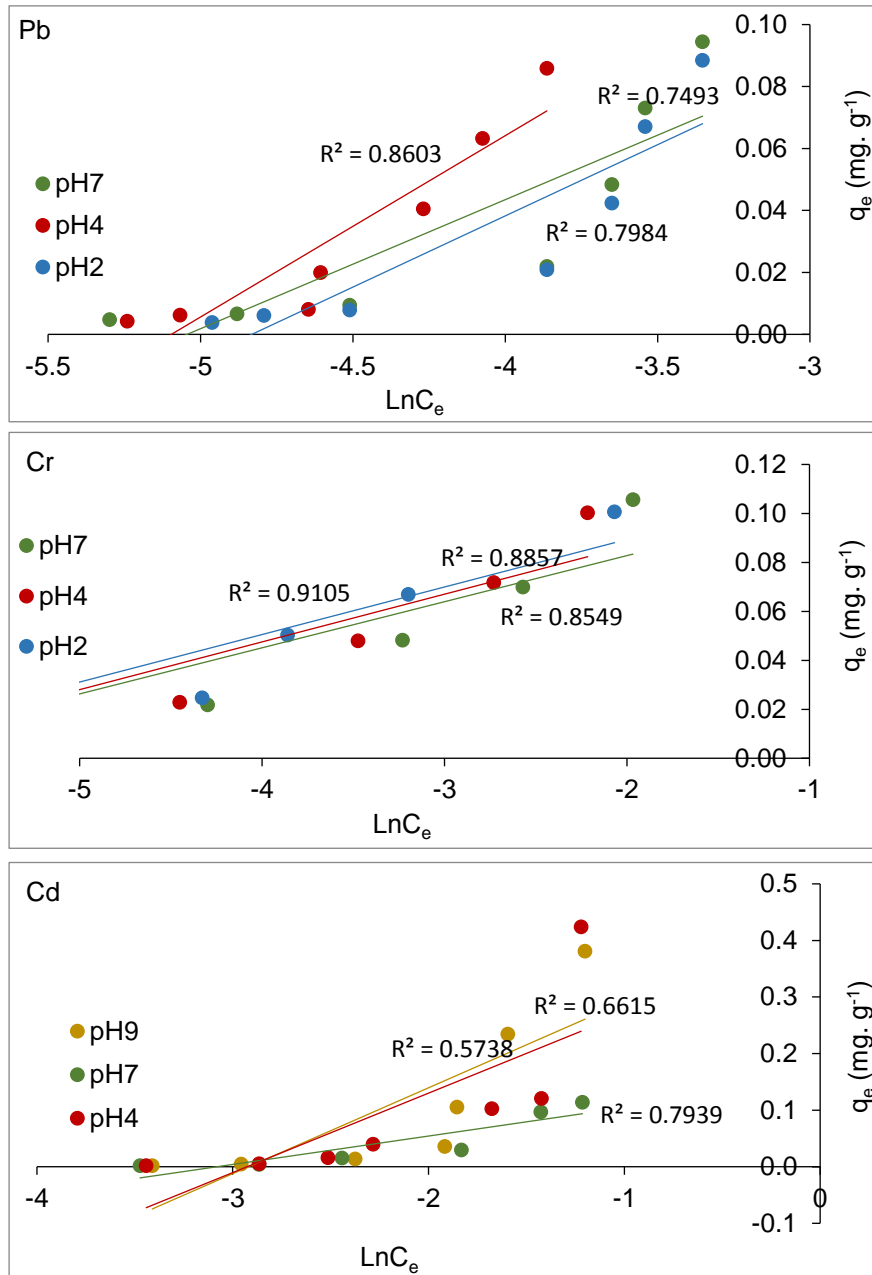


Figure 3. 7 Sorption isotherm of heavy metals onto DWS using Temkin isotherm model at different pHs (data refers to the HH sludge used as an example).

### 3.3.3.2.4 Frumkin isotherm model

The Frumkin isotherm model, which takes into consideration the interaction between adsorbed species, was found to give better fit for adsorption of Pb than for the other metals. The parameter  $a$  (interaction coefficient) was positive for all the sludges and this indicates that there is attractive interaction between Pb molecules and the sludges (Babatunde and Zhao, 2010).

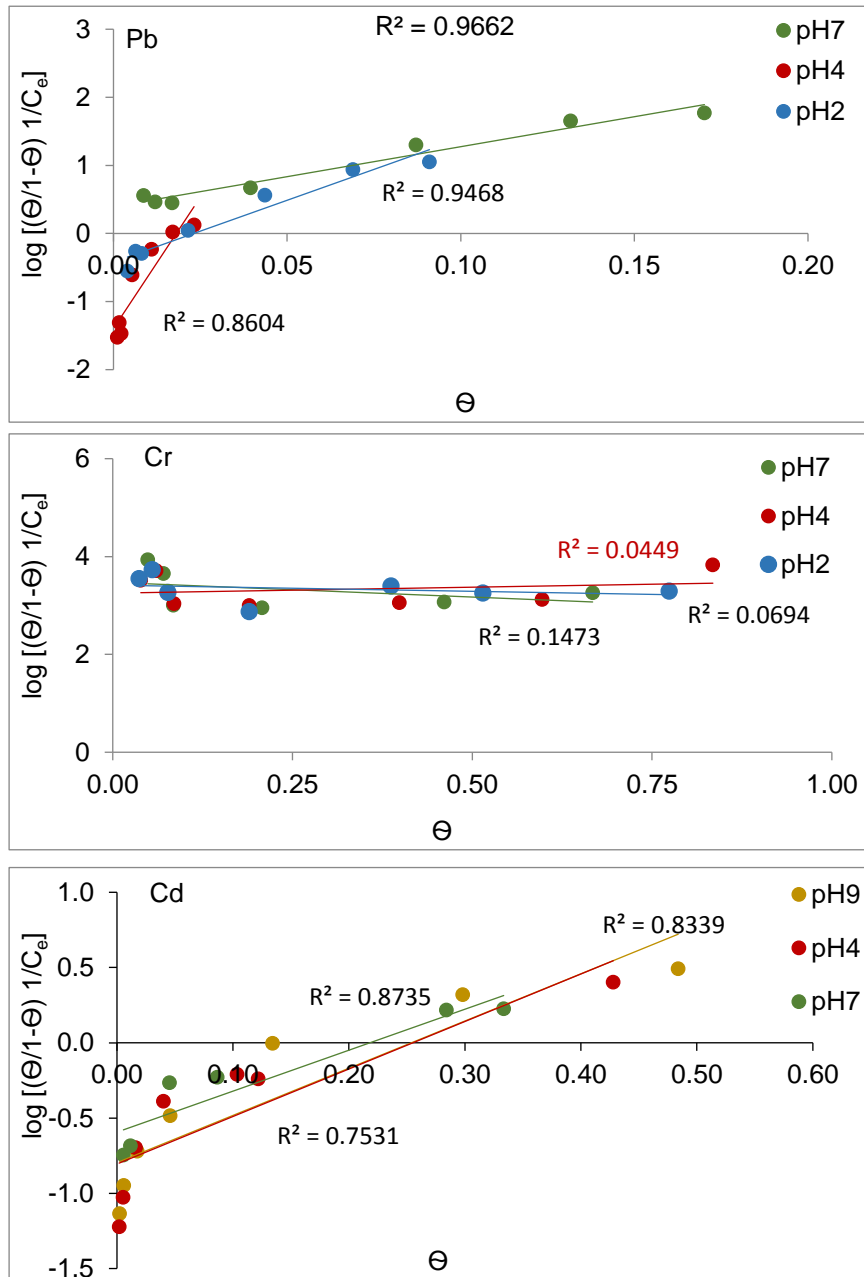


Figure 3. 8 Sorption isotherm of heavy metals onto DWS using Frumkin isotherm model at different pHs (data refers to the HH sludge used as an example).

### 3.3.3.2.5 Harkins- Jura isotherm model

The Harkins- Jura model gave the lowest  $R^2$  values and this shows that the model could not describe any of the adsorption data. The model implies multilayer adsorption with the existence of a heterogeneous pore distribution (Başar 2006). However, the  $R^2$  for Pb (except the  $R^2$  of GU and WD sludges) ranged from 0.72 to 0.97 (see data in Tables B6, B7 and B8).

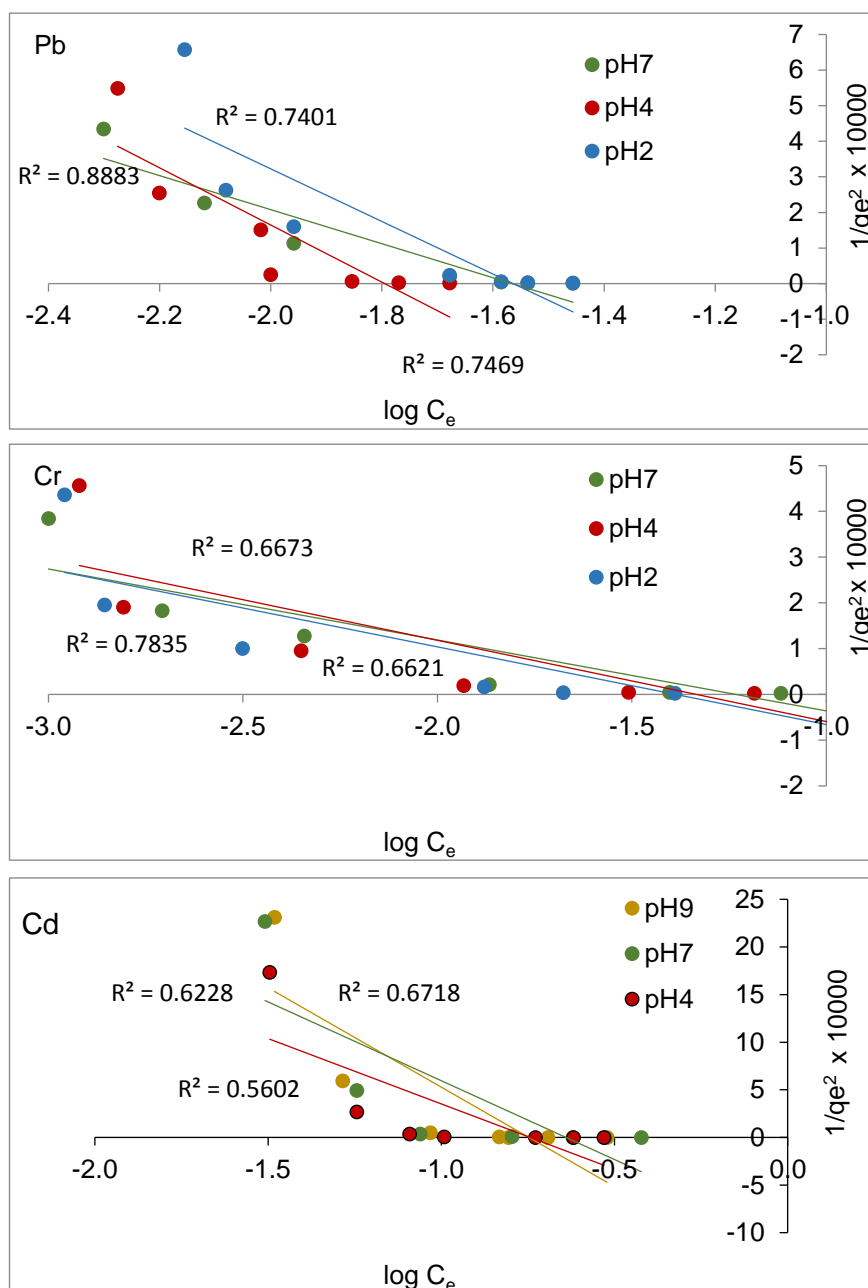
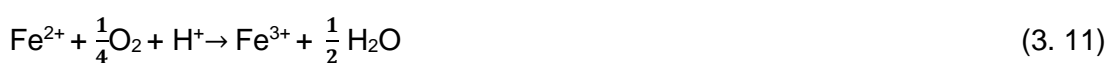


Figure 3. 9 Sorption isotherm of heavy metals onto DWS using Harkins- Jura model at different pHs (data refers to the HH sludge used as an example).

### 3.3.3.3 Fe removal

The correlation coefficients for all the isotherm models for Fe removal were low. In addition,  $Q_m$  from Langmuir model was negative, this could possibly be explained by the fact that the removal of Fe was by precipitation and not by adsorption (Table B9). Since in an oxygenated environment and in acidic condition, Fe can either be in insoluble oxyhydroxide (FeOOH) form (Equation 3.11 and 3.12), or joined with the hydroxide ion to form  $Fe(OH)_3$ , which gives the water reddish-brown colour. This formation of iron then either settles or remains in suspension (Kadlce and Wallace, 2008).



### 3.3.4 Differences in heavy metals removal by DWSs

To assess the difference between the two main types of waterworks sludges for heavy metal removal, kinetic studies were carried out by equilibrating 1g of each sludge sample in individual solutions of Pb, Cr, Cd at different contact times (1- 96h). Results as presented in Figures A.5- A.12 reveal that both Al and Fe-based sludges exhibited the same trend for the removal of the heavy metals. The removal of Pb and Cr reached 98% and 90%, respectively, during the first hour; and then increased to 99% after 24 h for the two sludge types. This indicates that there was no difference in removal of these metals between the two main types of DWSs. Kruskal-Wallis analysis of the equilibrium data at pH 4 also shows that there was no significant difference in maximum adsorption capacity for Al- and Fe-based sludges ( $p > 0.05$ ). Accordingly, both types of sludges performed similarly at adsorbing Pb, Cr, and Cd. The WD, WA, CA, MO and WY sludges were excluded from the analysis of Pb adsorption, whilst the two Al-based sludges (GU, HU) and the two Fe-based sludges (MO, HH) were used for the analysis of Cd adsorption. Whereas all sludges were used with the exception of AR to explain the differences in  $Q_m$  for Cr adsorption. The sludges that were not used in the Kruskal-Wallis analysis had a low  $R^2$  in the fitting with the Langmuir model, indicating that the adsorption was onto a heterogeneous surface (where  $R^2$  for Freundlich isotherm were high, see Tables B6- B8), and not monolayer adsorption on active sites, and therefore the model coefficients ( $Q_m, b$ ) do not give an accurate representation of the data.

### 3.4 Conclusion

The adsorption of heavy metals (Cr, Cd, Pb and Fe) on fourteen samples of alum and ferric dewatered water treatment sludges was investigated in this chapter. The main conclusions were:

- i. DWSs can be used as effective adsorbent for heavy metals (Cr, Cd and Pb) removal from landfill leachate.
- ii. Langmuir, Freundlich and Temkin adsorption isotherm models fitted the adsorption data for Cr and Pb quite well, and Temkin model fitted the Cd data quite well too. However, low  $R^2$  values were obtained from the fit of the models to the Fe data, indicating that Fe removal was by precipitation rather than adsorption.
- iii. Adsorption capacities in  $\text{mg g}^{-1}$  as determined by the Langmuir model were between (0.01- 0.02) ;( 0.03- 0.16) and (0.01- 0.13), respectively for Pb, Cr and Cd, and these were generally found to be maximum at pH 4.
- iv. Kinetic data was well fitted with the pseudo first-order model for Pb, pseudo second-order model for Cr indicated that the rate-limiting step for Cr adsorption is chemisorption, while intraparticle diffusion model was more applicable to the kinetic behaviour of Cd.

# **Chapter 4**

## **Mechanistic study of Pb, Cr and Cd uptake by DWSs**

## 4.1 Introduction

This chapter investigates the heavy metal attenuation capabilities of fourteen dewatered waterworks sludges towards selected individual heavy metals found in landfill leachate (Pb, Cr and Cd). Adsorption is a major process responsible for attenuation of heavy metals contaminants in wastewater. Not only total content of heavy metals in sorbent are important for an estimation of environmental risk, but also information about the way the metals are bound is necessary as it can be used to predict the heavy metals availability, mobility and toxicity. Therefore, the study of adsorption mechanism is of utmost importance for the understanding of how heavy metals are transferred from a liquid mobile phase to the surface of a solid phase (Castaldi et al. 2015). Whilst dewatered waterworks sludges have been shown to have large surface areas and high affinity for heavy metals such as Cd, Cr, Cu, Hg, Zn, Pb and Se (Chiang et al. 2012), there are limited studies on the removal of heavy metals using dewatered waterworks sludges from various sources, at typical concentration found in landfill leachate, and their potential effectiveness at decreasing the solubility of divalent metal cations such as Pb, Cr and Cd. Likewise, the role of the inorganic and organic fractions of DWSs in the adsorption processes of metals is unknown. Moreover, the relation between physicochemical characterization of sludges and the removal mechanisms of these heavy metals is unclear. Therefore, the main objectives of this chapter are:

- 1) To Use principal component analyses (PCA) and canonical correlation analysis (CCA) to evaluate the relationship between physicochemical properties of different DWSs and heavy metals attenuation,
- 2) To study the nature of the interactions established between the metal ions and the surfaces of dewatered waterworks sludges, and
- 3) To ascertain the role of the inorganic and organic fractions of dewatered waterworks sludges in the metal attenuation processes.

---

Part of this Chapter has already been published as 'Attenuation of metal contamination in landfill leachate by dewatered waterworks sludges' - A. Mohammed; T. Al-Tahmazi; A.O. Babatunde, (2016), J Ecological Engineering, 94, 656-667.

## 4.2 Material and Methods

### 4.2.1 Total extraction carbon (TEC)

In order to investigate the role of organic matter on metal sorption dewatered waterworks sludges, total extractable carbon (TEC) was separated from the sludge samples using the protocol proposed by Ciavatta et al. (1990).

2 g of dewatered waterworks sludge was placed in a 150-mL centrifuge tube with 100 mL of 0.1 M sodium hydroxide plus 0.1 M  $\text{Na}_4\text{P}_2\text{O}_7$  (NaOH + PP). Nitrogen bubble was passed through the solution for 2 min and, the tube was plugged immediately. Thereafter, a rotary shaker was used for 2 h at 160 rpm at room temperature, then centrifuged at 13000 g for 20 min. After centrifugation and filtration through a 0.45- $\mu\text{m}$  Millipore filter using a vacuum pump, the sludge on the 0.45- $\mu\text{m}$  Millipore filter was collected, air dried and stored. A 25 mL of the extract (total extract, TE) was transferred into a centrifuge tube (usually 40 mL) and acidified to pH < 2 by adding a small volume (0.3-0.5 mL) of 50% sulphuric acid. This was centrifuged at 5000 g for 20 minutes, thereafter the precipitate (apparent humic substance, HS) was then collected and stored.

### 4.2.2 Sequential extraction of Pb, Cr and Cd sorbed by DWSs

Sequential extraction is an analytical process that chemically leaches metals out of sludge samples. The purpose of sequential extraction is to mimic the release of the selective metals into solution under various environmental conditions. One commonly used sequential extraction procedure is designed to partition different trace metals based on their chemical nature. In this study, the chemical forms of Pb, Cr or Cd bound to the dewatered waterworks sludges were determined using the sequential extraction procedure of Castaldi et al. (2015). The sludge samples saturated with Pb, Cr, and Cd at pH 4 (i.e. those deriving from the last point of the isotherms in Chapter 3 (3.2.2.2.1.)) were washed with 25 mL of distilled water, in order to remove the salts deposited in the sorbents, thereafter they were agitated for 2 mins. Washings were repeated three times.

Subsequently, the solid samples (0.1 g) were placed in 50 mL centrifugation tubes, treated with 25 mL of distilled water and shaken for 2 h to extract soluble metal (Castaldi et al., 2015). Samples were then treated with 25 mL of 0.1 N  $\text{Ca}(\text{NO}_3)_2$  to

extract the exchangeable phase, and subsequently with 25 mL of 0.02 M EDTA to extract the complexed phase (Castaldi et al., 2015). After each step of the extraction process, the samples were centrifuged at 7000 rpm for 10 min, filtered to completely separate the liquid and solid phases, and the content of Pb, Cr and Cd was analysed using inductively coupled plasma optical emission spectroscopy (ICP–OES).

The same procedures were repeated for the sludges after total extracted carbon.

### **4.2.3 FTIR spectroscopy**

Fourier transform infrared spectroscopy (FTIR) is a technique which is used to obtain an infrared spectrum of absorption or emission of a solid, liquid or gas. An FTIR spectrometer simultaneously collects high spectral resolution data over a wide spectral range. FTIR is an important technique in organic chemistry. It is an easy way to identify the presence of certain functional groups in a molecule. Also, one can use the unique collection of absorption bands to confirm the identity of a pure compound or to detect the presence of specific impurities.

The FTIR spectra of the HH- sludge (ferric sludge) samples were recorded at room temperature using a Shimadzu IR Affinity-1s spectrophotometer. The samples included HH sludge and HH sludge after total extracted carbon, doped and not doped with Pb, Cr or Cd at pH 4, together with humic substance (HS) extracted from HH (relative to the last point of the batch). The FTIR spectra were recorded in the 4000–500  $\text{cm}^{-1}$  range, and were collected after 320 scans at 4  $\text{cm}^{-1}$  resolution.

### **4.2.4 Statistical analysis**

Multivariate statistical analysis is a useful technique for identifying common patterns in data distribution, leading to a reduction of the initial dimension of data sets and facilitating its interpretation (Janos et al. 2004). In order to evaluate the relationship between physicochemical characterisation of the dewatered waterworks sludges and the maximum uptake of heavy metals by these sludges, correlation analysis, PCA and CCA were used.

All statistical analysis were performed using software package IBM SPSS 20.

#### **4.2.4.1 Principal component analyses**

PCA is widely used to reduce data and to extract a small number of latent factors (principal components, PCs) for analysing relationships among the observed variables.

PCA was used to obtain an overview of the relationships between the physicochemical characteristics of dewatered waterworks sludges. PCA was performed with Varimax rotation, while Pearson correlation coefficient, R, measures the strength of a linear relationship between two quantitative variables.

#### **4.2.4.2 Canonical correlation analysis**

Canonical correlation analysis is a multivariate statistical model that facilitates the study of linear interrelationships between two sets of variables. One set of variables is referred to as independent variable and the others are considered dependent variables (Hair et al. 2010).

CCA was applied to quantify correlations between maximum uptake of heavy metals (Pb, Cr and Cd) which is derived from the Langmuir model in Chapter 3 (3.3.3.2.1), and the principal components of physicochemical characteristics of dewatered waterworks sludges.

### **4.3 Results and Discussions**

#### **4.3.1 Sequential extraction**

Sequential extraction of Pb, Cr and Cd from DWS samples loaded with the HM using distilled water to extract soluble metal. Thereafter, using  $\text{Ca}(\text{NO}_3)_2$  to extract the exchangeable phase. Finally, using EDTA to extract the complexed phase before and after extract total carbon from DWSs is discussed below:

##### **4.3.1.1 Sequential extraction before total extraction carbon**

Fourteen samples of Fe and Al DWSs loaded with Pb, Cr and Cd were subjected to sequential extraction following the procedure proposed by Castaldi et al. (2015). The aim was to determine the pathway of their metal binding, thus allowing the prediction

of the metals' availability, mobility and toxicity. The metals' extraction efficiencies obtained with the single extraction procedures are presented in Figure 4.1a. The amount of Pb, Cr and Cd soluble in H<sub>2</sub>O were respectively 2%, 0.4-7.3% and 1-15.9% in Fe- based sludges; and 2-17%, 2-19% and 5-19.5% respectively in the Al- based sludges. The concentration of the water-soluble metals correlates with the dissolved organic matter, and this suggests the formation of soluble complexes between the dissolved organic matter and the heavy metals (Bradl 2004). The extractabilities of Pb and Cr obtained with Ca(NO<sub>3</sub>)<sub>2</sub> were generally lower than 4% of total metals sorbed, whilst 27% of the Cd was extracted by Ca(NO<sub>3</sub>)<sub>2</sub>. Such pattern seems not only governed by the charge density of divalent metals cations (especially for Cd), but also by the tendency of Pb and Cr to form inner sphere complexes with Fe- or Al-(oxy)hydroxides and organic matter (Garau et al. 2014).

The metal fractions which were not readily bio-available or leachable i.e. those extracted with EDTA, were in the ranked order Pb (71%) > Cd (35%) > Cr (30%) in Fe-sludges; and Cd (49%) > Pb (34%) > Cr (12.5%) in the Al-sludges. These high percentages extracted by EDTA may be because of the acidic condition of the experiment, where pH of initial solution was 4, as EDTA method was originally developed for acidic soils (Chen et al. 2009). Additionally, the metal cations are pushed out with the H<sup>+</sup> from certain kind of binding site by ion exchange mechanism (Janos et al. 2004).

The residual fractions of Pb and Cr in the dewatered waterworks sludges were high especially in the ferric sludge, reaching 85% and 99% respectively, whilst the range of non-extractable Cd ion from the two species of DWSs was between 28% and 80%. This indicates specific strong and irreversible adsorption. With the exception of WD, all the DWSs showed strong binding with the metal ions. This is due to the different interaction mechanisms involving organic and inorganic component of the DWSs. The high affinity of amorphous Fe- or Al- (oxy) hydroxide (inorganic fraction) to heavy metals may result in fixation into the micropore wall in subsurface (Axe and Trivedi 2002). For instance, the adsorption capacity of Fe- based sludges for Cr can reach up to 0.1M of Cr/ M of Fe at pH <5.5 (Zachara et al. 1987), reflecting the high capacity of Fe- based sludges to retain this metal ion since it has low solubility and high sorptive capacity (Kantar et al. 2013). On the other hand, there is a complexation reaction between metal ions and organic matter such as humic acids occurring in macro and/or micropores.

#### 4.3.1.2 Sequential extraction after total extraction carbon

Organic matter content can significantly influence metal solubility and bioavailability. To study the effect of organic fraction on the HM retention capacity of the water sludges, samples of DWSs doped with Pb, Cr and Cd were subjected again to sequential extraction after removal of total organic matter from the sludges. The main difference between DWSs before and after TEC is the decrease of water-soluble fraction and exchangeable metal (i.e. extraction with H<sub>2</sub>O and Ca(NO<sub>3</sub>)<sub>2</sub>) for Pb and Cd after TEC (Figures 4.1 b and 4.3 b), this confirms the formation of soluble Pb or Cd organic complex. Whilst there were increases of immobile fraction (i.e. extraction with EDTA) for both of these metals reaching up to 70% and 64% for Pb and Cd respectively. EDTA is a strong chelating reagent and can extract metals from DWSs (Bermond et al. 1998). However, the more striking difference between DWSs and DWSs after TEC was in Cr where no fraction was extracted with Ca(NO<sub>3</sub>)<sub>2</sub> and EDTA. This result can be due to the available number of inorganic sites, after extraction of the organic matter which can interact electrostatically with metal ions (Castaldi et al., 2015).

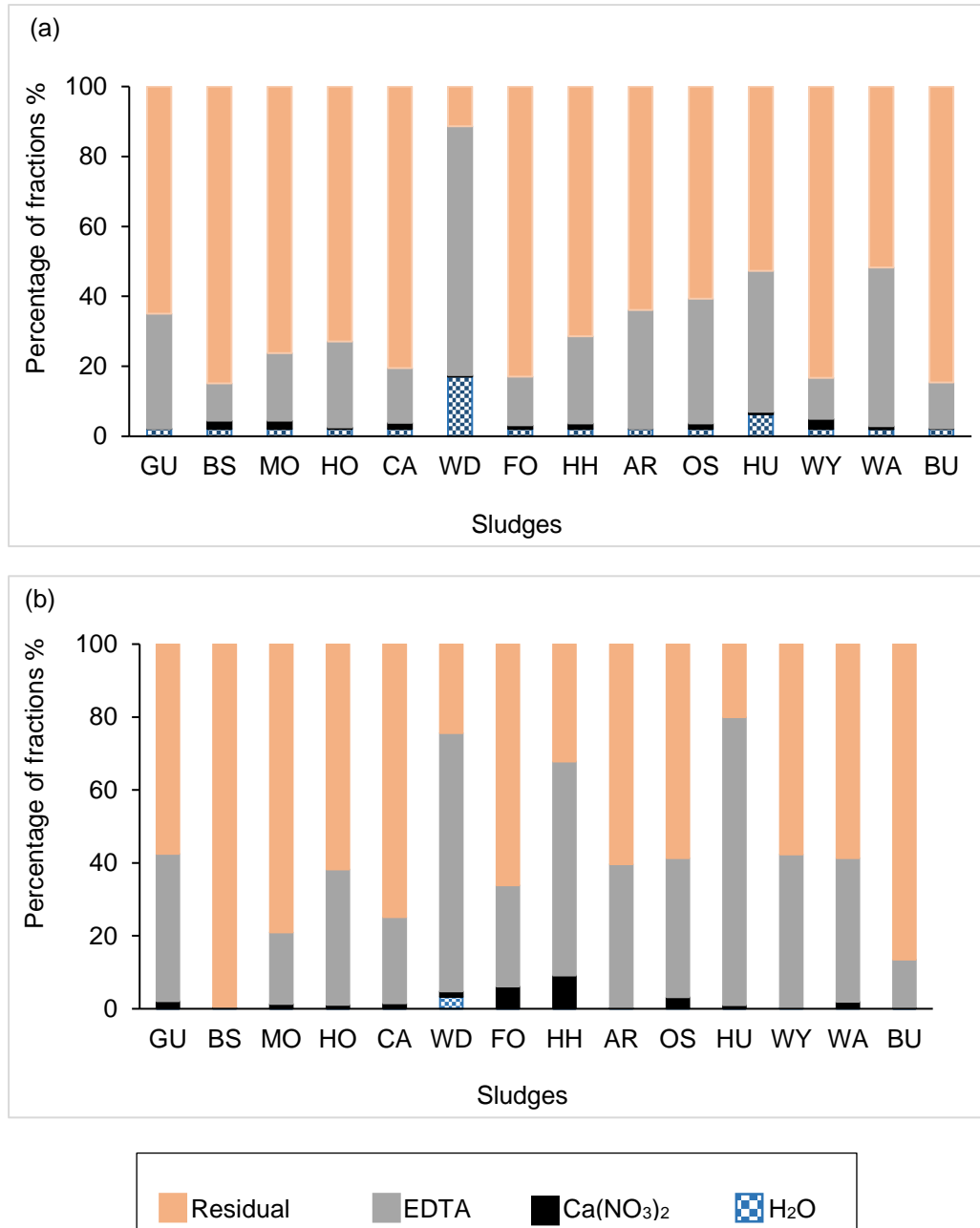


**Figure 4. 1 Percentage distribution of lead between various fractions determined by the sequence extraction test (a) before total extraction carbon (b) after total extraction carbon.**

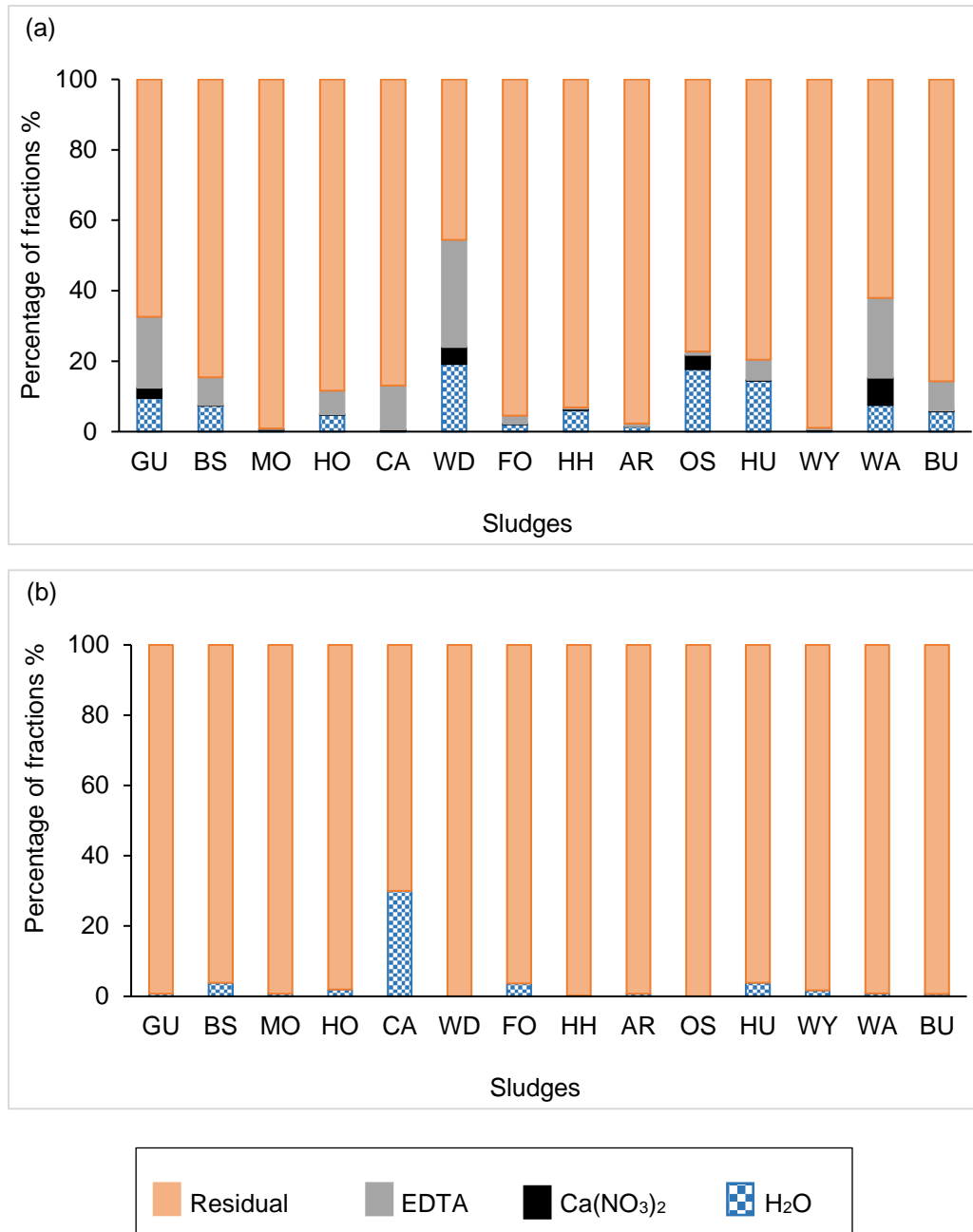


**Figure 4. 2 Percentage distribution of chromium between various fractions determined by the sequence extraction test (a) before total extraction carbon (b) after total extraction carbon.**

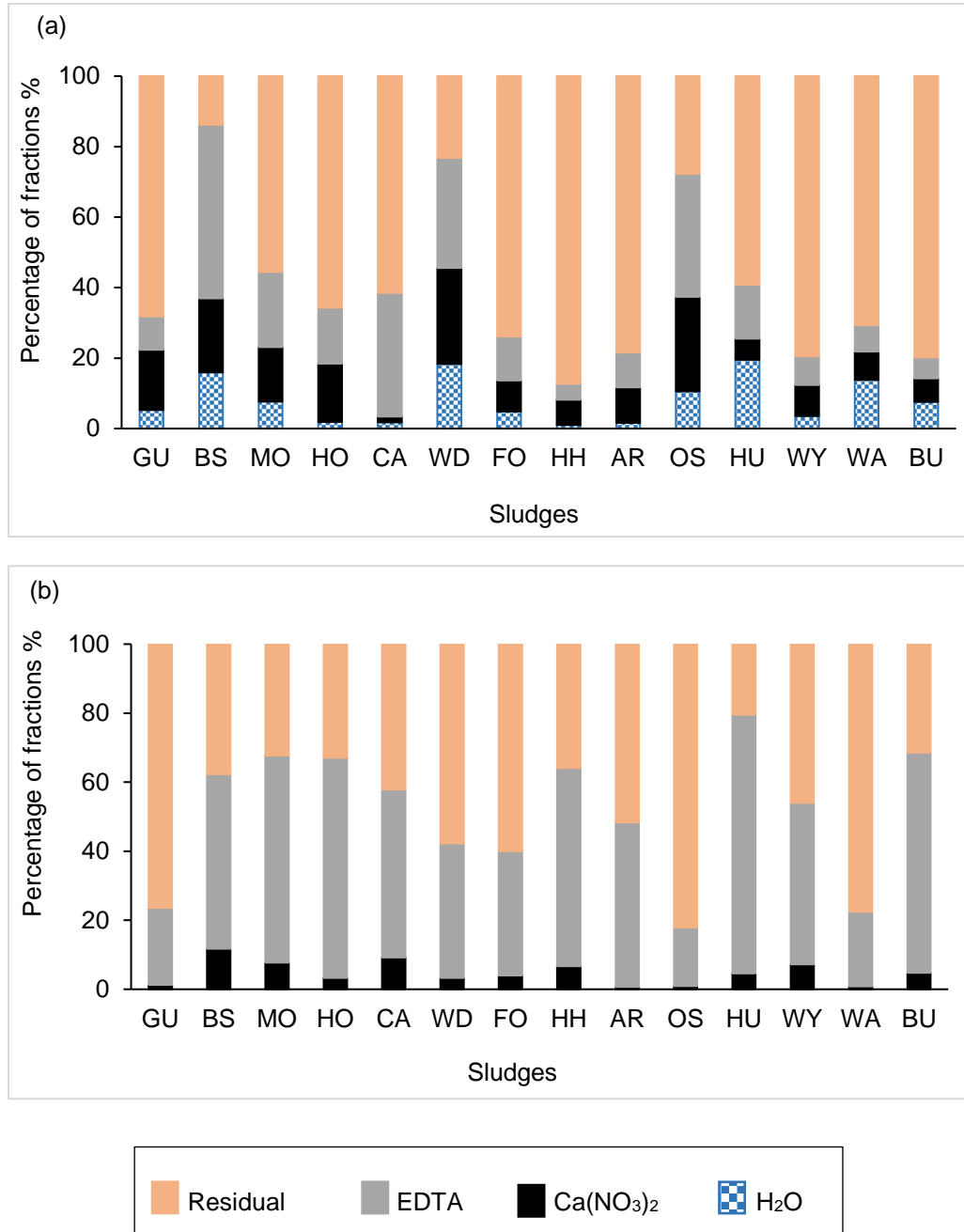


**Figure 4. 3 Percentage distribution of cadmium between various fractions determined by the sequence extraction test (a) before total extraction carbon (b) after total extraction carbon.**

## 4.3.2 FTIR spectroscopy

### 4.3.2.1 FTIR spectroscopy before total extracted carbon

To investigate the involvement of the organic and inorganic components of the HH dewatered waterworks sludge in the sorption process of the metal ions, HH- sludge loaded and not loaded with Pb, Cr and Cd were analysed, together with humic substances (HS) extracted by the sorbent through FTIR spectroscopy. The HH-sludge was chosen among the fourteen sludges because it had the highest adsorption capacity for the heavy metals studied, and so it can be used for practical application such as main media in constructed wetland. The FTIR spectra of HH sludge (Figure 4.4a) showed a broad band in the 3600–700  $\text{cm}^{-1}$  region, which could likely be the result of the superposition of several bands deriving from the heterogeneity of dewatered waterworks sludge which, as final residues of the water treatment process, they would incorporate organic and inorganic substances. From Figure 4.4 a, the broad band as derived from the FTIR spectra of the humic substances can be considered as the result of the overlapping of a band at  $\sim 1610 \text{ cm}^{-1}$  which refers to C=O stretching of carboxylic group ( $\nu_{asCOO^-}$ ) (Lambert et al. 1987). Moreover, the band at  $\sim 1400 \text{ cm}^{-1}$  referred to COO<sup>-</sup> group in carboxylic acid salts ( $\nu_{sCOO^-}$ ) (Lambert et al. 1987). The FTIR spectra of the HH- sludge doped with Pb, Cr and Cd showed a shift and an increase of the intensity of bands in the  $\sim 1610 \text{ cm}^{-1}$  and  $\sim 1400 \text{ cm}^{-1}$  which are attributable respectively, to the asymmetric and symmetric stretching of the carboxylate group of the humic fraction as reported above.

The difference between the frequencies of  $\nu_{asCOO^-}$  and  $\nu_{sCOO^-}$  ( $\Delta\nu$ ) gives useful information about the type of interaction between the carboxylate groups and the metal ions (Castaldi et al. 2015). If the  $\Delta\nu$  value of the complex is lower than that recorded for the HS, a bidentate chelating mode can be assumed; while a monodentate chelating mode is proposed if the  $\Delta\nu$  of the complex is higher than that of the HS (Castaldi et al., 2010). A  $\Delta\nu$  value of 198, 187 and 180 is measured for the spectra of HH- sludge doped with Pb, Cr and Cd respectively, and 204 for the extracted HS. These values of  $\Delta\nu$  suggest a bidentate chelating mode of these HM with the carboxylate groups of the HS.

The band at  $\sim 1660\text{ cm}^{-1}$  which refers to the OH bending mode of  $\text{H}_2\text{O}$  associated with the Fe surface (Castaldi et al. 2015) disappeared after heavy metals adsorption. On the other hand, the peaks attributed to the Si–O–Si antisymmetric stretch at  $1107\text{ cm}^{-1}$  and  $1036\text{ cm}^{-1}$  overlapped into one sharp peak at  $\sim 1020\text{ cm}^{-1}$  (Lambert et al. 1987); this suggests that silica develops a negative charge on the sludge and this contributes to adsorption of the HM.

The peak attributed to sulfonyl chlorides (C–S stretch) in the HH- sludge reduced and shifted from  $754\text{ cm}^{-1}$  to  $777\text{ cm}^{-1}$ ,  $743\text{ cm}^{-1}$  and  $748\text{ cm}^{-1}$  respectively, after Pb, Cr and Cd adsorption. This indicates that sulfonyl halide groups participates in the heavy metals adsorption (Lambert et al. 1987). Figure 4.4 a also showed a sharp band in the HH- sludge at  $2972\text{ cm}^{-1}$  which was caused respectively by the asymmetric vibration of –CH and the symmetric vibration of –CH (Cheng et al. 2015). This band disappeared after HM adsorption suggesting that metal ions could form surface complexes with aliphatic compounds. Finally, the intensity of the broad band of the –OH stretching vibration at the wavenumber  $\sim 3250\text{ cm}^{-1}$  in HH- sludge decreased due to the HM adsorption (Lambert et al. 1987).

#### 4.3.2.2 FTIR spectroscopy after total extracted carbon

The FTIR spectra of HH- sludge after TEC, loaded and not loaded with Pb, Cr and Cd were very similar to those of amorphous Fe-hydroxides (Goldberg and Johnston 2001) (Figure 4.4 b). The broad band at  $2160\text{ cm}^{-1}$  decreased and shifted to  $2156\text{ cm}^{-1}$ ,  $2156\text{ cm}^{-1}$  and  $2181\text{ cm}^{-1}$  after Pb, Cr and Cd adsorption respectively. This suggests that the asymmetric stretch of N in azides group contributed to the adsorption of these heavy metals (Lambert et al. 1987). The strong band  $\sim 1560\text{ cm}^{-1}$  assigned to the  $\text{NO}_2$  in aliphatic nitro compounds group (Lambert et al. 1987), shifted to lower frequencies  $1553\text{ cm}^{-1}$ ,  $1584\text{ cm}^{-1}$  and  $1539\text{ cm}^{-1}$  respectively after the sludge was loaded with Pb, Cr and Cd. A wave number  $\sim 890\text{ cm}^{-1}$  bending mode assigned to Fe surface and to the stretching vibrations of FeOOH (Balasubramaniam and Kumar 2000) shifted to  $907\text{ cm}^{-1}$  after Cd sorption, suggesting the involvement of the Fe–O and OH stretching sites in the coordination of Cd. The HH- sludge loaded with Cr showed increase in vibrational frequencies at band  $\sim 3600\text{ cm}^{-1}$ -  $3900\text{ cm}^{-1}$ , and this suggests that the –OH groups in alcohols and phenols (OH stretch mode) participated in the Cr adsorption (Lambert et al. 1987).

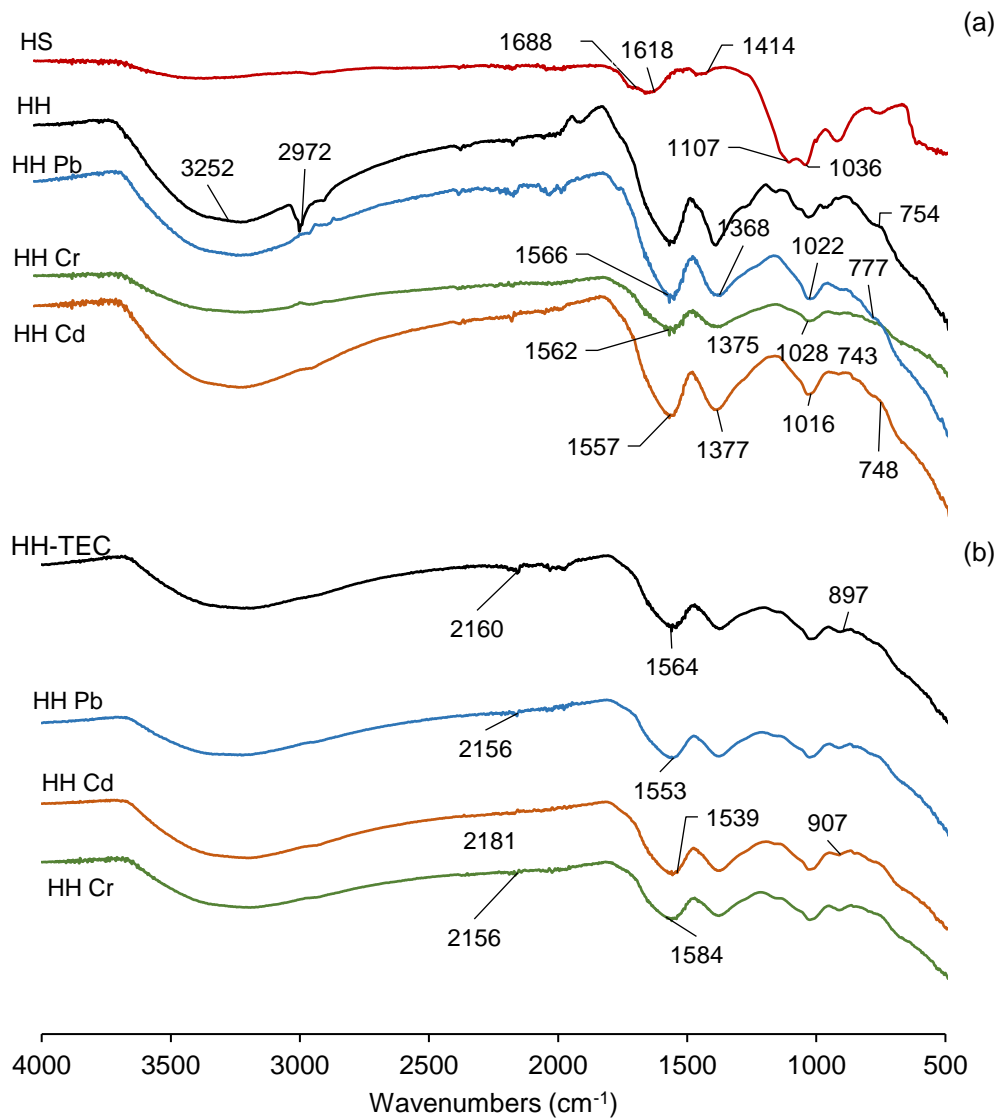


Figure 4. 4 FTIR spectra of HH dewatered waterworks sludge (a) before and (b) after total carbon extraction loaded ad not loaded with Pb, Cr and Cd at pH 4.

### 4.3.3 Statistical analysis

#### 4.3.3.1 Principal component analysis

Pearson's correlation coefficients for the physicochemical characteristics of the sludges are presented in Table 4.1. The highest positive correlation pairs of total carbon and organic carbon (TC-OC (1.0)) at 95% confidence level indicates that most of the total carbon in the sludges is organic carbon. The other high correlation pairs were oxalate aluminium and aluminium (Al-Oxl-Al (0.973)), and oxalate iron and iron (Fe-Oxl-Fe (0.986)). These high correlations may be due to the fact that 85% of the total Al in the Al-sludges is oxalate Al, whilst 53% of the total Fe in the Fe-sludges is oxalate Fe (table 1). The pairing of Fe-SO<sub>4</sub> (0.83) and Al-SO<sub>4</sub> (-0.756) suggests a common origin, such as using aluminium and iron sulphate as coagulants during the water purification process. The pairings between aluminium and specific surface area (Al-SSA (0.726)); and iron and specific surface area (Fe-SSA (-0.642)) relates to the Al and Fe hydroxides in the sludges, and this is mainly due to the amorphous nature of the sludges resulting in relatively high surface areas.

By extracting the eigenvalues and eigenvectors from the correlation matrix, the number of significant factors and the percentage of variance explained by each of them were calculated and the results are presented in table 5. The results in table 5 showed that only two eigenvalues were >1.00 and they both explain 79.9% of total variance.

Table 6 shows the two factor loadings with a varimax rotation. The first factor (PC1) explains about 54.8% of the total variance and loads heavily on Fe-Oxl, Fe, Al-Oxl, Al, SSA, pH and SO<sub>4</sub>. The source for this factor may be coagulants used during the water treatment processes. The second factor (PC2) is loaded primarily by TC and OC, and this can be adduced to impurities attached to the suspended particles in the raw water. This factor accounted for 25.1% of the total variance.

#### 4.3.3.2 Canonical component analysis

When performing the CCA, two PCs each from the predictor variables (i.e the physicochemical characteristics of the sludges) and the predicted variable (i.e. the maximum uptake of heavy metals at pH 4 from unpublished data) were used. The result showed high correlation between PC1 and maximum uptake of Cd (0.93). This

result indicates that the sorption of Cd could be by Fe- or Al-(oxy) hydroxides and this is in agreement with similar study by Janos et al. (2004). The authors found that most of the Cd was bound to Fe oxides when sequential extraction was used to extract heavy metals from the iron humate. The second higher correlation was between PC2 and maximum uptake of Cr (-0.64) followed by maximum uptake of Pb (0.46). These indicate that the adsorption of these heavy metals is influenced by the presence of organic carbon. In a study by Bradl (2004), it was shown that the adsorption of Cr and Pb increased with an increase in the organic matter in the soil, whilst the presence of dissolved organic carbon could restrict the adsorption of Cd.

**Table 4. 1 Correlation matrix for the physicochemical characterization of the DWSs.**

Element	TC	SSA	pH	pH <sub>pcz</sub>	OC	Al	Fe	Al-Oxl	Fe-Oxl	SO <sub>4</sub>	Mn
TC	1.000	-0.355	-0.293	-0.481	1.000	0.003	-0.046	0.030	0.058	-0.411	-0.306
SSA		1.000	0.451	0.443	-0.362	0.726	-0.642	0.672	-0.674	-0.352	-0.296
pH			1.000	0.866	-0.300	0.735	-0.714	0.730	-0.762	-0.580	-0.111
pH <sub>pcz</sub>				1.000	-0.488	0.491	-0.553	0.465	-0.635	-0.270	-0.208
OC					1.000	-0.006	-0.036	0.021	0.068	-0.403	-0.301
Al						1.000	-0.892	0.973	-0.892	-0.756	-0.208
Fe							1.000	-0.854	0.986	0.830	0.358
Al-Oxl								1.000	-0.849	-0.750	-0.184
Fe-Oxl									1.000	0.745	0.304
SO <sub>4</sub>										1.000	0.418
Mn											1.000

Table 4. 2 Principal component analysis of physicochemical characterisation of DWSs (n=14).

Component	Initial Eigenvalues			Extraction Sums of Squared Loadings			Rotation Sums of Squared Loadings		
	Total	% of Variance	Cumulative %	Total	% of Variance	Cumulative %	Total	% of Variance	Cumulative %
1	6.030	54.820	54.820	6.030	54.820	54.820	6.030	54.816	54.816
2	2.759	25.083	79.903	2.759	25.083	79.903	2.760	25.087	79.903
3	0.907	8.246	88.149						
4	0.769	6.899	95.137						
5	0.230	2.090	97.227						
6	0.178	1.616	98.843						
7	0.086	0.784	99.627						
8	0.023	0.209	99.836						
9	0.017	0.156	99.992						
10	0.001	0.007	100.000						
11	1.513E-005	0.000	100.000						

Extraction method: principal component analysis.

**Table 4. 3 Varimax rotated loadings for the dewatered waterworks sludges**

(N=14)

	Principal Component	
	1	2
<b>Fe-Oxl</b>	-0.961	
<b>Fe</b>	-0.953	
<b>Al</b>	0.945	
<b>Al-Oxl</b>	0.919	
<b>pH</b>	0.843	
<b>SO<sub>4</sub></b>	-0.781	-0.517
<b>SSA</b>	0.732	
<b>pH<sub>pcz</sub></b>	0.684	-0.483
<b>TC</b>		0.979
<b>OC</b>		0.977
<b>Mn</b>	-0.345	-0.407

Extraction Method: Principal Component Analysis. Rotation Method: Varimax with Kaiser Normalization.

#### 4.4 Conclusion

The mechanism of HM (Pb, Cr and Cd) attenuation by fourteen samples of alum and ferric DWSs was investigated in this chapter using sequential extraction, FTIR spectra and statistical analysis (PCA and CCA). The main conclusions were:

(i) The sequential extraction procedure showed that low concentrations of the HM sorbed by DWSs were in the form of water-soluble and exchangeable fractions, while the greatest concentrations of the metals sorbed were strongly bound and would not be expected to be readily released under natural conditions.

(ii) The FTIR spectra of HH- sludge doped with Pb, Cr and Cd suggested a predominant bidentate chelating mode for these HM with the carboxylate groups of the humic substances.

(iii) The correlation analysis, PCA and CCA showed high correlation between Cd uptake and Fe- or Al-(oxy) hydroxide while Cr and Pb uptake correlated with organic carbon.

# **Chapter 5**

**General performance and  
design of a novel engineered  
wetland system for landfill  
leachate treatment**

## 5.1 Introduction

Landfill leachate is highly contaminated with organic contaminants, ammonia and HM. The presence of HM and OM at high concentrations in landfill leachate usually causes toxic effects to microbes and inhibits ammonia oxidation (Metcalf 2003; Sun et al. 2005). In most cases, the evaluation of the treatment potential of CWs is focussed separately on biodegradable organic matters and nutrients on the one hand, and toxic pollutants on the other, without considering the effect of the presence of the latter type of pollutants on the removal efficiency of the former. Little work has been carried out to date to investigate the effect of HM on the removal efficiency of biodegradable pollutants in CWs.

Aluminium- sludge based CW tidal flow presents a recent development in treatment wetlands. Initiated at University College Dublin (UCD), aluminium- sludge based CW tidal flow uses dewatered alum sludge as the main wetland medium instead of the generally applied medium-gravel (Babatunde et al. 2007; Zhao et al. 2008). However, the results from Chapters 3 and 4 show that HH sludge (ferric-based sludge) can serve as the sorbent for HM adsorption which is not expected to be readily released under natural conditions, therefore it can be used for engineering applications, such as constructed wetlands.

Tidal flow operation greatly enhances the oxygen transfer into the wetland matrix, and this enables the CWs to achieve effective nitrification under a high nitrogen-loading rate, such as those for found in landfill leachate treatment.

In addition, anoxic conditions can be established to prolong HM- ferric-based sludge contact and which favours the adsorption process on the one hand, and the denitrification process on the other hand. Therefore, objectives of this chapter are:

1. To assess the overall performance of ferric- sludge based CWs for HM, OM, and nitrogen removal and of the impact of their relative concentrations.

---

Part of this Chapter has already been published as 'Understanding Integrated Removal of Heavy Metals, Organic Matter and Nitrogen in a Constructed Wetland System Receiving Simulated Landfill Leachate' by A. Mohammed; A. Babatunde, International Journal of Environmental, Chemical, Ecological, Geological and Geophysical Engineering, Presented at the Conference on ICWTWQ 2017, Dubia, Volume 11, Issue 4, April 2017, 279- 285. **(This paper was selected as the best paper in the conference)**

2. To evaluate the effect of high pollutant-loading rate and different operational conditions (anoxic condition and aerobic condition) on the treatment performance.

## 5.2 Materials and Methods

### 5.2.1 System configuration

Experiments were conducted in two periods. The first period, which lasted for 220 days, consisted of four stages while the second period, which lasted for 185 days, consisted of the same four stages as period 1 in addition to column B, which was added to enhance the operation of system this is discussed further in 5.5.3. A photograph of the outdoor setup at Cardiff University School of Engineering is shown in Figure 5.1.

The CWs were operated as sub-surface vertical down-flow systems, and different operating conditions were applied depending on the variables that each individual unit was being used to investigate (see Tables 5.1 and 5.2).

**Table 5. 1 Operating scheme for the first period constructed wetland system.**

Stages	Input points	Distribution ratio (%)	Cycle time (h)	Wet/dry (h)
Stage A	Influent	100	4	3.83 : 0.17
Stage C	Stage A	100	4	1.00 : 3.00
Stage D	Stage C, Effluent	50:50	4	1.00 : 3.00
Stage E	Stage D	100	4	3.90: 0.10

**Table 5. 2 Operating scheme for the second period constructed wetland system.**

Stages	Input points	Distribution ratio (%)	Cycle time (h)	Wet/dry (h)
Stage A	Influent	100	4	3.83 : 0.17
Stage B	Stage A	100	4	3.83: 0.17
Stage C	Stage B	100	4	1.00 : 3.00
Stage D	Stage C, Effluent	50:50	4	1.00 : 3.00
Stage E	Stage D	100	4	3.90: 0.10



**Figure 5. 1** Constructed wetland system showing: (1) first period of operation on the left, and (2) second period of operation on the right.

### 5.2.1.1 Perspex columns

Each stage consist of a single lab-scale CW constructed with Perspex columns of 100 mm in diameter and 1100 mm in height. The pipes were sealed off at one end with a plastic cap, thus providing the base of the CW. A main outlet valve was fitted on the base in the centre of the sealed end, and four more valves were fitted along the length of the media in the pipe every 15 cm, 10 cm from the top of the media, to allow wastewater samples to be taken at different depths. An additional three holes were fitted for media (ferric sludge) to be taken if required at depths of 15 cm, 30 cm and 45 cm from the bottom of the CW. A schematic of a single CW can be seen in Figure 5.2.

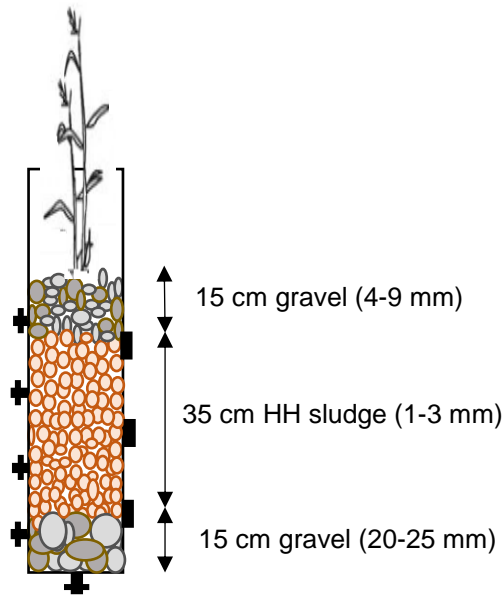


**Figure 5. 2 Schematic of a single Stage CWs for the landfill leachate treatment**

### 5.2.1.2 Media and plants

Ferric-based sludge is a by-product that can be used as an adsorbent for HM removal from landfill leachate. It is low cost and easily available worldwide, and it is generated during the drinking-water treatment process. The HH-sludge used in this study is primarily composed of Fe oxy-hydroxides, which are often amorphous species, and it contains sediment and humic substances from the raw water. HM are one of the major pollutants in landfill leachate, and they can affect the removal other pollutants, such as organic matter and ammonia. In addition, HH-sludge has been shown to have a high affinity and strong bonding toward selected HM (Pb, Cr and Cd) found in landfill leachate (Chapters 3 and 4). Therefore, HH-sludge was selected as the main medium for the CWs in this study.

The columns were filled with  $22\pm 3$  mm round gravel to a depth of 150 mm as a drainage layer. Air-dried HH-sludge (particle size 1-3 mm) was used as the main medium layer (350 mm), followed by  $7\pm 2$  mm washed gravel with a depth of 150 mm, giving an average porosity value of 0.43. The gravel layer (150 mm top layer) was employed to enhance air diffusion to the second layer (ferric-based sludge). Zhao et al. (2004c) reported that the coarse layer can provide relatively wide pore channels to

allow the rapid and strong diffusion of O<sub>2</sub> during the tidal flow operation strategy. This strong O<sub>2</sub> flux may enhance pollutant removal. Moreover, this layer facilitates the distribution of wastewater and the growth of plants.

*Phragmites australis*, known as common reed, was planted on the top layer of each stage, and good growth with lush vegetation was observed after 2 months. *Phragmites australis* is used as it is the main reference plant for CWs in Europe (Brix 1994; Sun et al. 2005; Kadlec and Wallace 2008). This plant can withstand extreme environmental conditions, including the presence of toxic contaminants, such as HM and nutrients (Baldantoni et al. 2004; Quan et al. 2007). Therefore, the plant was selected to be used in the CWs.

### 5.2.2 Synthetic wastewater

In order to minimize variability in the experiment, all systems in this study were fed with synthetic landfill leachate, which was prepared using C<sub>2</sub>H<sub>3</sub>NaO<sub>2</sub> and (NH<sub>4</sub>)<sub>2</sub>SO<sub>4</sub> for COD and NH<sub>4</sub> respectively, and CdSO<sub>4</sub>· $\frac{8}{3}$ H<sub>2</sub>O salt, Cr(SO<sub>4</sub>)<sub>2</sub>·12H<sub>2</sub>O salt, FeSO<sub>4</sub>·7H<sub>2</sub>O and PbCl<sub>2</sub> salt, respectively for Cd, Cr, Fe (II) and Pb dissolved in tap water. Artificial landfill leachate was synthesised in the laboratory to simulate young landfill leachates in the UK, as identified in the literature review (see Table 2.1)

Several pollutants were not selected for the experiment due to the lack of data regarding their typical concentrations in landfill leachate in the UK, for example phosphorus.

### 5.2.3 System operation

The wetland system consisted of four stages in the first period and five stages in the second period. The system was operated under the anoxic conditions and tidal flow strategies.

Four parallel laboratory scale CWs (A, C, D and E) were operated under different operating conditions for 220 days in the first period, this started from 10 May 2015 to 20 December 2015. Cycles of wet/dry periods were generated by a peristaltic pump (333.33 mL min<sup>-1</sup>) and controlled by a timer. Synthetic wastewater was batch loaded to the first stage and sequentially passed through the other stages, generating wet/dry periods in the individual stages. About 2 litres of synthetic wastewater was pumped

into the system in each cycle, giving 12 litres per day going into the system. Before starting the experiment and loading the synthetic wastewater, the system was inoculated with activated sludge obtained from a local municipal wastewater treatment plant to let the bacterial communities become attached to the media (HH-sludge).

Anoxic conditions were employed for stages A and E. This enabled prolonged HM-ferric-based sludge contact in stage A, and it enhanced the denitrification process in stage E. The wet period started as the wastewater began to fill the column, whereas the dry period was between the wastewater being pumped to the next stage, according to the settings of the timer, and a new batch of wastewater arriving from the preceding stage. The wet period for anoxic conditions was 3 hours and 50 minutes, giving a 10-minute unsaturated period for stage A while for stage E, the wet period was 3 hours and 54 minutes.

The tide, that is cycles of wet/dry periods, was generated in stages C and D. The cycle was set to take place every 4 hours, giving each wetland 1 hour of wastewater-media contact and 3 hours of aeration in each cycle. Air was drawn into the porous space of the wetland from the top when the wastewater began to drain until the wetland was completely drained during the wet/dry cycle of the tidal flow operation. In addition, the recirculation (recirculation flow rate: feed flow rate) from the effluent tank to stage D at a ratio of 1:1 was employed (Tables 5.1 and 5.2). Kantawanichkul & Neamkam (2003) found that this ratio (1:1) is optimum to allow the highest nitrogen removal.

The second period (185 days) started from 20 December 2015 to 26 June 2016. As it will be explained in more detail later in section 5.3.2, a clogging problem was encountered during this period in stage C, therefore an additional stage (column) was added to the system as a second stage (B) to enhance the removal of HM through the media (Figure 5.1). When the clogging phenomenon occurs, the active void volume of the medium is blocked, resulting in a reduction in the infiltration rate. Consequently, the O<sub>2</sub> supply is reduced and the treatment efficiency decreases.

#### **5.2.4 Sampling and process**

Inflow and outflow sampling were conducted once per week. Weekly sampling was sufficient to conduct a comprehensive analysis due to the extensive period of time over which the experiment was run. Inflow sampling was conducted from the feed

tank, while outflow samples were taken from the outlet at the bottom of each stage. Additional, samples were collected from the effluent tank.

The parameters measured were chemical oxygen demand (COD), total nitrogen (TN), ammonium-nitrogen ( $\text{NH}_4\text{-N}$ ), nitrite-nitrogen ( $\text{NO}_2\text{-N}$ ), nitrate-nitrogen ( $\text{NO}_3\text{-N}$ ), Fe, Pb, Cd, Cr, pH, dissolved oxygen (DO) and temperature T.

In-situ measurements were taken for DO, pH and temperature from four collection points (i.e. from each valve on the column), as shown in Figure 5.2, while all other pollutant concentrations were determined in the laboratory using the samples taken at the time of dosing (for influent) or release (for effluent). Samples were collected in 300 mL polyethylene bottles. For metal analysis, 40 mL volumes were acidified with nitric acid and stored at  $<4^\circ\text{C}$ , as recommended in the standard methods (APHA 2012).

Measurements for DO, pH and temperature were recorded using a HANNA HI 991301 probe. HM were determined using an Optima 210 DV ICP OES while COD, TN,  $\text{NH}_4\text{-N}$ ,  $\text{NO}_2\text{-N}$  and  $\text{NO}_3\text{-N}$  concentrations were measured with a Hach Lange DR3900 benchtop spectrophotometer.

COD, TN and  $\text{NH}_4\text{-N}$  were measured using Hach Lange's cuvette tests, for which all the required analytical reagents are provided, along with vessels for analysis. Digestion at  $148^\circ\text{C}$  and  $100^\circ\text{C}$  was required, respectively for COD and TN prior, by using a Hach Lange LT-200 thermostat.  $\text{NO}_2\text{-N}$  and  $\text{NO}_3\text{-N}$  were determined using powder pillow reagents (diazotization and cadmium reduction methods, respectively).

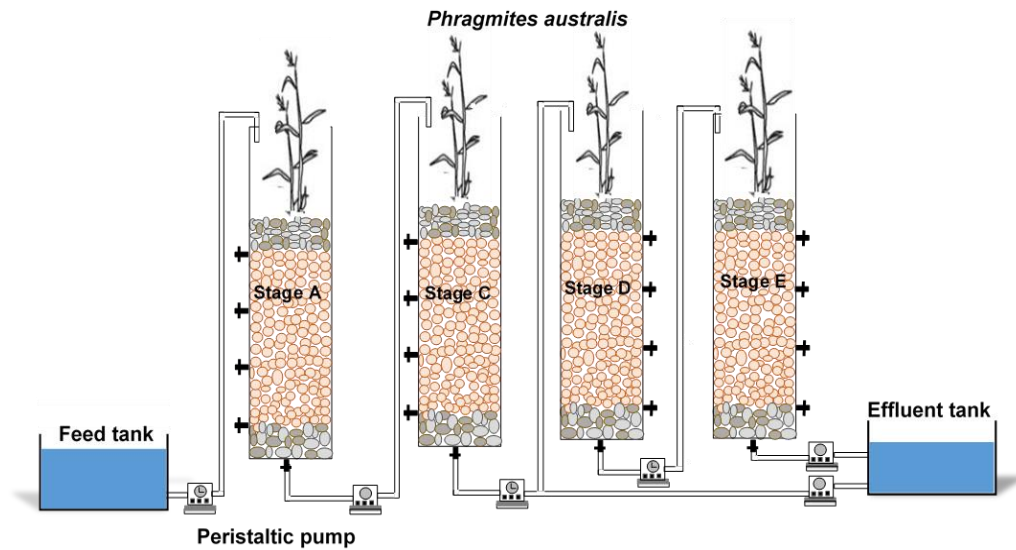


Figure 5. 3 Schematic of CWs in first period (0-220 days)

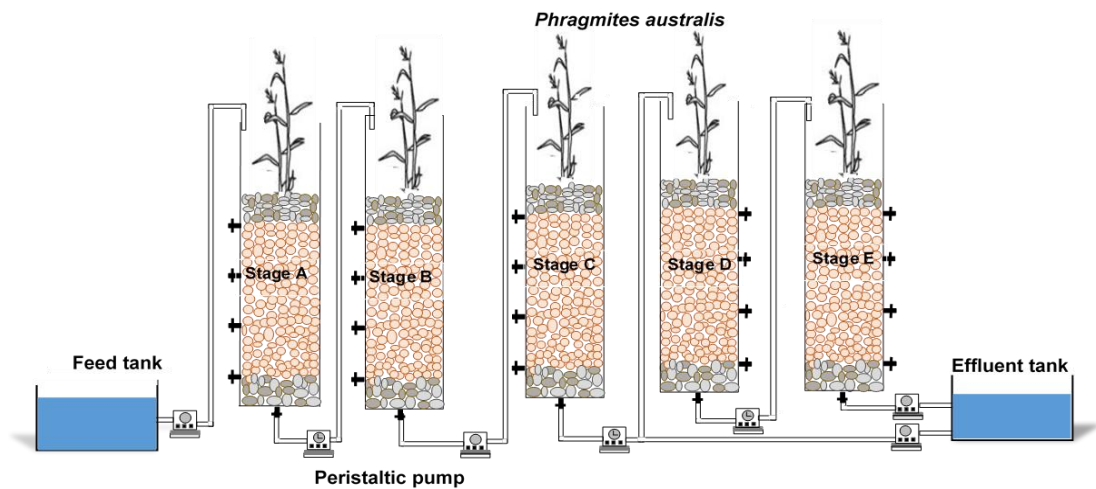


Figure 5. 4 Schematic of CWs in second period (220-405 days)

## 5.3 Results and Discussion

### 5.3.1 Overall performance of CWs

The experiment was carried out over 14 months (from May 2015 to July 2016) including the start-up period, and it was divided into two periods.

The overall treatment performance under different conditions i.e., anoxic conditions (stage A, B and E) and tidal flow (stage C and D), is summarized in Figure 5.5 and 5.6, while the mean influent and effluent of the parameters and pollutant concentrations from each stage are represented in Tables 5.3 and 5.4 for period 1 and period 2 respectively. From these Tables, the average values for pH were between 6.52 and 7.88 for period 1 and between 6.42 and 7.58 for period 2. These pH values indicate that the wastewater was slightly alkaline. The organic matter degradation, nitrification and denitrification processes were affected by temperature values, which in this study remained at around 15°C (Tables 5.3 and 5.4). Not only did temperature affect these processes, but also these process were affected DO concentrations. The influent DO concentrations in this study were in the range of 0.85 mg L<sup>-1</sup>- 5.67 mg L<sup>-1</sup> in period 1, and 0.83 mg L<sup>-1</sup>- 6.26 mg L<sup>-1</sup> in period 2.

The results show that the HM studied were effectively removed in the CWs; however, the removal efficiency was more pronounced in stage A reaching 62%, 75% and 66%, for Pb, Cr and Cd respectively in period 1; and 74%, 71% and 72% for Pb, Cr and Cd respectively in period 2. Fe was totally removed in the influent tank by the oxidation/precipitation basins' technique where the wastewater was left for 24 h in an open influent tank, in order to provide aeration for iron precipitation as recommended by Kadlce and Wallace (2008). The overall removal efficiency of COD across the four stages was significant; however, there was a sharp decline in COD removal efficiency in period 1 between days 80 and 100 due to clogging. Figures 5.6 also show that the pollutant removal was almost stable in period 2. Tables 5.3 and 5.4 show clearly that a significant reduction in NH<sub>4</sub>-N was achieved during the operation of the system, especially in stage D in the first and second period, when the 1:1 recirculation was employed. Moreover, there was evidence of nitrification taking place, as the values of nitrite and nitrate in the wastewater increased, as shown in Tables 5.3 and 5.4. Denitrification processes occurred simultaneously with nitrification in all stages, and especially in stage E in both periods in the CWs.

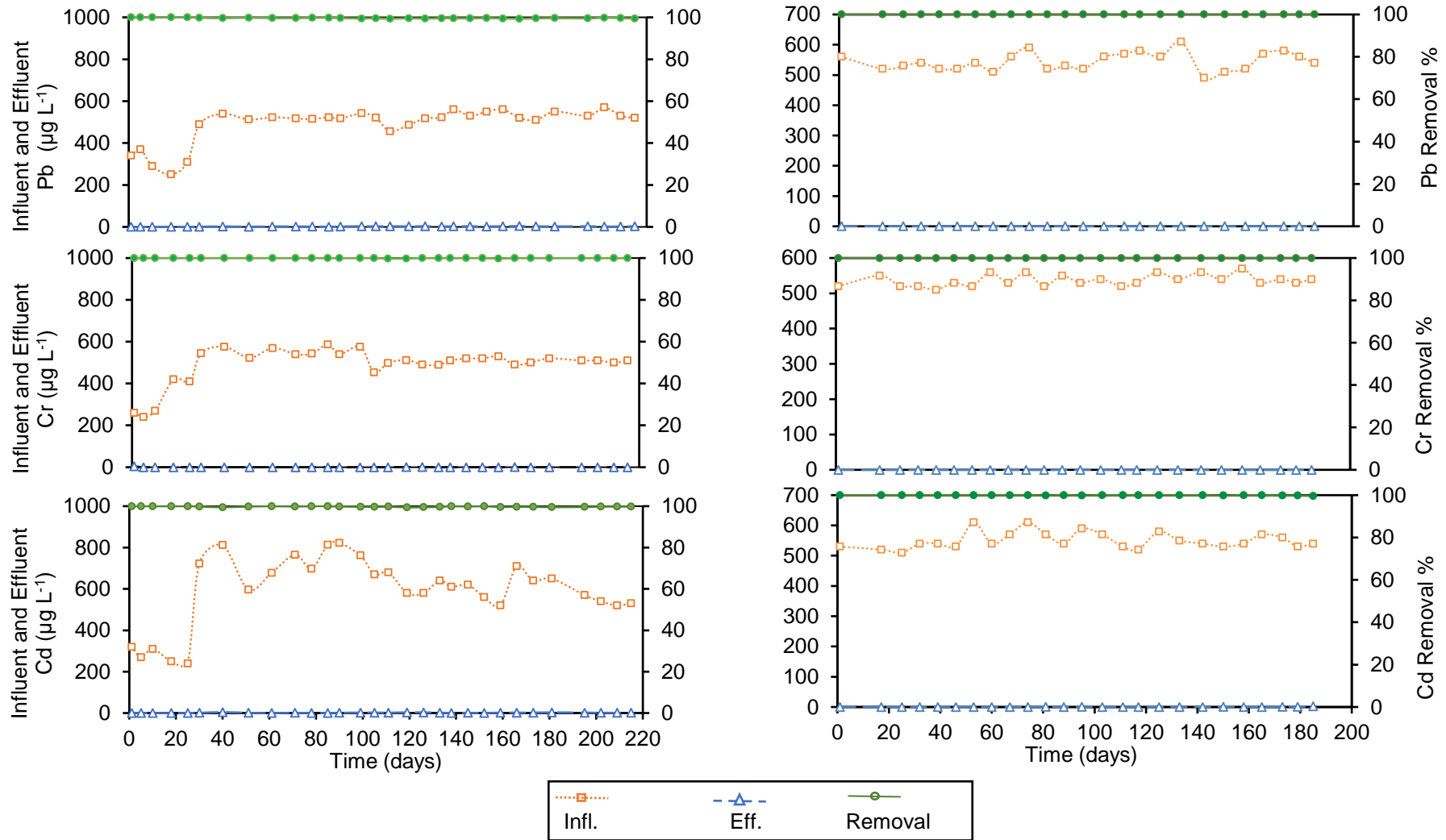


Figure 5. 5 Dynamics of HM concentrations in the influent and effluent and HM removal in CWs during period 1 to the left and period 2 to the right.

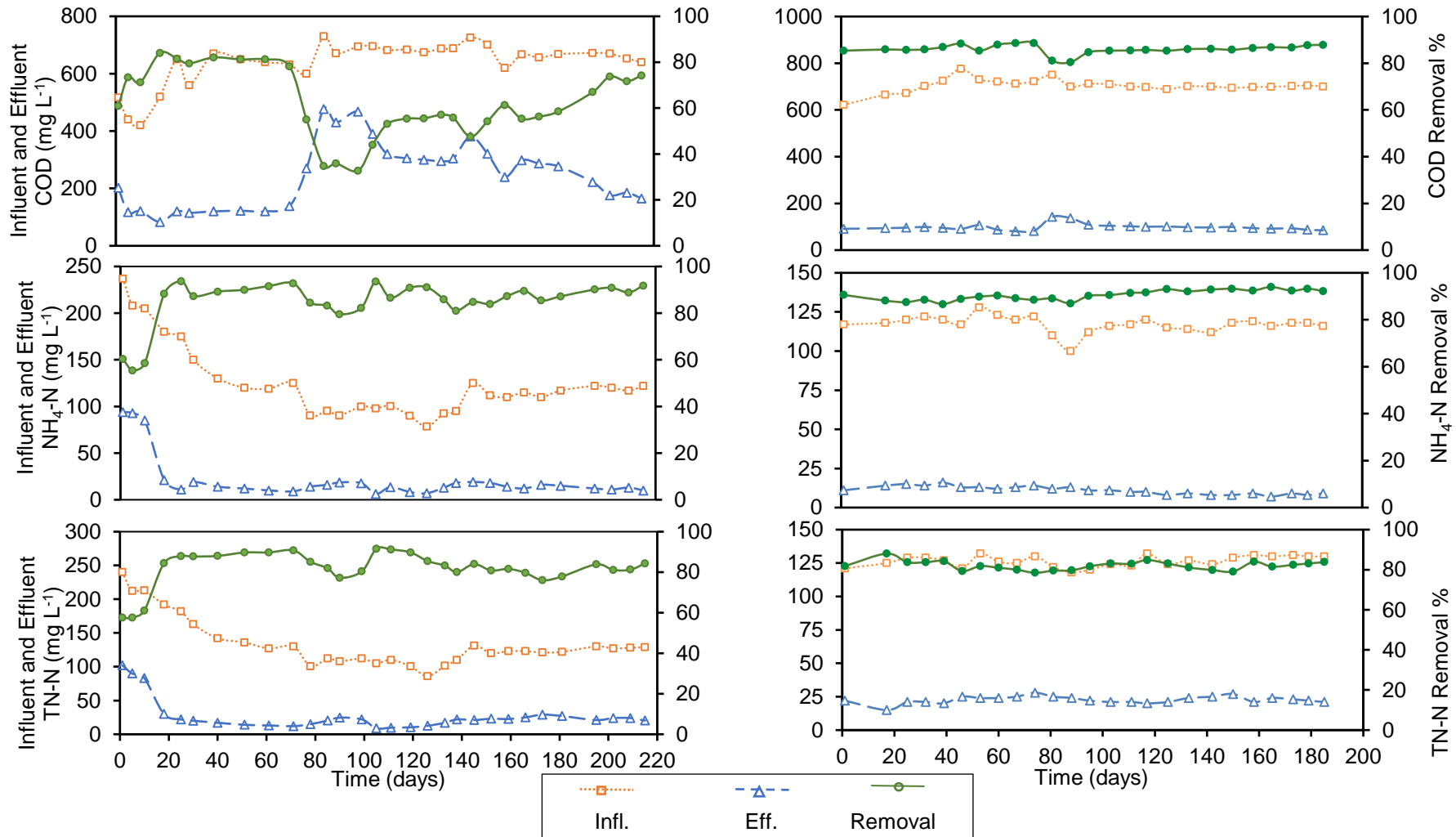


Figure 5. 6 Dynamics of pollutant concentrations in the influent and effluent and pollutant removal in CWs during period 1 (left) and period 2 (right).

**Table 5. 3 Characteristics of influent and effluent of the CWs for the four stages (Mean  $\pm$  SD)**

Parameter	Influent	Stage A	Stage C	Stage D	Stage E
DO (mg L <sup>-1</sup> )	-	1.67 $\pm$ 0.45	5.13 $\pm$ 0.67	5.67 $\pm$ 0.89	0.85 $\pm$ 0.12
pH	7.88 $\pm$ 0.23	7.81 $\pm$ 0.23	6.52 $\pm$ 0.38	7.14 $\pm$ 0.26	7.42 $\pm$ 0.24
Temperature °C	16.25 $\pm$ 4.15	15.85 $\pm$ 4.2	15.7 $\pm$ 4	15.23 $\pm$ 4.1	16.1 $\pm$ 4.21
Pb ( $\mu$ g L <sup>-1</sup> )	489 $\pm$ 84	185 $\pm$ 48	33 $\pm$ 8.9	8 $\pm$ 2.3	1.87 $\pm$ 1.0
Cr ( $\mu$ g L <sup>-1</sup> )	488 $\pm$ 86	123 $\pm$ 64	11.8 $\pm$ 5.6	1.65 $\pm$ 0.6	0.1 $\pm$ 0.3
Cd ( $\mu$ g L <sup>-1</sup> )	589 $\pm$ 95	200 $\pm$ 70	41 $\pm$ 17.2	4.7 $\pm$ 2.4	1.24 $\pm$ 0.1
COD (mg L <sup>-1</sup> )	639 $\pm$ 64	561 $\pm$ 62	405 $\pm$ 102	281 $\pm$ 111	241 $\pm$ 109
NH <sub>4</sub> -N (mg L <sup>-1</sup> )	125 $\pm$ 32	106 $\pm$ 28	77 $\pm$ 26	35 $\pm$ 15	21 $\pm$ 20
NO <sub>2</sub> -N (mg L <sup>-1</sup> )	0.19 $\pm$ 0.39	0.30 $\pm$ 0.75	0.28 $\pm$ 0.20	0.32 $\pm$ 0.20	0.23 $\pm$ 0.14
NO <sub>3</sub> -N (mg L <sup>-1</sup> )	0.39 $\pm$ 0.42	2.47 $\pm$ 1.18	3.42 $\pm$ 1.8	3.60 $\pm$ 1.6	2.52 $\pm$ 1.4
TN-N (mg L <sup>-1</sup> )	135 $\pm$ 36	118 $\pm$ 33	96 $\pm$ 27	56 $\pm$ 24	27 $\pm$ 2

**Table 5. 4 Characteristics of influent and effluent of the CWs for the five stages (Mean  $\pm$  SD)**

Parameter	Influent	Stage A	Stage B	Stage C	Stage D	Stage E
DO (mg L <sup>-1</sup> )	-	2.59 $\pm$ 0.36	1.63 $\pm$ 0.07	6.26 $\pm$ 0.58	5.19 $\pm$ 0.38	0.76 $\pm$ 0.07
pH	7.11 $\pm$ 0.15	7.47 $\pm$ 0.18	7.53 $\pm$ 0.17	6.42 $\pm$ 0.25	7.39 $\pm$ 0.10	7.58 $\pm$ 0.17
Temperature °C	14.5 $\pm$ 2.8	14.3 $\pm$ 2.9	14.13 $\pm$ 2.7	14.2 $\pm$ 2.4	14.5 $\pm$ 2.1	14.2 $\pm$ 2.3
Pb ( $\mu$ g L <sup>-1</sup> )	544.4 $\pm$ 28.8	173.2 $\pm$ 34	47.7 $\pm$ 13.4	6.88 $\pm$ 1.46	3.6 $\pm$ 3.6	0
Cr ( $\mu$ g L <sup>-1</sup> )	536.8 $\pm$ 15.9	191.2 $\pm$ 20	16.5 $\pm$ 4.8	3.4 $\pm$ 1.3	0.24 $\pm$ 0.42	0
Cd ( $\mu$ g L <sup>-1</sup> )	551.6 $\pm$ 26.2	205.6 $\pm$ 28.8	57.3 $\pm$ 13.3	6.36 $\pm$ 2.3	3.04 $\pm$ 1.5	0.36 $\pm$ 0.62
COD (mg L <sup>-1</sup> )	704 $\pm$ 27.5	596 $\pm$ 40.5	487 $\pm$ 39.4	253.5 $\pm$ 28.4	132.1 $\pm$ 20.4	98.5 $\pm$ 13.9
NH <sub>4</sub> -N (mg L <sup>-1</sup> )	117 $\pm$ 5.1	89 $\pm$ 5	75 $\pm$ 5.6	60.4 $\pm$ 4.6	18.6 $\pm$ 1.9	11.1 $\pm$ 2.5
NO <sub>2</sub> -N (mg L <sup>-1</sup> )	0.009 $\pm$ 0.004	0.043 $\pm$ 0.04	0.082 $\pm$ 0.06	0.11 $\pm$ 0.05	0.094 $\pm$ 0.047	0.009 $\pm$ 0.0002
NO <sub>3</sub> -N (mg L <sup>-1</sup> )	0.34 $\pm$ 0.18	1.33 $\pm$ 0.68	3.3 $\pm$ 1.2	4.59 $\pm$ 1.2	6.32 $\pm$ 1.4	4.33 $\pm$ 1.42
TN-N (mg L <sup>-1</sup> )	126 $\pm$ 37	107 $\pm$ 33.8	89.5 $\pm$ 28	71.2 $\pm$ 25	51.4 $\pm$ 9.6	22.64 $\pm$ 2.6

### 5.3.2 Heavy metals removal in CWs

Unlike other pollutants, such as nutrients and toxic organic components, HM are not degradable. Therefore, HM accumulate in the environment and in the long term, part of the HM can reach humans through the food chain. The main HM of interest in this study are Fe, Pb, Cr and Cd, all of which were present in the CWs in dissolved form. The main removal mechanisms are adsorption, co-precipitation with iron oxyhydroxide, and plant uptake. Tables 5.3 and 5.4 show that the HM were effectively removed during both periods. However, the removal efficiency was more pronounced in stage A, as mentioned above, leaving remaining HM to be removed in stage C during period 1, as shown in Figure 5.7.

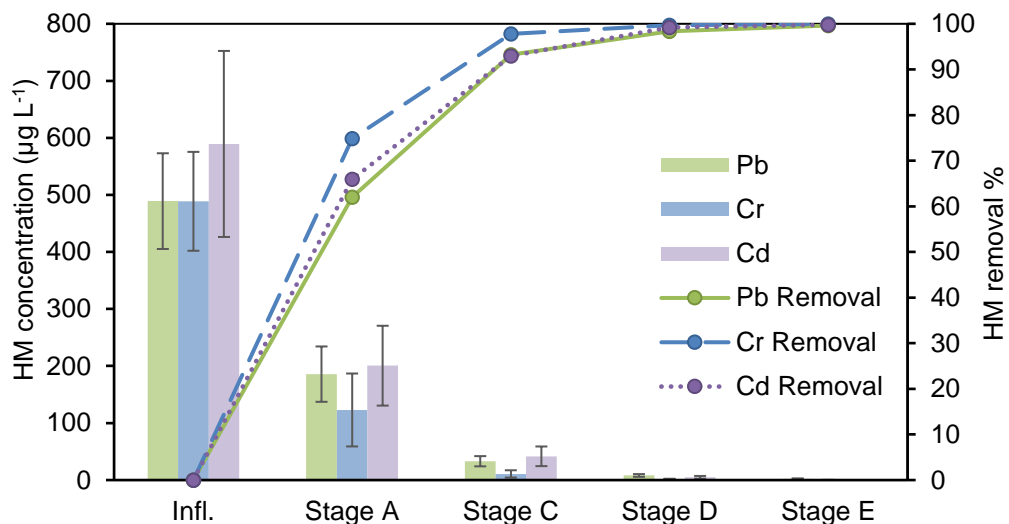


**Figure 5. 7 HM concentrations in each stage and removal efficiency (Mean ± SD) for period 1**

Stage A was operated to be fully saturated for 3 hours and 50 minutes and unsaturated for 10 minutes. Due to a limitation of DO diffusion within HH-sludge (Wang et al. 2008), there are aerobic and anaerobic conditions along the height of the column, as shown in Figure 5.8.

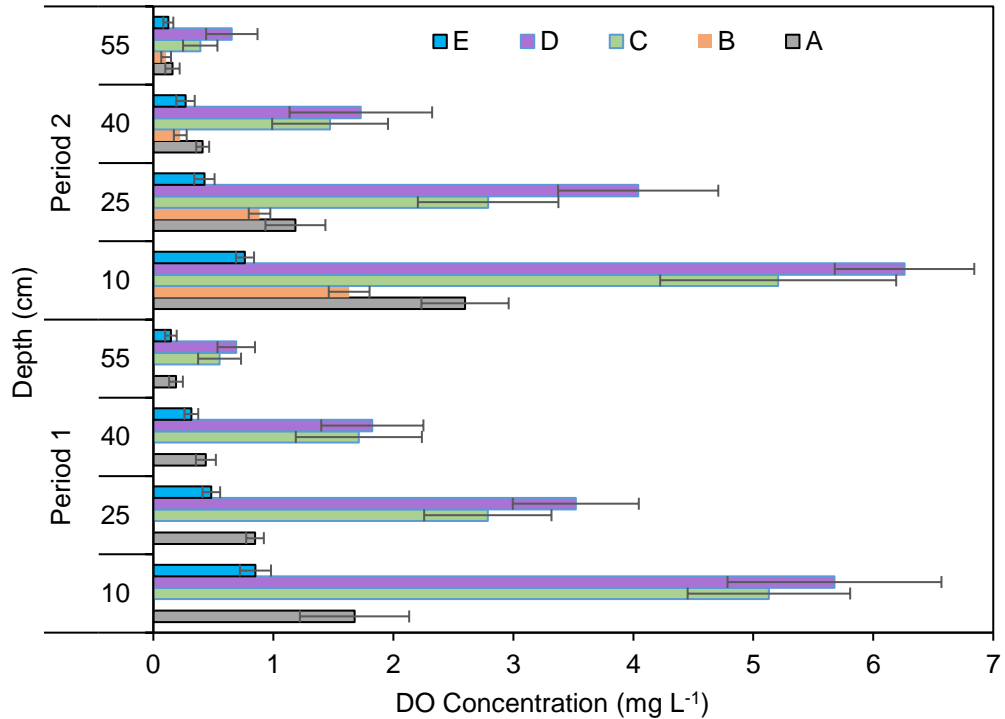


**Figure 5. 8 Vertical DO distribution (Mean  $\pm$  SD) at different depth (from top layer to bottom) in all stages of CWs**

Under aerobic conditions and within first 25 cm depth in stage A, precipitation as Fe oxide could occur. However, Fe oxide is highly dependent on DO variations, so the binding of metals with Fe oxide cannot be a long-term removal mechanism, as metals may be released back into the system. Moreover, Fe oxide has a high affinity to metals that have a similar size to Fe, such as Cd; however, the co-precipitate is limited when there is a sufficient amount of  $\text{SO}_4$  which reduces the potential for metal removal (Marchand et al. 2010). In this study, the source of  $\text{SO}_4$  was from the sulphate salts used to prepare most of pollutants in the synthetic landfill leachate as described in section 5.2.2. Another source for  $\text{SO}_4$  is HH-sludge; Table 3.3 (Chapter 3) shows that there is about  $4.51 \text{ mg g}^{-1}$  of  $\text{SO}_4$  in HH-sludge.

In addition, under anaerobic conditions when the  $\text{DO} < 0.5 \text{ mg L}^{-1}$ , our hypothesis is that precipitation as metal sulphides cannot occur. This could be because there is no sufficient carbon source ( $\text{CH}_2\text{O}$ ), which is required by sulphate-reducing bacteria to produce sulphides since the carbon source used in this study was sodium acetate ( $\text{C}_2\text{H}_3\text{NaO}_2$ ), which restricted the growth of the sulphate-reducing bacteria (Webb et al. 1998). Moreover, these bacteria cause a reduction in the sulphate concentration and as a result, the pH value decreases (Kosolapov et al. 2004). However, in this

study, there was no significant reduction in the pH value between the influent and the effluent for stage A (Table 5.3). This confirms our hypothesis.

It seems that adsorption is the main process for HM removal in this stage where there is a high contact time between the landfill leachate and HH-sludge (Stefanakis et al. 2011). However, the influent pH plays an important role in adsorption (Stefanakis et al. 2011). The mean value of the influent pH for this stage was 7.88 (Table 5.3). The maximum adsorption capacity of HH-sludge for HM at pH 7 was found to be  $20 \mu\text{g g}^{-1}$ ,  $130 \mu\text{g g}^{-1}$  and  $30 \mu\text{g g}^{-1}$  for Pb, Cr and Cd respectively, using the Langmuir isotherm model (Tables B6- B8 in Appendix B).

The rest of the HM, which had not been removed in stage A were introduced in stage C. The removal of HM in this stage reached up to 98% for Cr and 93% for Pb and Cd (Figure 5.7). In this stage, the aerobic condition was the dominant condition along the depth of the column where  $\text{DO} > 0.5 \text{ mg L}^{-1}$  as shown in Figure 5.10. The oxygenated environment promotes HM oxidation and subsequent hydroxylation, and this causes metal precipitation (Kosolapov et al. 2004). In addition, the presence of iron in the HH-sludge, (Table 3.3 in Chapter 3) and sulphate in the wastewater and the HH-sludge as described above, can enhance the precipitation of metals. Iron in the aerobic environment can oxidise and hydrolyse, and consequently this results in the removal of metals by co-precipitation (Marchand et al. 2010), or the precipitation of iron oxyhydroxide could absorb the metals (Kosolapov et al. 2004). The process of iron oxyhydroxide can lower the pH of the wastewater (Kosolapov et al. 2004). The pH value in this stage had been reduced from 7.81 in the influent to 6.52 in the effluent. It seems that the removal of HM in this stage was dominated by precipitation or co-precipitation, and this caused the clogging problem in this stage, as discussed below in section 5.3.3. Stage B had been added to the system on 20 of December to solve the clogging problem. The operation of this stage was similar to stage A to enhance HM removal by the adsorption process. The removal of HM was up to 91%, 97% and 90% for Pb, Cr and Cd respectively in stage B, as shown in Figure 5.9 leaving insignificant amounts of HM to produce in stage C, thus solving the clogging problem.

The uptake of HM by plants was insignificant compared to the total amount of HM removed in CWs. The HM removed by plants in this study was found to be 6%, 5.1% and 5.2% for Pb, Cr and Cd respectively as shown through the STELLA simulation result in Section 7.3.3 (Chapter 7). Garcia et al. (2010) and Stefanakis and Tsihrintzis (2011) reported that up to 5% of HM can be assimilated by plants. However, the presence of a high concentration of HM in synthetic landfill leachate may inhibit the

growth of plants (Batty and Younger 2004). This was seen as a reduction in shoot height as shown in Figure 5.1 in both stages A and C.

However, plants make an indirect contribution to HM removal in CWs; for example, a plant's roots provide an attractive attachment area for microbial populations (Brix 1997) and enhance aeration of the bed (Brix 1994), while plant roots release organic carbon as well as oxygen (Brix 1997).

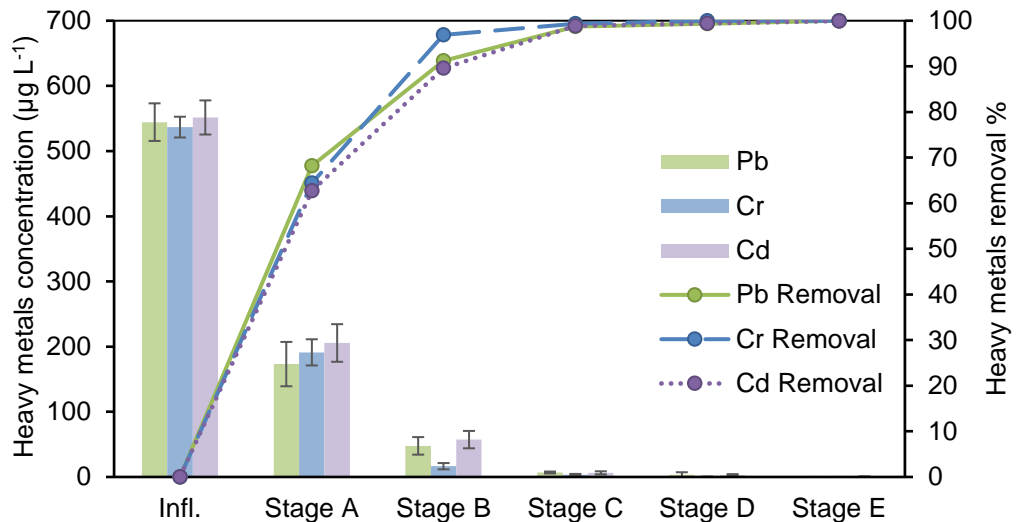


**Figure 5. 9 HM concentrations in each stage and removal efficiency (Mean ± SD) for period 2**

### 5.3.2.1 Iron removal

The concentration of Fe was found to be up to 448 mg L<sup>-1</sup> in young landfill in the UK (Table 2.1 in Chapter 2), mostly in soluble form because of the anaerobic conditions of the leachate in the landfill. At such high concentration, iron precipitation causes serious clogging threat in CWs. Consequently, Hoover et al. (1998) and Loer et al. (1999) recommended pre-treatment of the leachate using aeration and precipitation steps to produce a clear water discharge to the CW. In this study, the concentration of Fe was 500 mg L<sup>-1</sup> and the synthetic wastewater was left in open basin for 24 h. Fe<sup>3+</sup> is dominant in the oxidized condition and at pH > 6.5; Fe<sup>3+</sup> then joins with hydroxide ions to form reddish-brown ferric hydroxide (Fe(OH)<sub>3</sub>). After ferric hydroxide precipitation, the clear water was discharged to stage A. The influent tank was rinsed after the wastewater was used to remove ferric hydroxide before the next filling. It seems that this ferric hydroxide can adsorb other metals in the wastewater solution

(i.e. Pb, Cr and Cd). Therefore, the concentrations of these HM were low during first 20 days, and were about 250  $\mu\text{g L}^{-1}$  for Pb and 240  $\mu\text{g L}^{-1}$  for Cr and Cd as shown in Figure 5.5. Thereafter, the concentrations of the HM increased to around 550  $\mu\text{g L}^{-1}$ .

### 5.3.2.2 Lead removal

Lead was completely removed in both periods, and the removal efficiency was more pronounced in stage A. The removal of Pb in this stage could be by adsorption to the HH-sludge, to the carboxylate groups of the humic substances in this sludge, or to the Fe-oxyhydroxide, as described in section 4.3.2.1. In the aerobic zone, such as in stage C, Pb can form insoluble compounds with sulphate, as shown in Equation (5.1).



The removal efficiency of Pb in the CWs was up to 100% higher than the 50% and 81% reported in the literature by Khan et al. (2009) and Lesage et al. (2007) respectively. This can be attributed to the use of HH-sludge as the main medium in this study to enhance the adsorption and removal of HM.

### 5.3.2.3 Chromium removal

Chromium was also completely removed in the CWs, compared to 86% and 89% removal achieved, respectively by Maine et al. (2009) and Khan et al. (2009). The adsorption process to the HH-sludge was through the carboxylate groups of the humic substances or to the Fe-oxyhydroxide, as shown in Chapter 4 (Section 4.3.2.1).

Chromium can also undergo co-precipitation with iron oxyhydroxide and especially at  $\text{pH} > 6$  (Coelho et al. 2014).

### 5.3.2.4 Cadmium removal

In this study, the removal of cadmium from CWs could either be by adsorption or by co-precipitation with iron oxyhydroxide, as discussed in section 4.3.3.1. However, cadmium precipitation can occur at  $\text{pH} > 8$  (Chen et al. 2015a), and in this study, the pH value was up to 7.88 (Tables 5.3 and 5.4). In addition, the adsorption of cadmium could be by carboxylate groups of the humic substances in the HH-sludge, as described in section 4.3.2.1. The removal of Cd in this study reached up to 99.7% in period 1 and 99.9% in period 2 (Figures 5.9 and 5.11). In general, this value is in

agreement with the findings of previous studies (Yang 2006; Kanagy et al. 2008; Khan et al. 2009).

### **5.3.3 Clogging Phenomena in stage C**

Clogging is defined as the process that develops over the operational time of CWs, and which leads to the blockage of substrate pores, and the subsequent diminution of the corresponding hydraulic conductivity, as induced by the accumulation of solids within the wetland (Stefanakis et al. 2014). Clogging can obstruct the oxygen transport and consequently decrease the treatment performance of CWs. Over the past two decades, there has been a motivation to understand and control clogging, and so the desire to mitigate clogging has directly influenced the design evolution of CWs (Murphy and Cooper 2010).

In this study, it was visually observed during the system operation that stage C experienced clogging. In addition, there was a drop in the wastewater treatment performance in stage C in the period between 26/07/2015 to 14/08/2015. It was noted that there was ponding of wastewater on the surface of this stage leading to bypass of untreated wastewater. To solve this problem, the stage was firstly left to rest for two weeks (from 14/08/2015 to 28/08/2015) as shown in Figure 5.10. This is because it was thought that the clogging was due to excessive microbial growth. When this did not work, backwash was used. Thereafter, the wastewater treatment was enhanced until 18/12/2015 when it was noticed that there was a reduction in both treatment performance and wastewater infiltration. It seemed that the chemical treatment process (adsorption and precipitation) could be the main factor in clogging. However, the adsorption films did not become thick enough to create the clogging problem, as adsorption was limited in this stage. Chemical precipitation as HM hydroxide or co precipitation with iron oxyhydroxide may form a film-like coating on the media surface (Knowles et al. 2011). The additional stage (stage B) was added to the system on 20/12/2015 and was designed to work in anoxic conditions to enhance the removal of the rest of the HM which had not been removed by the adsorption process in stage A.

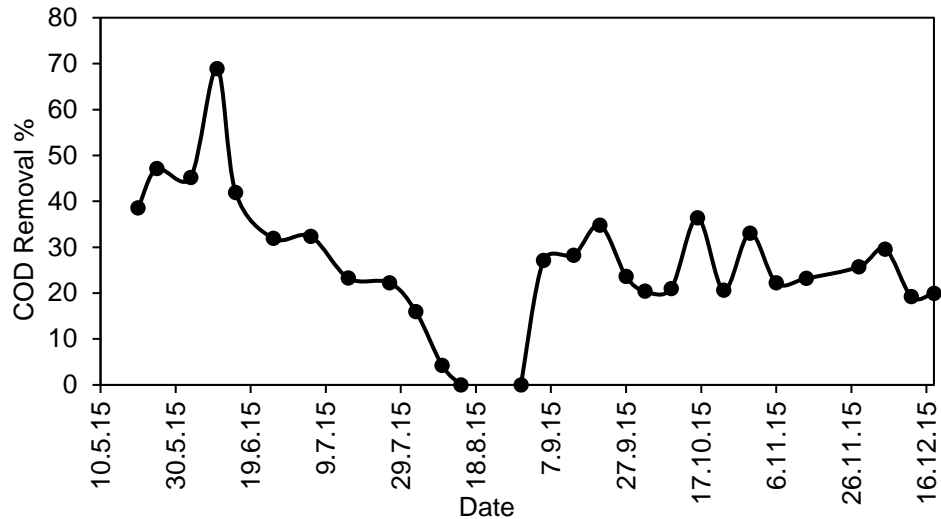


Figure 5. 10 COD removal in stage C in first period

### 5.3.4 Organic matter removal in CWs

Chemical oxygen demand (COD) is a major pollutant in wastewater and decomposes both aerobically and anaerobically. The aerobic decomposition of organic matter demands a high oxygen supply which is utilized as an electron acceptor. It is also reported that most organic matter is removed within the first 10 - 20 cm of the bed since the top layer is dominated by aerobic conditions and higher microbial density (Stefanakis and Tsihrintzis 2012; Kadlce and Wallace 2008). Anaerobic degradation takes place in the absence of oxygen by acid- or methane-forming bacteria.

The overall removal efficiency of COD across the stages is presented in Figure 5.11 for period 1 and Figure 5.12 for period 2. These Figures indicate that a shorter saturated time and a longer unsaturated time resulted in greater COD removal efficiency. It is noted from Figures 5.11 and 5.12 that the removal percentages of COD are enhanced during continuous runs under the same operating conditions. It can be suggested that enhanced aeration by convection and diffusion during the unsaturated time may have played a key role in the removal of COD in stages C and D. The removal efficiency in stage C reached up to 69% within the first 20 days; and thereafter a sharp reduction in COD removal occurred due to clogging, as described in section 5.3.3. When the clogging problem was solved, the removal of COD started to increase up to 36% in this stage until 18 December 2015, when this stage began to experience clogging problems again. While the COD removal in this stage for period 2 was almost stable and reached up to 52%, stage D also was responsible for COD removal, with the removal efficiency reach the up to 61% and 59% in this stage

in period 1 and period 2 respectively. The significant aerobic COD removal obtained during these two stages is predominantly due to the enhanced oxygenation ability of the tidal flow strategy that was employed in these two stages (Zhao et al. 2004b; Hu et al. 2012; Chang et al. 2014). The time of filling and draining of these two stages ensured that oxygen was present in the system beds, where the DO concentrations ranged from 0.55 mg L<sup>-1</sup> to 5.13 mg L<sup>-1</sup> and 0.69 mg L<sup>-1</sup> to 5.67 mg L<sup>-1</sup> in stages C and D respectively in period 1 (Figure 5.10). In period 2, the DO concentrations ranged from 0.39 mg L<sup>-1</sup> to 5.21 mg L<sup>-1</sup> and 0.65 mg L<sup>-1</sup> to 6.25 mg L<sup>-1</sup> in stages C and D respectively, indicating good oxygen conditions within these stages. In such prevailing aerobic conditions, organic matter is oxidized by heterotrophic bacteria that uses oxygen as an electron acceptor (García et al. 2010).

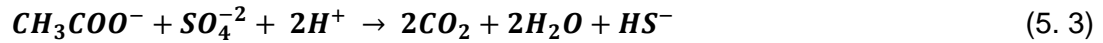
Anaerobic COD removal was achieved in stage E; the removal efficiency in this stage was up to 30% and 33% during period 1 and period 2 respectively, as shown in Figures 5.11 and 5.12. Denitrification is the most important process in removing organic matter in CWs and especially with a depth of 0.27 m (García et al. 2010). Under anoxic conditions, heterotrophic bacteria have the ability to oxidize organic matter that uses nitrate as an electron acceptor (García et al. 2010).

In this study, the average concentration of DO at a depth of 25 cm was 0.43 mg L<sup>-1</sup> and 0.42 mg L<sup>-1</sup> in periods 1 and 2 respectively, which means denitrification can occur at this depth. The concentration of DO is not the only important factor for COD removal in anaerobic conditions, such as in stage E, but the abundantly available NO<sub>3</sub>-N in this stage could directly lead to more denitrification with simultaneous consumption of COD as a required organic source (Fan et al. 2013a). However, the first and most significant nitrogen transformation that occurred in stage D was nitrification (NH<sub>4</sub>-N → NO<sub>3</sub>-N), and this did not contribute to COD consumption. Nitrification was also the rate-limiting step for providing NO<sub>3</sub>-N for denitrification and COD consumption.

Anaerobically COD removal can also be achieved through iron and sulfate reduction when acetate is used as substrate. In stage E and at depth 60 cm, the DO concentrations were respectively 0.14 mg L<sup>-1</sup> and 0.12 mg L<sup>-1</sup> for period 1 and 2. Fe<sup>3+</sup> from HH- sludge can be reduced as in Equation below:



In addition, the sulfate from the synthetic wastewater can also be removed as per the Equation below:



During the operation (220 days), the system achieved average COD removal efficiency of  $62\% \pm 14\%$  in period 1 and  $86\% \pm 2\%$  in period 2, respectively for COD loading rates of  $977 \text{ g m}^{-2} \text{ day}^{-1}$  and  $1076 \text{ g m}^{-2} \text{ day}^{-1}$  for period 1 and period 2. To our knowledge, the COD removal efficiency in period 1 was lower than those used to treat landfill leachate in vertical flow CWs. The typical removal efficiencies of 96% (Lavrova and Koumanova 2010) and 77% (De Feo 2007). However, the COD removal reached up to 84% after 20 days of operation in period 1, as shown in Figure 5.6, and especially in stage C, as shown in Figure 5.11.

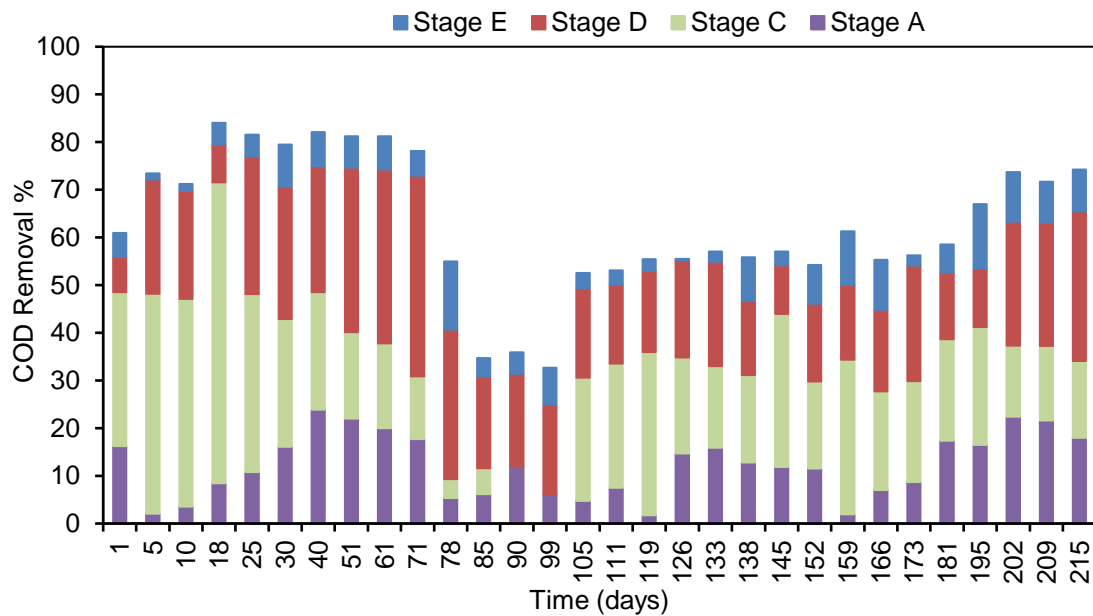


**Figure 5. 11** Variation and removal efficiency of COD in the four stages of CWs during period 1.

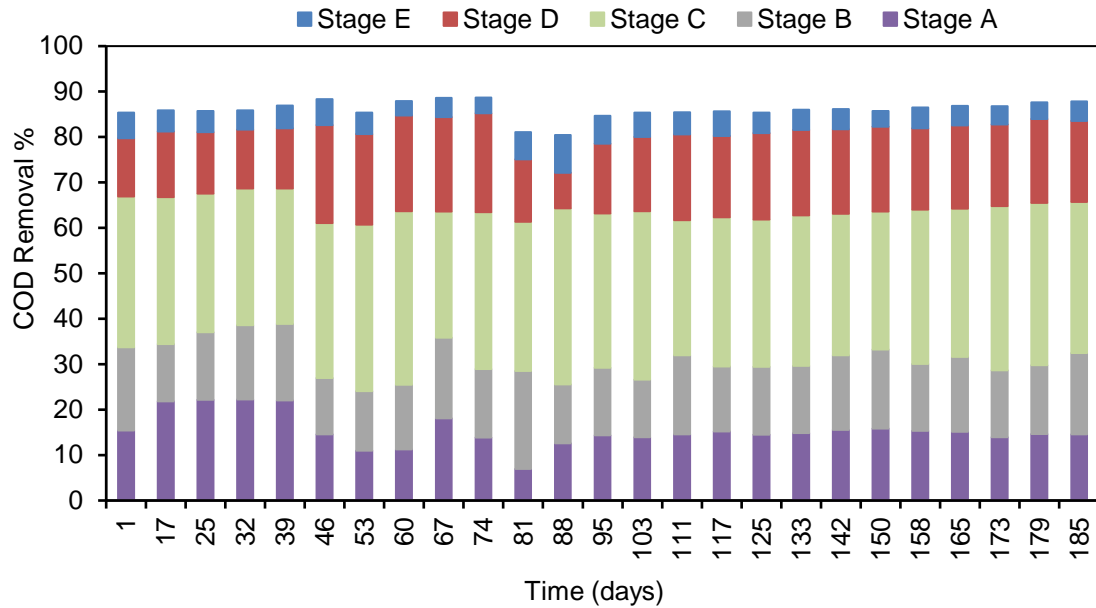


**Figure 5.12** Variation and removal efficiency of COD in the four stages of CWs during period 2.

### 5.3.5 Nitrogen removal in CWs

There is great interest in removing nitrogen from wastewater. When released into surface water, nitrate constitutes a major risk for eutrophication and reduced water quality through altering the DO balance to insufficient levels for living organisms in water.

Usually, analytical methods include the determination of  $\text{NH}_4$ , oxidized nitrogen ( $\text{NO}_2$  and  $\text{NO}_3$ ) and TN (organic nitrogen,  $\text{NH}_4$  and oxidized nitrogen).

The focus of the design of the CWs in this study was to treat nitrogen-rich synthetic wastewater. Figures 5.13 and 5.14 present variations of nitrogen forms including  $\text{NH}_4\text{-N}$ ,  $\text{NO}_2\text{-N}$ ,  $\text{NO}_3\text{-N}$  and TN-N, across the CWs in period 1 and period 2 respectively. The transformation and removal of nitrogen in CWs could be accomplished by nitrification–denitrification, plant and microbial uptake, adsorption, ammonia volatilization etc. (Fan et al., 2013; Chang et al. 2014).

Nitrogen removal through plant uptake was considered to be negligible due to the high nitrogen loading rate applied, as shown in Tables 5.3 and 5.4 ( $205.7 \text{ gN m}^{-2} \text{ day}^{-1}$  and  $192.6 \text{ gN m}^{-2} \text{ day}^{-1}$ , respectively for periods 1 and 2).

The amount of nitrogen removed by adsorption in stage C and D will be discussed in Chapter 6 (section 6.4.3). The Freundlich constant  $K_f$  ( $L \text{ mg}^{-1}$ ), which is used as adsorption isotherm coefficient in the HYDRUS software, is found to be equal to  $0.047 \text{ L g}^{-1}$ . In practical terms, the ammonia adsorbed by HH-sludge could enhance nitrification to nitrate during the resting time between loadings.

Volatilization, the process by which unionized ammonia ( $\text{NH}_3$ ) diffuses to the atmosphere from the water surface, depends mainly on pH. The pH value for this process is higher than 8 and for pH 9.3, the conversion of  $\text{NH}_4\text{-N}$  to  $\text{NH}_3$  gas increases (Vymazal 2007; Saeed and Sun 2012). In this study, the maximum value of pH in both periods was 7.88 (Tables 5.3 and 5.4); thus the extent of ammonia volatilization can be considered negligible.

From the above, it seems that the classical route of nitrification, coupled with simultaneous nitrification and denitrification, is the major removal process for nitrogen retention in this study.

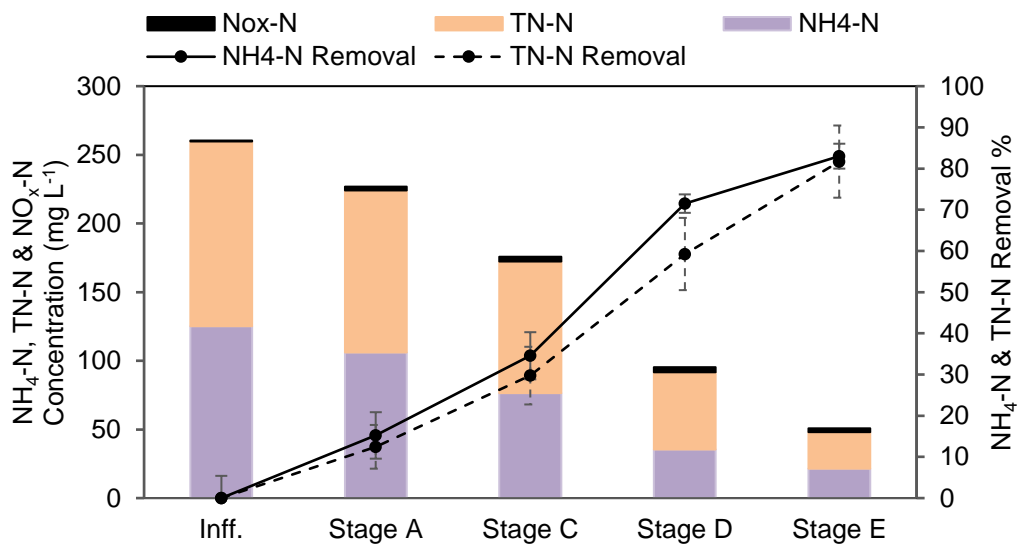


**Figure 5. 13**  $\text{NH}_4\text{-N}$ ,  $\text{NO}_x\text{-N}$  and  $\text{TN-N}$  profile and removal efficiency of  $\text{NH}_4\text{-N}$  and  $\text{TN-N}$  across the four stages of the CWs in period 1

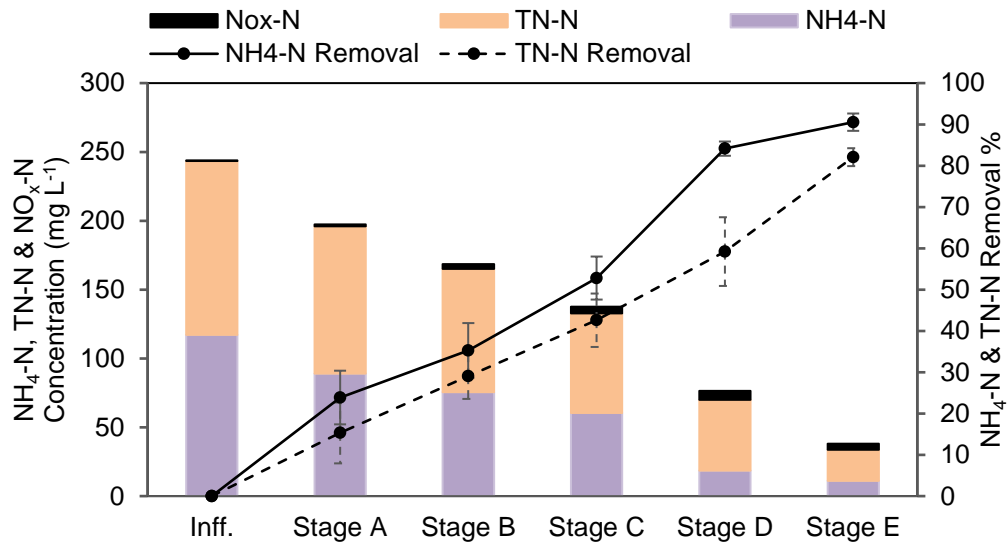
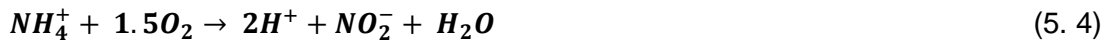


**Figure 5. 14 NH<sub>4</sub>-N, NO<sub>x</sub>-N and TN-N profile and removal efficiency of NH<sub>4</sub>-N and TN-N across the five stages of the CWs in period 2**

### 5.3.5.1 NH<sub>4</sub>-N removal

Nitrification is probably the major removal process for NH<sub>4</sub>-N removal in this study. First, NH<sub>4</sub>-N is oxidized to NO<sub>2</sub>-N under aerobic conditions and then to NO<sub>3</sub>-N. The two processes can be written as (Metcalf and Eddy 2003):



From these equations, nitrification is seen to be an oxygen-consumption process. Complete NH<sub>4</sub>-N oxidation requires about 4.6 mgO<sub>2</sub> (mgN)<sup>-1</sup> (optimum DO concentration of 3-4 mg L<sup>-1</sup>) and consumes 8.64 mgHCO<sub>3</sub> (mgNH<sub>4</sub>-N)<sup>-1</sup> (Vymazal 2007; Saeed and Sun 2012; Faulwetter et al. 2009). Other parameters that can affect nitrification are temperature, pH value, moisture, alkalinity of water, microbial population and NH<sub>4</sub>-N concentration (Vymazal 2007; Lee et al. 2009). The optimum temperature range for nitrification is 25°C to 35°C, and the process is inhibited at temperatures 4-5°C, while the optimum pH values vary from 6.6 to 8 (Vymazal 2007).

Figures 5.13 and 5.14 show clearly that a significant reduction in NH<sub>4</sub>-N was achieved during the operation of the system (83.2% ± 2.4%) and (90.5% ± 2.1%) in periods 1 and 2 respectively. Other studies reported the removal of NH<sub>4</sub>-N to be higher than these values. Fan et al. (2013a) achieved 99% when they used a sufficient carbon source of COD/N =10 and Hu et al. (2014) recorded 96% of NH<sub>4</sub>-N removal when

they extended the resting time to 1 hour. Meanwhile, a study by Chang et al. (2014) showed just 55% of  $\text{NH}_4\text{-N}$  removal in tidal flow CWs with 3:3 hours of feed:dry period.

Intermittent aeration of 1 hour per 3 hours in stages C and D led to a well-developed aerobic condition where  $\text{NH}_4\text{-N}$  nitrifies. The removal of both these stages reached an average of 56.2% and 48.9% for the first and second period respectively. The DO concentrations were  $> 3 \text{ mg L}^{-1}$  within 25 cm depth in both stages (Figure 5.8). The pH values were 6.5 - 7.14 and 6.42 - 7.39, while the temperature values were 15.7 - 15.2 and 14.2 - 14.5 (Tables 5.3 and 5.4) for periods 1 and 2 respectively. In addition, there was the availability of a carbon source from aerobic COD removal when oxygen was utilized for carbon oxidization; all of these enhanced the nitrification process in both these stages. However, the removal efficiency was more pronounced in stage D, which employed a 1:1 recirculation, this resulted in prolonged wastewater-biofilm contact. Nitrification of  $\text{NH}_4\text{-N}$  by autotrophic nitrifying bacteria, which have a lower respiration rate, is slower than the decomposition of organic matter (Sun et al. 2005). Thus, by recirculation, the nitrifying bacteria will have enough time to convert  $\text{NH}_4\text{-N}$  to  $\text{NO}_2\text{-N}$  and  $\text{NO}_3\text{-N}$ . In addition, there will be a reduction in organic load. The  $\text{NH}_4\text{-N}$  removal increased from 34% to 72% (Figure 5.13) with an organic loading rate reduction from  $619 \text{ gCOD m}^{-2} \text{ day}^{-1}$  to  $430 \text{ gCOD m}^{-2} \text{ day}^{-1}$  in this stage in period 1 (Table 5.3). Meanwhile, the  $\text{NH}_4\text{-N}$  removal in period 2 increased from 53% to 84% (Figure 5.14) with an organic loading rate decreased from  $387 \text{ gCOD m}^{-2} \text{ day}^{-1}$  to  $202 \text{ gCOD m}^{-2} \text{ day}^{-1}$  in stage D (Table 5.4).

### 5.3.5.2 Total nitrogen removal

Denitrification is considered as a combined process with nitrification for TN removal. The process involves heterotrophic bacteria when N oxide or oxygen serve as electron acceptors and organic materials serve as electron donors (Vymazal et al., 1998; Kadlec and Wallace 2008; Saeed and Sun 2012).

The main factors that affect this process include redox potential, the availability of nitrate and organic source, pH value, the concentration of DO, moisture content and temperature (Vymazal 2007; Faulwetter et al. 2009; Lee et al. 2009). The optimum temperature for the denitrification process is between  $60^\circ\text{C}$  and  $75^\circ\text{C}$ , and the process is inhibited at temperatures below  $5^\circ\text{C}$ . DO concentration should be maintained at  $<0.3\text{-}0.5 \text{ mg L}^{-1}$  while the pH value ranges from 6 to 8 (Lee et al. 2009; Saeed and Sun 2012; Stefanakis et al. 2014).

In all stages, nitrification and denitrification processes may have occurred simultaneously in the CWs, resulting in a decrease in  $\text{NO}_2\text{-N}$  and  $\text{NO}_3\text{-N}$  levels; this phenomenon is termed as simultaneous nitrification and denitrification (SND) (Lavrova and Koumanova 2010). The intermittent aeration strategy creates anaerobic and aerobic conditions in CWs and facilitates nitrification and denitrification simultaneously (Fan et al. 2013b).

Total nitrogen losses of up to 30% and 60% have been noted in aerobic conditions in stages C and D respectively in period 1, and 43% and 59% in these stages respectively in period 2. These losses may be due to denitrification occurring in the anoxic microzone inside the sludge floc. However, autotrophic nitrification may occur on the surface of the flocs, and this could be because of high oxygen diffusion resistance within the sludge flocs (Hu et al. 2014). According to Bakti & Dick (1992), the dissolved oxygen gradient is controlled by several factors such as bulk dissolved oxygen level, the particle size of the floc (HH-sludge), the loading of organic substrate, and the aeration cycle. This phenomenon emphasises the denitrification developed in aerobic conditions using both oxygen and nitrate as a terminal electron acceptor (Hu et al. 2014). Several studies have shown aerobic denitrification in wastewater treatment processes and natural sediment (Gao et al. 2009; Zhang et al. 2011). Moreover, there is sufficient organic carbon (COD/N) of 4.2 and 5 in stages C and D in period 1, and 3.6 and 2.6 in these stages in period 2 respectively. This ratio is essential as an electron donor for nitrate reduction, and it provides an energy source for denitrifying microorganisms (Fan et al. 2013a). Zhao et al. (2010) found that high nitrogen removal efficiency occurred at COD/N ratio ranging from 2.5- 5. In addition, the pH values for both these stages were within the optimum value. The pH values in period 1 ranged from 6.5 to 7.14 while in period 2, they were from 6.42 to 7.39, as shown in Tables 5.3 and 5.4.

The effective TN-N removal in stage E (up to 91% in period 1 and 85% in period 2) could be attributed to the remaining carbon source in stage E (Figures 5.13 and 5.14). The influent COD/N ratios of 9 in period 1 and 4.5 in period 2 were sufficient to support the full denitrification of the nitrified nitrogen. Nitrification was shown to be a limiting factor for TN elimination. In this stage, about 10% of  $\text{NH}_4\text{-N}$  had been removed. Other studies have shown a high efficiency of nitrification and denitrification occurring simultaneously at COD/N = 5 (Fan et al. 2013a; Hu et al. 2014). Chang et al. (2014) demonstrated a significant improvement in TN-N removal efficiency, which increased from 25% to 70% when COD/N ratio increased from 2.5 to 10. Moreover, anoxic

conditions were applied in this stage, whereas the dissolved oxygen was less than 1, as shown in Figure 5.8, and pH values were 7.42 and 7.58 in periods 1 and 2 respectively. All these factors could enhance the TN removal in this study. However, the average TN removal in this study was 82% in both periods, which is lower than the 90% reported by Fan, et al. (2013a) and the 85% achieved by Hu et al. (2014). In the studies, the authors used intermittent aeration combined with a high influent COD/N ratio up to 20 and multiple tides respectively.

## 5.4 Conclusions

Overall, this study has demonstrated the effectiveness of combining anoxic conditions and the tidal flow strategy in CWs using ferric sludge as main media to achieve enhanced pollutant removal from high strength wastewater (landfill leachate). Sufficient bed resting time promotes COD removal and nitrified  $\text{NH}_4\text{-N}$  while anoxic conditions were shown to be the key factor in maintaining effective HM and total nitrogen removal. The main conclusions were as follows:

- (i) High removal rate of HM was obtained by adsorption in anoxic conditions and precipitation to ferric dewatered sludge in oxidizing conditions.
- (ii) Clogging problems in stage C in period 1 seem to occur due to the chemical precipitation of HM hydroxide and co-precipitation of HM with iron oxyhydroxide. The problem was solved by enhancing HM removal by the adsorption process.
- (iii) The removal efficiency of COD in this study could be ascribed to aerobic conditions in stages C and D, and anoxic microbial processes for denitrification in stage E. However, bed clogging was observed to be a serious problem, which affects COD removal in stage C in period 1.
- (iv) An intermittent aeration strategy can effectively develop alternate aerobic and anaerobic conditions in vertical flow CWs, so simultaneous nitrification and denitrification could occur under a sufficient COD/N ratio range from 2.5 to 10.

# **Chapter 6**

## **Modelling organic matter and nitrogen removal in CWs treating landfill leachate using HYDRUS CW2D**

## 6.1 Introduction

This chapter focuses on the development of a numerical model for the CWs treating landfill leachate. CWs is a complex system that is difficult to understand where the interaction between soil, vegetation, water and microorganisms are active in parallel and were they mutually influence each other (Kadlce and Wallace 2008). Because of this complexity, the design guidelines of CWs are mostly based on empirical rules of thumb, such as using specific surface area requirement (Brix and Johansen 2004), maximum nitrogen loading rate (Molle et al. 2008), simple first order decay models (Kadlce and Wallace 2008) or as black box (Pastor et al. 2003; Tomenko et al. 2007).

Numerical simulators can represent valuable tools for analysing and improving our understanding of the processes governing the biological and chemical transformation and degradation process in CWs. CW2D module allows further investigation with transport and reaction in vertical flow subsurface flow CWs, and implemented it into HYDRUS variably saturated flow and solute transport program (Langergraber and Šimůnek 2006).

In this study, we use Version 2 of HYDRUS was used and this includes the biokinetic model formulation CW2D that considers aerobic and anoxic transformation and degradation process for organic matter. Although this model was mostly tested for sand or gravel vertical flow CWs, in this study it had been evaluated for ferric dewatered sludge (HH- sludge) vertical flow CWs. The main aims were:

- To develop and validate a numerical model of the CWs with emphasis on nitarian prediction.
- To increase our understanding of the fundamental processes of transformation and elimination of pollutants in the system, understanding of the system, and contribute to unravelling the (black box).

## 6.2 HYDRUS

The software selected to develop the numerical model was HYDRUS 2D. HYDRUS was selected because of its ability to simulate water flow and solute transport in variably-saturated porous media and, importantly, because of the availability to incorporate with a multi- components reactive transport module (CW2D), this allows

for the simulation of aerobic and anoxic transformation processes for organic matter, nitrogen and phosphorus removal.

In the following sections, the water flow, unsaturated soil hydraulic properties and solute transport capabilities of HYDRUS used, and the governing equations through which the program carries out the modelling processes are described. In addition, the descriptions of the numerical analysis techniques used in the HYDRUS and the components and processes of the CW2D module are defined.

### 6.2.1 Water transport in HYDRUS

The governing equation for transient variably saturated flow used in the CW2D module is based on the modified Richards Equation (Equation 6.1), which assumes two-dimensional isothermal Darcie flow of water in a rigid porous media, with insignificant role from the air phase of the liquid flow.

$$\frac{\partial \theta(h)}{\partial t} = \frac{\partial}{\partial x_i} \left[ K(h) \left( K_{ij}^A \frac{\partial h}{\partial x_j} + K_{iz}^A \right) \right] - S \quad (6.1)$$

where:  $\theta(h)$  is volumetric water content ( $L^3 L^{-3}$ ),  $h$  is pressure head (L),  $S$  is sink term ( $T^{-1}$ ),  $x_i$  are the spatial coordinates ( $i = 1,2$ ) (L),  $K_{ij}^A$  are components of the dimensionless anisotropy tensor  $K^A$ . For an isotropic medium the diagonal elements of  $K_{ij}^A$  are one and the off-diagonal elements are zero,  $t$  is time (T),  $K(h)$  is unsaturated hydraulic conductivity function ( $L T^{-1}$ ), L is length unit after preference, T is time unit after preference.

### 6.2.2 The unsaturated soil hydraulic properties

The unsaturated soil hydraulic properties  $\theta(h)$  and  $K(h)$  for Equation 6.1. are nonlinear function of the pressure head. HYDRUS uses van Genuchten's analytical models (1980) to calculate these parameters and as shown in Equations 6.2 and 6.3.

$$\theta(h) = \begin{cases} \theta_r + \frac{\theta_s - \theta_r}{[1 + |\alpha h|^n]^m}, & h < 0 \\ \theta_s, & h \geq 0 \end{cases} \quad (6.2)$$

$$K(h) = K_s S_e^l \left[ 1 - \left( 1 - S_e^{\frac{1}{m}} \right)^m \right]^2 \quad (6.3)$$

Where:

$$S_e = \frac{\theta - \theta_r}{\theta_s - \theta_r} \quad (6.4)$$

$$m = 1 - \frac{1}{n}, \quad n > 1 \quad (6.5)$$

$K_s$  is saturated hydraulic conductivity.

The following parameters are the van Genuchten (1980) parameters:

$\theta_r$  is Residual water content ( $L^3 L^{-3}$ ),  $\theta_s$  is Saturated water content ( $L^3 L^{-3}$ ),  $\alpha$  is Inverse of air-entry value or bubbling pressure ( $L^{-1}$ ),  $n$  is pore size distribution index and  $l$  is pore connectivity parameter.

### 6.2.3 Solute transport in HYDRUS

The theory of the solute transport in HYDRUS CW2D module is similar to that of an activated sludge reactor. Thus, the mathematical structure of the CW2D multi-component solute transport module is based on the structure of activated sludge models (ASMs) proposed by Henze et al. (2000). The governing equation for the macroscopic transport of component  $i$  is as below with major assumptions of: (a) constant pH value, (b) constant coefficients in the rate equations and (c) constant stoichiometric factors.

$$\frac{\partial \theta}{\partial t} c_i + \frac{\partial \rho}{\partial t} s_i = \nabla(\theta D_i \nabla c_i) - \nabla(q c_i) + S c_{S,i} + r_i \quad (6.6)$$

where:  $i$  is 1, 2, 3,...etc: No. of components,  $c_i$  is concentration in the liquid phase ( $M L^{-3}$ ),  $s_i$  is concentration in the solid phase ( $M M^{-1}$ ),  $\rho$  is soil bulk density ( $M L^{-3}$ ),  $D_i$  is effect dispersion tensor ( $L^2$ ),  $q$  is volumetric flux density ( $L^3 L^{-2} T^{-1}$ ),  $c_{S,i}$  is concentration of source/sink ( $M L^{-3}$ ),  $r_i$  is reaction time ( $M L^{-3} T^{-1}$ ) and  $M$  is mass unit after preference.

In addition, HYDRUS assume non-equilibrium interaction between the liquid (c) and solid phase (s) concentrations. The adsorption isotherm relating  $s_k$  and  $c_k$  is described using nonlinear Equation of the form:

$$s_k = \frac{k_{s,k} c_k^{\beta_k}}{1 + \eta_k c_k^{\beta_k}} \quad (6.7)$$

where  $k_{s,k}$  ( $L^3 M^{-1}$ ),  $\beta^k$  (-) and  $\eta_k$  ( $L^3 M^{-1}$ ) are empirical coefficients. The linear equations of Langmuir and Freundlich isotherm adsorption are special cases of Equation (6.7). When  $\beta^k = 1$ , then Equation (6.7) becomes Langmuir equation and when  $\eta_k = 0$ , Equation (7.6) becomes Freundlich equation.

#### 6.2.4 Numerical solution to governing flow and solute Equations

The flow Equation (6.1) is solved numerically via Galerkin finite element method with linear basis functions. Depending upon the size of the problem and the type of matrix utilised from the discretisation of the governing equations, HYDRUS implements direct Gaussian elimination method, the conjugate gradient method. While for solute transport using, the ORTHOMIN method is used (Mendoza et al. 1991).

#### 6.2.5 CW2D solute transport: components and processes

There are 12 components (pollutants and bacteria) and 9 processes (biochemical transformations and degradation processes) that can be simulated in the CW2D module. Tables 6.1 and 6.2 define the components and processes (respectively). Organic P and Organic N are modelled as P and N content of the COD components.

**Table 6. 1 Components simulated in CW2D multi-component solute transport**  
(Langergraber and Slmunek 2005)

Symbol	Unit	Description
<b>O2</b>	mg <sub>O2</sub> L <sup>-1</sup>	Dissolved oxygen
<b>CR</b>	mg <sub>COD</sub> L <sup>-1</sup>	Readily biodegradable chemical oxygen demand
<b>CS</b>	mg <sub>COD</sub> L <sup>-1</sup>	Slowly biodegradable chemical oxygen demand
<b>CI</b>	mg <sub>COD</sub> L <sup>-1</sup>	Inert chemical oxygen demand
<b>XH</b>	mg <sub>COD</sub> L <sup>-1</sup>	Heterotrophic microorganism
<b>XANs</b>	mg <sub>COD</sub> L <sup>-1</sup>	<i>Nitrosomonas</i> spp. (autotrophic bacteria 1)
<b>XANb</b>	mg <sub>COD</sub> L <sup>-1</sup>	<i>Nitrobacter</i> spp. (autotrophic bacteria 2)
<b>NH4N</b>	mg <sub>N</sub> L <sup>-1</sup>	Ammonia, $NH_4^+$
<b>NO2N</b>	mg <sub>N</sub> L <sup>-1</sup>	Nitrite, $NO_2^-$
<b>NO3N</b>	mg <sub>N</sub> L <sup>-1</sup>	Nitrate, $NO_3^-$
<b>N2N</b>	mg <sub>N</sub> L <sup>-1</sup>	Dinitrogen gas, $N_2$
<b>IP</b>	mg <sub>P</sub> L <sup>-1</sup>	Inorganic phosphorus

**Table 6. 2 Processes simulated in CW2D multi-component solute transport (Langergraber and Šimůnek 2006).**

Processes	Description
<b>Hydrolysis</b>	Conversion of <i>CS</i> into <i>CR</i> , with a small fraction being converted into <i>CI</i> . $NH_4^+$ and <i>IP</i> are released during this transformation process.
<b>Aerobic growth of <i>XH</i></b>	This process consumes <i>O2</i> and <i>CR</i> while $NH_4^+$ and <i>IP</i> are incorporated in the biomass.
<b>Anoxic growth of <i>XH</i></b>	This process produces $N_2$ (due to denitrification on $NO_2^-$ ) and consume <i>CR</i> , $NH_4^+$ and <i>IP</i> .
<b>Anoxic growth of <i>XH</i></b>	This process produces $N_2$ (due to denitrification on $NO_3^-$ ) and consume <i>CR</i> , $NH_4^+$ and <i>IP</i> .
<b>Lysis of <i>XH</i></b>	Produces organic matter ( <i>CR</i> , <i>CS</i> and <i>CI</i> ), $NH_4^+$ , and <i>IP</i>
<b>Aerobic growth of <i>XANs</i></b>	This process consumes $NH_4^+$ and <i>O2</i> , and produces $NO_2^-$ . <i>IP</i> and a small portion of $NH_4^+$ are incorporated in the biomass.
<b>Lysis of <i>XANs</i></b>	Produces organic matter ( <i>CR</i> , <i>CS</i> and <i>CI</i> ), $NH_4^+$ , and <i>IP</i> .
<b>Aerobic growth of <i>XANb</i></b>	This process consumes $NO_2^-$ and produces $NO_3^-$ . <i>IP</i> and $NH_4^+$ are incorporated in the biomass.
<b>Lysis of <i>XANb</i></b>	Produces organic matter ( <i>CR</i> , <i>CS</i> and <i>CI</i> ), $NH_4^+$ , and <i>IP</i> .

## 6.3 Materials and Methods

### 6.3.1 Physical models

Three of the five columns used for the CWs were selected as the physical models which would be simulated by HYDRUS. These stages (C, D and E) were chosen because they were designed to remove organic matter and ammonia in the experiment. In the two periods, stage C was used to model organic matter, while stages D and E were chosen to simulate ammonia, nitrite and nitrate. Further details on the dimensions, configuration, components and loading regimes of the systems can be found in chapter 5 (Section 5.2).

### 6.3.2 Initial modelling considerations

Two sets of input data, hydraulic properties and solute transport parameters are essential to model CWs to study nutrient behaviour using HYDRUS-2D/ CW2D. Hydraulic parameters include the inflow volume, inflow rate and hydraulic properties of the CW media. The media hydraulic properties were obtained by

laboratory tests (hydraulic conductivity ( $K_s$ ), moisture content ( $\theta$ )) and the use of the soil water characteristics curve to find the other hydraulic properties of HH sludge. Further laboratory tests were carried out to obtain bulk density and Freundlich adsorption parameter for ammonia.

Solute transport parameters include the pollutant concentrations of the inflow synthetic landfill leachate in the CWs. The inflow solute concentrations were obtained from the measurements taken from each inflow dose of synthetic landfill leachate, carried out over the length of the experiment during the two periods.

### 6.3.2.1 Soil laboratory tests and hydraulic properties

Two of the most important soil hydraulic parameters,  $K_s$  and  $\theta_s$ , were obtained from laboratory tests carried out on the air dried HH sludge. Further laboratory tests were carried out to obtain the other hydraulic properties of the media and bulk density.

The  $K_s$  value of the air dried HH sludge was determined by undertaking a permeability test using the constant head method in accordance with clause 5 of BS 1377-5:1990. The  $K_s$  value was calculated using 4 different flow rates ( $4.31 \text{ cm}^3 \text{ sec}^{-1}$ ,  $14.92 \text{ cm}^3 \text{ sec}^{-1}$ ,  $16.94 \text{ cm}^3 \text{ sec}^{-1}$  and  $18.18 \text{ cm}^3 \text{ sec}^{-1}$ ) and their respective hydraulic gradients (4.2, 21.8, 26.6 and 31.4).

The undisturbed sample was used to determine the bulk density ( $\rho$ ) of the air dried HH sludge samples, adhering to BS 1377-2:1990. This method introduces a risk of human error in the physical measurement of sampling tube dimensions (necessary to determine the dimensions of the soil sample), thus an uncertainty of  $\pm 2 \text{ mm}$  was applied. This uncertainty equates to an approximate error of  $\pm 0.05 \text{ g cm}^{-3}$  in the final values of  $\rho$ . A mean value from five readings was taken in order to minimise the effect of the error.

The soil water characteristic curve was used to find the hydraulic properties of air dried HH sludge using Van Genuchten model (Equation 6.2). A series of specimens are prepared at different volumetric water content, measured soil suction ( $\psi$ ) using chilled- mirror hygrometer. Firstly, six samples of air dried HH sludge were prepared at different moisture content (10%, 20%, 30%, 40%, 50% and 60% of samples weight), and allowed to equilibrate for 24 h. After equilibration, part of the samples was used to measure gravimetric moisture content while, about  $8 \text{ cm}^3$  of each

specimen was used for the total suction measurement. The measurement environment of the device was set to 25°C.

Gravimetric moisture content ( $m$ ) values of the air dried HH sludge samples were determined using oven drying in accordance with ASTM D2216. A drying temperature of 60°C was specified for the samples to prevent oxidation of organic content. This lower temperature needed longer drying periods which was set to 48 h, and check on the mass was made at 2 to 4 h intervals to until a constant mass is reached.

In order to calculate the volumetric moisture content ( $\theta$ ) value of the air dried HH sludge, the bulk density ( $\rho$ ), water density ( $\rho_w$ ) and  $m$  are required. The volumetric moisture content was calculated using Equation 6.8.

$$\theta = \frac{\rho}{\rho_w} m \quad (6.8)$$

Under the conditions of available measured data of the soil suction and volumetric water content, the other parameters of Van Genuchten model have been estimated. Therefore, it is required to quantify the amount by which the measured value differs from an estimated value. Such quantification was made using the root mean square error (RMSE) to evaluate how well the estimator described the measure value as below:

$$RMSE = \sqrt{\left(\frac{1}{n} (\sum_{i=1}^N P_i - M_i)^2\right)} \quad (6.9)$$

Here  $P_i$  and  $M_i$  are, respectively the predicted and measured values of the  $i$ -th measured data (Yang and You 2013).

### 6.3.2.2 Influent pollutant concentrations

Influent pollutant concentration values of the synthetic landfill leachate were measured throughout the experiment during the two period for columns C, D and E. These concentrations were thus available as input values for HYDRUS.

The CW2D module models 12 components in its solute transport equations. These are shown in Table 6.1. Values for all 12 components are required prior to running the model. Of the 12 components,  $NH_4-N$ ,  $NO_2-N$ ,  $NO_3-N$ , and  $O_2$  were measured in the CWs experiment, while  $N_2N$  was set to zero. Because the concentration of

phosphorus was negligible in young landfill leachate in the UK as mentioned in chapter 2 (Table 2.1), therefore the HYDRUS input parameter of PO<sub>4</sub>-P is set to 1 mg L<sup>-1</sup> as it used as nutrient for growth of microorganisms. Concentrations of CR, CS, CI, XH, XANs and XANb (see Table 6.1) were not recorded in the experiment. Influent concentrations of heterotrophic (XH) and autotrophic (XANs and XANb) bacteria were set to zero, as HYDRUS assumes that they are immobile.

Values for CR, CS and CI were estimated. According to the Contrera et al. (2015), the major part of the organic compounds in leachates is volatile fatty acids. This component is readily biodegradable substrate (Pasztor et al. 2009), therefore in this study the COD fraction used is 60:20:20 for CR:CS:CI.

The full list of CW2D solute transport components and the selected input values is shown in Tables 6.3 and 6.4 for periods one and two, and Table 6.5 for one cycle period (4 h).

**Table 6. 3 CW2D solute transport component input concentrations for period 1.**

Stage s	O <sub>2</sub>	CR	CS	CI	XH	XAN s	XAN b	NH <sub>4</sub> N	NO <sub>2</sub> N	NO <sub>3</sub> N	N <sub>2</sub> N	IP
C	5.1	336	112	112	0	0	0	106	0.30	2.47	0	1
D	5.7	215	71	71	0	0	0	76	0.28	3.42	0	1
E	1.8	183	60	60	0	0	0	35	0.31	3.59	0	1

**Table 6. 4 CW2D solute transport component input concentrations for period 2.**

Stage s	O <sub>2</sub>	CR	CS	CI	XH	XAN s	XAN b	NH <sub>4</sub> N	NO <sub>2</sub> N	NO <sub>3</sub> N	N <sub>2</sub> N	IP
C	6.2	261	87	87	0	0	0	75	0.08	3.31	0	1
D	5.2	154	52	51	0	0	0	60	0.11	4.59	0	1
E	0.8	96	32	32	0	0	0	19	0.09	6.13	0	1

**Table 6. 5 CW2D solute transport component input concentrations for one cycle**

Stage s	O <sub>2</sub>	CR	CS	CI	XH	XAN s	XAN b	NH <sub>4</sub> N	NO <sub>2</sub> N	NO <sub>3</sub> N	N <sub>2</sub> N	IP
C	5.1	450	150	150	0	0	0	85	0.08	2.7	0	1
D	5.2	186	62	62	0	0	0	27	0.06	5.2	0	1
E	0.8	126	42	42	0	0	0	17	0.02	7.5	0	1

### 6.3.2.3 Ammonia adsorption isotherm

The adsorption of NH<sub>4</sub>-N on HH sludge was carried out using the batch method. According to Langergraber and Šimůnek (2006), ammonia adsorption is assumed as

a kinetic process. The batch experiments was conducted using the procedure by Karadag et al. (2006). The optimum conditions for the adsorption batch study, such as equilibrium time and adsorbent dosage, were taken from previous study (Karadag et al. 2006). A different initial concentration of ammonia solutions (50 ml) ranging from 20 mg L<sup>-1</sup> to 200 mg L<sup>-1</sup> were equilibrated with 0.5 g of HH sludge. Synthetic ammonia solutions were prepared by dissolving (NH<sub>4</sub>)<sub>2</sub>SO<sub>4</sub> salt in deionised water. The bottles were placed in shaker for 60 minutes and then centrifuged at 200 rpm. After the set equilibrium time, the mixtures were withdrawn, filtered and analysed for residual ammonia concentration using Hach DR/3900 spectrophotometer according to its standard operating procedures. Ammonium uptake ( $q_e$ ) was calculated using the following Equation:

$$q_e = \frac{(C_o - C_e) v}{m} \quad (6. 10)$$

where  $C_o$  and  $C_e$  (both in mg L<sup>-1</sup>) are the initial (t=0) and final ammonia concentrations at equilibrium ( $q_e$ ), respectively,  $q_e$  is the mass of ammonia adsorbed on the adsorbent (HH sludge) at equilibrium (mg g<sup>-1</sup>),  $v$  is the volume of the solution (L) and  $m$  is the mass of HH sludge used (g).

### 6.3.3 HYDRUS modelling

Modelling in HYDRUS was conducted in 3 stages. These were:

1. Simulation of the columns C, D and E CWs. Model calibration was conducted hydraulically using soil water characteristic curve to estimate values of the HH sludge hydraulic properties
2. Simulation of the validated model to test nutrient (COD and NH<sub>4</sub>-N) removal efficiencies against real data for two cycles (8 h).
3. Further investigation of the use of the validated model to test nutrient (COD and NH<sub>4</sub>-N) removal efficiencies against real data within first period (220 days) and second period (185 days).

The 2D finite element meshes of 96 nodes and 120 triangle finite elements were used for simulation as shown in Figure 6.1. In particular, the vertical rectangular transport domain 65 cm deep and 10 cm width (2 columns and 30 row) was constructed in

HYDRUS similar to the dimensions of the column CWS (dimensions described in chapter 5 section (5.2.1.1)).

Time steps were discretized for the numerical simulation using initial, minimum and maximum time steps of 0.001 h, 0.0001 h and 1 h respectively for the flow simulation.

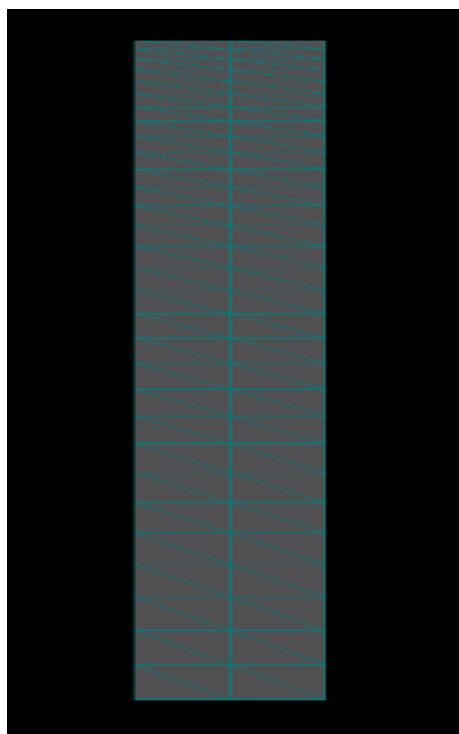


**Figure 6. 1 Finite element mesh as displayed in HYDRUS**

The model was firstly run over a 24 h simulation period. Water flow parameters were initially calculated by selecting sand soil. Sand from soil catalogue was chosen because the value of  $K_s$  for HH sludge was within the range of the sand soil.

The  $K_s$  and  $\theta_s$  values were then replaced with the value obtained from experiments to increase model accuracy. Finally and for improved model accuracy, the values of  $\theta_r$ ,  $\alpha$  and  $n$  for HH sludge were then replaced with the values obtained from experiments (soil water characteristic curve).

The influent flow rate (as determined in chapter 5) was converted to a precipitation rate:  $255 \text{ cm h}^{-1}$  applied over 0.1 h over the surface of the C, D and E CW model. Variable flow (for 0.1 h) was set to same number as top and bottom boundary conditions to guarantee that the same amount of water that is loaded comes out for column C and D. Here, the inflow and outflow was set in such a way that the top of the columns remain unsaturated. While for column E, the upper boundary of the CW

profile was designated an atmospheric boundary condition and the lower boundary was designated as constant head to create fully saturated condition in this column.

The model was run for a simulated time of 24 hours, with the inflow being applied at time  $t = 0$ . After the simulation, the final modelled boundary flux values throughout the CW was checked and due to unstable boundary flux, the result was saved and imported into a duplicate model. This duplicate model was then run with the same flow parameters as the original and its final water conditions were saved and imported into a second duplicate model. The process was repeated until steady state behaviour for water flux was achieved.

The same iterative process was used to establish the initial background solute concentrations in the model media. In the first iteration, the pollutant concentrations were set to the concentrations found in the synthetic landfill leachate (Table 6.3 for first period, Table 6.4 for second period and 6.5 for one cycle). The maximum time step for solute transport was set to 0.02 due to fast oxygen consumption.

## 6.4 Results and Discussions

### 6.4.1 Results of soil laboratory tests

The saturated hydraulic conductivity analysis gave a result of  $K_s = 39.6 \text{ cm h}^{-1}$  while average bulk density was calculated as  $\rho = 723 \text{ Kg m}^{-3}$ .

The result of gravimetric and volumetric moisture content was calculated using Equation 6.8 shown in Table 6.6 where  $\rho_w$  assume equal to  $1 \text{ g cm}^{-3}$ .

**Table 6. 6 Gravimetric and volumetric moisture content for HH sludge.**

Sample no.	$m \%$	$\theta \%$
1	7.60	5.50
2	16.60	12.00
3	26.86	19.42
4	38.00	27.45
5	61.10	44.22
6	66.22	47.88

## 6.4.2 Hydraulic properties

The hydraulic properties of HH sludge were determined using Van Genuchten model and soil water characteristic curve. Under the condition of variable measured data of the sludge water content and water potential, the Van Genuchten parameter can be estimated by trial and error method. The difference between estimated and measured values were quantified using root mean square error (Equation 6.9) as shown in Table 6.7 and Figure 6.2. The summation value of root mean square error =  $7.47 \times 10^{-4}$ .

**Table 6. 7 Measured and predicted values of volumetric water content at different section.**

Sample no.	Section $\psi$ (Kpa)	Measured $\theta$ ( $\text{cm}^3 \text{cm}^{-3}$ )	Predicted $\theta$ ( $\text{cm}^3 \text{cm}^{-3}$ )	RMSE
1	121450	0.05500069	0.053526	$2.18 \times 10^{-6}$
2	4300	0.1203552	0.117204	$9.93 \times 10^{-6}$
3	2100	0.1941557	0.174895	$3.72 \times 10^{-4}$
4	1000	0.2705056	0.264202	$3.97 \times 10^{-5}$
5	120	0.442215	0.449853	$5.83 \times 10^{-5}$
6	60	0.478754	0.462488	$2.65 \times 10^{-4}$

From Table 6.7 and Figure 6.2 and with exception of  $l$  value, the hydraulic properties of HH sludge are summarised in Table 6.8, whilst the hydraulic properties for other layers (15 cm of gravel on the top and 10 cm of drainage layer (Chapter 5 section 5.2.1.1)) and  $l$  value were obtained using literature values (Langergraber and Slmunek 2005; Langergraber 2008). Table 6.8 shows the soil hydraulic parameters for three layers in column C, D and E.

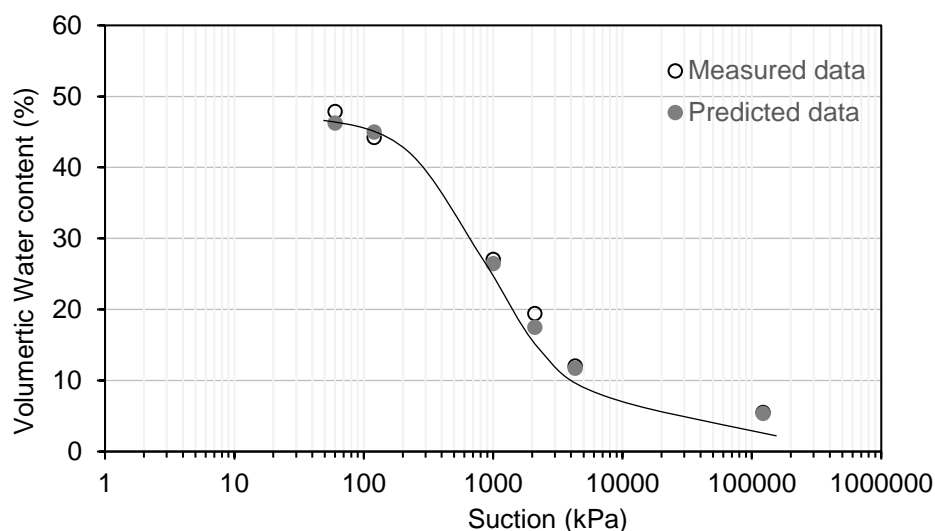


Figure 6. 2 Soil water characteristic curve

Table 6. 8 Van Genuchten – Mualem soil hydraulic parameters for column C, D and E.

Layers	Residual water Content $\theta_r$ ( $m^3 m^{-3}$ )	Saturated water Content $\theta_s$ ( $m^3 m^{-3}$ )	Parameter			Saturated hydraulic conductivity $k_s$ ( $cm h^{-1}$ )
			$\alpha$ ( $cm^{-1}$ )	$n$	$l$	
Top layer	0.045	0.41	0.145	5	0.5	600
Main layer	0.051	0.47	0.0015	1.48	0.5	39.6
Drainage layer	0.056	0.289	0.126	1.92	0.5	840

### 6.4.3 Freundlich isotherm model for ammonia adsorption

The linear form of Freundlich Equation is shown in Table (3.1) chapter 3. The isotherm equation and correlation coefficient are given in Figure 6.3. From this figure, the Freundlich constant  $K_f$  ( $L mg^{-1}$ ) which was used as adsorption isotherm coefficient in the model, is equal to  $0.047 L g^{-1}$ .

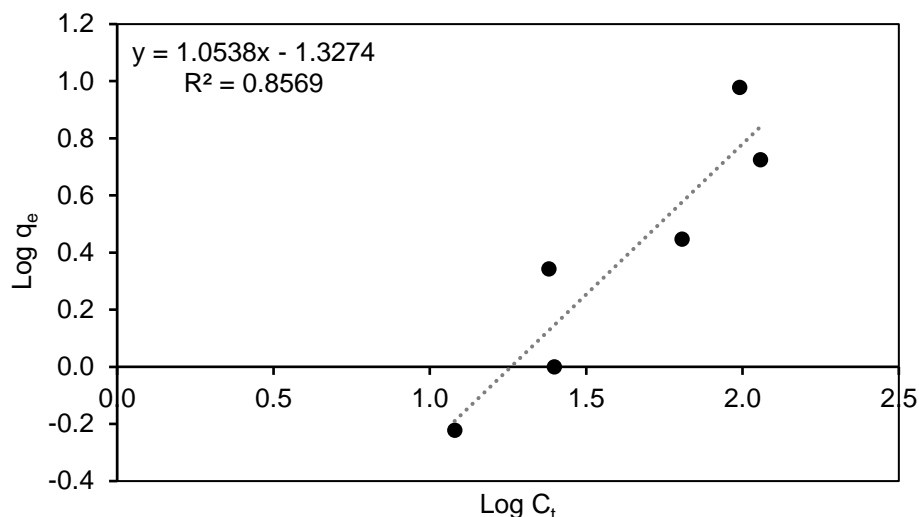


Figure 6. 3 Freunlich plot for ammonia adsorption

#### 6.4.4 HYDRUS modelling result

##### 6.4.4.1 Water flow

The flux effluent results from the measured and HYDRUS software are shown in Figure 6.4 for column C and D, and Figure 6.5 for column E. The results of the step-by-step adjustment through the use of  $K_s$  and  $\theta_s$  values and then other hydraulic parameter is also shown. It was apparent that the calibration of the hydraulic parameters of the model sand soil was required through the use of soil water characteristic curve as described in 6.4.2. The simulation results using these parameters showed good match with measured effluent flux as shown in Figures 6.4 and 6.5. These results indicate that a good calibration of the flow model requires measurement of at least the  $K_s$  and  $\theta_s$  of the main layer.

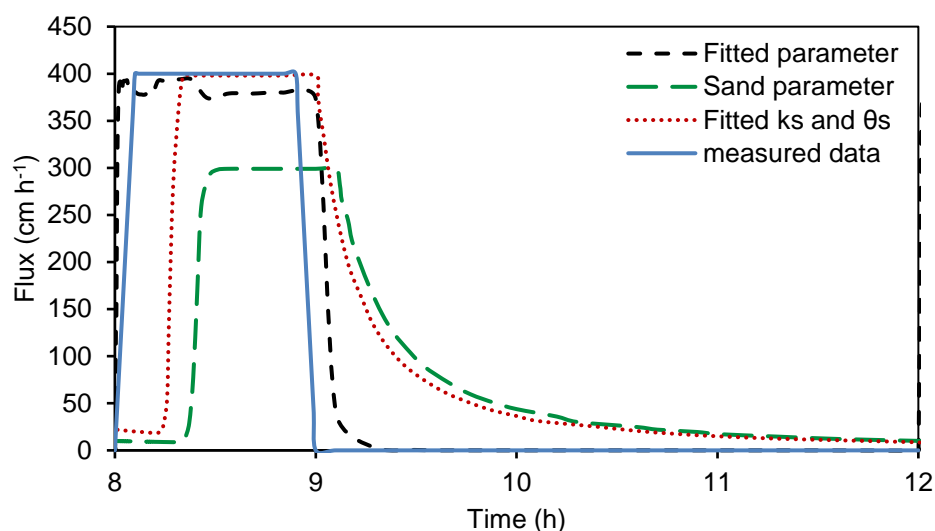


Figure 6. 4 Flux effluent results of measured data and HYDRUS model output, per calibrated parameter for column C and D.

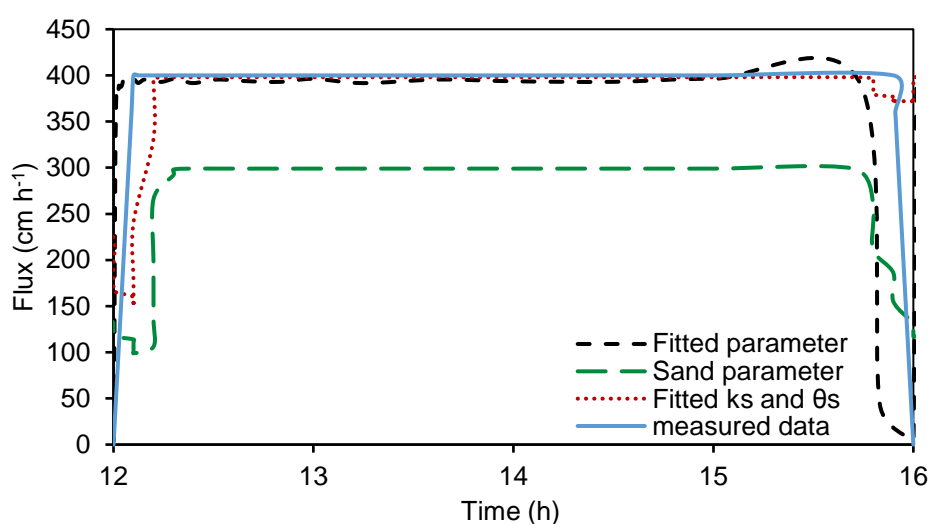


Figure 6. 5 Flux effluent results of measured data and HYDRUS model output, per calibrated parameter for column E.

#### 6.4.4.2 Simulation result for one cycle

##### 6.4.4.2.1 Column C CWs Simulation result

Since column C was designed to remove organic pollutants by employing tidal flow strategy as discussed in section 5.2.3 chapter 5, this section is focused on the result for simulated and measured COD effluent concentration. Figures 6.6 and 6.7 shows time series of DO and COD effluent concentration for two consecutive loadings to the

main layers. During the aeration period, the DO concentration increases to reach the maximum value ( $5.5 \text{ mg L}^{-1}$ ) within one hour for the first layer, and more than one hour for the second layer. This could be due to limited DO diffusion within HH sludge (Wang et al. 2008). Diffusion and water flow then moved oxygen through the column where it was consumed by heterotrophic or autotrophic bacteria. With a high concentration of oxygen such as in this stage, heterotrophs grow quickly until readily biodegradable organic matter reached a threshold low concentration. COD fate was clearly related to oxygen concentration, where oxygen was available COD decreased immediately after loading (Figure 6.7).

Simulation result in Figure 6.7 showed a good match between simulated data and measured data for COD effluent concentration for two cycles, with a mean percent error ( $\text{MPE} = ((m-s)/m) \times 100$ ) of 14.7%. Where  $m$  and  $s$  represent measured and simulated values respectively.

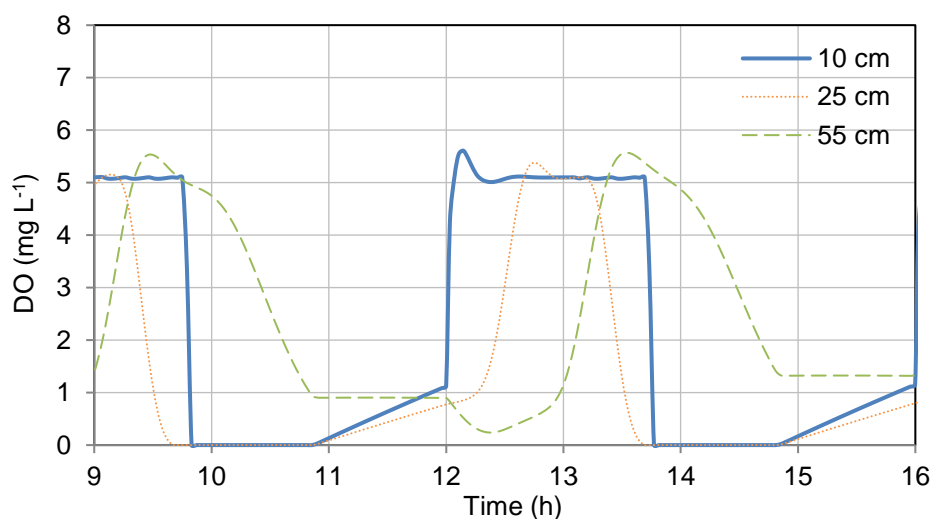


**Figure 6. 6 Simulated time series for DO within two main layers for two consecutive loadings for column C**

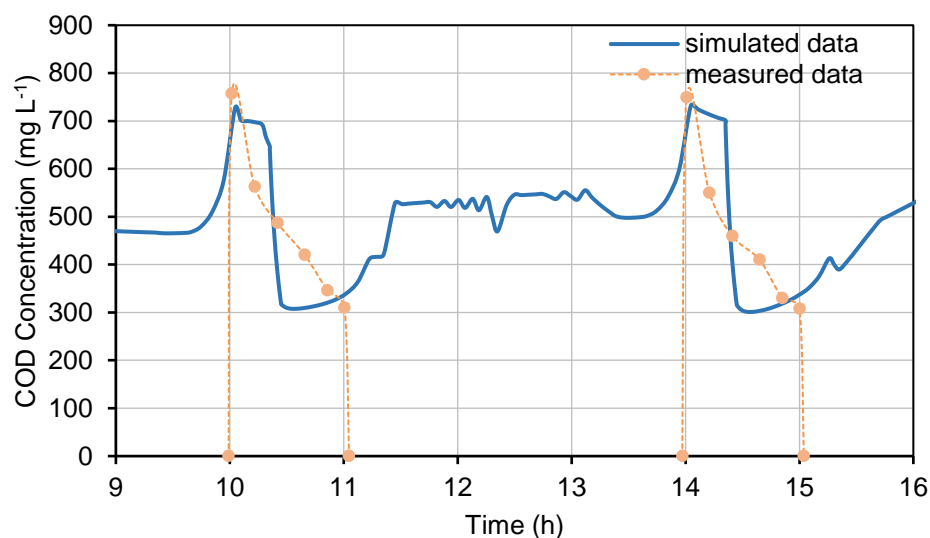


Figure 6. 7 Simulated and measured effluent concentration of COD for two consecutive loadings for column C

#### 6.4.4.2.2 Column D CWs Simulation result

Column D was designed to remove  $\text{NH}_4\text{-N}$  by applying tidal flow strategy and recirculating the effluent at ratio 1:1, as discussed in section 5.2.3 chapter 5. The simulation results for  $\text{NH}_4\text{-N}$  and  $\text{NO}_3\text{-N}$  effluent concentration are presented in Figures 6.8 and 6.9 respectively.

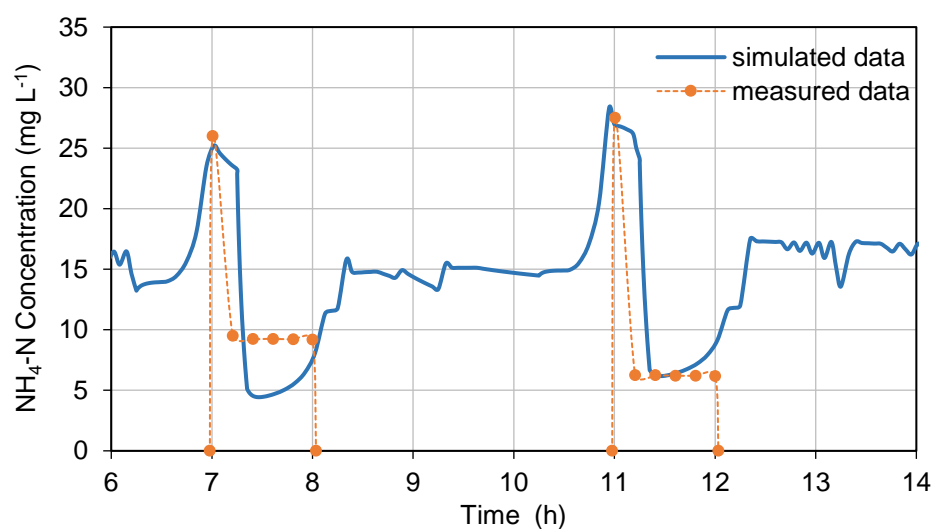
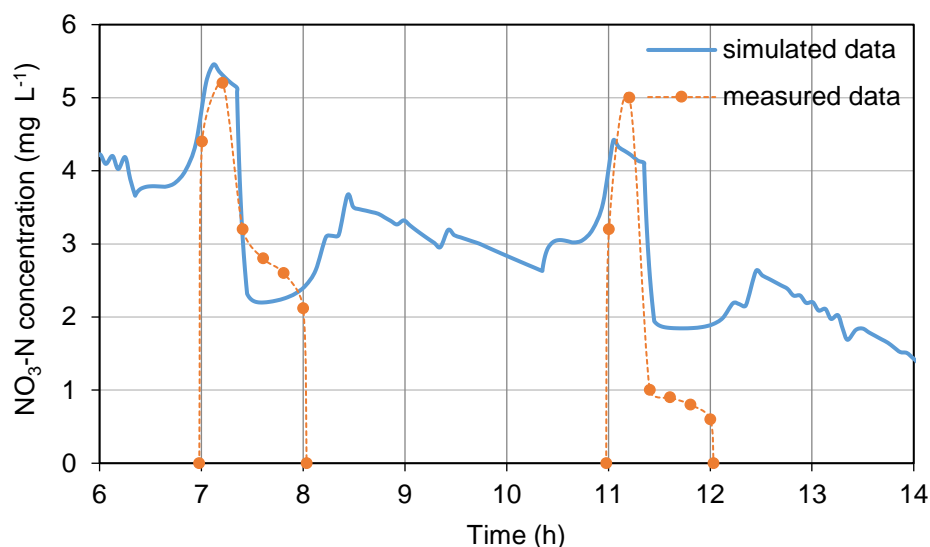


Figure 6. 8 Simulated and measured effluent concentration of  $\text{NH}_4\text{-N}$  for two consecutive loadings for column D



**Figure 6. 9 Simulated and measured effluent concentration of NO<sub>3</sub>-N for two consecutive loadings for column D**

The simulation results show an initial increase of NH<sub>4</sub>-N concentration during loading. Thereafter, there was a sharp decrease due to nitrification process. It was also noticed that there was a small increase in NH<sub>4</sub>-N concentration, and this may be due to the lysis of heterotrophic and autotrophic bacteria, or due to the fact that the model cannot predict pollutant degradation during dry periods (Stefanakis et al. 2014). The measured data had a good match with simulated data for two consecutive cycles with MPE of 27%. The measured result also showed that the tidal flow column had high oxygen availability so all the influent NH<sub>4</sub>-N was quickly oxidized within first 20 minutes.

The result from simulated and measured NO<sub>3</sub>-N effluent concentration showed the same trend of NH<sub>4</sub>-N (Figure 6.9). After initial increase due to loading, there was a sharp decrease in simulated and measured values of NO<sub>3</sub>-N which confirms that simultaneous nitrification and denitrification can occur as discussed in section 5.3.5.2 chapter 5.

#### 6.4.4.2.3 Column E CWs Simulation result

Column E was designed to enhance total nitrogen removal, therefore anoxic condition was employed in this column as explained in section 5.2.3 chapter 5.

Figures 6.10, 6.11 and 6.12 show the time series of DO, NH<sub>4</sub>-N and NO<sub>3</sub>-N effluent values for two consecutive loadings to the main layers.

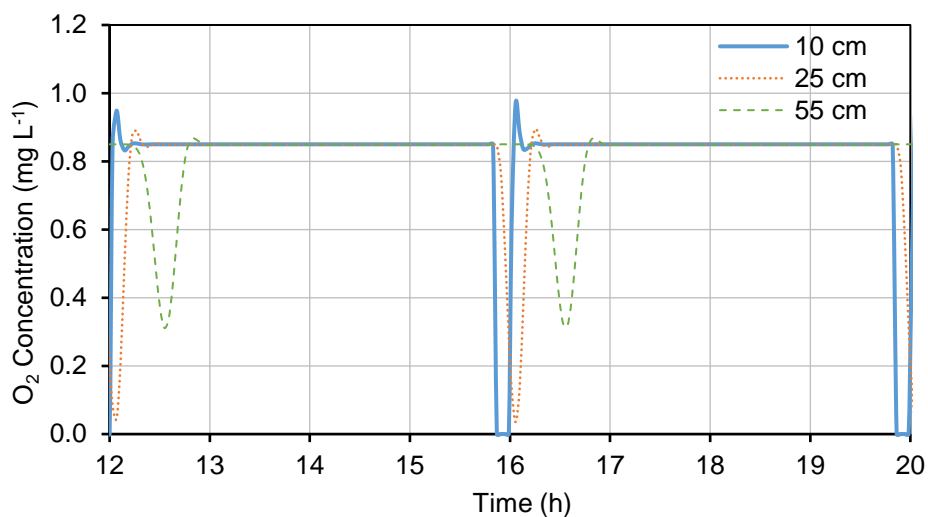


Figure 6. 10 Simulated time series for DO within two main layers for two consecutive loadings for column E

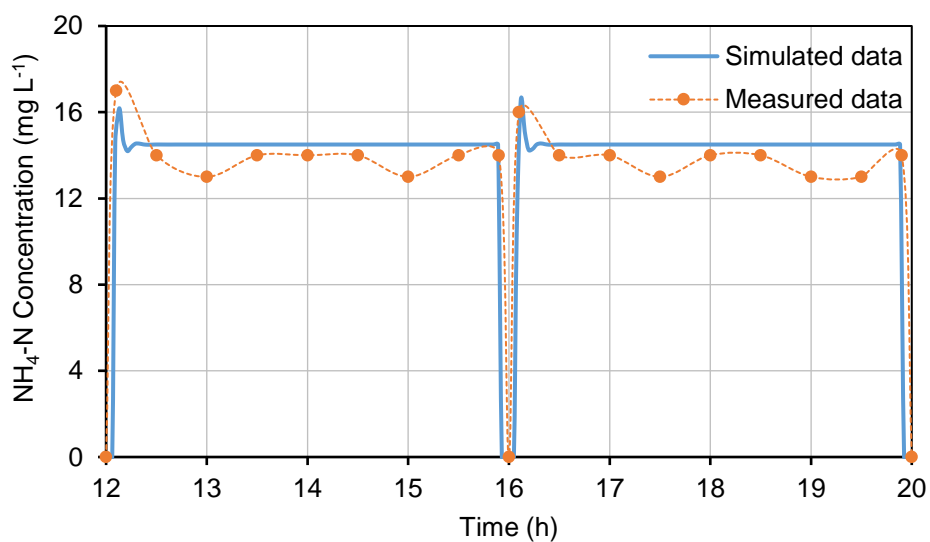
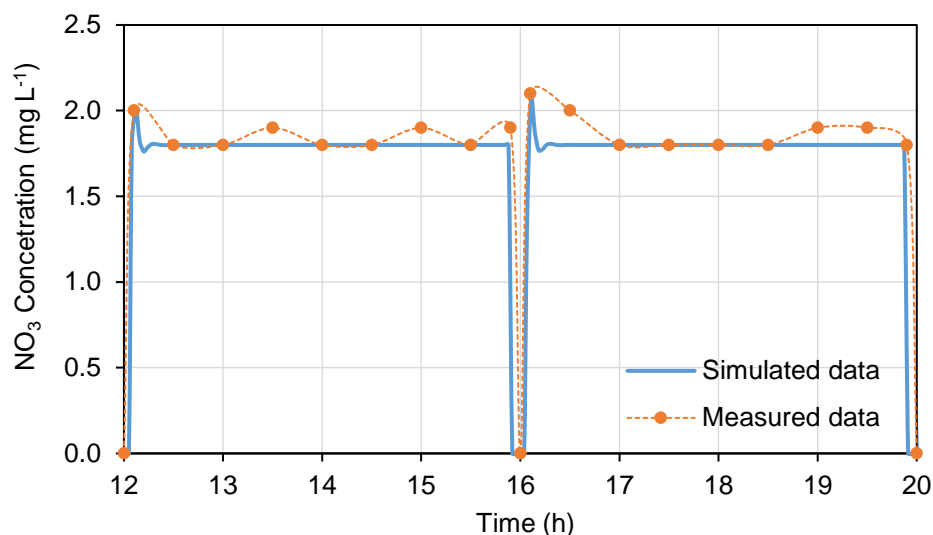


Figure 6. 11 Simulated and measured effluent concentration of NH<sub>4</sub>-N for two consecutive loadings for column E



**Figure 6. 12 Simulated and measured effluent concentration of NO<sub>3</sub>-N for two consecutive loadings for column E**

The simulated data for DO, NH<sub>4</sub>-N and NO<sub>3</sub>-N revealed that there is no oxygen consumption at depths 10 cm and 25 cm, and as a result there is no nitrification occurring in this depths. However, at depth 55 cm there is oxygen consumption which means that even in saturated condition, oxygen diffusion allowed for nitrification process at depth 55 cm below the water surface although oxygen diffusion was very slow in saturated sludge. The measured data for NH<sub>4</sub>-N effluent concentration (Figure 6.11) indicates that some NH<sub>4</sub>-N had been convert to NO<sub>3</sub>-N by nitrification. In this stage, oxygen in the wastewater influent was quickly consumed by the heterotrophs. Autotrophic growth occurred as well, but because the oxygen was quickly depleted, nitrification was less than in the other stages which used the tidal flow strategy. However there is simultaneous nitrification and denitrification occurring in this stage as well as in stage D where tidal flow strategy was employed.

### 6.4.4.3 Simulation result for first and second periods

#### 6.4.4.3.1 Column C CWs simulation result

The result from measured and simulated COD effluent concentrations are reported in Figures 6.13 and 6.14 for periods 1 and 2 respectively. Quasi-steady-state conditions have been obtained after about 20 days of simulation time for each period.

Figure 6.13 highlight a good match between measured and simulated values of COD concentrations with a MPE of 23.42% for the first period. From Figure 6.13, it can be seen that the model did not simulate the high value of effluent COD concentrations at between 80 and 180 days. This could be due to the clogging which occurred in August 2015 and in November 2015 as discussed in chapter 5 (Section 5.3.3). To solve the clogging problem, column C was firstly left to rest for 2 weeks and this may have had an effect on the growth of heterotrophic bacteria, and therefore affect the removal efficiency of COD for the next period. Thereafter backwashing was applied when the resting of column C did not solve the clogging problem. Finally column B had was added to the system in period 2 as described in chapter 5 (Section 5.2.3). Clogging can cause pore size reduction and affect the hydraulic properties of the substrate (Langergraber and Slmůnek 2005). One limitation of HYDRUS software is clogging phenomena, since HYDRUS software only considers the dissolved solute (Langergraber and Slmůnek 2005).

The result for the second period as shown in Figure 6.14 indicates that there is a very good match between the measured and simulated data for effluent concentration of COD, with MPE of 8.7% for the second period. This was expected since the problem of clogging had been solved by adding column B to the system as explained in chapter 5 (Section 5.2.3). However, the model did not simulate the low values of COD. The influent of COD was more likely divided between readily biodegradable, slowly biodegradable and inert organic matter. In this study, COD fractions were estimated as explained in section 6.3.2.2, but it seems to be inappropriate because the simulation created slow biodegradation of COD rather than removing up to  $268 \text{ mg L}^{-1}$  as observed in the laboratory experiments (Figure 6.14). Slowly biodegradable organic matter decays too slow through hydrolysis or is produced too quickly by biological decay (Fuchs 2009).

#### **6.4.4.3.2 Column D CWs simulation result**

Figures 6.15 and 6.16 show time series for  $\text{NH}_4\text{-N}$  in period 1 and period 2 respectively. The simulation result show a very good match with measured  $\text{NH}_4\text{-N}$  effluent values with MPE of 13.3% and 6.4% for periods 1 and 2 respectively. However, the model did not simulate the high and low  $\text{NH}_4\text{-N}$  measured values for both periods. It is likely that these parameters are dependent on environmental conditions such as temperature, soil characteristics, and wastewater constituents (Fuchs 2009). A second reason that the model might have underestimated nitrogen

removal is that it did not include the influence of plant presence and this is because of high nitrogen loading rate in this study which about  $117 \text{ gN m}^{-2} \text{ day}^{-1}$  for period 1 and  $92 \text{ gN m}^{-2} \text{ day}^{-1}$  for period 2, which is far beyond nitrogen uptake by plant of  $0.083 \text{ gN m}^{-2} \text{ day}^{-1}$  (Kadlce and Wallace 2008). However, plant can release DO which contribute in nitrification process (Brix 1994; Toscano et al. 2009).

#### **6.4.4.3.3 Column E CWs simulation result**

Figures 6.17 and 6.18 show time series for  $\text{NO}_3\text{-N}$  effluent concentration in period 1 and period 2 respectively. The simulation result shown a good match with measured  $\text{NO}_3\text{-N}$  effluent values with MPE of 14.8% and 14% for periods 1 and 2 respectively. Initial DO was high enough causing nitrification in this stage (Figure 6.10) and increasing  $\text{NO}_3\text{-N}$  concentration. However, there is sharp decrease in  $\text{NO}_3\text{-N}$  concentration (Figures 6.17, 6.18) in this stage as denitrification process occur simultaneously as explained in Section 5.3.5.2 chapter 5. COD and  $\text{NO}_3\text{-N}$  were balanced in the laboratory synthetic wastewater so that there would be enough carbon to denitrify all potential nitrate. The  $\text{CR}/\text{NO}_3\text{-N}$  ratio were  $50 \text{ mgCR}/ \text{mgNO}_3\text{-N}$  and  $15 \text{ mgCR}/ \text{mgNO}_3\text{-N}$  for periods 1 and 2 respectively, which means there was enough readily available carbon in the fractionation used in this study for denitrification.

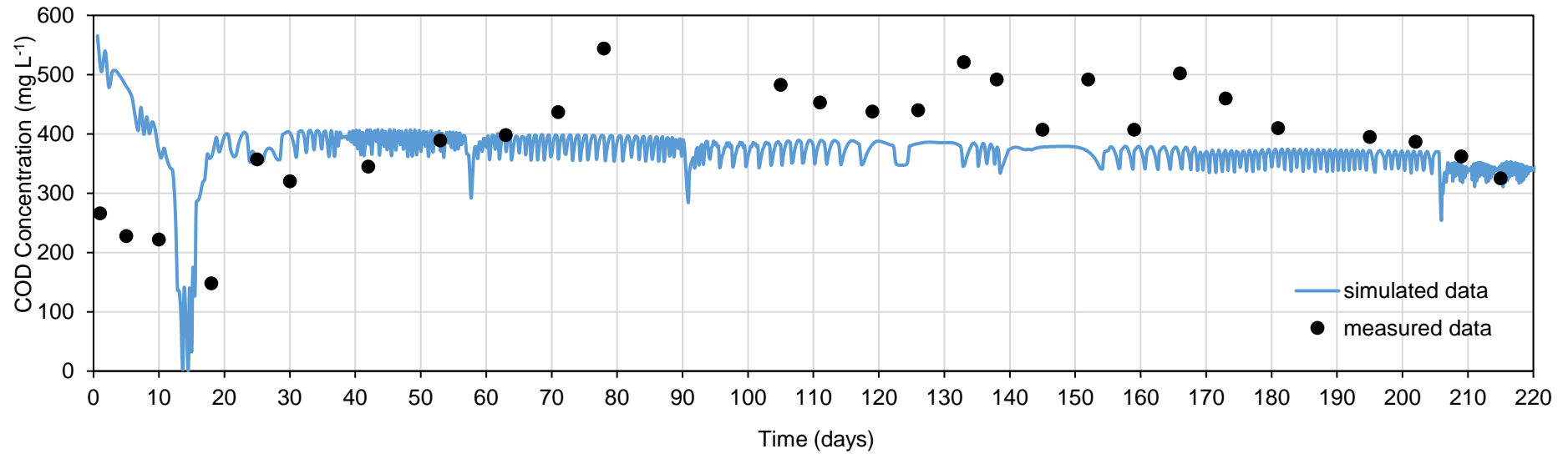


Figure 6. 13 Measured and simulated data of effluent COD for Column C at 215 days for period 1.

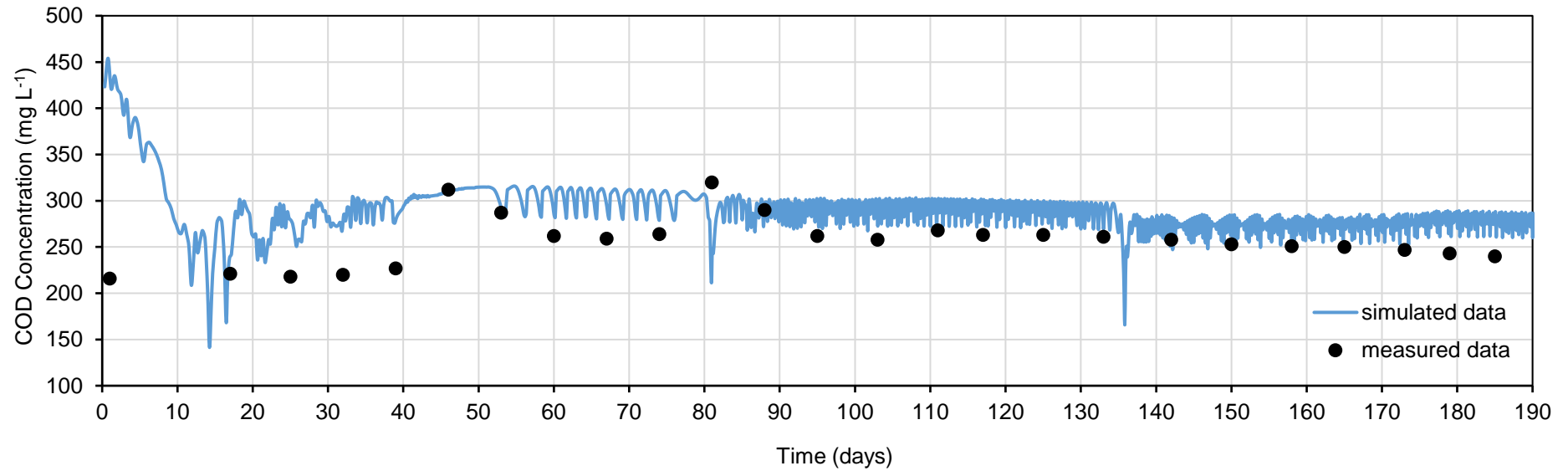


Figure 6. 14 Measured and simulated data of effluent COD for Column C at 185 days for period 2.

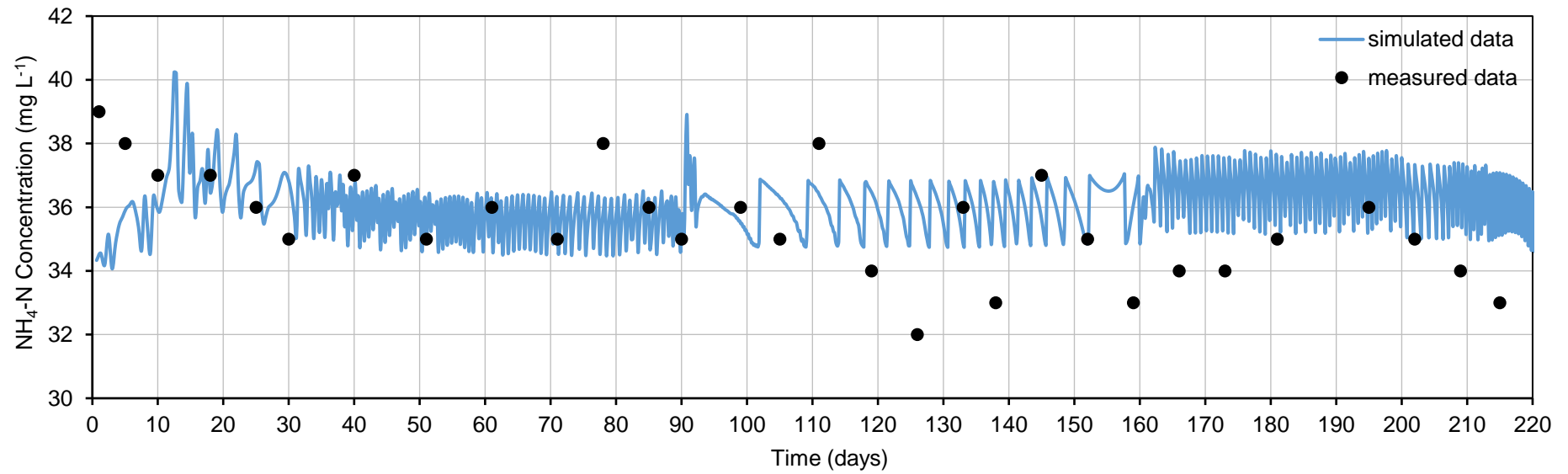


Figure 6. 15 Measured and simulated data of effluent  $\text{NH}_4\text{-N}$  for Column D at 215 days for period 1.

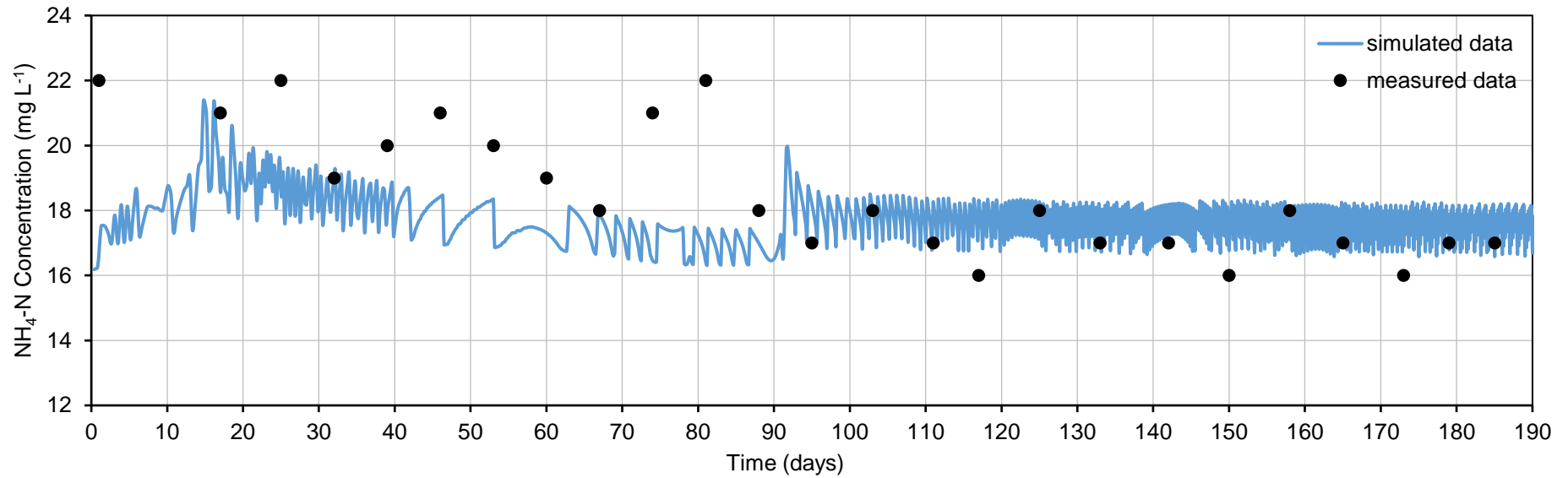


Figure 6. 16 Measured and simulated data of effluent NH<sub>4</sub>-N for Column D at 185 days for period 2.

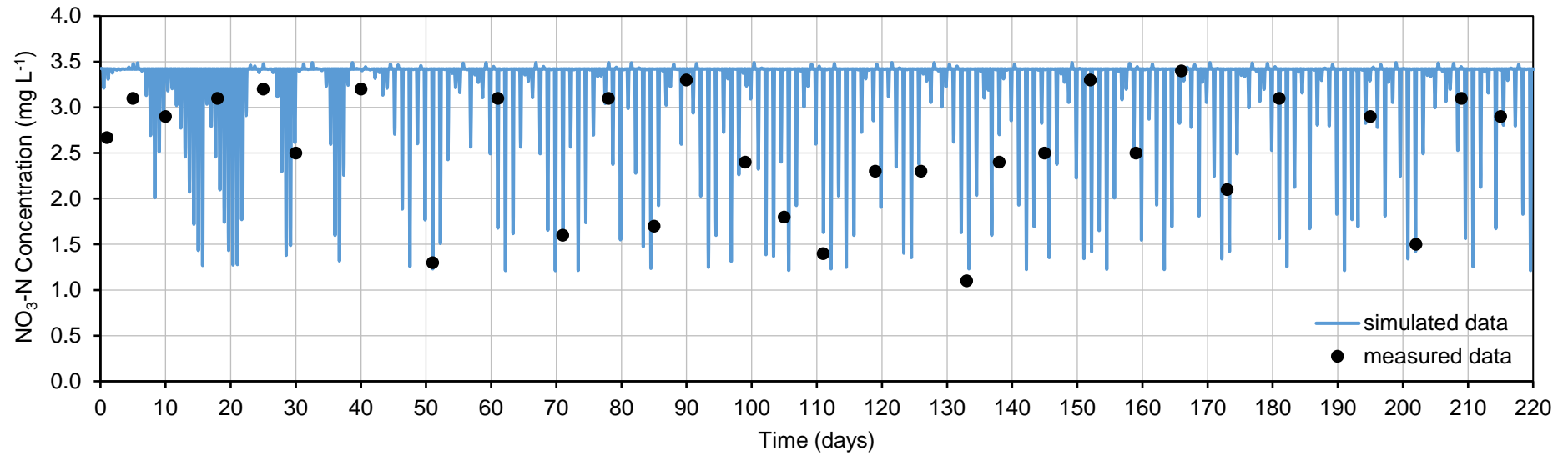


Figure 6. 17 Measured and simulated data of effluent NO<sub>3</sub>-N for Column E at 215 days for period 1.

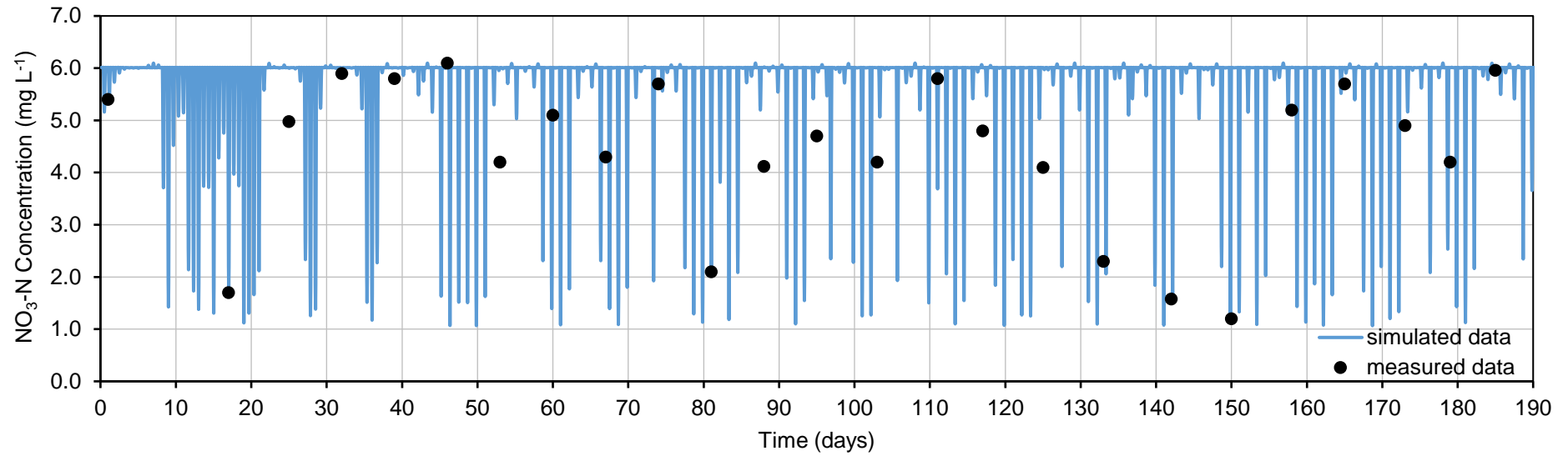


Figure 6. 18 Measured and simulated data of effluent NO<sub>3</sub>-N for Column E at 185 days for period 2.

## 6.5 Conclusion

HYDRUS-2D/CW2D is a complex module and high-quality data was collected for many processes and characteristics of vertical flow wetland columns that can be described by the model.

A good match between simulated data and experimental result was achieved when sufficient data was available to describe the hydraulic behaviour of the HH sludge. Thus, the flow model was successfully calibrated in this study by using the hydraulic parameter derived from Van Genuchten model.

The result for COD effluent concentration from the measured data for the first period showed that 55% of these data were higher than the simulated data. This is mainly because of clogging phenomena which is not considered by the model, and it is one of the limitation of the model.

The model did not simulate the high and low values of  $\text{NH}_4\text{-N}$  effluent concentration. A reason that the model might have underestimated nitrogen removal is that it did not include the influence of plant presence. Plants may increase oxygen as compared to the model, decrease ammonium, and decrease nitrate. In addition the model confirm that the removal of nitrogen in this study was through simultaneous nitrification and denitrification which occurred in the tidal flow and in anoxic condition.

# **Chapter 7**

## **Modelling heavy metals transformation in CWs treating landfill leachate**

## 7.1 Introduction

The efficiency of CWs systems for wastewater treatment is commonly evaluated by a comparison between influent and effluent concentrations. However, this is considered to be figurative black-box since there is no information about the biological and physicochemical processes occurring in the CWs. Unlike organic pollutants, HM cannot be degraded through biological processes. Understanding the mechanism of HM removal has expanded concurrently with increased adoption and usage of CWs (Kosolapov et al. 2004). Marchand et al. (2010) indicated that there are four main processes for metals removal in CWs. These include adsorption to fine textured sediments and organic matter; precipitation as insoluble salts (mainly sulphides and oxyhydroxides); absorption and induced changes in biogeochemical cycles by plants and bacteria; and deposition of suspended solids due to low flow rates. However, adsorption represents an important mechanism for removal of metals in CWs. Therefore, to ensure efficient HM removal, it is important to use substrates with high HM removal capacity and suitable physicochemical properties. A low-cost material that can enhance HM removal is dewatered sludge from drinking water treatment processes. It is available worldwide and is mostly landfilled at huge costs since it is regarded as a waste with little known reuse value. Previous investigations (Table 3.3, in chapter 3) had identified a particular drinking water treatment sludge, HH as having physicochemical properties that gives it a highly reactive surface and strong affinity for HM.

Plants can also play an important role in CWs for the removal of pollutants. They take up nutrients and they are also able to adsorb and accumulate metals (Cheng et al. 2002). Moreover, *Phragmites australis*, known as common reed, is widely used in CWs for treatment of urban and industrial wastewaters containing metals (Bonanno and Lo Giudice 2010).

Modelling of HM removal in CWs is important with regards to understanding the HM behaviour in the integrated treatment processes. Various modelling tools including FITOVERT, CW2D, PHWAT and CWM1 have been used to understand the processes in CWSs (Kumar and Zhao 2011). However, all these models have been used to simulate the hydraulic properties or degradation of pollutants. In this chapter,

---

Part of this Chapter has already been published as 'Modelling heavy metals transformation in vertical flow constructed wetlands' - A. Mohammed; A.O. Babatunde, Journal of Ecological Modelling, Volume 345, March 2017, 62- 71.

the fate of Pb, Cr and Cd in a VF CWs was investigated through the development of a mathematical model using STELLA v9.0.2 software. STELLA's is a quantitative systems modelling software that was developed to allow modellers specify system element, their interrelationships and whether the elements are positively or negatively correlated. At the same time, this model necessitate the modeller to specify exact values and mathematical equations to describe model elements and relationships. In contrast, the behaviour of individual is allowed to be controlled and tracked by the modeller (Jeyakumar 2013).

Several authors have used STELLA to describe the adsorption processes in CWs which use different kinds of substrate and for different types of pollutant. However, the use of this model to study the fate of HM is limited. Pimpan and Jindal (2009) explained the adsorption, desorption and plant uptake in laboratory scale FWF CWs planted with bulrush using the STELLA software. However, they used clay loam soil and sand mixture as a main media.

In this chapter the fate and transformation of HM in a VF CWs was investigated through the development of a model using the information on STELLA presented by Jørgensen & Fath (2011) and Jeyakumar (2013). The key objectives were:

- (1) To develop a dynamic model for simulating adsorption, plant uptake and growth from the VF CWs, which uses ferric dewatered sludge (HH) as main substrate.
- (2) To calibrate the model using the available experimental data.
- (3) To apply the model to simulate the fate of HM in the VF CWs.

## **7.2 Material and Method**

### **7.2.1 Setup of HH sludge dewatered sludge VFCW**

A laboratory scale VF CWs system was set up outdoors and operated using anoxic condition for a first period of 220 days using one column (A), and 185 days for the second period using two columns (A+B) as described in chapter five (5.2.1).

## 7.2.2 Description of the model

According to Jay Forrester's systems dynamics language (Jeyakumar 2013), STELLA is a graphic and dynamic simulation software. Using iconographic modelling techniques made the model a flexible simulation tool that makes it easy for the user to make change and calibrate. The user can immediately view the effect of changes, thereby model development time (Jørgensen and Fath 2011).

In this chapter, a conceptual diagram illustrating the adsorption processes, plant uptake and plant growth are shown in STELLA diagrams (Figure. 7.1- 7.3) for Pb, Cr and Cd respectively. The major mechanisms for HM dynamics in CWs considered in this study were adsorption and plant uptake. The system was operated to be fully saturated for 3 hours and 50 minutes and unsaturated for 10 minutes. Such high HRT allow for higher contact between wastewater and HH sludge and enhance adsorption process (Stefanakis et al. 2014). The developed models have five state variables (STOCK) including dissolved HM (DISPb, DISCr and DISCd), plant HM (PLPb, PLCr and PLCd) which means the heavy metals that are available for plant uptake and those that are present as soluble components in the soil solution, plant biomass (PLBPb, PLBCr and PLBCd) which means certain heavy metals required for plant growth and upkeep, detritus HM (DETPb, DETCr and DETCd) is the HM bond to the organic material with a wide range of biodegradable and adsorption (ADSPb, ADSCr and ADSCd), all the state variables are expressed in the unit of mg of HM per days. In STELLA terminology, STOCK is a noun and represent anything that accumulates which means flows coming in or out of them. While a STOCK is a noun in the language of STELLA, a FLOW is a verb that has activity to change the magnitudes of a STOCK. The FLOW in this study includes (INPb, INCr and INCd), (OPb, OCr and OCd), Up, Mp, De, Ad and Gr. Converter is used in model to modify FLOWS and calculate the initial values of STOCK. The converters in this model are (OUTPb, OUTCr and OUTCd), (OBSPb, OBSCr and OBSCd), (PbP, CrP and CdP), (Pbmin, Crmin and Cdmin), (Pbmax, Crmax and Cdmax), C0, F, Um, Ku, Mr, Mm, T, V, Fa, TA, KF, n, Gm and Kr. Finally, an action connector represent relationships between two items in STELLA model have been transmitted an input or an output.

Adsorbent type, HM concentration and temperature were considered as a major forcing function in the model. Detailed description of STELLA window responsible for removal and HM dynamics are presented below (Figures 7.1- 7.3). The state



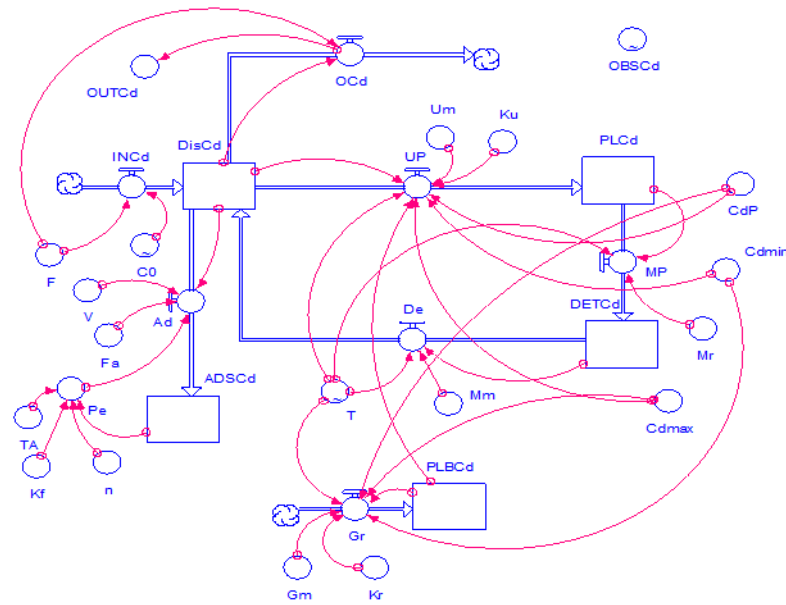


Figure 7. 3 STELLA diagram for the Cd model.

### 7.2.3 Michaelis- Menten equation for plant uptake and growth

In order to find the maximum uptake rate of plants, uptake rate of HM, maximum HM for growth rate of plant and plant growth rate, Michaelis- Menton half saturated equation was used.

#### 7.2.3.1 Plant germination and HM uptake

The effects of different concentrations of Pb ( $0.2 \text{ mg L}^{-1}$ -  $3 \text{ mg L}^{-1}$ ), Cr ( $0.2 \text{ mg L}^{-1}$ -  $2 \text{ mg L}^{-1}$ ) and Cd ( $0.05 \text{ mg L}^{-1}$ - $1.5 \text{ mg L}^{-1}$ ) on plant uptake were evaluated. The concentration of HM has been chosen according to the concentration of HM found in *Phragmites australis* in CWs (Kadlec and Wallace 2008). The Pb, Cr and Cd solutions were freshly prepared by dissolving  $\text{PbCl}_2$  salt,  $\text{Cr}(\text{SO}_4)_2 \cdot 12\text{H}_2\text{O}$  salt and  $\text{CdSO}_4 \cdot \text{H}_2\text{O}$  salt in deionized water. A total of 42 samples of rhizome fragments (14 for each HM) were placed in 100 mL glass flask filled with tap water. The rhizome fragments were then incubated in the Cardiff University's CLEER laboratory at  $20 \pm 3^\circ\text{C}$  for 10 days. Rhizome fragments were considered to have germinated when both the plumule and radicle growth were over 2 cm long (Figure 7.4). They were then rinsed with deionized water. Three germinated rhizome fragments were analysed for initial HM in the plant as described in (7.2.3.2). 18 germinated rhizome fragments were transferred to 100 mL glass flasks, each flask filled with solution which have particular concentration of HM (6 of them with solution of Pb, and each one with concentration of (0.25, 0.5, 1,

1.5, 2, and 3 mgPb L<sup>-1</sup>), the other 6 with solution of Cr and each one with concentration of (0.2, 0.5, 1, 1.25, 1.5 and 2 mgCr L<sup>-1</sup>), and the last 6 with solution of Cd and each one with concentration of (0.075, 0.15, 0.3, 0.75, 1 and 1.5 mgCd L<sup>-1</sup>). The solutions were renewed every day to avoid any changes in the concentration. After 21 days' growth, the plants from each HM solution were analysed for plant uptake. The 21 days were chosen based on experimental observation. The growth of plants was particularly slow as the experiments was run during winter and spring (from 05 of December 2015 to 20 March 2016). However, the plant growth started in spring but the high concentration of HM could have inhibited the plant growth (Batty and Younger 2004).



Figure 7. 4 *Phragmites australis* after ten days of growth

### 7.2.3.2 Analysis of HM in *Phragmites australis* plants

After 10 days' growth, three germinated rhizome fragments were dried in oven for 2 days at 70°C, weighted ( $W_0$ ) and ground to powder and then analysed for initial HM. The initial HM concentration in the plant was determined after mineralisation of 400 mg of powdered dry *Phragmites australis* in a microwave oven (Milestone Ethos 1600) with 5 ml of nitric acid (69% v/v), 5 ml deionised water and 2 mL H<sub>2</sub>O<sub>2</sub> (30% v/v). Using deionised water in order to make the final volume 25 ml. Thereafter, the sample was filtered using 0.45 µm, Millipore and then analysed for Pb, Cr and Cd using ICP/OES (Bragato et al. 2006).

Following the procedure of Bragato et al. 2006; the HM concentration in plant after 21 days of growth in different HM concentration solution (Section 7.2.3.1) was determined.

### 7.2.3.3 Michaelis- Menten equation for plant uptake

Uptake rate of HM was studied as a function of HM concentration with *Phragmites australis* using Michaelis- Menten equation (Equation. 7.1).

$$v_u = U_m C / K_u + C \quad (7. 1)$$

Where  $v_u$  is the rate of uptake in  $\text{mg (L day)}^{-1}$ ,  $C$  is HM concentration in  $\text{mg L}^{-1}$ ,  $U_m$  is maximum plant uptake in  $\text{day}^{-1}$  and  $K_u$  is Michaelis- Menten half- saturated constant (the concentration supporting half the maximum uptake rate) in  $\text{mg (L day)}^{-1}$ .

A linear transformation of the Michaelis- Menten equation for plant uptake is given as:

$$\frac{C}{v_u} = \frac{C}{U_m} + \frac{K_u}{U_m} \quad (7. 2)$$

The  $\frac{C}{v_u}$  vs.  $C$  plot was used to calculate  $U_m$  and  $K_u$  as shown in figure 7.5.

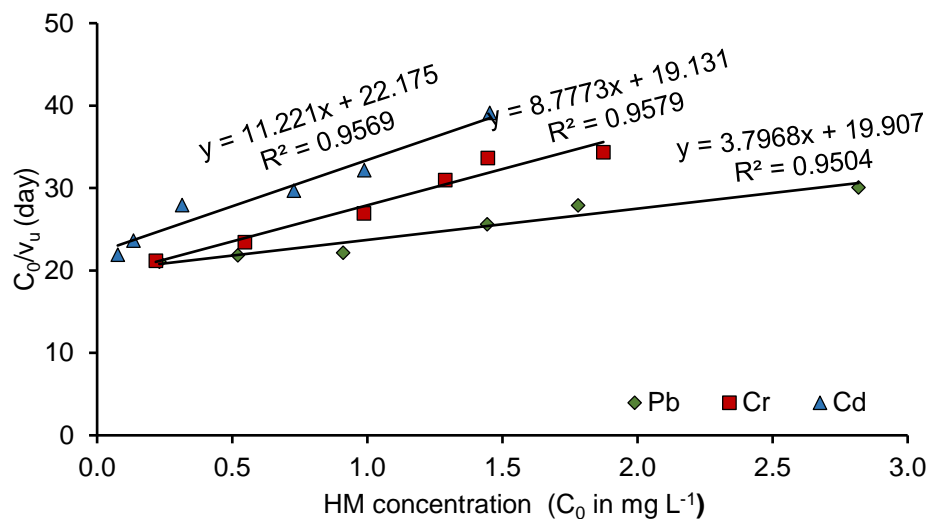


Figure 7. 5 The linear regression of  $C_0/v_u$  vs.  $C_0$  for  $K_u$  and  $U_m$  determination for Pb, Cr and Cd.

### 7.2.3.4 Impact of HM on plant growth

The effect of different concentrations of Pb (0.2 mg L<sup>-1</sup>- 3 mg L<sup>-1</sup>), Cr (0.2 mg L<sup>-1</sup>- 2 mg L<sup>-1</sup>) and Cd (0.05 mg L<sup>-1</sup>-1.5 mg L<sup>-1</sup>) on plant growth was also evaluated. After 10 days of growth (Section 7.2.3.1), 18 of the plants were placed in 100 mL glass flasks, each flask filled with solution which have particular concentration of HM (6 of them with solution of Pb and each one with concentration of (0.25, 0.5, 1, 1.5, 2, and 3 mgPb L<sup>-1</sup>), the other six with solution of Cr, and each one with concentration of (0.2, 0.5, 1, 1.25, 1.5 and 2 mgCr L<sup>-1</sup>) and the last 6 with solution of Cd, and each one with concentration of (0.075, 0.15, 0.3, 0.75, 1 and 1.5 mgCd L<sup>-1</sup>)). The solutions were renewed every day to avoid any changes in the concentration. After 21 days of growth one plant from each HM solution was taken (0.25 mgPb L<sup>-1</sup>, 0.2 mgCr L<sup>-1</sup> and 0.075 mgCd L<sup>-1</sup>), dried in oven for 2 days at 70°C and weighted (W). The deference between initial weight W<sub>0</sub> as described in section 7.2.3.2 and final weight W represent the plant growth. This procedure was repeated for the other plants at other HM concentrations within 21 days' durations.

### 7.2.3.5 Michaelis- Menten equation for plant growth

Growth rate of plant was also studied as a function of HM concentration using Michaelis- Menten equation as given below

$$v_G = G_m C / K_r + C \quad (7.3)$$

Where  $v_G$  is the rate of growth in g day<sup>-1</sup>,  $G_m$  is maximum plant growth in mg (L day)<sup>-1</sup> and  $K_r$  is Michaelis- Menten half- saturated constant (the concentration supporting half the maximum uptake rate) in mg (L day)<sup>-1</sup>.

A linear transformtion of the Michaelis- Menten equation for plant growth is given as equation 7.4

$$\frac{C}{v_G} = \frac{C}{G_m} + \frac{K_r}{G_m} \quad (7.4)$$

The  $\frac{C}{v_G}$  vs. C plot was used to calculate  $G_m$  and  $K_r$  as shown in Figure 7.6.

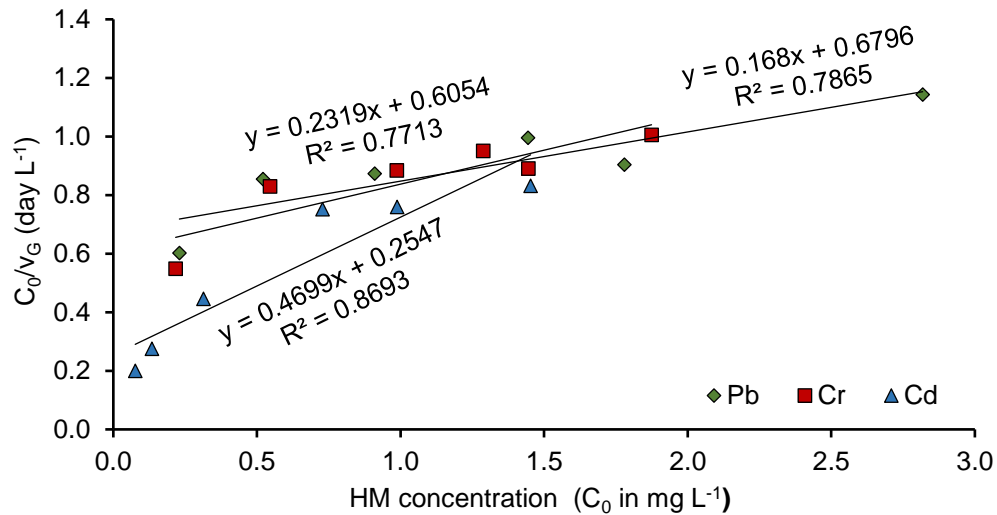


Figure 7. 6 The linear regression of  $C_0/v_G$  vs.  $C_0$  for  $K_r$  and  $G_m$  determination for Pb, Cr and Cd Process equations

### 7.2.3.6 Adsorption of HM by dewatered ferric sludge

The adsorption process was described by the equilibrium between HM in water and HM in the adsorbent. Unlike other processes, this process is fast and reaches equilibrium in hours based on the batch results (Section 3.3.2.2 in chapter 3). Therefore, 0.02 delta time (DT) was selected as the time step. DT refers to the time interval between calculations in STELLA software, in other words, it controls how frequently calculations are applied each unit of time. A small DT means smoother, more continuous change in variables within the model. In addition, the adsorption process was multiplied by a factor ( $Fa$ ) of 2.5, 5 and 3, respectively for Pb, Cr and Cd for column A; and 3.5, 14 and 5, respectively for Pb, Cr and Cd for column B. These factors were based on experimental results, and it is expected that they will vary according to the type of media, HM concentrations, type of pollutant, type of CWs, etc.

Adsorption processes can be described using Equation 7.5, where  $Fa$  is a factor,  $DISHM$  is dissolved HM (either Pb, Cr or Cd) ( $\text{mg day}^{-1}$ ),  $P_e$  is the equilibrium concentration ( $\text{mg L}^{-1} \text{day}^{-1}$ ) and  $V$  is the volume of wastewater (L).

$$Ad = Fa(DISHM - P_e \times V) \quad (7.5)$$

$P_e$  can be calculated using Equation 7.6, where  $ADSHM$  is adsorption of HM (either Pb, Cr or Cd) ( $\text{mg day}^{-1}$ ),  $T_A$  is the total amount of adsorbent (g),  $K_F$  is the Freundlich constant ( $\text{L g}^{-1}$ ) and  $n$  is the heterogeneity factor.

$$P_e = \left( \frac{ADSHM}{T_A \times K_F} \right)^n \quad (7.6)$$

The result from chapter 3 (Section 3.3.3.2) shows that the Freundlich adsorption model was well fitted to describe the adsorption behaviour of Pb, Cr and Cd, with correlation coefficients of 0.97, 0.98 and 0.98 for Pb, Cr and Cd, respectively (Table B6-B9).

### 7.2.3.7 Impact of HM on plant growth

The growth of the plant, *phragmites australis* depends on the amount of HM in the plant, since the presence of high concentration of HM in wastewater have adverse effect on plant growth (Batty and Younger 2004). Plant growth can be described as a function of maximum growth rate at the optimum temperature (Jeyakumar 2013). Furthermore, the plant's growth can be expressed by Michaelis-Menton equation. The following equation was used to describe plant growth (Jeyakumar 2013):

$$Gr = \frac{G_m \times PLB \times (HM_p - HM_{min}) \times 1.05^{(T-20)}}{K_r \times (HM_{max} - HM_{min})} \quad (7.7)$$

Here,  $G_m$  and  $K_r$  are maximum HM growth rate of the plant and the plant's growth rate (Michaelis-Menton half saturated constant for growth);  $PLB$  is plant biomass;  $HM_p$ ,  $HM_{min}$  and  $HM_{max}$  are heavy metal in the plant, minimum heavy metal in the plant and maximum heavy metal in the plant, respectively; and  $T$  is temperature.

### 7.2.3.8 Plant uptake

Plant uptake (*phragmites australis*) is defined as a function of maximum uptake rate at the optimum temperature as explained in Equation 7.8, where  $U_m$  and  $K_u$  respectively, are the maximum uptake rates of plants and the uptake rate of HM (Michaelis-Menton half saturated constant for uptake).

$$Up = \frac{U_{max} \times PLB \times (HM_{max} - HM_p) \times DISHM \times 1.05^{(T-20)}}{(DISHM - K_u) \times (HM_{max} - HM_{min})} \quad (7.8)$$

### 7.2.3.9 Plant mortality

The first order reaction with Arrhenius function of temperature was used to express the plant mortality and the detritus and as shown below.

$$MHM = PLHM \times M_r \times 1.07^{(T-20)} \quad (7.9)$$

$$De = DETHM \times M_m \times 1.07^{(T-20)} \quad (7.10)$$

$$KT = K_{20} \theta^{(T-20)} \quad (7.11)$$

Here,  $M_r$  and  $M_m$  are the mortality rate and maximum HM mineralization, respectively;  $KT$  is the removal rate constant at  $T^\circ\text{C}$ ;  $K_{20}$  is the removal rate constant at  $20^\circ\text{C}$ ;  $\theta$  is dimensionless; and  $T$  is the water temperature ( $^\circ\text{C}$ ). The value of  $\theta$  is 1.05 for plant growth and plant uptake, whereas the plant's mortality decomposition is more sensitive to temperature changes. Therefore, the  $\theta$  value ranges from 1.07 to 1.08 (Kumar et al. 2011).

### 7.2.4 Calibration and sensitivity analysis

Before applying the developed STELLA model to estimate the removal of HM, the model was calibrated and validated using standard trial and error procedure. In general, model calibration is a process of adjusting the selected parameter values to obtain the best fit between the observed data and simulated results. In practical modelling, sensitivity analysis is carried out to aid in model calibration. This is done by changing the parameters and observing the corresponding response on the selected parameters. Thus, the sensitivity ( $S$ ) of a parameter ( $P$ ) is defined as follows:

$$S = \frac{\delta X / X}{\delta P / P} \quad (7.12)$$

Here,  $X$  is the model output. The higher the value of  $S$ , the more important the parameter (Jørgensen and Fath 2011). The relative change in the parameter is chosen based on experimental knowledge as to the certainty of the parameters.

**Table 7. 1 Summary of the state variables, processes, parameters and their associated units in the model development for Pb.**

Symbol	Description	Value	Unit	Source
<b>State variables</b>				
<b>ADSPb</b>	Amount of Pb adsorbed in HH sludge	-	mg Pb day <sup>-1</sup>	Calculated
<b>DISPb</b>	Dissolved amount of Pb in HH sludge	-	mg Pb day <sup>-1</sup>	Observed data
<b>PLPb</b>	Amount of Pb found in plants	-	mg Pb day <sup>-1</sup>	Estimated
<b>PLBPb</b>	Amount of Pb found in plants biomass	-	mg Pb day <sup>-1</sup>	Estimated
<b>DETPb</b>	Amount of Pb found in detritus and used by bacteria	-	mg Pb day <sup>-1</sup>	Estimated
<b>Processes</b>				
<b>Gr</b>	Pb requirement for growth	Eq.(7.7)	mg Pb day <sup>-1</sup>	-
<b>Up</b>	Pb through plants	Eq.(7.8)	mg Pb day <sup>-1</sup>	-
<b>Mp</b>	Mortality of plant	Eq.(7.9)	mg Pb day <sup>-1</sup>	-
<b>De</b>	Decomposition of detritus	Eq.(7.10)	mg Pb day <sup>-1</sup>	-
<b>Ad</b>	Pb adsorption	Eq.(7.5)	mg Pb day <sup>-1</sup>	-
<b>Parameters</b>				
<b>Pbmax</b>	Maximum Pb in plants	0.11	g (100g) <sup>-1</sup>	Estimated
<b>Pbmin</b>	Minimum Pb in plants	0.001	g (100g) <sup>-1</sup>	Estimated
<b>Um</b>	Maximum uptake of Pb from plants	0.26	day <sup>-1</sup>	Calculated
<b>Ku</b>	Michaelis Menton for uptake	5.24	mg Pb (L day) <sup>-1</sup>	Calculated
<b>Mm</b>	Maximum mineralization	0.2	day <sup>-1</sup>	(Kumar et al. 2011)
<b>Pe</b>	Pb equilibrium concentration	-	mg Pb (L day) <sup>-1</sup>	Calculated
<b>Pbp</b>	Pb in plant	0.000024	mg mg <sup>-1</sup>	Calculated
<b>Mr</b>	Mortality rate	0.001	mg Pb (L day) <sup>-1</sup>	(Kumar et al. 2011)
<b>Gm</b>	Maximum growth of plant	2.08	mg Pb (L day) <sup>-1</sup>	Calculated
<b>Kr</b>	Michaelis Menton plant growth rate	2.8	mg Pb (L day) <sup>-1</sup>	Calculated
<b>Others</b>				
<b>INPb</b>	Inflow of Pb	TF	mgPb day <sup>-1</sup>	Observed data
<b>C0</b>	Pb concentration of inflow	TF	mgPb L <sup>-1</sup>	Observed data
<b>T</b>	Temperature requirement of plant growth	TF	°C	Observed data
<b>V</b>	Volume of wastewater	12	L	Experiment
<b>F</b>	Flow rate of wastewater into the CW	12	L day <sup>-1</sup>	Experiment
<b>TA</b>	Amount of adsorbent	2500	g	Calculated

TF is a Table function which is incorporated into the model.

**Table 7. 2 Summary of the state variables, processes, parameters and their associated units in the model development for Cr.**

Symbol	Description	Value	Unit	Source
<b>State variables</b>				
<b>ADSCr</b>	Amount of Cr adsorbed in HH sludge	-	mg Cr day <sup>-1</sup>	Calculated
<b>DISCr</b>	Dissolved amount of Cr in HH sludge	-	mg Cr day <sup>-1</sup>	Observed data
<b>PLCr</b>	Amount of Cr found in plants	-	mg Cr day <sup>-1</sup>	Estimated
<b>PLBCr</b>	Amount of Cr found in plants biomass	-	mg Cr day <sup>-1</sup>	Estimated
<b>DETCr</b>	Amount of Cr found in detritus and used by bacteria	-	mg Cr day <sup>-1</sup>	Estimated
<b>Processes</b>				
<b>Gr</b>	Cr requirement for growth	Eq.(7.7)	mg Cr day <sup>-1</sup>	-
<b>Up</b>	Cr through plants	Eq.(7.8)	mg Cr day <sup>-1</sup>	-
<b>Mp</b>	Mortality of plant	Eq.(7.9)	mg Cr day <sup>-1</sup>	-
<b>De</b>	Decomposition of detritus	Eq.(7.10)	mg Cr day <sup>-1</sup>	-
<b>Ad</b>	Cr adsorption	Eq.(7.5)	mg Cr day <sup>-1</sup>	-
<b>Parameters</b>				
<b>Crmax</b>	Maximum Cr in plants	1	g (100g) <sup>-1</sup>	Estimated
<b>Crmin</b>	Minimum Cr in plants	0.195	g (100g) <sup>-1</sup>	Estimated
<b>Um</b>	Maximum uptake of Cr from plants	0.114	day <sup>-1</sup>	Calculated
<b>Ku</b>	Michaelis Menton for uptake	2.18	mg Cr (L day) <sup>-1</sup>	Calculated
<b>Mm</b>	Maximum mineralization	0.2	day <sup>-1</sup>	(Kumar et al. 2011)
<b>Pe</b>	Cr in plant	-	mg Cr (L day) <sup>-1</sup>	Calculated
<b>Crp</b>	Mortality rate	0.00052	mg mg <sup>-1</sup>	Calculated
<b>Mr</b>		0.001	mg Cr (L day) <sup>-1</sup>	(Kumar et al. 2011)
<b>Gm</b>	Maximum growth of plant	3	mg Cr (L day) <sup>-1</sup>	Calculated
<b>Kr</b>	Michaelis Menton plant growth rate	3	mg Cr (L day) <sup>-1</sup>	Calculated
<b>Others</b>				
<b>INCr</b>	Inflow of Cr	TF	mgCr day <sup>-1</sup>	Observed data
<b>C0</b>	Cr concentration of inflow	TF	mgCr L <sup>-1</sup>	Observed data
<b>T</b>	Temperature requirement of plant growth	TF	°C	Observed data
<b>V</b>	Volume of wastewater	12	L	Experiment
<b>F</b>	Flow rate of wastewater into the CW	12	L day <sup>-1</sup>	Experiment
<b>TA</b>	Amount of adsorbent	2500	g	Calculated

TF is a Table function which is incorporated into the model.

**Table 7. 3** Summary of the state variables, processes, parameters and their associated units in the model development for Cd.

Symbol	Description	Value	Unit	Source
<b>State variables</b>				
<b>ADSCd</b>	Amount of Cd adsorbed in HH sludge	-	mg Cd day <sup>-1</sup>	Calculated
<b>DISCd</b>	Dissolved amount of Cd in HH sludge	-	mg Cd day <sup>-1</sup>	Observed data
<b>PLCd</b>	Amount of Cd found in plants	-	mg Cd day <sup>-1</sup>	Estimated
<b>PLBCd</b>	Amount of Cd found in plants biomass	-	mg Cd day <sup>-1</sup>	Estimated
<b>DETCd</b>	Amount of Cd found in detritus and used by bacteria	-	mg Cd day <sup>-1</sup>	Estimated
<b>Processes</b>				
<b>Gr</b>	Cd requirement for growth	Eq.(7.7)	mg Cd day <sup>-1</sup>	-
<b>Up</b>	Cd through plants	Eq.(7.8)	mg Cd day <sup>-1</sup>	-
<b>Mp</b>	Mortality of plant	Eq.(7.9)	mg Cd day <sup>-1</sup>	-
<b>De</b>	Decomposition of detritus	Eq.(7.10)	mg Cd day <sup>-1</sup>	-
<b>Ad</b>	Cd adsorption	Eq.(7.5)	mg Cd day <sup>-1</sup>	-
<b>Parameters</b>				
<b>Cdmax</b>	Maximum Cd in plants	1.5	g (100g) <sup>-1</sup>	Estimated
<b>Cdmin</b>	Minimum Cd in plants	0.016	g (100g) <sup>-1</sup>	Estimated
<b>Um</b>	Maximum uptake of Cd from plants	0.09	day <sup>-1</sup>	Calculated
<b>Ku</b>	Michaelis Menton for uptake	2	mg Cd (L day) <sup>-1</sup>	Calculated
<b>Mm</b>	Maximum mineralization	0.2	day <sup>-1</sup>	(Kumar et al. 2011)
<b>Pe</b>	Cd equilibrium concentration	-	mg Cd (L day) <sup>-1</sup>	Calculated
<b>Cdp</b>	Cd in plant	0.00002	mg mg <sup>-1</sup>	Calculated
<b>Mr</b>	Mortality rate	0.001	mg Cd (L day) <sup>-1</sup>	(Kumar et al. 2011)
<b>Gm</b>	Maximum growth of plant	0.82	mg Cd (L day) <sup>-1</sup>	Calculated
<b>Kr</b>	Michaelis Menton plant growth rate	1.26	mg Cd (L day) <sup>-1</sup>	Calculated
<b>Others</b>				
<b>INCd</b>	Inflow of Cd	TF	mgCd day <sup>-1</sup>	Observed data
<b>C0</b>	Cd concentration of inflow	TF	mgCd L <sup>-1</sup>	Observed data
<b>T</b>	Temperature requirement of plant growth	TF	°C	Observed data
<b>V</b>	Volume of wastewater	12	L	Experiment
<b>F</b>	Flow rate of wastewater into the CW	12	L day <sup>-1</sup>	Experiment
<b>TA</b>	Amount of adsorbent	2500	g	Calculated

TF is a Table function which is incorporated into the model.

## 7.3 Results and Discussion

### 7.3.1 Simulation of heavy metals using STELLA software

Experiments were carried out in two periods using column A (220 days) for Period 1, and columns A and B (185 days) for Period 2. A comparison of the measured and modelled data was undertaken using Period 1 (0- 220 days) for calibration and Period 2 (220- 405 days) for validation. During the calibration, the input parameters were

obtained from experimental measurements, theoretical calculations or existing literature (Tables 7.7- 7.9). The model was calibrated by trial and error adjustment of the key parameters (within a reasonable range) until predictions under similar conditions had good agreement with the observed data. The measured HM concentrations ranged from 54  $\mu\text{g L}^{-1}$ - 264  $\mu\text{g L}^{-1}$ , 21  $\mu\text{g L}^{-1}$ - 190  $\mu\text{g L}^{-1}$  and 87  $\mu\text{g L}^{-1}$ - 342  $\mu\text{g L}^{-1}$ , respectively, for Pb, Cr and Cd. Whereas the simulation ranged from 92  $\mu\text{g L}^{-1}$ - 255  $\mu\text{g L}^{-1}$ , 38  $\mu\text{g L}^{-1}$ - 262  $\mu\text{g L}^{-1}$  and 80  $\mu\text{g L}^{-1}$ -324  $\mu\text{g L}^{-1}$ , respectively, for Pb, Cr and Cd during the calibration period. The maximum value of the measured effluent concentration (OBS) for all the HM was very close to the value simulated by the STELLA model. However, the predicted data were slightly higher than the measured data for all the HM, with the exception of a few data points. In addition, the model did not simulate very low values for all the HM. This may be because there are other processes contributing to HM removal in the CWs which were not taken into consideration during the model built and as the removal of HM by precipitation as explained in section 5.3.2 chapter 5. Figure 7.7 shows the trend of model calibration and validation for column A. The mean percent error ( $\text{MPE} = (\text{OBS} - \text{OUT})/\text{OBS} \times 100$ ) was 38%, 33% and 30%, respectively for Pb, Cr and Cd during the calibration period; and 15%, 20% and 10%, respectively, for Pb, Cr and Cd during the validation period. It is worth noting that the validated data for the HM was quite close to the observed data, despite the fact that the simulation data was higher than the observation data for the period of 320- 405 days in the case of Cr within the validation period. This slight fluctuation in the model simulation and the experimental data could be due to experimental error or accumulation of biomass within the CWs (growth of microorganism). This could also be attributed to the fact that the plants were not harvested during the experimental period. The uptake of HM by plant is not significant (up to 6%) compared to the total amount removal in CWs. HM are taken up by roots and distributed to the other parts of the plant. However, a small portion is translocated to the other plant parts. Therefore, harvesting of the aboveground plant contributes only a small percent of the total HM removal in vertical flow CWs (Cheng et al. 2002; Kosolapov et al. 2004; Marchand et al. 2010). Another possible reason may be that apart from the adsorption process, the HM in CW can be removed by other processes such as precipitation, oxidation, ion exchange and redox reaction (Galletti et al. 2010). However, the system was operated to be fully saturated for 3 hour and 50 minutes and unsaturated for 10 minutes; and due to a limitation of DO diffusion within HH sludge (Wang et al. 2008), there is aerobic and anaerobic condition along of the depth

of the column as discussed in chapter 5 Section 5.3.2, it shows that the precipitation of metals as metal sulphide cannot occur.

A comparison of the observed and predicted Pb, Cr and Cd concentration values in the effluent during the model calibration process was obtained using linear regression as shown in Figure 7.8. The  $R^2$  values for Pb, Cr and Cd outlet concentration values were 0.75, 0.69 and 0.62, respectively. The  $R^2$  values for comparisons of the observed and predicted Pb, Cr and Cd outlet concentration values during the model validation process (Figure 7.9.) were 0.78, 0.65 and 0.74, respectively for Pb, Cr and Cd concentration. These values represent good correlations between the model predictions and the experimental measurements.

Based on these results, the mathematical model developed in this study could be used to describe the HM removal process in the VF CWs using HH sludge as the primary media. The model was run using STELLA software for a period of 185 days for column B. Since the results of the validation data in column A displayed a good match between simulated and experimental data, the calibration for column B was performed with the column A data. The experimental effluent HM concentrations ranged from 25  $\mu\text{g L}^{-1}$  to 76  $\mu\text{g L}^{-1}$ , 8  $\mu\text{g L}^{-1}$  to 22  $\mu\text{g L}^{-1}$  and 24  $\mu\text{g L}^{-1}$  to 76  $\mu\text{g L}^{-1}$ , respectively for Pb, Cr and Cd. On the other hand, the simulation data for Pb, Cr and Cd ranged, respectively from 23  $\mu\text{g L}^{-1}$  to 63  $\mu\text{g L}^{-1}$ , 11  $\mu\text{g L}^{-1}$  to 24  $\mu\text{g L}^{-1}$  and 27  $\mu\text{g L}^{-1}$  to 68  $\mu\text{g L}^{-1}$ , as shown in Figure 7.10. This figure shows that the mean concentration values of HM for the measured and simulated values were very close and therefore, the overall simulation is acceptable for column B. The MPEs for this column were 17% for Pb, 17% for Cr and 17% for Cd. A comparison between the observed and predicted Pb, Cr and Cd concentrations in effluent during the model validation process for column B showed good correlations between the model predictions and the experimental measurements, with  $R^2$  being 0.82, 0.71 and 0.76, respectively for the Pb, Cr and Cd outlet concentrations (Figure 7.11).

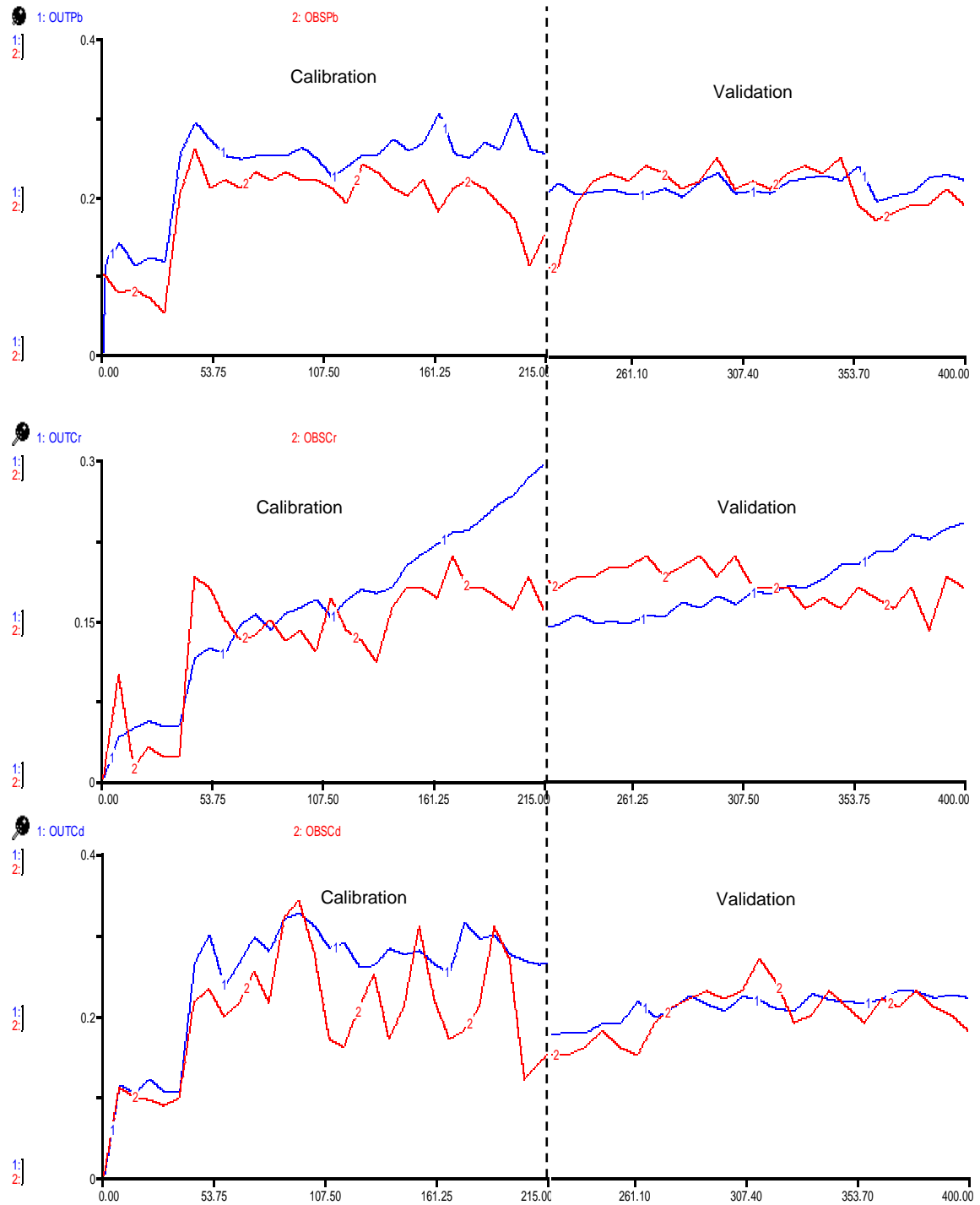


Figure 7. 7 Model calibration and validation for (a) Pb, (b) Cr and (c) Cd removal in mg L<sup>-1</sup> in the CWs using column A.

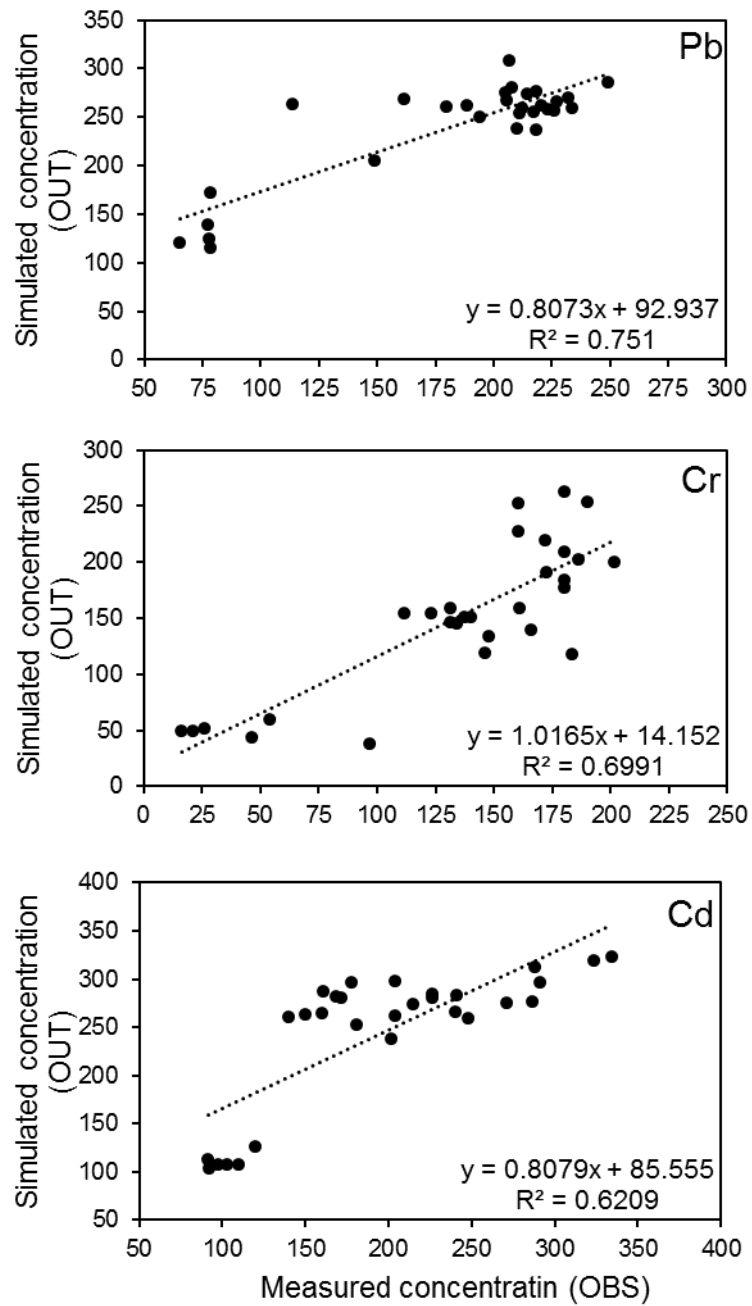


Figure 7. 8 Comparison of model predicted and field measured of Pb, Cr and Cd removal in  $\mu\text{g L}^{-1}$  in the CWs using column A during model calibration.

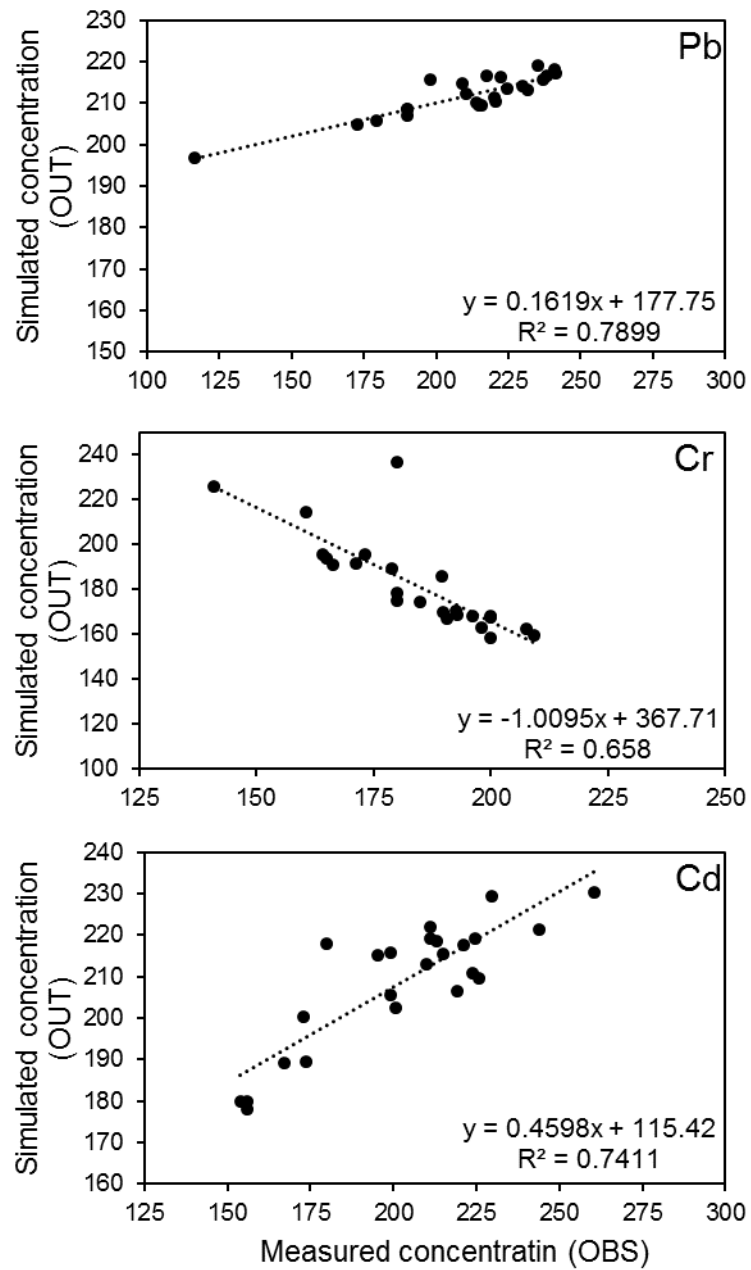


Figure 7. 9 Comparison of model predicted and field measured of Pb, Cr and Cd removal in  $\mu\text{g L}^{-1}$  in the CWs using column A during model validation.

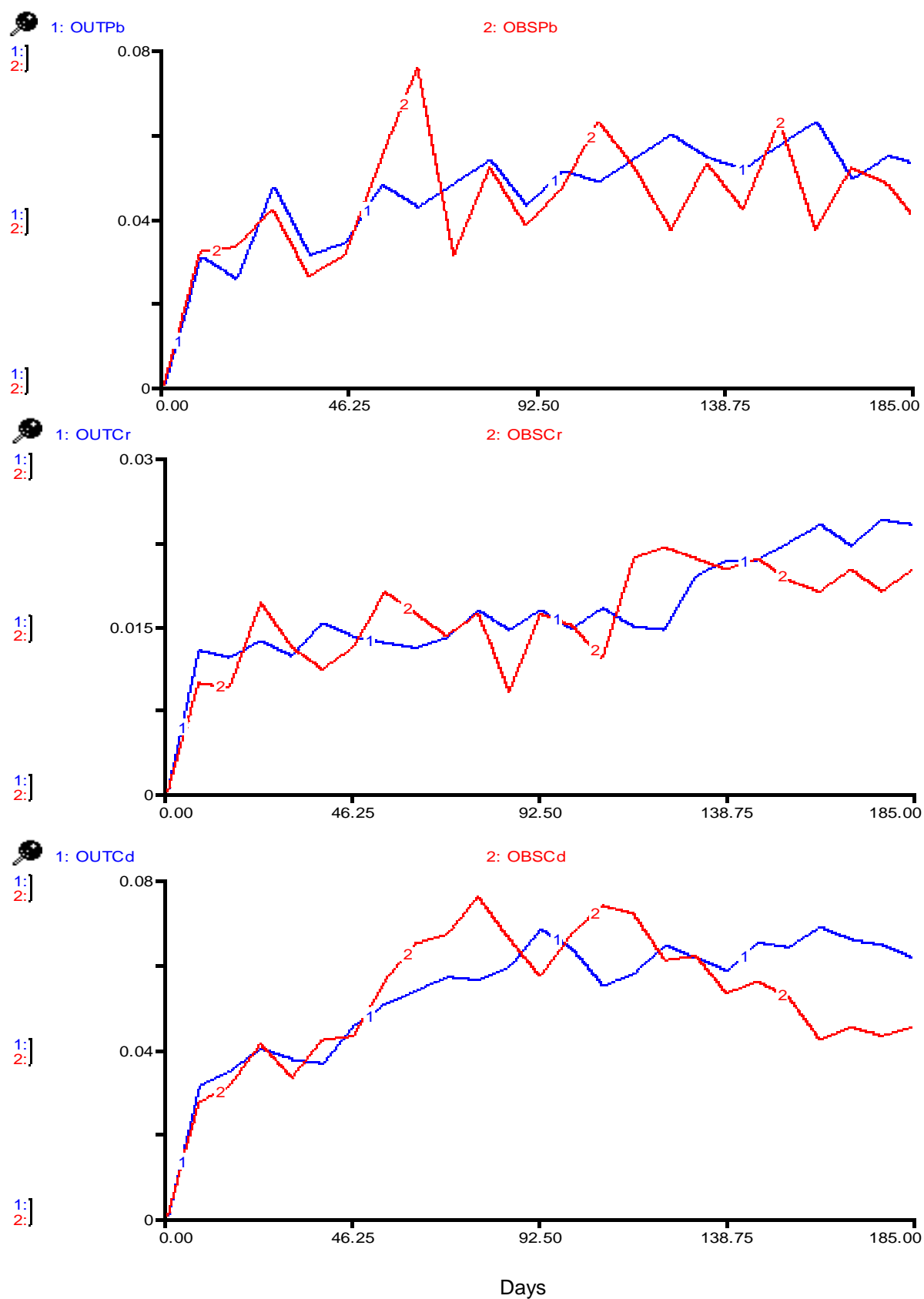


Figure 7. 10 Model validation for (a) Pb, (b) Cr and (c) Cd removal in mg L<sup>-1</sup> in the CWs using column B.

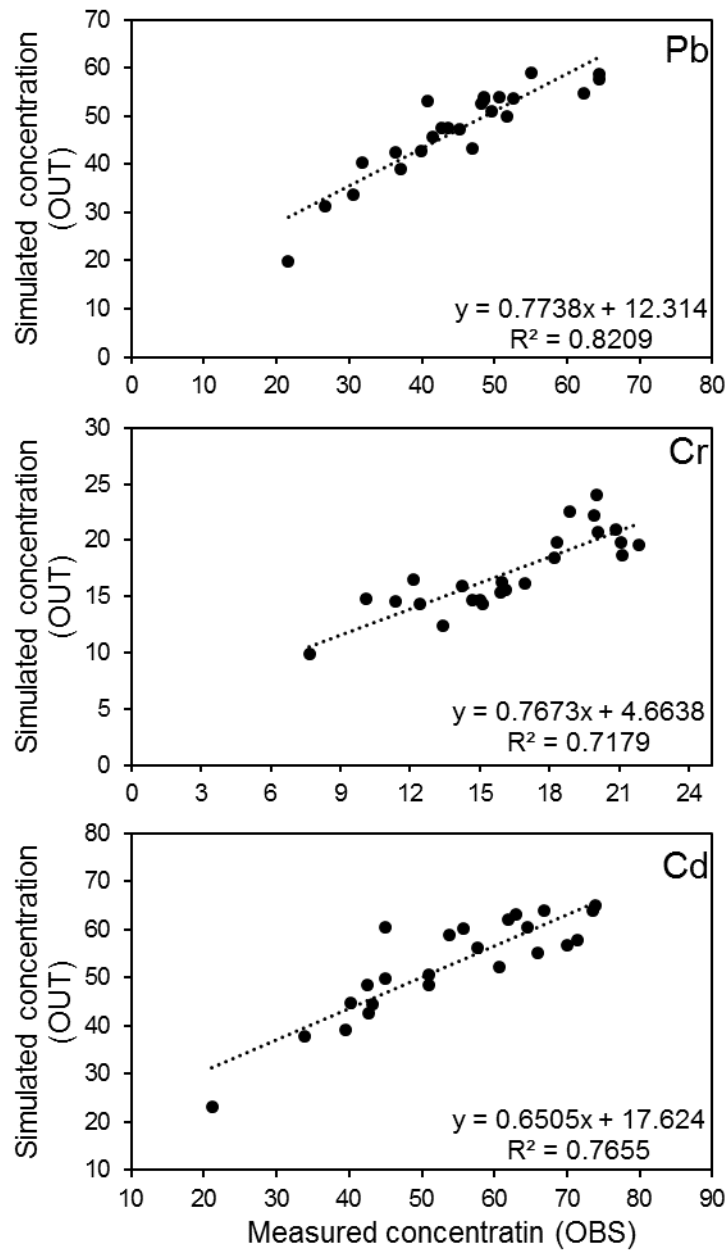


Figure 7. 11 Comparison of model predicted and field measured of Pb, Cr and Cd removal in  $\mu\text{g L}^{-1}$  in the CWs using column B during model validation.

### 7.3.2 Sensitivity analysis

Sensitivity analysis provides a good overview of the most sensitive components in the model. sensitivity analysis provides a measure of the sensitivity of the parameters, forcing functions, initial values of the state variables of the sub models, or sub model to the state variables of greatest interest in the model (Jørgensen and Fath 2011).

The sensitivity of the model was tested using the 10 parameters which were the most likely to be important:  $G_m$ ,  $K_r$ ,  $U_m$ ,  $K_u$ ,  $M_m$ ,  $M_r$ ,  $HM_{max}$ ,  $HM_{min}$ ,  $n$  and  $K_f$  (Table 7.10). All these parameters are related to the main processes of HM removal in this study ( $G_r$ ,  $U_p$ ,  $M_p$ ,  $D_e$  and  $A_d$ ). This was done by examining the relative change in the model output and dividing it by the relative change in the value of the tested parameter. The magnitude of the changes in the parameter values may be proportional to the value of the parameter; this also depends on the possible range of the parameter. Most changes were made between -50% and +50% (Van der Peiji and Verhoeven 1999). In this study, changes were made at  $\pm 40\%$ . Table 7.10 shows that the increase and decrease of  $n$  caused a significant change in the corresponding state variable of the model. Similarly, the change in  $K_f$  also caused changes in the model output and the corresponding state variables. This is primarily because the adsorption process is supposed as the main process for the removal of HM by the HH sludge in the CWs. The rigid structure and fixed set of parameters do not accurately reflect the changes in the output of the VF CW.

**Table 7. 4 Sensitivity analysis for the selected parameters included in the model.**

Change of	Parameter value			$S_{(+40\%)}$			$S_{(-40\%)}$		
	Pb	Cr	Cd	Pb	Cr	Cd	Pb	Cr	Cd
Gm	2.08	3	0.82	$1.08 \times 10^{-8}$ - $1.33 \times 10^{-7}$	$2.18 \times 10^{-8}$ - $1.43 \times 10^{-7}$	$1.64 \times 10^{-7}$ - $3.22 \times 10^{-7}$	$2.10 \times 10^{-8}$ - $1.32 \times 10^{-7}$	$2.18 \times 10^{-7}$ - $6.23 \times 10^{-7}$	$7.08 \times 10^{-8}$ - $2.47 \times 10^{-7}$
Kr	2.8	3	1.26	$1.43 \times 10^{-8}$ - $2.1 \times 10^{-8}$	$1.98 \times 10^{-7}$ - $2.13 \times 10^{-6}$	$1.08 \times 10^{-8}$ - $2.33 \times 10^{-8}$	$1.08 \times 10^{-8}$ - $1.33 \times 10^{-7}$	$1.11 \times 10^{-7}$ - $5.01 \times 10^{-6}$	$2.08 \times 10^{-7}$ - $4.91 \times 10^{-7}$
Um	0.26	0.114	0.09	$1.48 \times 10^{-5}$ - $3.69 \times 10^{-5}$	$0.41 \times 10^{-5}$ - $0.55 \times 10^{-3}$	$6.63 \times 10^{-6}$ - $2.02 \times 10^{-5}$	$1.56 \times 10^{-5}$ - $3.92 \times 10^{-5}$	$0.41 \times 10^{-3}$ - $0.55 \times 10^{-3}$	$6.63 \times 10^{-6}$ - $2.02 \times 10^{-5}$
Ku	5.24	2.18	2	$3.91 \times 10^{-6}$ - $2.38 \times 10^{-5}$	$0.19 \times 10^{-3}$ - $0.33 \times 10^{-3}$	$2.14 \times 10^{-6}$ - $1.00 \times 10^{-5}$	$1.41 \times 10^{-5}$ - $4.72 \times 10^{-5}$	$0.31 \times 10^{-3}$ - $0.63 \times 10^{-3}$	$2.71 \times 10^{-6}$ - $1.47 \times 10^{-5}$
HMmax	0.11	1	1.5	$2.01 \times 10^{-5}$ - $8.75 \times 10^{-5}$	$6.67 \times 10^{-5}$ - $8.93 \times 10^{-5}$	$5.08 \times 10^{-8}$ - $1.55 \times 10^{-7}$	$1.45 \times 10^{-5}$ - $6.33 \times 10^{-5}$	$0.19 \times 10^{-3}$ - $0.26 \times 10^{-3}$	$1.19 \times 10^{-7}$ - $3.65 \times 10^{-7}$
HMmin	0.001	0.195	0.016	$2.32 \times 10^{-5}$ - $0.11 \times 10^{-3}$	$0.11 \times 10^{-3}$ - $0.15 \times 10^{-3}$	$7.17 \times 10^{-8}$ - $2.18 \times 10^{-7}$	$8.83 \times 10^{-9}$ - $3.51 \times 10^{-7}$	$0.15 \times 10^{-5}$ - $0.12 \times 10^{-3}$	$7.12 \times 10^{-8}$ - $2.16 \times 10^{-7}$
Mr	0.001	0.001	0.001	$2.48 \times 10^{-6}$ - $8.48 \times 10^{-6}$	$7.73 \times 10^{-5}$ - $0.18 \times 10^{-3}$	$1.32 \times 10^{-6}$ - $5.97 \times 10^{-6}$	$2.67 \times 10^{-6}$ - $8.61 \times 10^{-6}$	$8.03 \times 10^{-5}$ - $0.18 \times 10^{-3}$	$1.41 \times 10^{-6}$ - $6.09 \times 10^{-6}$
Mm	0.2	0.2	0.2	$1.16 \times 10^{-5}$ - $9.86 \times 10^{-5}$	$1.82 \times 10^{-6}$ - $4.72 \times 10^{-5}$	$5.84 \times 10^{-8}$ - $8.68 \times 10^{-6}$	$1.09 \times 10^{-7}$ - $1.16 \times 10^{-5}$	$5.05 \times 10^{-6}$ - $0.10 \times 10^{-3}$	$1.41 \times 10^{-6}$ - $6.09 \times 10^{-6}$
n	0.53	1.52	0.5	$0.60 \times 10^{-1}$ - $2.00 \times 10^{-1}$	$2.72 \times 10^{-3}$ - $3.36 \times 10^{-1}$	$1.32 \times 10^{-1}$ - $3.20 \times 10^{-1}$	$3.10 \times 10^{-1}$ - $6.41 \times 10^{-1}$	$4.70 \times 10^{-3}$ - $5.91 \times 10^{-1}$	$2.03 \times 10^{-1}$ - $6.70 \times 10^{-1}$
Kf	43	1.7	0.43	$0.12 \times 10^{-1}$ - $0.54 \times 10^{-1}$	$1.4 \times 10^{-3}$ - $4.44 \times 10^{-1}$	$0.3 \times 10^{-1}$ - $1.43 \times 10^{-1}$	$0.23 \times 10^{-1}$ - $1.03 \times 10^{-1}$	$7.50 \times 10^{-3}$ - $22.70 \times 10^{-1}$	$5.00 \times 10^{-1}$ - $2.60 \times 10^{-1}$

### 7.3.3 Fate of heavy metals in VFCW

To assess the performance of the VF CWs for the removal of HM from landfill leachate, a scenario was simulated to investigate the HM dynamics for the anoxic condition, using HH sludge as the primary media in the VF CWs. The input data of the HMs were inserted into the STELLA software during model calibration and integrated by using the second order Runge-Kutta method with a time step of 0.02 day. Once the model finished its run (i.e. at the end of 220 days), the amount of HM that accumulates into the state variables, and the processes of the model show how much HM is removed by the individual pathways. Therefore, it is possible to calculate the efficiency of the individual processes, such as  $A_d$  (Eq. 7.5),  $U_p$  (Eq. 7.8) and  $M_p$  (Eq. 7.9) and  $D_e$  (Eq. 7.10). A mass balance for all state variables as simulated by the model revealed approximately 89%, 91% and 91% for  $A_d$ ; 6%, 5.1% and 5.2% for  $U_p$ ; and 1%, 1.15% and 1% for  $M_p$  and  $D_e$  for respectively Pb, Cr and Cd. The results from the mass balance show that the major HM transformation routes in this study were adsorption, with a small amount of uptake by the plant. The effect of various parameters on adsorption was studied via batch experiments (Chapter 3). The adsorption results of Pb, Cr and Cd ions by HH sludge showed a slightly better fit with the Freundlich compared to Langmuir. The Langmuir isotherms data found that HH sludge had  $40 \mu\text{g g}^{-1}$ ,  $130 \mu\text{g g}^{-1}$  and  $30 \mu\text{g g}^{-1}$  adsorption capacities, respectively for Pb, Cr and Cd. On the other hand, the Freundlich isotherm results showed that a precipitation reaction may occur for Pb and Cd removal where  $n$  values  $> 1$ . Lead and cadmium could precipitate to form insoluble compounds with sulphide in anaerobic zones of CWs (Kadlec and Wallace 2008). The results from effect of contact time on HM removal (Section 3.3.2.2 in chapter 3) shows a sharp rise in Pb and Cr removal within the first hour, indicating the instant at which the removal of these HM takes place. This can be adduced to the excess of binding sites on highly accessible surfaces like particles and macropores. Over time, the curve starts to plateau because the rate of removal is much slower. This is due to the accumulation of metal ions on the binding sites until it reaches equilibrium; and thereafter, sorption would be via intraparticle diffusion in meso- and micropores and/or sorption by the organic matter (Zhou and Haynes 2011).

The adsorption process in STELLA was described to calculate the  $P_e$  concentration using the Freundlich isotherm. From the model simulation, approximately  $526 \mu\text{g}$ ,  $518 \mu\text{g}$  and  $640 \mu\text{g}$  of Pb, Cr and Cd, respectively adsorbed during the calibration stage

of the model run, and the corresponding inflow of these heavy metals amounts were 591 µg, 570 µg and 712 µg for Pb, Cr and Cd, respectively. The high amount of HM adsorbed by the media was as a result of using HH sludge as the main substrate and an anoxic condition to elongate the contact time between the media and HM. The overall simulation of Ad is reasonably good in the STELLA model, especially for the adsorption process.

Unfortunately, no data from the use of HH sludge as a substrate in CWs for HM removal were found in the literature. Therefore, direct comparison was not possible. However, several authors used the STELLA program to describe the adsorption process in CWs and using different kinds of substrates and pollutants. Pimpan and Jindal (2009) showed that the maximum cadmium removal simulated by the STELLA software occurred via accumulation in soil with mass fraction values of 33.6–76.6% at different hydraulic retention times. Kumar et al. (2011) revealed that 72% of phosphorus was removed via the adsorption process as simulated by the STELLA software using VF CWs and alum sludge as main substrate. Accordingly, adsorption seems to be the main process to remove Cd and phosphorous in CWS.

The uptake of HM by plants in this study was low. This was primarily because the plants in CWs contribute to HM removal through substrate stabilization, rhizosphere oxidation, supply of organic matter for microorganisms for their growth and the transportation of water to wetland soil, rather than through the direct uptake of metals (Kosolapov et al. 2004).

## **7.4 Conclusion**

In this chapter, a dynamic model for HM transformation in a novel CWs, using dewatered drinking water treatment sludge as main substance was developed using STELLA. The mechanisms used in the modelling included adsorption, plant uptake and growth. The most significant pathway of HM retention was adsorption. In terms of the model's sensitivity, the adsorption parameter was the most important factor. The model was calibrated in order to achieve predictions that were close to the experimental data. A reasonable agreement was obtained between the measured and predicted results. A mass balance showed that up to 89%, 91% and 91% of the removal of HM was through adsorption, which is highly significant; whereas removal through plants was about 6%, 5.1% and 5.2% for Pb, Cr and Cd, respectively. This study demonstrates that the model could be used to describe the Pb, Cr and Cd

removal process from landfill leachate in CWs using ferric dewatered sludge as substrate.

# **Chapter 8**

## **Conclusion and Recommendations**

## 8.1 Conclusion

This thesis focused on the design and assessment of a novel constructed wetland systems for landfill leachate treatment. In the following sections, the main conclusions from the research are presented. Result from the adsorption kinetics and equilibrium tests showed that the adsorption rate of all metals to both types of DWS (Al- based and Fe- based) was quick, and with the majority of the reaction taking place within the first hour for Pb and Cr, while the majority of the reaction for Cd took place within 6 hours. The reaction rate was well described by the pseudo-second-order model for Cr adsorption; this indicates that chemisorption was the controlling factor in the adsorption of Cr to DWSs. On the other hand, pseudo-first-order model showed better fit for Pb adsorption. Diffusion as opposed to chemical reaction can also be the rate-limiting step in the case of Cd adsorption. The Langmuir, Freundlich, Temkin, Frumkin and Harkins-Jura isotherms were all found to give reliable representations of metal adsorption in the experiments. The HH-sludge had a particularly high capacity for adsorption of Pb, Cr and Cd.

The mechanistic study using sequential extraction, FTIR spectra and statistical analysis (PCA and CCA) showed that low concentrations of heavy metals sorbed by dewatered waterworks sludges were in the form of water-soluble and exchangeable fractions, whilst the greatest concentrations of the metals sorbed were strongly bound and would not be expected to be readily released under natural conditions. In addition, the FTIR spectra of HH sludge loaded with Pb, Cr and Cd suggested a predominant bidentate chelating mode for these heavy metals with the carboxylate groups of the humic substances. The correlation analysis, PCA and CCA showed high correlation between Cd uptake and Fe- or Al-(oxy) hydroxide, while Cr and Pb uptake correlated with organic carbon.

Based on these result, the suitable drinking water sludge was selected for the design and development of a novel CWs for landfill leachate treatment. The two design variables (CW media and wetting/drying regime) were found to have significant impacts on the removal of different pollutants. High removal rate of heavy metals was obtained by adsorption in anoxic condition, and precipitation to ferric dewatered sludge in oxidising condition. However, the removal efficiency was more pronounced when the anoxic condition employed, reaching up to 62%, 75% and 66% respectively for Pb, Cr and Cd in the first operational period, and 74%, 71% and 72% for Pb, Cr and Cd respectively in the second operational period.

A dynamic model for HM transformation was also developed using STELLA. The mechanisms used in the modelling included adsorption, plant uptake and growth. The result from model shows that the most significant pathway of HM removal was adsorption. In terms of the model's sensitivity, the adsorption parameter was the most important factor. The model was calibrated in order to achieve predictions that were close to the experimental data. A reasonable agreement was obtained between the measured and predicted results. Mass balance analysis showed that up to 89%, 91% and 91% of the removal of HM was through adsorption, which is highly significant; whereas the removal through the plants was about 6%, 5.1% and 5.2% for Pb, Cr and Cd, respectively.

Due to the exceptional high pollutant loading rate applied, bed clogging could be a major problem. In this study, it seemed that the chemical treatment process for HM (adsorption and precipitation) could be the main factor contributing to clogging in stage C. Although, the adsorption films do not become thick enough to create clogging problem as adsorption was limited in this stage. Chemical precipitation as HM hydroxide or co precipitate with iron oxyhydroxide may form film like coating on media surface.

It was clearly demonstrated that with a shorter saturated time and longer unsaturated time, the CW system was more efficient in the removal of various pollutants due to the enhanced oxygen supply into the CW. The removal efficiency of COD in this study could be ascribed to the aerobic conditions, and anoxic microbial processes for denitrification. Bed clogging was shown to be a serious problem which affects COD removal. The main removal pathway for  $\text{NH}_4\text{-N}$  was through nitrification particularly when a 1:1 recirculation was employed, resulting in prolonged wastewater-biofilm contact. Total nitrogen losses were observed in the aerobic and anoxic conditions. The losses in the aerobic condition may be due to denitrification occurring in the anoxic microzone inside sludge floc. Whereas nitrification may occur on the surface of the flocs, and this could be because of the high oxygen diffusion resistance within the sludge flocs.

The successful development of a HYDRUS model enhanced a deeper understanding of the landfill leachate treatment in CWs, confirming that a good match between simulation data and experimental result can be achieved when sufficient data is available to describe the hydraulic behaviour of the sludge media. Therefore, the flow model can be successfully calibrated, as in this study by using the hydraulic parameter derived from the Van Genuchten model. The result for COD effluent concentration

from the measured data for the long-term period were higher than simulated data (55% of measured data was higher than simulation data). This is mainly because of clogging which is not considered by the model, and it is one of the limitations of the model. The model also did not simulate the high and low values of  $\text{NH}_4\text{-N}$  effluent concentration. A reason that the model might have underestimated nitrogen removal is that it did not include the influence of plants.

## 8.2 Recommendations for further work

1. The batch adsorption results presented in chapters 3 and 4 are based on the use of a single metal adsorbate solution. Therefore, it is possible that different results may have been produced with the use of a multi-metal adsorbate solution. This would have been more representative of the synthetic landfill leachate used in the CW inflow (and indeed real landfill leachate), but was not investigated due to time and financial constraints. Thus a simple series of batch adsorption tests using multi-metal adsorbate solution would further refine the understanding of metal adsorption to the media used in the CWs.
2. Any future experimental work carried out on pilot-scale or field-scale tidal-flow landfill leachate CWs would benefit from the continuous measurement of dissolved oxygen and redox potential in the systems. It is felt that measurement of these parameters would have given a greater understanding of the OM and N transformation process in the tidal-flow CWs, indicating the times during the inflow/outflow cycle at which oxygen concentrations were highest/lowest, impacting on oxidation, organic matter degradation and nitrification/denitrification processes.
3. Future experimental work should also include investigating the structure of the microbial communities (i.e. characteristics and composition) and their impact on and contribution to organic matter and nitrogen removal in the system.
4. The kinetics of OM and  $\text{NH}_4\text{-N}$  adsorption and OM degradation and nitrification during bed resting should be further investigated. This can provide key information to determine the operational parameters (loading rate, contact and rest time) and optimize the OM and nitrogen conversion processes.

## References

Abdul Aziz, H., Adlan, M.N., Zahari, M.S. and Alias, S. 2004. Removal of Ammoniacal Nitrogen (N-NH<sub>3</sub>) from Municipal Solid Waste Leachate by Using Activated Carbon and Limestone. *Waste Management & Research* · 23, pp. 371–375.

Akhtar, N., Iqbal, M., Zafar, S.I., Iqbal and Javed 2008. Biosorption characteristics of unicellular green alga *Chlorella sorokiniana* immobilized in loofa sponge for removal of Cr(III). *Journal of Environmental Sciences* 20(2), pp. 231–239.

Akratos, C.S., Papaspyros, J.N.E. and Tsihrintzis, V.A. 2009. Total nitrogen and ammonia removal prediction in horizontal subsurface flow constructed wetlands: Use of artificial neural networks and development of a design equation. *Bioresource Technology* 100(2), pp. 586–596.

Akratos, C.S. and Tsihrintzis, V.A. 2006. Effect of temperature, HRT, vegetation and porous media on removal efficiency of pilot-scale horizontal subsurface flow constructed wetlands. *Ecological Engineering* 29, pp. 173–191.

Albuquerque, A., Arendacz, M., Gajewska, M., Obarska-Pempkowiak, H., Randerson, P. and Kowalik, P. 2009. Removal of organic matter and nitrogen in an horizontal subsurface flow (HSSF) constructed wetland under transient loads. *Water Science and Technology* 60(7), pp. 1677–1682.

Albuquerque, A., Oliveira, J., Semitela, S. and Amaral, L. 2009. Influence of bed media characteristics on ammonia and nitrate removal in shallow horizontal subsurface flow constructed wetlands. *Bioresource Technology* 100(24), pp. 6269–6277.

Alvarez-Vazquez, E., Jefferson, B. and Judd, S.J. 2004. Review Membrane bioreactors vs conventional biological treatment of landfill leachate: a brief review. *Journal of Chemical Technology and Biotechnology* 79, pp. 1043–1049.

APHA (American Public Health Association), AWWA (American Water Works Association), and W. (Water E.F. 2012. *Standard methods for the examination of water and wastewater*. 22nd ed. Washington: American Public Health Association.

Axe, L. and Trivedi, P. 2002. Intraparticle surface diffusion of metal contaminants and their attenuation in microporous amorphous Al, Fe, and Mn oxides. *Journal of colloid*

and interface science 247(2), pp. 259–265.

Babatunde, a. O. and Zhao, Y.Q. 2010. Equilibrium and kinetic analysis of phosphorus adsorption from aqueous solution using waste alum sludge. *Journal of Hazardous Materials* 184(1-3), pp. 746–752.

Babatunde, a. O., Zhao, Y.Q., Burke, a. M., Morris, M. a. and Hanrahan, J.P. 2009. Characterization of aluminium-based water treatment residual for potential phosphorus removal in engineered wetlands. *Environmental Pollution* 157(10), pp. 2830–2836.

Babatunde, A.O., Zhao, Y.Q., O'Neill, M. and O'Sullivan, B. 2008. Constructed wetlands for environmental pollution control : a review of developments, research and practice in Ireland. *Environment International* 34(1), pp. 116–126.

Babatunde, A.O., Zhao, Y.Q., Yang, Y. and Kearney, P. 2007. From 'fills' to filter : insights into the reuse of dewatered alum sludge as a filter media in a constructed wetland. *Journal of Residuals Science & Technology* 4(3), pp. 147–152.

Bakti, N.A.K. and Dick, R.I. 1992. A model for a nitrifying suspended-growth reactor incorporating intraparticle diffusional limitation. *Water Research* 26(12), pp. 1681–1690.

Balasubramaniam, R. and Kumar, A.V.R. 2000. Characterization of Delhi iron pillar rust by X-ray diffraction, Fourier transform infrared spectroscopy and Mössbauer spectroscopy. *Corrosion Science* 42, pp. 2085–2101.

Baldantoni, D., Alfani, A., Di Tommasi, P., Bartoli, G. and De Santo, A.V. 2004. Assessment of macro and microelement accumulation capability of two aquatic plants. *Environmental Pollution* 130(2), pp. 149–156.

Bang, J., Kamala-Kannan, S., Lee, K.-J., Cho, M., Kim, C.-H., Kim, Y.-J., Bae, J.-H., Kim, K.-H., Myung, H. and Oh, B.-T. 2015. Phytoremediation of Heavy Metals in Contaminated Water and Soil Using *Miscanthus sp. Goedae-Uksae* 1. *International Journal of Phytoremediation* 17(6), pp. 515–520.

Başar, C.A. 2006. Applicability of the various adsorption models of three dyes adsorption onto activated carbon prepared waste apricot. *Journal of Hazardous Materials* 135(1-3), pp. 232–241.

Batty, L.C. and Younger, P.L. 2004. Growth of *Phragmites australis* (Cav.) Trin ex. Steudel in mine water treatment wetlands: Effects of metal and nutrient uptake. *Environmental Pollution* 132(1), pp. 85–93.

Batty, L.C. and Younger, P.L. 2007. The effect of pH on plant litter decomposition and metal cycling in wetland mesocosms supplied with mine drainage. *Chemosphere* 66(1), pp. 158–164.

Batzias, A.F. and Siontorou, C.G. 2008. A new scheme for biomonitoring heavy metal concentrations in semi-natural wetlands. *Journal of Hazardous Materials* 158(2-3), pp. 340–358.

Baun, D.L. and Christensen, T.H. 2004. Speciation of heavy metals in landfill leachate: a review. *Waste management & research* 22(1), pp. 3–23.

Behnamfard, A. and Salarirad, M.M. 2009. Equilibrium and kinetic studies on free cyanide adsorption from aqueous solution by activated carbon. *Journal of Hazardous Materials* 170(1), pp. 127–133.

Beining, B.A. and Otte, M.L. 1996. Retention of metals originating from an abandoned lead-zinc mine by a wetland at Glendalough, Co. Wicklow. *Biology and Environment* 96(2), pp. 117–126.

Beining, B.A. and Otte, M.L. 1997. Retention of Metals and Longevity of a Wetland Receiving Mine Leachate. *Journal American Society of Mining and Reclamation* 96(1), pp. 43–48.

Bermond, A., Yousfi, I., Ghestem, J. and Analytique, L.D.C. 1998. Kinetic approach to the chemical speciation of trace metals in soils. *Analyst* 123(May), pp. 785–789.

Bernet, N., Habouzit, F. and Moletta, R. 1996. Use of an industrial effluent as a carbon source for denitrification of a high-strength wastewater. *Applied Microbiology and Biotechnology* 46(1), pp. 92–97.

Birkbeck, A.E., Reil, D. and Hunter, R. 1990. Application of natural and engineered wetlands for treatment of low-strength leachate. In: *Constructed Wetlands in Water Pollution Control. Proceedings International Conference on the use of Constructed Wetlands in Water Pollution Control.*, pp. 411–418.

Bonanno, G. and Lo Giudice, R. 2010. Heavy metal bioaccumulation by the organs of

- Phragmites australis (common reed) and their potential use as contamination indicators. *Ecological Indicators* 10(3), pp. 639–645.
- Bou-Zeid, E. and El-Fadel, M. 2004. Parametric sensitivity analysis of leachate transport simulations at landfills. *Waste Management* 24(7), pp. 681–689.
- Božić, D., Gorgievski, M., Stanković, V., Štrbac, N., Šerbula, S. and Petrović, N. 2013. Adsorption of heavy metal ions by beech sawdust - Kinetics, mechanism and equilibrium of the process. *Ecological Engineering* 58, pp. 202–206.
- Bradl, H.B. 2004. Adsorption of heavy metal ions on soils and soils constituents. *Journal of Colloid and Interface Science* 277(1), pp. 1–18.
- Bragato, C., Brix, H. and Malagoli, M. 2006. Accumulation of nutrients and heavy metals in *Phragmites australis* (Cav.) Trin. ex Steudel and *Bolboschoenus maritimus* (L.) Palla in a constructed wetland of the Venice lagoon watershed. *Environmental Pollution* 144(3), pp. 967–975.
- Brix, H. 1994. Functions of macrophytes in constructed wetlands. *Water Science and Technology* 29(4), pp. 71–78.
- Brix, H. 1997. Do Macrophytes Play a Role in Constructed Treatment. *Water Science and Technology* 35(5), pp. 11–17.
- Brix, H. 1999. How 'green' are aquaculture, constructed wetlands and conventional wastewater treatment systems? *Water Science and Technology* 40(3), pp. 45–50.
- Brix, H. and Johansen, N.H. 2004. Guidelines for vertical flow constructed wetland systems up to 30 PE. *Økologisk Byfornyelse og Spildevandsrensning* (52)
- Brovelli, A., Malaguerra, F. and Barry, D.A. 2009. Bioclogging in porous media: Model development and sensitivity to initial conditions. *Environmental Modelling and Software* 24(5), pp. 611–626.
- Castaldi, P., Lauro, G., Senette, C. and Deiana, S. 2010. Role of the Ca-pectates on the accumulation of heavy metals in the root apoplasm. *Plant Physiology and Biochemistry* 48(12), pp. 1008–1014.
- Castaldi, P., Mele, E., Silvetti, M., Garau, G. and Deiana, S. 2014. Water treatment residues as accumulators of oxoanions in soil. Sorption of arsenate and phosphate

- anions from an aqueous solution. *Journal of Hazardous Materials* 264, pp. 144–152.
- Castaldi, P., Silveti, M., Garau, G., Demurtas, D. and Deiana, S. 2015. Copper(II) and lead(II) removal from aqueous solution by water treatment residues. *Journal of Hazardous Materials* 283, pp. 140–147.
- Cerato, A.B. and Lutenegeger, A.J. 2002. Determination of surface area of fine-grained soils by the ethylene glycol monoethyl ether (EGME) method. *Geotechnical Testing Journal* 25(3), pp. 315–321.
- Chang, Y., Wu, S., Zhang, T., Mazur, R., Pang, C. and Dong, R. 2014. Dynamics of nitrogen transformation depending on different operational strategies in laboratory-scale tidal flow constructed wetlands. *Science of the Total Environment* 487(1), pp. 49–56.
- Chen, S., Sun, L., Chao, L., Zhou, Q. and Sun, T. 2009. Estimation of lead bioavailability in smelter-contaminated soils by single and sequential extraction procedure. *Bulletin of Environmental Contamination and Toxicology* 82(1), pp. 43–47.
- Chen, T., Zhou, Z., Han, R., Meng, R., Wang, H. and Lu, W. 2015a. Adsorption of cadmium by biochar derived from municipal sewage sludge: Impact factors and adsorption mechanism. *Chemosphere* 134, pp. 286–293.
- Chen, T., Zhou, Z., Han, R., Meng, R., Wang, H. and Lu, W. 2015b. Adsorption of cadmium by biochar derived from municipal sewage sludge: Impact factors and adsorption mechanism. *Chemosphere* 134, pp. 286–293.
- Chen, T.Y., Kao, C.M., Yeh, T.Y., Chien, H.Y. and Chao, A.C. 2006. Application of a constructed wetland for industrial wastewater treatment: A pilot-scale study. *Chemosphere* 64(3), pp. 497–502.
- Cheng, S., Grosse, W., Karrenbrock, F. and Thoennessen, M. 2002. Efficiency of constructed wetlands in decontamination of water polluted by heavy metals. *Ecological Engineering* 18(3), pp. 317–325.
- Cheng, Y., Yang, C., He, H., Zeng, G., Zhao, K. and Yan, Z. 2015. Biosorption of Pb (II) Ions from Aqueous Solutions by Waste Biomass from Biotrickling Filters : Kinetics , Isotherms , and Thermodynamics. *Environmental Engineering* 142(9), pp. 1–7.
- Chiang, Y.W., Ghyselbrecht, K., Santos, R.M., Martens, J. a., Swennen, R.,

- Cappuyns, V. and Meesschaert, B. 2012. Adsorption of multi-heavy metals onto water treatment residuals: Sorption capacities and applications. *Chemical Engineering Journal* 200-202, pp. 405–415.
- Chiemchaisri, C., Chiemchaisri, W., Junsod, J., Threedeach, S. and Wicranarachchi, P.N. 2009. Leachate treatment and greenhouse gas emission in subsurface horizontal flow constructed wetland. *Bioresource Technology* 100(16), pp. 3808–3814.
- Choudhary, A.K., Kumar, S. and Sharma, C. 2011. Constructed wetlands: an approach for wastewater treatment. *pollution* 37, pp. 3666–3672.
- Christensen, T.H., Kjeldsen, P., Albrechtsen, H.-J., Heron, G., Nielsen, P.H., Bjerg, P.L. and Holm, P.E. 1994. Attenuation of landfill leachate pollutants in aquifers. *Critical Reviews in Environmental Science and Technology* 24(2), pp. 119–202.
- Christensen, T.H., Kjeldsen, P., Bjerg, P.L., Jensen, D.L., Christensen, J.B., Baun, A., Albrechtsen, H. and Heron, G. 2001. Biogeochemistry of land leachate plumes. *Applied Geochemistry* 16, pp. 659–718.
- Chu, W. 2001. DYE REMOVAL FROM TEXTILE DYE WASTEWATER USING RECYCLED ALUM SLUDGE. *Water Research* 35(13), pp. 3147–3152.
- Ciavatta, C., Govi, M., Antisari, L.V. and Sequi, P. 1990. Characterization of humified compounds by extraction and fractionation on solid polyvinylpyrrolidone. *J. Chromatogr. A* 509(1), pp. 141–146.
- Coelho, G.F., Gonçalves, A.C., Tarley, C.R.T., Casarin, J., Nacke, H. and Francziskowski, M.A. 2014. Removal of metal ions Cd (II), Pb (II), and Cr (III) from water by the cashew nut shell *Anacardium occidentale* L. *Ecological Engineering* 73, pp. 514–525.
- Coleman, J., Hench, K., Garbutt, K. and Sexstone, A. 2001. Treatment of Domestic Wastewater by Three Plant Species in Constructed Wetlands. *Water Air and Soil Pollution* 128, pp. 283–295.
- Contrera, C.R., da Cruz Silva, K., Ribeiro, G.H., Morita, D.M., Zaiat, M. and Schalch, V. 2015. The ‘ chemical oxygen demand / total volatile acids ’ ratio as an anaerobic treatability indicator for landfill leachates. *Brazilian journal of Chemical Engineering/ Engineering* 32(01), pp. 73–86.

- Cooper, P.F., Job, G.D., Green, M.B. and Shutes, R.B.E. 1996. *Reed beds and constructed wetlands for wastewater treatment*. Water Research Centre Swindon, UK.
- Danh, L.T., Truong, P., Mammucari, R., Tran, T. and Foster, N. 2009. Vetiver grass, *vetiveria zizanioides*: A choice plant for phytoremediation of heavy metals and organic wastes. *International Journal of Phytoremediation* 11(8), pp. 664–691.
- Dorman, L., Castle, J.W. and Rodgers, J.H. 2009. Performance of a pilot-scale constructed wetland system for treating simulated ash basin water. *Chemosphere* 75(7), pp. 939–947.
- Fan, J., Wang, W., Zhang, B., Guo, Y., Ngo, H.H., Guo, W., Zhang, J. and Wu, H. 2013a. Nitrogen removal in intermittently aerated vertical flow constructed wetlands: Impact of influent COD/N ratios. *Bioresource Technology* 143, pp. 461–466.
- Fan, J., Zhang, B., Zhang, J., Ngo, H.H., Guo, W., Liu, F., Guo, Y. and Wu, H. 2013b. Intermittent aeration strategy to enhance organics and nitrogen removal in subsurface flow constructed wetlands. *Bioresource Technology* 141, pp. 117–122.
- Faulwetter, J.L., Gagnon, V., Sundberg, C., Chazarenc, F., Burr, M.D., Brisson, J., Camper, A.K. and Stein, O.R. 2009. Microbial processes influencing performance of treatment wetlands: A review. *Ecological Engineering* 35(6), pp. 987–1004.
- De Feo, G. 2007. Performance of vegetated and non-vegetated vertical flow reed beds in the treatment of diluted leachate. *Journal of Environmental Science and Health, Part A* 42(7), pp. 1013–1020.
- Ferreira, G., Celso, A., Jr, G., Ricardo, C., Tarley, T., Casarin, J., Nacke, H. and André, M. 2014. Removal of metal ions Cd ( II ), Pb ( II ), and Cr ( III ) from water by the cashew nut shell *Anacardium occidentale* L. *Ecological Engineering* 73, pp. 514–525.
- Fuchs, V. 2009. *Nitrogen removal and sustainability of vertical flow constructed wetlands for small scale wastewater treatment*. Michigan Technological University.
- Galletti, A., Verlicchi, P. and Ranieri, E. 2010. Removal and accumulation of Cu, Ni and Zn in horizontal subsurface flow constructed wetlands: Contribution of vegetation and filling medium. *Science of the Total Environment* 408(21), pp. 5097–5105.

Gao, H., Schreiber, F., Collins, G., Jensen, M.M., Kostka, J.E., Lavik, G., de Beer, D., Zhou, H. and Kuypers, M.M. 2009. Aerobic denitrification in permeable Wadden Sea sediments. *The ISME journal* 4(3), pp. 417–426.

Garau, G., Silveti, M., Castaldi, P., Mele, E., Deiana, P. and Deiana, S. 2014. Stabilising metal(loid)s in soil with iron and aluminium-based products: Microbial, biochemical and plant growth impact. *Journal of Environmental Management* 139, pp. 146–153.

García, J., Rousseau, D.P.L., MoratÓ, J., Lesage, E., Matamoros, V. and Bayona, J.M. 2010. Contaminant Removal Processes in Subsurface-Flow Constructed Wetlands: A Review. *Critical Reviews in Environmental Science and Technology* 40(7), pp. 561–661.

Garcia, J., Vivar, J., Aromir, M. and Mujeriego, R. 2003. Role of hydraulic retention time and granular medium in microbial removal in tertiary treatment reed beds. *Water Research* 37(11), pp. 2645–2653.

van Genuchten, M.T. 1980. A Closed-form Equation for Predicting the Hydraulic Conductivity of Unsaturated Soils<sup>1</sup>. *Soil Science Society of America Journal* 44(5), p. 892.

Goldberg, S. and Johnston, C.T. 2001. Mechanisms of Arsenic Adsorption on Amorphous Oxides Evaluated Using Macroscopic Measurements, Vibrational Spectroscopy, and Surface Complexation Modeling. *Journal of Colloid and Interface Science* 234(1), pp. 204–216.

Hagopian, D.S. and Riley, J.G. 1998. A closer look at the bacteriology of nitrification. *Aquacultural Engineering* 18(4), pp. 223–244.

Hair, J.F., Anderson, R.E., Babin, B.J. and Black, W.C. 2010. *Multivariate data analysis: A global perspective*. Seventh Ed. London: Pearson Upper Saddle River, NJ.

Hameed, B.H. 2008. Equilibrium and kinetic studies of methyl violet sorption by agricultural waste. *Journal of Hazardous Materials* 154(1-3), pp. 204–212.

Healy, M.G., Rodgers, M. and Mulqueen, J. 2007. Treatment of dairy wastewater using constructed wetlands and intermittent sand filters. *Bioresource Technology* 98(12), pp. 2268–2281.

Henze, M., Gujer, W., Mino, T. and Van Loosdrecht, M.C.M. 2000. *Activated sludge models ASM1, ASM2, ASM2d and ASM3*. IWA publishing.

Hong, M.S., Farmayan, W.F., Dortch, I.J., Chiang, C.Y., McMillan, S.K. and Schnoor, J.L. 2001. Phytoremediation of MTBE from a groundwater plume. *Environmental Science and Technology* 35(6), pp. 1231–1239.

Hoover, K.L., Rightnour, T.A., Collins, R. and Herd, R. 1998. *Applications of passive treatment to trace metals removal*. Proceeding of the American Power Conference in Chicago, Illinois; Pennwell Publishing: Tulsa, Oklahoma

Hu, Y., Zhao, Y. and Rymaszewicz, A. 2014. Robust biological nitrogen removal by creating multiple tides in a single bed tidal flow constructed wetland. *Science of the Total Environment* 470-471, pp. 1197–1204.

Hu, Y.S., Zhao, Y.Q., Zhao, X.H. and Kumar, J.L.G. 2012. Comprehensive analysis of step-feeding strategy to enhance biological nitrogen removal in alum sludge-based tidal flow constructed wetlands. *Bioresource Technology* 111, pp. 27–35.

Hua, T., Haynes, R.J., Zhou, Y.-F., Boulemant, a. and Chandrawana, I. 2015. Potential for use of industrial waste materials as filter media for removal of Al, Mo, As, V and Ga from alkaline drainage in constructed wetlands – Adsorption studies. *Water Research* 71, pp. 32–41.

Inamori, R., Gui, P., Dass, P., Matsumura, M., Xu, K. and Kondo, T. 2007. Investigating CH<sub>4</sub> and N<sub>2</sub>O emissions from eco-engineering wastewater treatment processes using constructed wetland microcosms. *Process Biochemistry* 42, pp. 363–373.

Ippolito, J.A., Barbarick, K.A. and Elliott, H.A. 2011. Drinking Water Treatment Residuals : A Review of Recent Uses. *Environmental Quality* 40, pp. 1–12.

ISO, N.F. 1994. 10390 (1994). *Soil quality, Determination of pH, AFNOR*

Jacob, D.L. and Otte, M.L. 2003. Conflicting Processes in the Wetland Plant. *Water, Air, & Soil Pollution* 3, pp. 91–104.

Jacob, D.L. and Otte, M.L. 2004. Long-term effects of submergence and wetland vegetation on metals in a 90-year old abandoned Pb-Zn mine tailings pond. *Environmental Pollution* 130(3), pp. 337–345.

Janos, P., Herzogová, L., Rejnek, J. and Hodslavská, J. 2004. Assessment of heavy metals leachability from metallo-organic sorbent-iron humate-with the aid of sequential extraction test. *Talanta* 62(3), pp. 497–501.

Jeyakumar, L. 2013. *Process based Modelling in Constructed Wetlands*. First Edit. Germany

Jönsson, J., Jönsson, J. and Lövgren, L. 2006. Precipitation of secondary Fe(III) minerals from acid mine drainage. *Applied Geochemistry* 21(3), pp. 437–445.

Jørgensen, S.E. and Fath, B.D. 2011. *Fundamentals of Ecological Modelling*. Fourth Edi. London: Elsevier.

Kadlce, R.H. and Wallace, S.D. 2008. *Treatment Wetlands*. Second edi. London

Kadlec, R.H. 1995. Overview: surface flow constructed wetlands. *Water Science and Technology* 32(3), pp. 1–12.

Kanagy, L.E., Johnson, B.M., Castle, J.W. and Rodgers, J.H. 2008. Design and performance of a pilot-scale constructed wetland treatment system for natural gas storage produced water. *Bioresource Technology* 99(6), pp. 1877–1885.

Kantar, C., Demir, A. and Koleli, N. 2013. Effect of exopolymeric substances on the kinetics of sorption and desorption of trivalent chromium in soil. *Chemical Papers* 68(1), pp. 112–120.

Kantawanichkul, S. and Neamkam, P. 2003. Optimum recirculation ratio for nitrogen removal in a combined system: vertical flow vegetated bed over horizontal flow sand bed. *Wetlands: Nutrients, Metals and Mass Cycling*. Backhuys Publishers, Leiden, The Netherlands , pp. 75–86.

Karadag, D., Koc, Y., Turan, M. and Armagan, B. 2006. Removal of ammonium ion from aqueous solution using natural Turkish clinoptilolite. *Journal of Hazardous Materials* 136(3), pp. 604–609.

Karathanasis, A.D., Potter, C.L. and Coyne, M.S. 2003. Vegetation effects on fecal bacteria, BOD, and suspended solid removal in constructed wetlands treating domestic wastewater. *Ecological Engineering* 20(2), pp. 157–169.

Keeney, D.R. 1973. The nitrogen cycle in sediment-water systems. *Journal of*

*Environmental Quality* 2(1), pp. 15–29.

Khan, S., Ahmad, I., Shah, M.T., Rehman, S. and Khaliq, A. 2009. Use of constructed wetland for the removal of heavy metals from industrial wastewater. *Journal of Environmental Management* 90(11), pp. 3451–3457.

Kjeldsen, P., Barlaz, M.A., Rooker, A.P., Baun, A., Ledin, A., Christensen, T.H., Kjeldsen, P., Barlaz, M.A., Rooker, A.P., Baun, A., Kjeldsen, P., Barlaz, M.A., Rooker, A.P., Ledin, A. and Christensen, T.H. 2002. Present and Long-Term Composition of MSW Landfill Leachate : A Review. *Critical Reviews in Environmental Science and Technology* 32(4), pp. 297–336.

Klomjek, P. and Nitisoravut, S. 2005. Constructed treatment wetland: A study of eight plant species under saline conditions. *Chemosphere* 58(5), pp. 585–593.

Knowles, P., Dotro, G., Nivala, J. and García, J. 2011. Clogging in subsurface-flow treatment wetlands : Occurrence and contributing factors. *Ecological Engineering* 37(2), pp. 99–112.

Kosolapov, D.B., Kuschik, P., Vainshtein, M.B., Vatsourina, A. V., Wießner, A., Kästner, M. and Müller, R.A. 2004. Microbial processes of heavy metal removal from carbon-deficient effluents in constructed wetlands. *Engineering in Life Sciences* 4(5), pp. 403–411.

Kulikowska, D. and Klimiuk, E. 2008. The effect of landfill age on municipal leachate composition. *Bioresource Technology* 99(13), pp. 5981–5985.

Kumar, J.L.G., Wang, Z.Y., Zhao, Y.Q., Babatunde, a O., Zhao, X.H. and Jørgensen, S.E. 2011. STELLA software as a tool for modelling phosphorus removal in a constructed wetland employing dewatered alum sludge as main substrate. *Journal of environmental science and health. Part A, Toxic/hazardous substances & environmental engineering* 46(7), pp. 751–757.

Kumar, J.L.G. and Zhao, Y.Q. 2011. A review on numerous modeling approaches for effective, economical and ecological treatment wetlands. *Journal of Environmental Management* 92(3), pp. 400–406.

Lambert, J.B., Shurvell, H.F., Lightner, D.A. and Cooks, R.G. 1987. *Introduction to organic spectroscopy*. First Edit. New York: Macmillan Publishing Company.

- Langergraber, G. 2008. Modeling of Processes in Subsurface Flow Constructed Wetlands: A Review. *Vadose Zone Journal* 7(2), pp. 830–842.
- Langergraber, G., Haberl, R., Laber, J. and Pressl, A. 2003. Evaluation of substrate clogging processes in vertical flow constructed wetlands. *Water Science and Technology* 48(5), pp. 25–34.
- Langergraber, G. and Slmůnek, J. 2005. Modeling Variably Saturated Water Flow and Multicomponent Reactive Transport in Constructed Wetlands. *Vadose Zone Journal* 4(4), pp. 924–938.
- Langergraber, G. and Šimůnek, J. 2006. *The multi-component reactive transport module CW2D FOR CONSTRUCTED WETLANDS FOR THE HYDRUS SOFTWARE PACKAGE*. Manual - V.
- Lavrova, S. and Koumanova, B. 2010. Influence of recirculation in a lab-scale vertical flow constructed wetland on the treatment efficiency of landfill leachate. *Bioresource Technology* 101(6), pp. 1756–1761.
- Lee, B.H. and Scholz, M. 2007. What is the role of *Phragmites australis* in experimental constructed wetland filters treating urban runoff? *Ecological Engineering* 29(1), pp. 87–95.
- Lee, B.-H. and Scholz, M. 2006. Application of the self-organizing map (SOM) to assess the heavy metal removal performance in experimental constructed wetlands. *Water research* 40(18), pp. 3367–74.
- Lee, C.G., Fletcher, T.D. and Sun, G. 2009. Nitrogen removal in constructed wetland systems. *Engineering in Life Sciences* 9(1), pp. 11–22.
- Lema, J., Mendez, R. and Blazquez, R. 1988. Characteristics of landfill leachates and alternatives for their treatment: a review. *Water, Air and Soil Pollution* 40, pp. 223–250.
- Lesage, E., Rousseau, D.P.L., Meers, E., Tack, F.M.G. and De Pauw, N. 2007. Accumulation of metals in a horizontal subsurface flow constructed wetland treating domestic wastewater in Flanders, Belgium. *Science of the Total Environment* 380(1-3), pp. 102–115.
- Li, X.Z. and Zhao, Q.L. 2001. Efficiency of biological treatment affected by high

strength of ammonium-nitrogen in leachate and chemical precipitation of ammonium-nitrogen as pretreatment. *Chemosphere* 44(1), pp. 37–43.

Li, X.Z., Zhao, Q.L., Hao, X.D., Engineering, S., Hom, H., Kong, H. and District, N. 1999. Ammonium removal from landfill leachate by chemical precipitation. *Waste Management* 19(6), pp. 409–415.

Lin, L.-Y. 1995. Wastewater treatment for inorganics. *Encyclopedia of environmental biology* 3, pp. 479–484.

Loer, J., Scholz-Barth, K., Kadlec, R.H., Wetzstein, D. and Julik, J. 1999. An integrated natural system for leachate treatment. *Constructed wetlands for the treatment of landfill leachates*, pp. 187–204.

Lu, S., Zhang, P., Jin, X., Xiang, C., Gui, M., Zhang, J. and Li, F. 2009. Nitrogen removal from agricultural runoff by full-scale constructed wetland in China. *Hydrobiologia* 621(1), pp. 115–126.

Ma, X. and Burken, J.G. 2003. TCE diffusion to the atmosphere in phytoremediation applications. *Environmental Science and Technology* 37(11), pp. 2534–2539.

Maine, M.A., Suñe, N., Hadad, H., Sánchez, G. and Bonetto, C. 2006. Nutrient and metal removal in a constructed wetland for wastewater treatment from a metallurgic industry. *Ecological Engineering* 26(4), pp. 341–347.

Maine, M.A., N.S.H.H.G.S.C.B. 2009. Influence of vegetation on the removal of heavy metals and nutrients in a constructed wetland. *Environmental Management* 90, pp. 355–363.

Makris, K.C., Sarkar, D. and Datta, R. 2006. Evaluating a drinking-water waste by-product as a novel sorbent for arsenic. *Chemosphere* 64(5), pp. 730–741.

Marchand, L., Mench, M., Jacob, D.L. and Otte, M.L. 2010. Metal and metalloid removal in constructed wetlands, with emphasis on the importance of plants and standardized measurements: A review. *Environmental Pollution* 158(12), pp. 3447–3461.

Martensson, A.M., Aulin, C., Wahlberg, O. and Agren, S. 1999. Effect of humic substances on the mobility of toxic metals in a mature landfill. *Waste Management & Research* 17(4), pp. 296–304.

- Martin, C.D., Moshiri, G.A. and Miller, C.C. 1993. *Mitigation of landfill leachate incorporating in-series constructed wetlands of a closed-loop design*. Lewis Publishers, Chelsea, MI.
- Matagi, S., Swai, D. and Mugabe, R. 1998. A review of Heavy Metal Removal Mechanisms in wetlands. *African Journal of Tropical Hydrobiology and Fisheries* 8(1), pp. 23–35.
- McKeague, J. a. and Day, J.H. 1966. Dithionite- and oxalate-extractable Fe and Al as aids in differentiating various classes of soils. *Canadian Journal of Soil Science* 46(1), pp. 13–22.
- Mendoza, C.A., Therrien, R. and Sudicky, E.A. 1991. ORTHOFEM Users Guide, Version 1.02. *Waterloo Centre for Groundwater Research, Univ. of Waterloo, Waterloo, ON*
- Metcalf and Eddy 2003. *Wastewater engineering: Treatment and reuse*. Fourth Edi. New York, USA: McGraw-Hill.
- Mitchell, C. and McNevin, D. 2001. Alternative analysis of BOD removal in subsurface flow constructed wetlands employing Monod kinetics. *Water Research* 35(5), pp. 1295–1303.
- Mohan, S. and Gandhimathi, R. 2009. Removal of heavy metal ions from municipal solid waste leachate using coal fly ash as an adsorbent. *Journal of Hazardous Materials* 169(1-3), pp. 351–359.
- Molle, P., Li??nard, A., Boutin, C., Merlin, G. and Iwema, A. 2005. How to treat raw sewage with constructed wetlands: An overview of the French systems. *Water Science and Technology* 51(9), pp. 11–21.
- Molle, P., Prost-Boucle, S. and Lienard, A. 2008. Potential for total nitrogen removal by combining vertical flow and horizontal flow constructed wetlands: A full-scale experiment study. *Ecological Engineering* 34(1), pp. 23–29.
- Mulder, A., Van de Graaf, A.A., Robertson, L. a. and Kuenen, J.G. 1995. Anaerobic ammonium oxidation discovered in a denitrifying fluidized bed reactor. *microbiology Ecology* 16, pp. 177–184.
- Murphy, C. and Cooper, D. 2010. The Evolution of Horizontal Subsurface Flow Reed

Bed Design for Tertiary Treatment of Sewage Effluents in the UK. In: *Water and Nutrient Management in Natural and Constructed Wetlands*. Springer., pp. 103–119.

Murray-Gulde, C.L., Berr, J. and Rodgers, J.H. 2005. Evaluation of a constructed wetland treatment system specifically designed to decrease bioavailable copper in a wastestream. *Ecotoxicology and Environmental Safety* 61(1), pp. 60–73.

Nakamoto, K. 1986. *Infrared and Raman spectra of inorganic and coordination compounds*. Wiley Online Library.

Ngah, W.S.W. and Fatinathan, S. 2010. Adsorption characterization of Pb(II) and Cu(II) ions onto chitosan-tripolyphosphate beads: Kinetic, equilibrium and thermodynamic studies. *Journal of Environmental Management* 91(4), pp. 958–969.

Nivala, J., Hoos, M.B., Cross, C., Wallace, S. and Parkin, G. 2007. Treatment of landfill leachate using an aerated, horizontal subsurface-flow constructed wetland. *Science of the Total Environment* 380(1-3), pp. 19–27.

Ogata, Y., Ishigaki, T., Ebie, Y., Sutthasil, N., Chiemchaisri, C. and Yamada, M. 2015. Water reduction by constructed wetlands treating waste landfill leachate in a tropical region. *Waste Management* 44, pp. 164–171.

Ojeda, E., Caldentey, J., Saaltink, M.W. and García, J. 2008. Evaluation of relative importance of different microbial reactions on organic matter removal in horizontal subsurface-flow constructed wetlands using a 2D simulation model. *Ecological Engineering* 34(1), pp. 65–75.

Ouyang, Y., Luo, S.M. and Cui, L.H. 2011. Estimation of nitrogen dynamics in a vertical-flow constructed wetland. *Ecological Engineering* 37(3), pp. 453–459.

Øygaard, J.K., Gjengedal, E. and Røyset, O. 2007. Size charge fractionation of metals in municipal solid waste landfill leachate. *Water Research* 41(1), pp. 47–54.

Pastor, R., Benqilou, C., Paz, D., Cardenas, G., Espuña, A. and Puigjaner, L. 2003. Design optimisation of constructed wetlands for wastewater treatment. *Resources, Conservation and Recycling* 37(3), pp. 193–204.

Pasztor, I., Thury, P. and Pulai, J. 2009. Chemical oxygen demand fractions of municipal wastewater. *International Journal of Environmental Science Technology* 6(1), pp. 51–56.

- Van der Peiji, M.J. and Verhoeven, J.T.A. 1999. A model of carbon, nitrogen and phosphorus dynamics and their interactions in river marginal wetlands. *Ecological Modelling* 118, pp. 95–130.
- Pimpan, P. and Jindal, R. 2009. Mathematical modeling of cadmium removal in free water surface constructed wetlands. *Journal of Hazardous Materials* 163(2-3), pp. 1322–1331.
- Platzer, C. and Mauch, K. 1997. Soil clogging in vertical flow reed beds - Mechanisms, parameters, consequences and.....solutions? *Water Science and Technology* 35(5), pp. 175–181.
- Quan, W.M., Han, J.D., Shen, A.L., Ping, X.Y., Qian, P.L., Li, C.J., Shi, L.Y. and Chen, Y.Q. 2007. Uptake and distribution of N, P and heavy metals in three dominant salt marsh macrophytes from Yangtze River estuary, China. *Marine Environmental Research* 64(1), pp. 21–37.
- Ray, C., Student, G. and Chan, P.C. 1986. Heavy metals in landfill leachate. *International Journal of Environmental Studies* 27(3-4), pp. 225–237.
- Reed, S.C., Crites, R.W. and Middlebrooks, E.J. 1995. *Natural systems for waste management and treatment*. 2nd Edition ed. New York: McGraw-Hill.
- Reinhart, D.R. 1996. Full-Scale Experiences With Leachate Recirculating Landfills : Case Studies. *Wast Management and Research* , pp. 347–365.
- Reinhart, D.R. and Al-Yousfi, A.B. 1996. The impact of leachate recirculation on municipal solid waste landfill operating characteristics. *Waste management and Research* 20(2), pp. 337–346.
- Renou, S., Givaudan, J.G., Poulain, S., Dirassouyan, F. and Moulin, P. 2008. Landfill leachate treatment: Review and opportunity. *Journal of Hazardous Materials* 150(3), pp. 468–493.
- Rong, L. 2009. *Management of Landfill Leachate*. TAMK University of Applied Sciences.
- Saeed, T., Afrin, R., Al, A. and Sun, G. 2012. Chemosphere Treatment of tannery wastewater in a pilot-scale hybrid constructed wetland system in Bangladesh. *Chemosphere* 88, pp. 1065–1073.

- Saeed, T. and Sun, G. 2012. A review on nitrogen and organics removal mechanisms in subsurface flow constructed wetlands: Dependency on environmental parameters, operating conditions and supporting media. *Journal of Environmental Management* 112, pp. 429–448.
- Seo, D.C., Yu, K. and DeLaune, R.D. 2008. Comparison of monometal and multimetal adsorption in Mississippi River alluvial wetland sediment: Batch and column experiments. *Chemosphere* 73(11), pp. 1757–1764.
- Sheoran, A.S. and Sheoran, V. 2006. Heavy metal removal mechanism of acid mine drainage in wetlands: A critical review. *Minerals Engineering* 19(2), pp. 105–116.
- Song, X., Ding, Y., Wang, Y., Wang, W., Wang, G. and Zhou, B. 2015. Comparative study of nitrogen removal and bio-film clogging for three filter media packing strategies in vertical flow constructed wetlands. *Ecological Engineering* 74, pp. 1–7.
- Song, Z., Zheng, Z., Li, J., Sun, X., Han, X., Wang, W. and Xu, M. 2006. Seasonal and annual performance of a full-scale constructed wetland system for sewage treatment in China. *Ecological Engineering* 26(3), pp. 272–282.
- Staubitz, W.W., Surface, J.M., Steenhuis, T.S., Peverly, J.H. and Lavine, M.J. 1989. Potential use of constructed wetlands to treat landfill leachate. *Constructed Wetlands for Wastewater Treatment: Municipal, Industrial and Agricultural*. Lewis Publishers, Chelsea Michigan. , pp. 735–742.
- Stefanakis, A., Akratos, C.S. and Tsihrintzis, V.A. 2014. *Vertical flow constructed wetlands: eco-engineering systems for wastewater and sludge treatment*. First Edit. London: Newnes.
- Stefanakis, A.I., Akratos, C.S. and Tsihrintzis, V.A. 2011. Effect of wastewater step-feeding on removal efficiency of pilot-scale horizontal subsurface flow constructed wetlands. *Ecological Engineering* 37(3), pp. 431–443.
- Stefanakis, A.I. and Tsihrintzis, V.A. 2011. Dewatering mechanisms in pilot-scale Sludge Drying Reed Beds: Effect of design and operational parameters. *Chemical Engineering Journal* 172(1), pp. 430–443.
- Stefanakis, A.I. and Tsihrintzis, V.A. 2012. Effects of loading, resting period, temperature, porous media, vegetation and aeration on performance of pilot-scale vertical flow constructed wetlands. *Chemical Engineering Journal* 181-182, pp. 416–

430.

Stottmeister, U., Wießner, A., Kusch, P., Kappelmeyer, U., Kästner, M., Bederski, O., Müller, R.A. and Moormann, H. 2003. Effects of plants and microorganisms in constructed wetlands for wastewater treatment. *Biotechnology Advances* 22(1-2), pp. 93–117.

Sun, G., Gray, K.R. and Biddlestone, A.J. 1999. Treatment of Agricultural Wastewater in a Pilot-Scale Tidal Flow Reed Bed System. *Environmental Technology* 20(2), pp. 233–237.

Sun, G., Gray, K.R., Biddlestone, A.J., Allen, S.J. and Cooper, D.J. 2003. Effect of effluent recirculation on the performance of a reed bed system treating agricultural wastewater. *Process Biochemistry* 39(3), pp. 351–357.

Sun, G., Zhao, Y. and Allen, S. 2005. Enhanced removal of organic matter and ammoniacal-nitrogen in a column experiment of tidal flow constructed wetland system. *Journal of Biotechnology* 115(2), pp. 189–197.

Sung, W. and Morgan, J.J. 1980. Kinetics and product of ferrous iron oxygenation in aqueous systems. *Environmental Science & Technology* 14(5), pp. 561–568.

Tahir, S.S. and Naseem, R. 2007. Removal of Cr(III) from tannery wastewater by adsorption onto bentonite clay. *Separation and Purification Technology* 53(3), pp. 312–321.

Tan, X., Liu, Y., Zeng, G., Wang, X., Hu, X., Gu, Y. and Yang, Z. 2015. Application of biochar for the removal of pollutants from aqueous solutions. *Chemosphere* 125, pp. 70–85.

Tang, X., Emeka, P., Scholz, M. and Huang, S. 2009. Bioresource Technology Processes impacting on benzene removal in vertical-flow constructed wetlands. *Bioresource Technology* 100, pp. 227–234.

Tanner, C.C., Kadlec, R.H., Gibbs, M.M. and Sukias, J.P.S. 2002. Nitrogen processing gradients in subsurface-flow treatment wetlands — influence of wastewater characteristics. *Ecological Engineering* 18, pp. 499–520.

Terzakis, S., Fountoulakis, M.S., Georgaki, I., Albantakis, D., Sabathianakis, I., Karathanasis, A.D., Kalogerakis, N. and Manios, T. 2008. Constructed wetlands

treating highway runoff in the central Mediterranean region. *Chemosphere* 72(2), pp. 141–149.

Third, K. a 2003. *Oxygen Management for Optimisation of Nitrogen Removal in a Sequencing Batch Reactor Katie Third*. Murdoch University, Western Australia.

Thornton, S.F., Bright, M.I., Lerner, D.N. and Tellam, J.H. 2000. Attenuation of landfill leachate by UK Triassic sandstone aquifer materials: 2. Sorption and degradation of organic pollutants in laboratory columns. *Journal of Contaminant Hydrology* 43(3-4), pp. 355–383.

Tomenko, V., Ahmed, S. and Popov, V. 2007. Modelling constructed wetland treatment system performance. *Ecological Modelling* 205(3-4), pp. 355–364.

Toscano, A., Langergraber, G., Consoli, S. and Cirelli, G.L. 2009. Modelling pollutant removal in a pilot-scale two-stage subsurface flow constructed wetlands. *Ecological Engineering* 35(2), pp. 281–289.

Trautmann, N.M., Martin, J.H., Porter, K.S. and Hawk, K.C. 1989. *Use of artificial wetlands for treatment of municipal solid waste landfill leachate*. Lewis Publishers, Chelsea, Michigan, USA.

Vijayaraghavan, K., Padmesh, T.V.N., Palanivelu, K. and Velan, M. 2006. Biosorption of nickel(II) ions onto *Sargassum wightii*: Application of two-parameter and three-parameter isotherm models. *Journal of Hazardous Materials* 133(1-3), pp. 304–308.

Vymazal, J. 2002. The use of sub-surface constructed wetlands for wastewater treatment in the Czech Republic: 10 years experience. *Ecological Engineering* 18(5), pp. 633–646.

Vymazal, J. 2007. Removal of nutrients in various types of constructed wetlands. *Science of the Total Environment* 380(1-3), pp. 48–65.

Vymazal, J. 2011. Constructed Wetlands for Wastewater Treatment: Five Decades of Experience. *Environmental Science & Technology* 45(1), pp. 61–69.

Vymazal, J. 2014. Constructed wetlands for treatment of industrial wastewaters: A review. *Ecological Engineering* 73, pp. 724–751.

Vymazal, J. and Brezinova, T. 2016. Removal of saccharin from municipal sewage:

The first results from constructed wetlands. *Chemical Engineering Journal* 306, pp. 1067–1070.

Vymazal, J., Březinová, T. and Koželuh, M. 2015. Occurrence and removal of estrogens, progesterone and testosterone in three constructed wetlands treating municipal sewage in the Czech Republic. *Science of the Total Environment* 536, pp. 625–631.

Vymazal, J., Brix, H., Cooper, P.F., Green, M.B. and Haberl, R. 1998. *Constructed wetlands for wastewater treatment in Europe*. Backhuys Leiden.

Vymazal, J., Švehla, J., Kröpfelová, L. and Chrastný, V. 2007. Trace metals in *Phragmites australis* and *Phalaris arundinacea* growing in constructed and natural wetlands. *Science of the Total Environment* 380(1-3), pp. 154–162.

Wang, B.M.C., Hull, J.Q., Jao, M., Dempsey, B.A. and Cornwell, D.A. 1993. Engineering behavior of water treatment sludge. *Environmental Engineering* 118(6), pp. 848–864.

Wang, J., Wang, X., Zhao, Z. and Li, J. 2008. Organics and nitrogen removal and sludge stability in aerobic granular sludge membrane bioreactor. *Applied Microbiology and Biotechnology* 79(4), pp. 679–685.

Warith, B.M.A., Smolkin, P.A. and Caldwell, J.G. 2001. Effect of leachate recirculation on enhancement of biological degradation of solid waste: Case study. *Practice Periodical of Hazardous, Toxic, and Radioactive Waste Management* 5(1), pp. 40–46.

Webb, J.S., McGinness, S. and Lappin-Scott, H.M. 1998. Metal removal by sulphate-reducing bacteria from natural and constructed wetlands. *Journal of Applied Microbiology* 84(2), pp. 240–248.

Winter, K.J. and Goetz, D. 2003. The impact of sewage composition on the soil clogging phenomena of vertical flow constructed wetlands. *Water Science and Technology* 48(5), pp. 9–14.

Wiszniewski, J., Robert, D., Surmacz-Gorska, J., Miksch, K. and Weber, J. V. 2006. Landfill leachate treatment methods: A review. *Environmental Chemistry Letters* 4(1), pp. 51–61.

Wu, H., Fan, J., Zhang, J., Ngo, H.H., Guo, W., Hu, Z. and Lv, J. 2015. Optimization

of organics and nitrogen removal in intermittently aerated vertical flow constructed wetlands: Effects of aeration time and aeration rate. *International Biodeterioration and Biodegradation* 113, pp. 139–145.

Wu, S., Zhang, D., Austin, D., Dong, R. and Pang, C. 2011. Evaluation of a lab-scale tidal flow constructed wetland performance: Oxygen transfer capacity, organic matter and ammonium removal. *Ecological Engineering* 37(11), pp. 1789–1795.

Wuchter, C., Abbas, B., Coolen, M.J.L., Herfort, L., van Bleijswijk, J., Timmers, P., Strous, M., Teira, E., Herndl, G.J., Middelburg, J.J., Schouten, S. and Sinninghe Damsté, J.S. 2006. Archaeal nitrification in the ocean. *Proceedings of the National Academy of Sciences of the United States of America* 103(33), pp. 12317–22.

Yalcuk, A. and Ugurlu, A. 2009. Comparison of horizontal and vertical constructed wetland systems for landfill leachate treatment. *Bioresource Technology* 100(9), pp. 2521–2526.

Yang, B. 2006. Long-term efficiency and stability of wetlands for treating wastewater of a lead/zinc mine and the concurrent ecosystem development. *Environmental Pollution* 143(3), pp. 1105–1112.

Yang, X. and You, X. 2013. Estimating parameters of van genuchten model for soil water retention curve by intelligent algorithms. *Applied Mathematics and Information Sciences* 7(5), pp. 1977–1983.

Yao, K.-M., Habibian, M. and O'Melia, C. 1971. Water and waste water filtration. Concepts and applications. *Environmental Science & Technology* 5(11), pp. 1105–1112.

Zachara, J.M., Girvin, D.C., Schmidt, R.L. and Resch, C.T. 1987. Chromate adsorption on amorphous iron oxyhydroxide in the presence of major groundwater ions. *Environmental science & technology* 21(6), pp. 589–594.

Zhang, J., Wu, P., Hao, B. and Yu, Z. 2011. Heterotrophic nitrification and aerobic denitrification by the bacterium *Pseudomonas stutzeri* YZN-001. *Bioresource Technology* 102(21), pp. 9866–9869.

Zhang, L., Scholz, M., Mustafa, A. and Harrington, R. 2008. Assessment of the nutrient removal performance in integrated constructed wetlands with the self-organizing map. *Water Research* 42(13), pp. 3519–3527.

- Zhang, L., Scholz, M., Mustafa, A. and Harrington, R. 2009. Application of the self-organizing map as a prediction tool for an integrated constructed wetland agroecosystem treating agricultural runoff. *Bioresource Technology* 100(2), pp. 559–565.
- Zhang, Q.Q., Tian, B.H., Zhang, X., Ghulam, A., Fang, C.R. and He, R. 2013. Investigation on characteristics of leachate and concentrated leachate in three landfill leachate treatment plants. *Waste Management* 33(11), pp. 2277–2286.
- Zhao, Y. Q.; Sun, G; Allen, S. 2004c. Anti-sized reed bed system for animal wastewater treatment : a comparative study. *Water Research* 38(12), pp. 2907–2917.
- Zhao, H.W., Mavinic, D.S., Oldham, W.K. and Koch, F. a. 1999. Controlling factors for simultaneous nitrification and denitrification in a two-stage intermittent aeration process treating domestic sewage. *Water Research* 33(4), pp. 961–970.
- Zhao, Y.J., Liu, B., Zhang, W.G., Ouyang, Y. and An, S.Q. 2010. Performance of pilot-scale vertical-flow constructed wetlands in responding to variation in influent C/N ratios of simulated urban sewage. *Bioresource Technology* 101(6), pp. 1693–1700.
- Zhao, Y.Q., Babatunde, a O., Razali, M. and Harty, F. 2008. Use of dewatered alum sludge as a substrate in reed bed treatment systems for wastewater treatment. *Journal of environmental science and health. Part A, Toxic/hazardous substances & environmental engineering* 43(1), pp. 105–110.
- Zhao, Y.Q., Babatunde, A.O., Hu, Y.S., Kumar, J.L.G. and Zhao, X.H. 2011. Pilot field-scale demonstration of a novel alum sludge-based constructed wetland system for enhanced wastewater treatment. *Biochemistry* 46(1), pp. 278–283.
- Zhao, Y.Q., Sun, G. and Allen, S.J. 2004b. Purification capacity of a highly loaded laboratory scale tidal flow reed bed system with effluent recirculation. *Science of the Total Environment* 330, pp. 1–8.
- Zhao, Y.Q., Sun, G., Lafferty, C. and Allen, S. 2004a. Optimising the performance of a lab-scale tidal flow reed bed system treating agricultural wastewater. *Water Science and Technology* 50(8), pp. 65– 72.
- Zhao, Y.Q., Zhao, X.H. and Babatunde, A.O. 2009. Use of dewatered alum sludge as main substrate in treatment reed bed receiving agricultural wastewater : long-term trial. *Bioresource Technology* 100(2), pp. 644–648.

Zhou, Y.F. and Haynes, R.J. 2011. Removal of Pb(II), Cr(III) and Cr(VI) from aqueous solutions using alum-derived water treatment sludge. *Water, Air, and Soil Pollution* 215(1-4), pp. 631–643.

# **Appendix A**

**Figures of physicochemical characterisation of DWSs  
and removal efficiency of HM by DWSs**

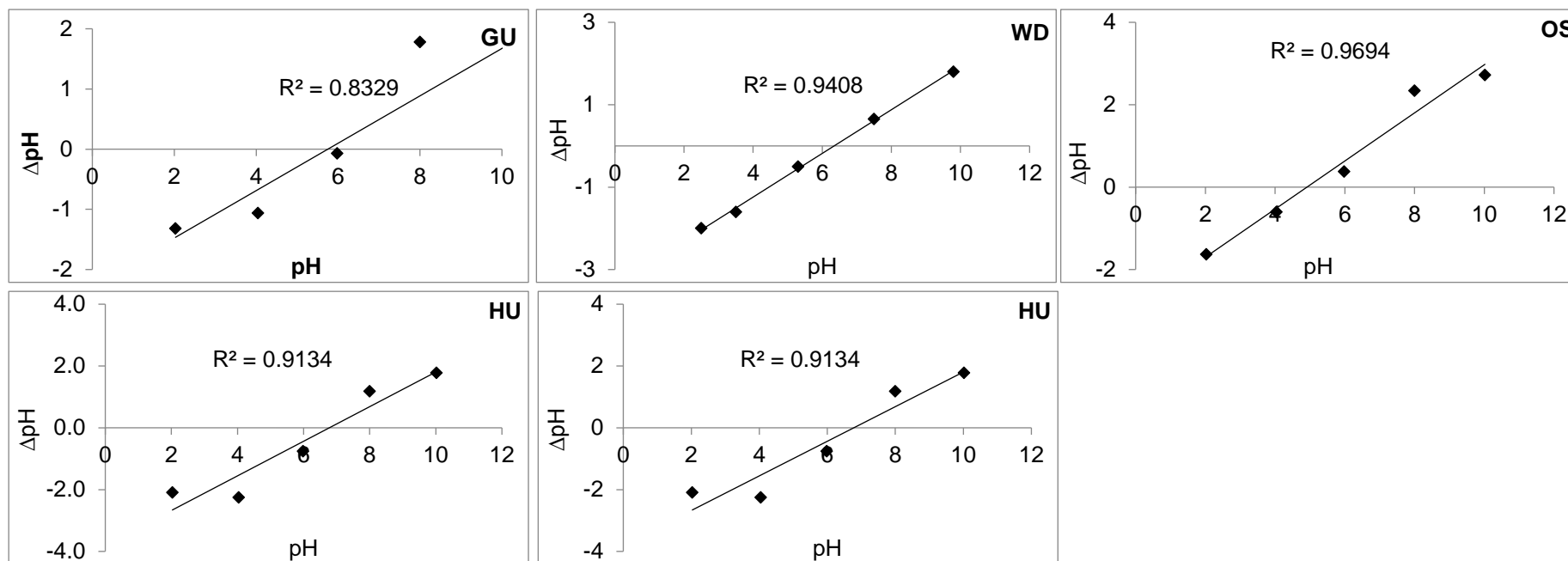


Figure A. 1 Point of zero charge (PZC) determination of aluminium- based sludges.

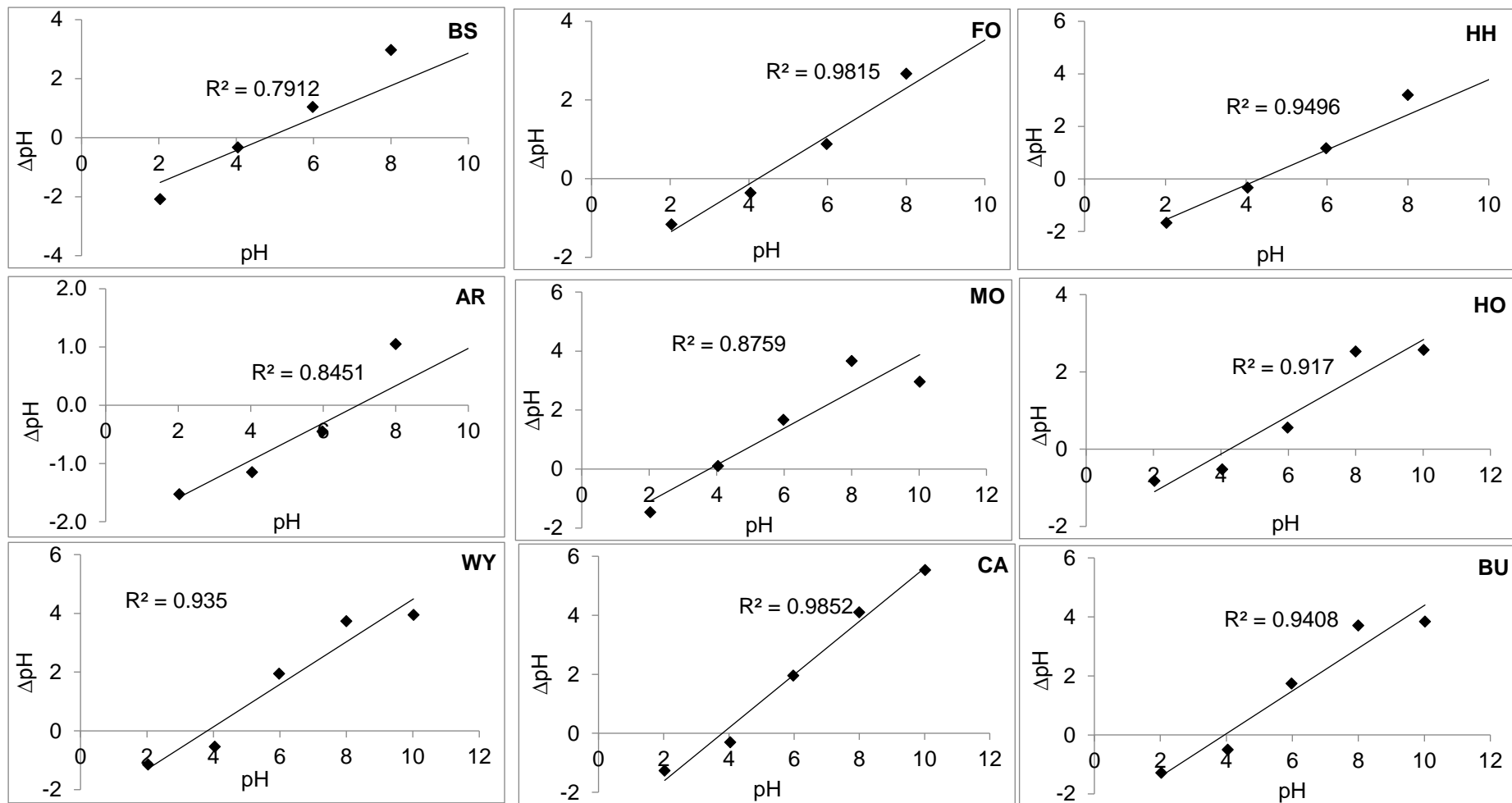


Figure A. 2 Point of zero charge (PZC) determination of ferric- based sludges.

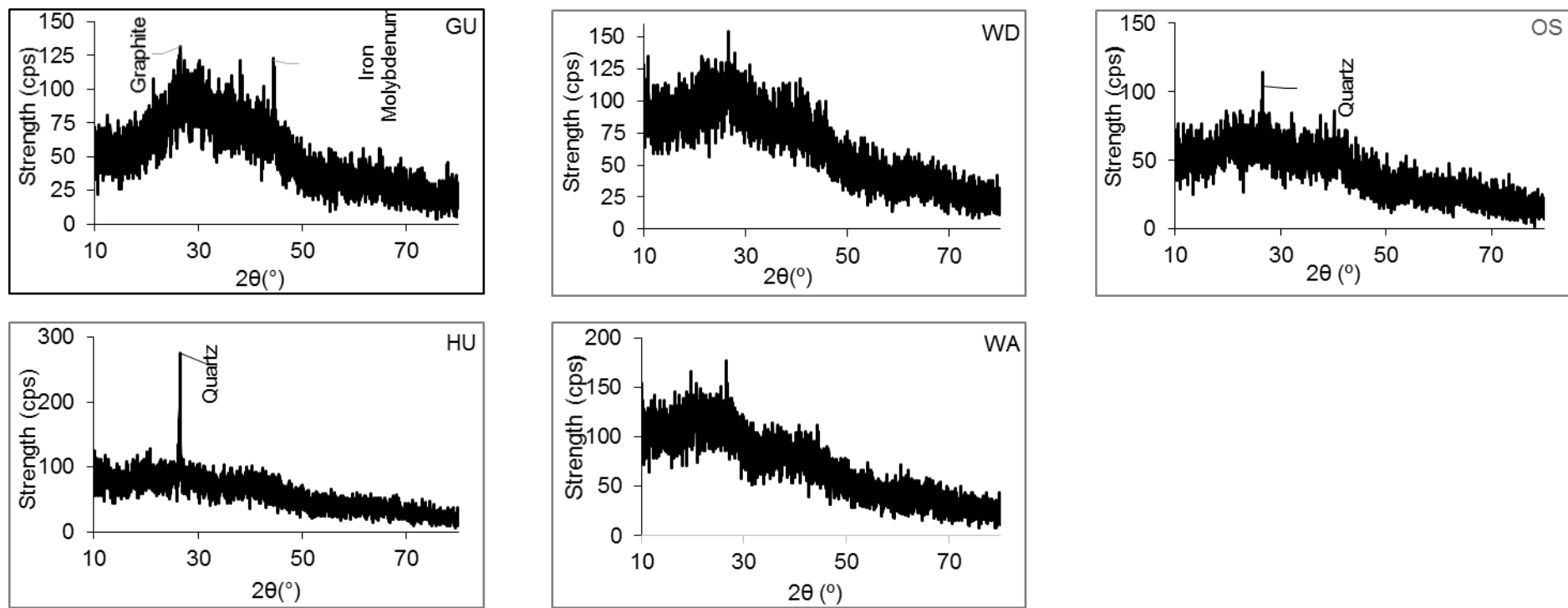


Figure A. 3 XRD patterns of aluminum-based sludges.

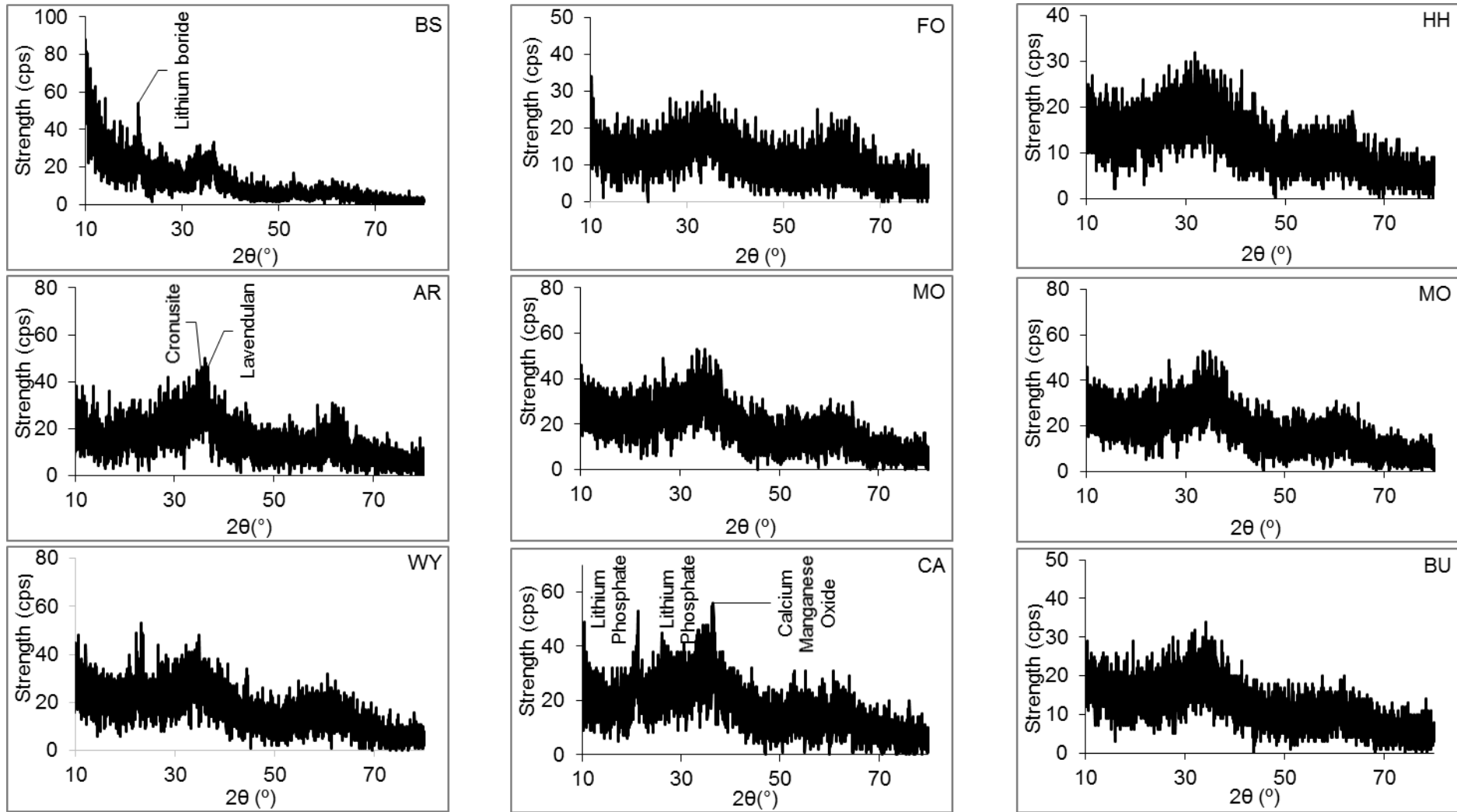


Figure A. 4 XRD patterns of ferric-based sludges.

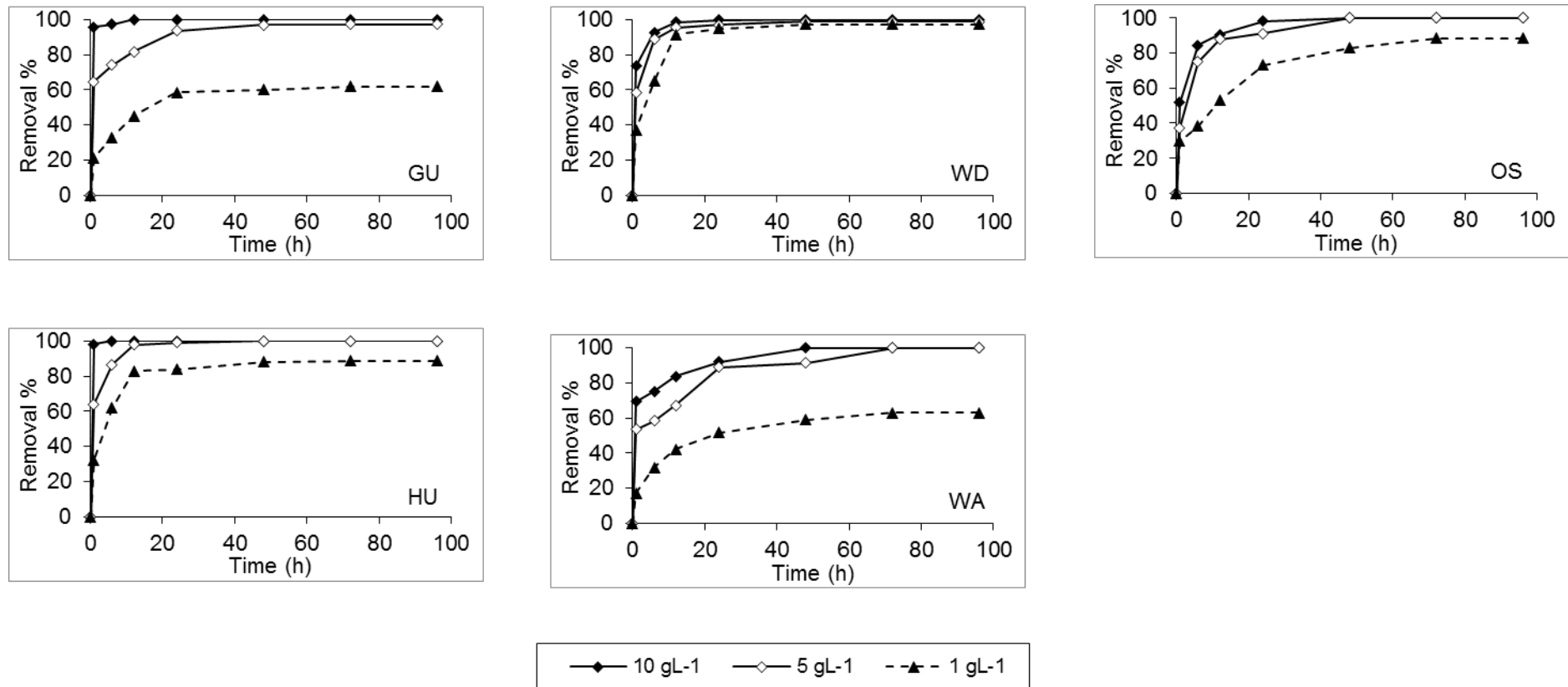


Figure A. 5 Removal efficiency of lead by aluminum- based sludges at different contact time and three different sludge dosages.

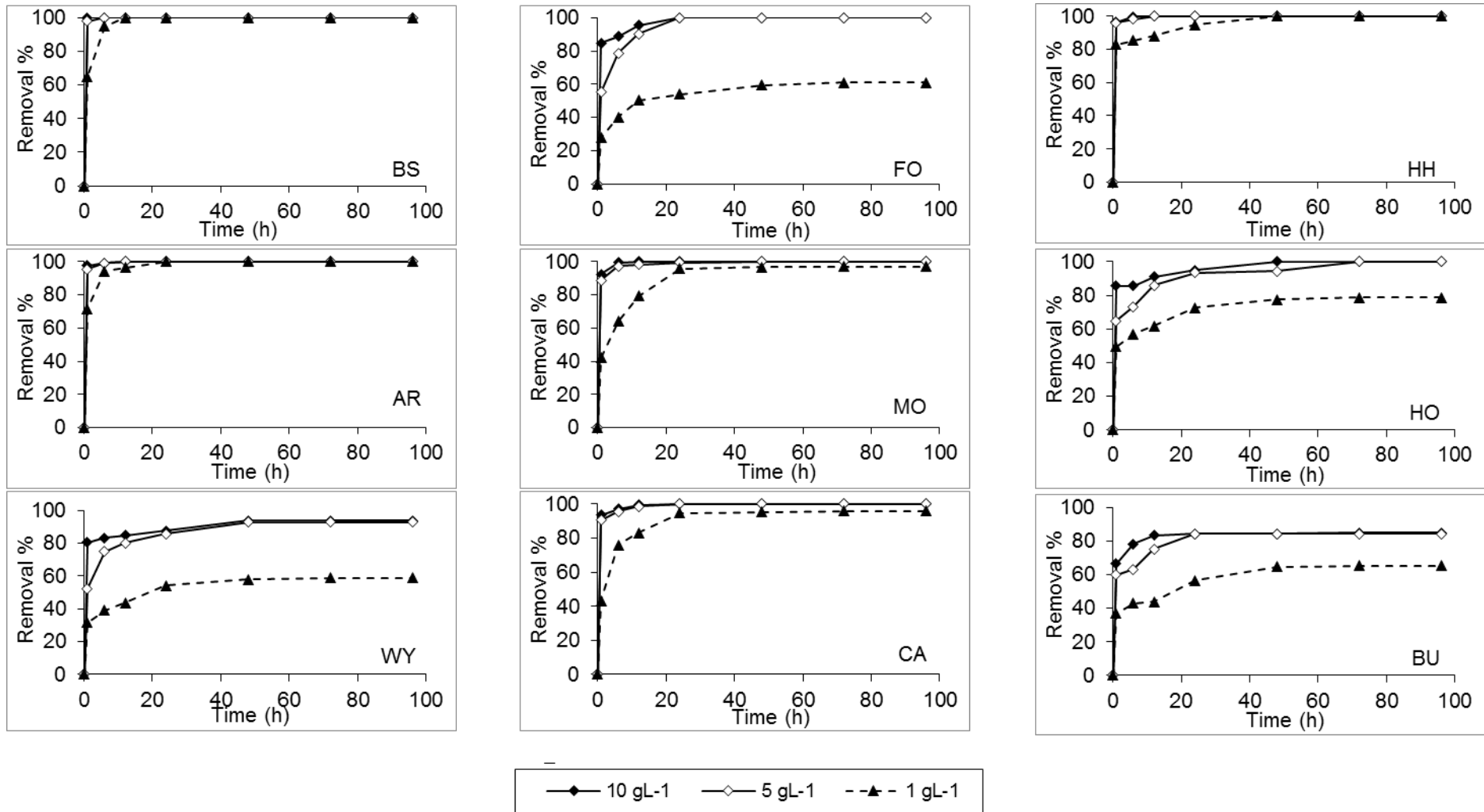


Figure A. 6 Removal efficiency of lead by ferric- based sludges at different contact time and three different sludge dosages.

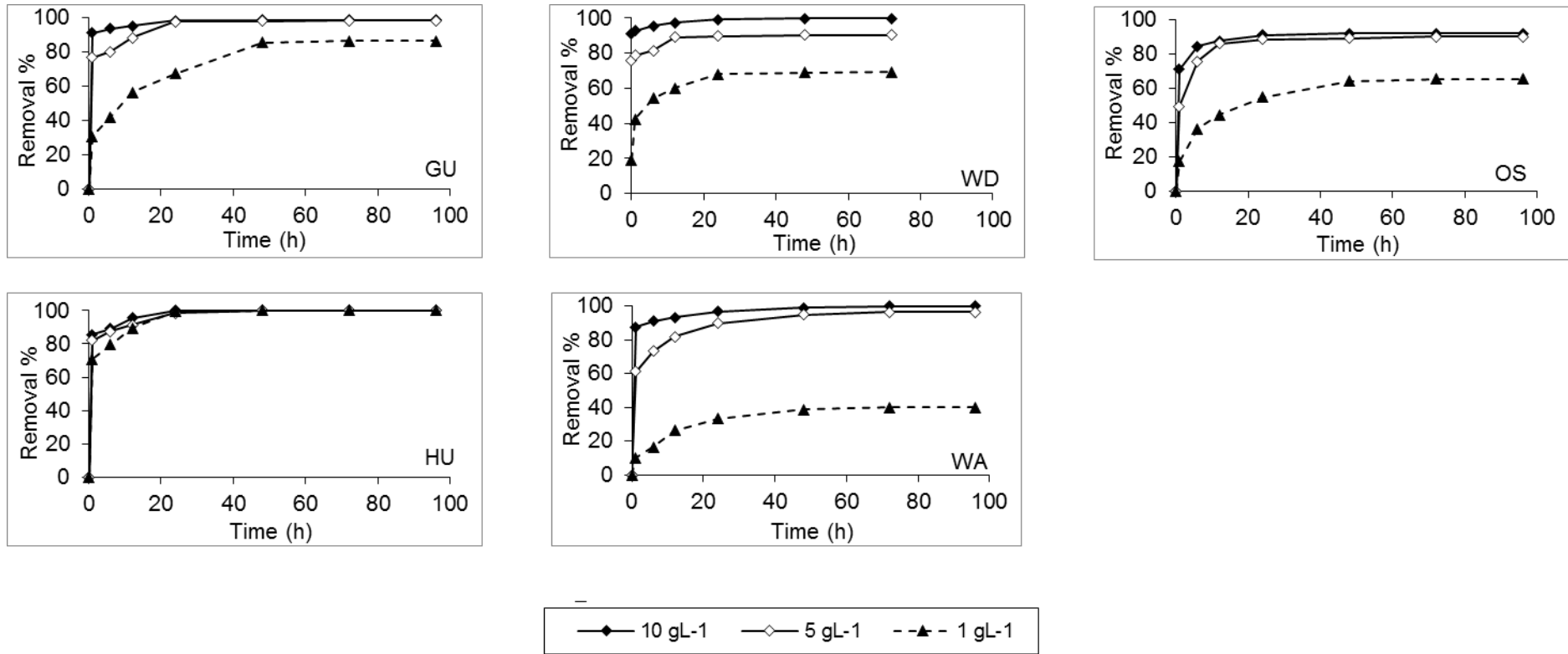


Figure A. 7 Removal efficiency of chromium by aluminium- based sludges at different contact time and three different sludge dosages.

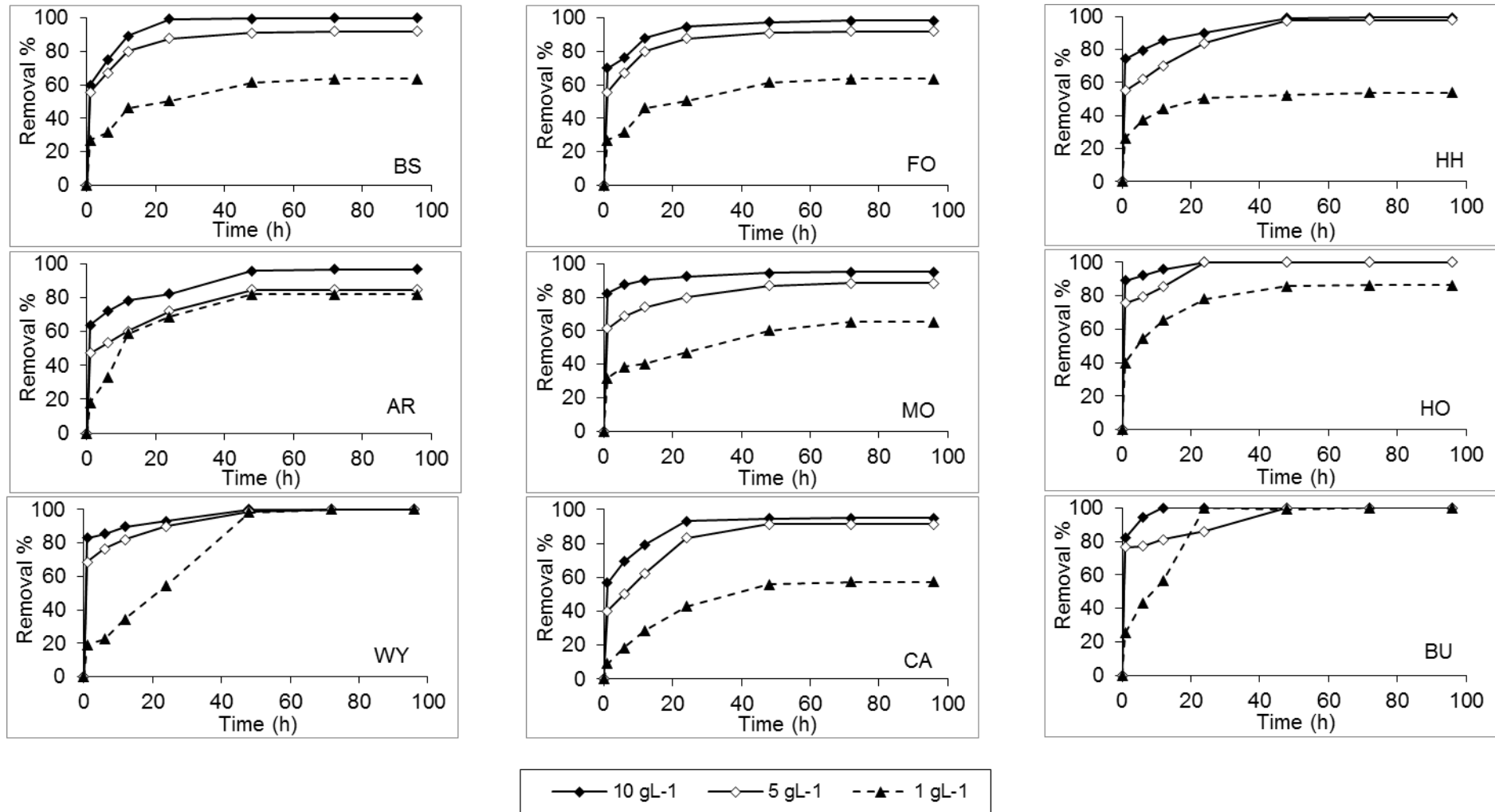


Figure A. 8 Removal efficiency of chromium by ferric-based sludges at different contact time and three different sludge dosages.

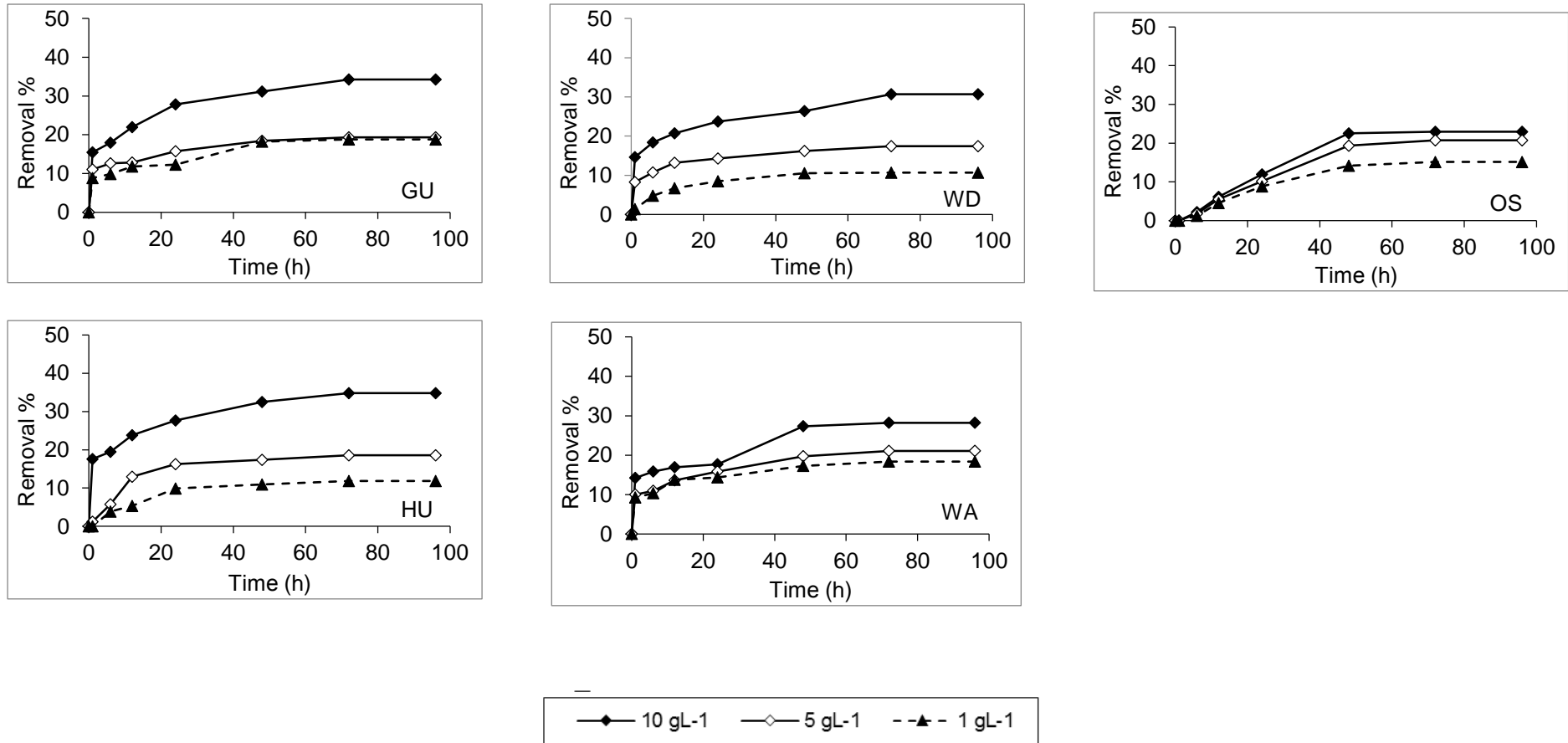


Figure A. 9 Removal efficiency of cadmium by aluminium- based sludges at different contact time and three different sludge dosages.

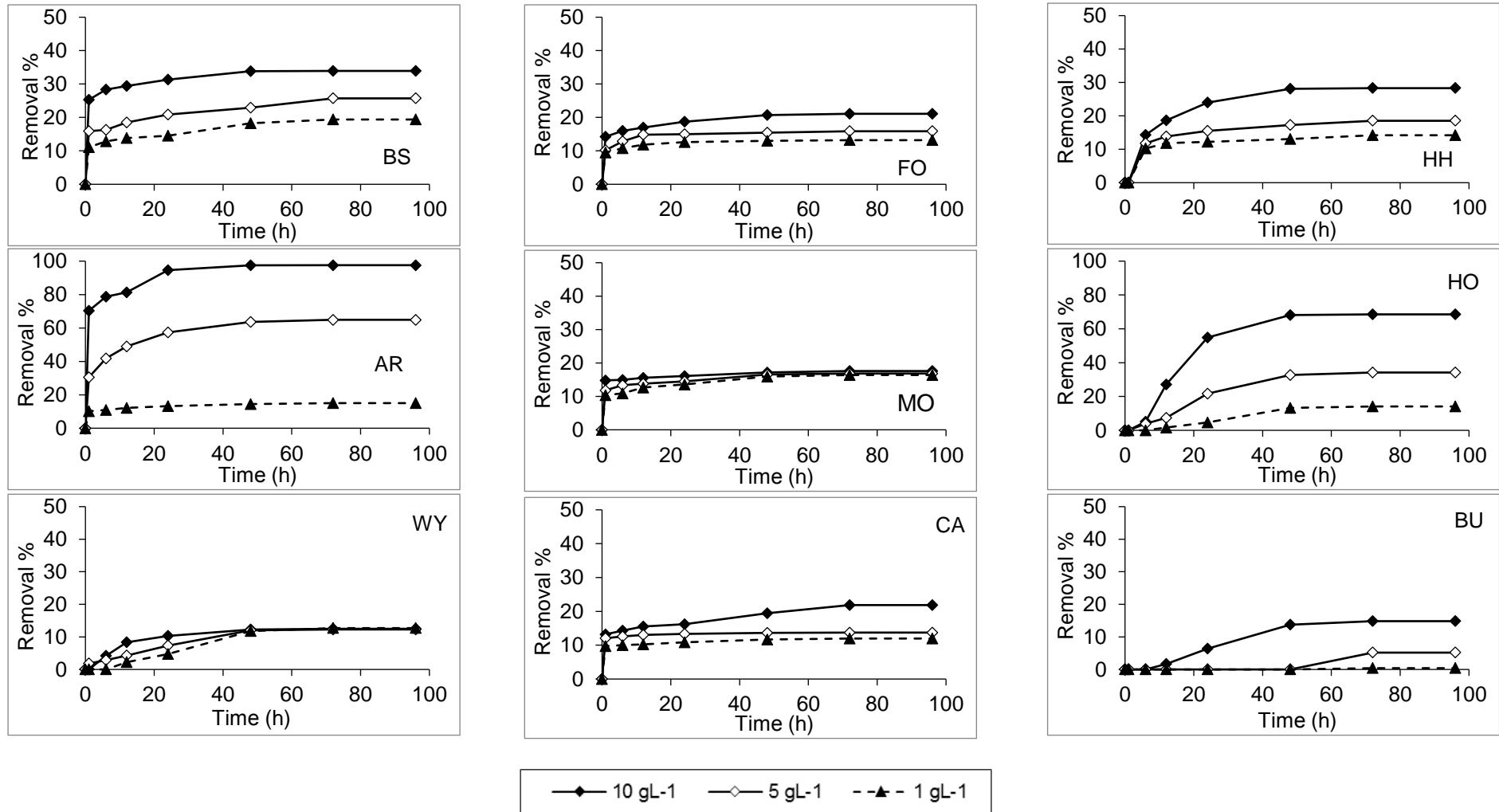


Figure A. 10 Removal efficiency of cadmium by ferric-based sludges at different contact time and three different sludge dosages.

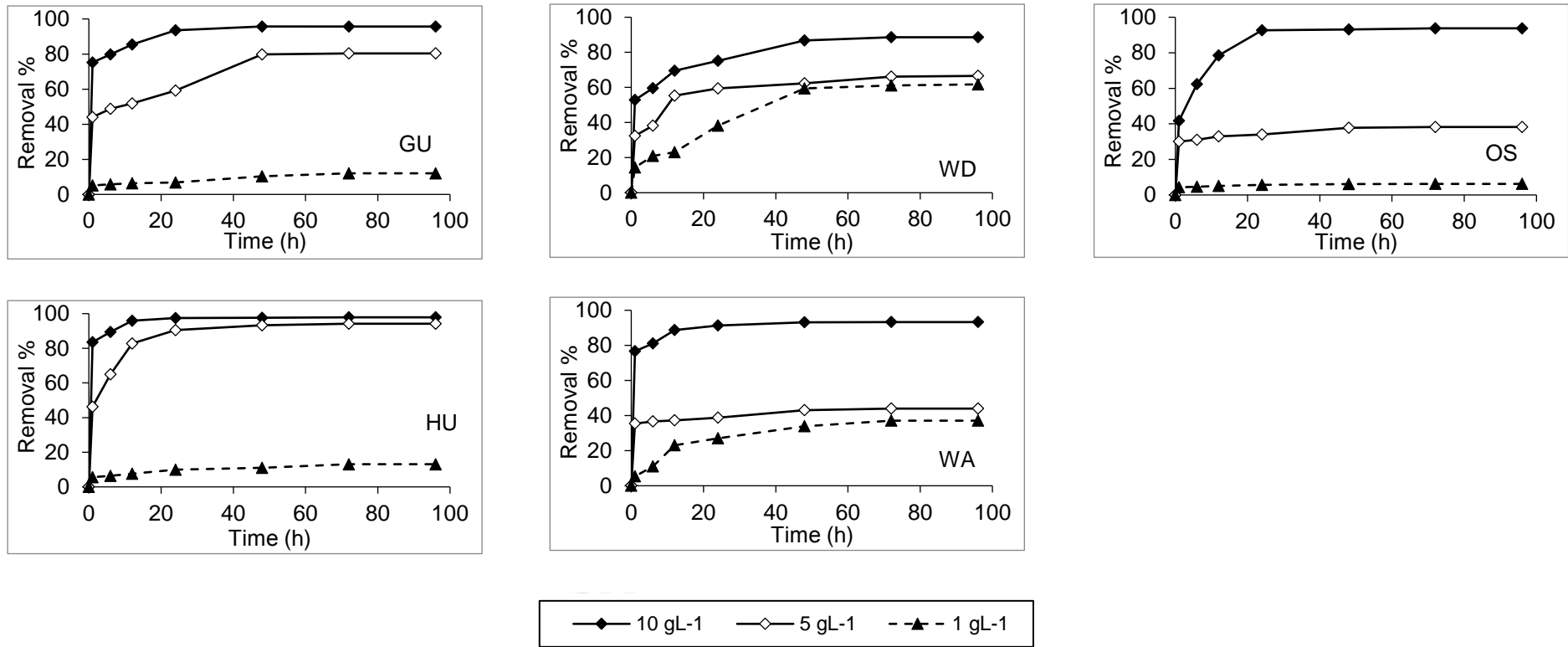


Figure A. 11 Removal efficiency of iron by aluminium- based sludges at different contact time and three different sludge dosages.

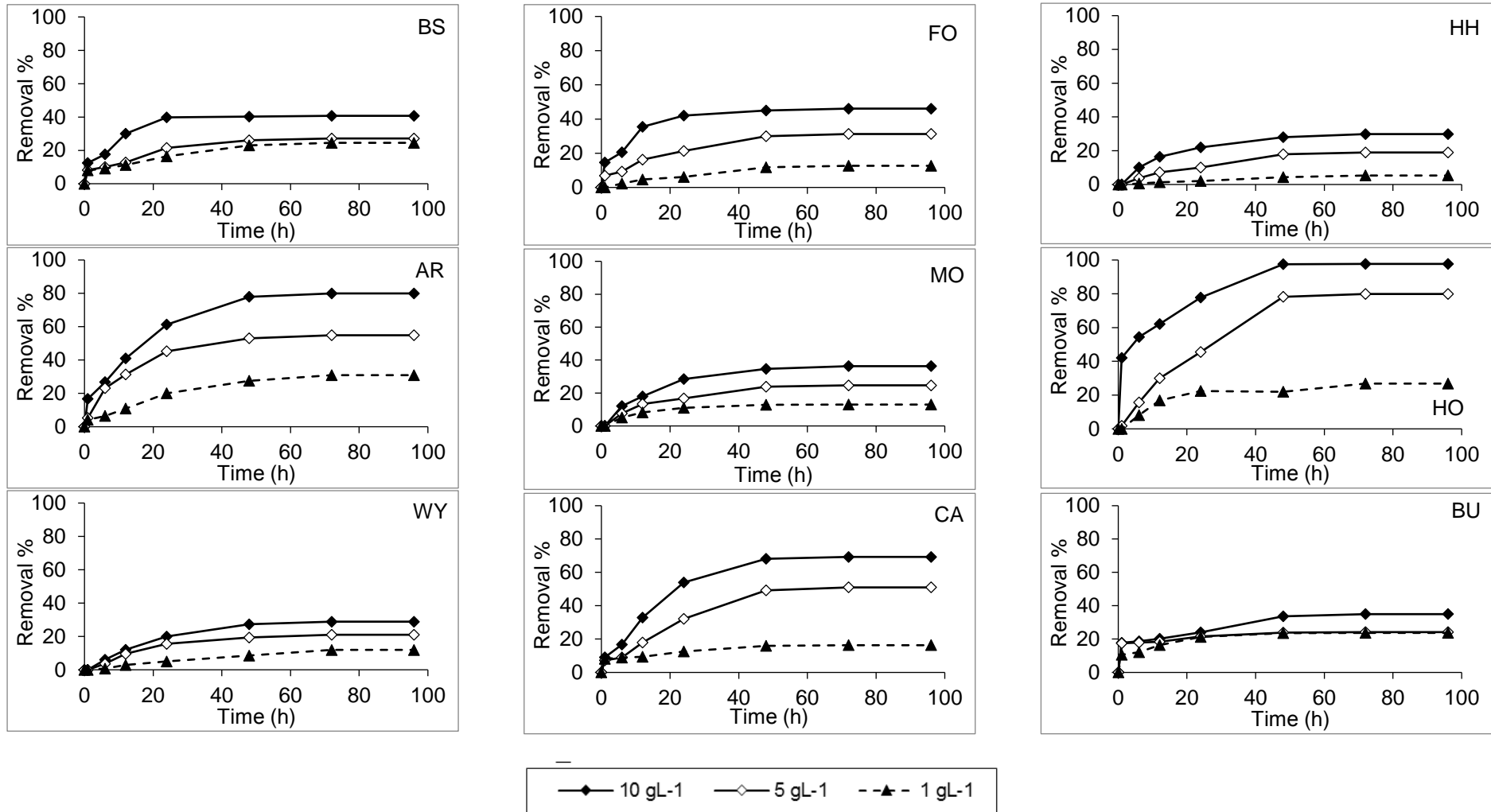


Figure A. 12 Removal efficiency of iron by ferric- based sludges at different contact time and three different sludge dosages

# **Appendix B**

**Tables of kinetic and adsorption  
isotherm parameters**

**Table B. 1 Adsorption rate constant and correlation coefficients for first order model for adsorption of heavy metals on DWSSs.**

Sludge	Heavy Metal	$q_e$ (mg g <sup>-1</sup> )	$K_1$ (min <sup>-1</sup> )	R <sup>2</sup>
GU	Cr	0.004	0.05	0.77
	Pb	0.002	0.06	0.91
	Cd	0.108	0.04	0.98
	Fe	18.70	0.14	0.98
WD	Cr	0.029	0.03	0.97
	Pb	0.005	0.09	0.93
	Cd	0.023	0.03	0.95
	Fe	21.96	0.06	0.97
OS	Cr	0.012	0.05	0.83
	Pb	0.020	0.11	0.98
	Cd	0.207	0.08	0.90
	Fe	22.10	0.10	0.87
HU	Cr	0.009	0.09	0.93
	Pb	0.001	0.07	0.91
	Cd	0.105	0.04	0.99
	Fe	4.540	0.08	0.82
WA	Cr	0.071	0.09	0.88
	Pb	0.010	0.07	0.90
	Cd	0.112	0.06	0.85
	Fe	7.110	0.10	0.96
BS	Cr	0.032	0.12	0.89
	Pb	0.001	0.09	1.00
	Cd	0.063	0.09	0.95
	Fe	12.08	0.09	0.88
MO	Cr	0.010	0.05	0.93
	Pb	0.001	0.08	0.66
	Cd	0.018	0.04	0.97
	Fe	11.58	0.06	0.90

*Appendix B: Tables of kinetic and adsorption isotherm parameters*

---

HO	Cr	0.008	0.07	0.95
	Pb	0.009	0.06	0.98
	Cd	0.516	0.04	0.94
	Fe	34.87	0.13	0.90
CA	Cr	0.039	0.10	0.95
	Pb	0.002	0.08	0.77
	Cd	0.051	0.03	0.96
	Fe	13.69	0.05	0.87
FO	Cr	0.025	0.07	0.98
	Pb	0.008	0.09	0.98
	Cd	0.043	0.06	0.98
	Fe	13.69	0.05	0.87
HH	Cr	0.026	0.12	0.95
	Pb	0.001	0.06	0.64
	Cd	0.159	0.09	0.99
	Fe	13.96	0.06	0.99
AR	Cr	0.038	0.08	0.99
	Pb	0.001	0.06	0.84
	Cd	0.218	0.11	0.98
	Fe	34.46	0.09	0.87
WY	Cr	0.022	0.08	0.93
	Pb	0.002	0.06	0.96
	Cd	0.066	0.07	0.99
	Fe	8.502	0.06	0.95
BU	Cr	0.007	0.07	0.77
	Pb	0.010	0.07	0.90
	Cd	0.125	0.05	0.83
	Fe	4.505	0.06	0.47

---

**Table B. 2 Adsorption rate constant and correlation coefficients for second order model for adsorption of heavy metals on DWSs.**

Sludge	Heavy Metal	$q_e$ (mg g <sup>-1</sup> )	$K_2 \times 10^{-2}$ (min <sup>-1</sup> )	R <sup>2</sup>
GU	Cr	0.08	3012	1.00
	Pb	0.53	9.90	0.95
	Cd	2.59	0.70	0.83
	Fe	500	0.01	0.94
WD	Cr	0.08	7.00	0.16
	Pb	0.54	9.09	0.95
	Cd	2.88	1.67	0.94
	Fe	526	0.01	0.89
OS	Cr	0.08	1855	1.00
	Pb	0.59	6.26	0.97
	Cd	0.78	1.19	0.46
	Fe	588	4.5X10 <sup>-7</sup>	0.97
HU	Cr	0.08	1855	1.00
	Pb	0.53	9.99	0.95
	Cd	2.52	0.88	0.84
	Fe	500	0.06	0.95
WA	Cr	0.24	2.05	0.05
	Pb	0.52	8.56	0.93
	Cd	2.19	0.83	0.66
	Fe	46.1	1.07	0.95
BS	Cr	0.09	847.1	1.00
	Pb	0.53	10.04	0.95
	Cd	2.06	1.91	0.93
	Fe	333	3.9x10 <sup>-7</sup>	0.89
MO	Cr	0.08	3012	1.00
	Pb	0.53	9.92	0.95
	Cd	1.04	3.99	0.92
	Fe	1000	4.0x10 <sup>-7</sup>	0.05

*Appendix B: Tables of kinetic and adsorption isotherm parameters*

---

HO	Cr	0.08	3012	1.00
	Pb	0.55	7.96	0.93
	Cd	0.94	1.46	0.48
	Fe	400	$3.1 \times 10^{-7}$	0.92
CA	Cr	0.08	94.67	0.99
	Pb	0.53	9.79	0.95
	Cd	1.34	2.52	0.91
	Fe	333	$1.9 \times 10^{-9}$	0.00
FO	Cr	0.08	4589	1.00
	Pb	0.54	8.54	0.95
	Cd	1.44	1.84	0.82
	Fe	625	$3.9 \times 10^{-7}$	0.93
HH	Cr	0.08	4589	1.00
	Pb	0.53	10.07	0.95
	Cd	3.74	0.12	0.05
	Fe	175	0.02	0.82
AR	Cr	0.08	507.3	0.99
	Pb	0.53	10.07	0.95
	Cd	6.03	0.63	0.93
	Fe	244	$4.3 \times 10^{-7}$	0.89
WY	Cr	0.08	1145	1.00
	Pb	0.52	8.56	0.93
	Cd	4.54	0.05	0.10
	Fe	1250	$0.4 \times 10^{-7}$	0.55
BU	Cr	0.08	4589	1.00
	Pb	0.53	9.84	0.95
	Cd	0.02	69.15	0.35
	Fe	909	$2.0 \times 10^{-8}$	0.04

---

**Table B. 3 Adsorption rate constant and correlation coefficients for Intraparticle diffusion model for adsorption of heavy metals on DWss.**

Sludge	Heavy Metal	$\bar{D} \times 10^{-7}$	$K_d \times 10^{-2}$ (mg g <sup>-1</sup> )	R <sup>2</sup>
GU	Cr	3.48	0.08	0.59
	Pb	290	0.02	0.76
	Cd	48.3	1.47	0.97
	Fe	145	150	0.87
WD	Cr	0.72	0.320	0.94
	Pb	290	0.080	0.72
	Cd	290	0.310	0.97
	Fe	72.5	259.4	0.96
OS	Cr	1.45	0.210	0.73
	Pb	145.	0.280	0.66
	Cd	72.5	1.870	0.94
	Fe	145.	342.9	0.77
HU	Cr	1.45	0.150	0.60
	Pb	580	0.010	0.83
	Cd	48.3	1.360	0.98
	Fe	290	87.40	0.71
WA	Cr	1.45	1.190	0.68
	Pb	72.5	0.09	0.95
	Cd	72.5	1.150	0.90
	Fe	580	96.11	0.66
BS	Cr	1.45	0.470	0.75
	Pb	3481	0.010	0.83
	Cd	72.5	0.650	0.94
	Fe	145	191.7	0.78
MO	Cr	1.45	0.150	0.84
	Pb	580	0.040	0.42
	Cd	580	0.230	0.98
	Fe	145	184.0	0.82
HO	Cr	1.45	0.120	0.85

*Appendix B: Tables of kinetic and adsorption isotherm parameters*

---

	Pb	72.5	0.110	0.94
	Cd	72.5	6.350	0.96
	Fe	145	382.9	0.81
CA	Cr	1.45	0.480	0.84
	Pb	290	0.040	0.62
	Cd	72.5	0.650	0.97
	Fe	145	423.0	0.82
FO	Cr	1.45	0.360	0.84
	Pb	145.	0.110	0.81
	Cd	72.5	0.540	0.97
	Fe	290	224.2	0.84
HH	Cr	1.74	0.330	0.78
	Pb	580	0.020	0.47
	Cd	72.5	1.870	0.84
	Fe	72.5	1.870	0.84
AR	Cr	1.45	0.450	0.92
	Pb	3481	0.010	0.65
	Cd	145	2.160	0.89
	Fe	145	456.3	0.84
WY	Cr	0.72	0.210	0.96
	Pb	72.5	0.090	0.95
	Cd	72.5	0.840	0.88
	Fe	72.5	1530	0.93
BU	Cr	2.90	0.160	0.58
	Pb	290	0.030	0.80
	Cd	72.5	0.130	0.86
	Fe	72.5	91.17	0.62

---

**Table B. 4 Kinetic model parameters by liner regression method for pseudo first order model for the sorption of heavy metals by DWSs.**

Sludges	Heavy Metals	R <sup>2</sup>	NSD	ARE	q <sub>e</sub> <sup>cal</sup>	q <sub>e</sub> <sup>exp</sup>
GU	Pb	0.92	0.512	0.339	0.052	0.052
	Cr	0.78	2.205	1.114	0.083	0.083
	Cd	0.99	3.278	2.432	0.189	0.191
	Fe	0.98	6.453	2.932	47.07	47.07
WD	Pb	0.93	2.134	1.197	0.052	0.052
	Cr	0.97	18.67	15.03	0.081	0.084
	Cd	0.96	36.37	33.65	0.188	0.274
	Fe	0.97	80.95	72.74	18.49	43.30
OS	Pb	0.99	11.29	4.692	0.052	0.052
	Cr	0.84	6.577	3.106	0.080	0.078
	Cd	0.90	503.4	232.2	0.098	0.128
	Fe	0.88	86.37	77.77	16.24	46.15
HU	Pb	0.91	0.251	0.209	0.052	0.052
	Cr	0.93	3.682	1.886	0.084	0.084
	Cd	0.99	201.4	180.2	0.451	0.194
	Fe	0.82	3.100	1.934	47.99	48.17
WA	Pb	0.91	7.160	6.115	0.052	0.049
	Cr	0.89	754.0	365.8	0.079	0.084
	Cd	0.86	43.91	33.93	0.122	0.157
	Fe	0.97	30.11	27.82	33.54	45.88
BS	Pb	1.00	7.6x10 <sup>-5</sup>	2.6x10 <sup>-5</sup>	0.052	0.052
	Cr	0.89	9.367	4.729	0.084	0.084
	Cd	0.95	52.81	48.75	0.274	0.189
	Fe	0.89	350.5	250.1	43.29	18.55
MO	Pb	0.66	2.644	1.077	0.052	0.052
	Cr	0.93	0.340	3.752	0.082	0.080
	Cd	0.97	23.44	21.63	0.118	0.098
	Fe	0.90	364.0	167.6	22.66	16.25
HO	Pb	0.99	17.157	0.804	0.052	0.052

*Appendix B: Tables of kinetic and adsorption isotherm parameters*

	Cr	0.95	1.030	0.874	0.083	0.084
	Cd	0.95	1717	799.7	0.145	0.452
	Fe	0.91	107.3	92.24	14.70	47.99
CA	Pb	0.78	1.620	0.810	0.052	0.052
	Cr	0.96	3652	1650	0.081	0.079
	Cd	0.96	490.9	446.4	0.541	0.122
	Fe	0.87	445.1	188.1	38.66	33.54
FO	Pb	0.99	0.996	0.604	0.052	0.052
	Cr	0.98	5.603	4.717	0.078	0.082
	Cd	0.989	9.892	9.059	0.128	0.118
	Fe	0.870	270.2	194.9	45.970	22.70
HH	Pb	0.645	1.044	0.470	0.052	0.052
	Cr	0.954	4.325	2.278	0.084	0.083
	Cd	0.991	196.2	90.72	0.194	0.158
	Fe	0.998	1214	705.7	48.107	14.70
AR	Pb	0.841	6.346	5.862	0.049	0.052
	Cr	0.995	5.367	4.585	0.084	0.081
	Cd	0.985	107.3	98.78	0.070	0.545
	Fe	0.879	191.8	133.1	12.17	38.84
WY	Pb	0.964	7.376	5.010	0.049	0.049
	Cr	0.932	3.720	1.931	0.084	0.084
	Cd	0.993	465.7	301.6	0.157	0.070
	Fe	0.959	756.7	533.4	45.85	12.18
BU	Pb	0.906	7.506	4.783	0.052	0.052
	Cr	0.772	5.293	2.349	0.084	0.084
	Cd	0.836	2943	1279	0.083	0.083
	Fe	0.475	18.47	12.83	15.00	15.02

**Table B. 5 Kinetic model parameters by liner regression method for pseudo second order model for the sorption of heavy metals by DWSs.**

Sludges	Heavy Metals	R <sup>2</sup>	NSD	ARE	q <sub>e</sub> <sup>cal</sup>	q <sub>e</sub> <sup>exp</sup>
GU	Pb	0.95	543.2	432.9	0.441	0.052
	Cr	1.00	8.292	3.895	0.084	0.083
	Cd	0.84	549.5	438.0	1.699	0.191
	Fe	0.95	538.6	429.6	400.8	47.07
WD	Pb	0.95	543.3	432.4	0.444	0.052
	Cr	0.17	93.32	85.65	0.027	0.084
	Cd	0.94	547.3	436.2	2.365	0.274
	Fe	0.89	551.9	439.6	382.1	43.30
OS	Pb	0.97	545.1	426.7	0.457	0.052
	Cr	1.00	8.714	3.573	0.078	0.078
	Cd	0.46	158.8	131.9	0.371	0.128
	Fe	0.98	557.3	433.7	423.2	46.15
HU	Pb	0.95	543.1	433.1	0.441	0.052
	Cr	1.00	15.8	11.59	0.078	0.084
	Cd	0.85	549.3	438.7	1.713	0.194
	Fe	0.96	812.9	713.5	482.6	48.17
WA	Pb	0.93	545.2	435.1	0.418	0.049
	Cr	0.05	58.32	48.46	0.074	0.084
	Cd	0.66	556.4	445.2	1.392	0.157
	Fe	0.95	26.08	14.77	45.12	45.88
BS	Pb	0.95	543.1	433.0	0.441	0.052
	Cr	1.00	9.978	5.614	0.084	0.084
	Cd	0.93	545.9	435.0	1.630	0.189
	Fe	0.89	565.6	424.8	184.1	18.55
MO	Pb	0.96	542.9	431.9	0.442	0.052
	Cr	1.00	7.771	6.990	0.084	0.080
	Cd	0.93	544.8	435.5	0.836	0.098
	Fe	0.05	902.3	674.8	262.6	16.25
HO	Pb	0.94	544.6	435.0	0.444	0.052

*Appendix B: Tables of kinetic and adsorption isotherm parameters*

	Cr	1.00	7.889	3.272	0.084	0.084
	Cd	0.48	64.61	37.63	0.538	0.452
	Fe	0.93	214.6	154.3	218.7	47.99
CA	Pb	0.95	543.0	432.5	0.442	0.052
	Cr	0.99	3721	1682	0.080	0.079
	Cd	0.91	563.0	457.0	1.023	0.122
	Fe	0.002	1324	1093	193.6	33.54
FO	Pb	0.95	543.8	433.3	0.446	0.052
	Cr	1.00	14.50	9.781	0.084	0.082
	Cd	0.82	533.3	418.7	1.032	0.118
	Fe	0.93	255.5	167.1	436.5	22.70
HH	Pb	0.95	543.0	432.6	0.441	0.052
	Cr	1.00	11.80	6.826	0.084	0.083
	Cd	0.05	352.6	253.6	1.122	0.158
	Fe	0.83	636.4	570.2	130.0	14.70
AR	Pb	0.95	543.0	432.8	0.441	0.052
	Cr	0.99	21.06	9.795	0.081	0.081
	Cd	0.94	546.2	435.2	4.730	0.545
	Fe	0.89	124.0	90.23	121.8	38.84
WY	Pb	0.93	545.2	435.1	0.418	0.049
	Cr	1.00	16.56	7.087	0.084	0.084
	Cd	0.11	623.3	449.6	0.832	0.070
	Fe	0.55	2128	1614	431.4	12.18
BU	Pb	0.95	543.2	432.9	0.441	0.052
	Cr	1.00	1.434	0.849	0.084	0.084
	Cd	0.35	158.6	103.8	0.015	0.083
	Fe	0.046	467.5	329.1	139.2	15.02

**Table B. 6 Constant parameters, adsorption capacity and correlation coefficient for lead calculated for the five-adsorption models at different pHs.**

Sludge	Model	Parameter	pH2	pH4	pH7
GU	Langmuir	Q <sub>m</sub>	0.01	0.011	0.010
		b	38.57	46.09	47.73
		R <sup>2</sup>	0.78	0.869	0.76
	Freundlich	K <sub>f</sub>	2481	1384.5	4526
		n	0.37	0.383	0.36
		R <sup>2</sup>	0.98	0.972	0.96
	Temkin	B <sub>1</sub>	0.07	0.067	0.08
		K <sub>T</sub>	135	119.86	114.3
		R <sup>2</sup>	0.91	0.882	0.92
	Frumkin	a	54.97	64.785	39.9
		ln k	-1.15	-2.181	-1.10
		R <sup>2</sup>	0.85	0.872	0.87
	H-J	A x10 <sup>-5</sup>	1.02	0.976	1.26
		B	-1.78	-1.703	-1.70
		R <sup>2</sup>	0.69	0.743	0.68
WD	Langmuir	Q <sub>m</sub>	0.02	0.017	0.01
		b	22.7	29.12	36.75
		R <sup>2</sup>	0.65	0.890	0.77
	Freundlich	K <sub>f</sub>	47.4	54.752	259.3
		n	0.52	0.505	0.45
		R <sup>2</sup>	0.98	0.980	0.95
	Temkin	B <sub>1</sub>	0.05	0.050	0.05
		K <sub>T</sub>	137	109.22	108.6
		R <sup>2</sup>	0.81	0.873	0.82
	Frumkin	a	10.57	10.930	4.12
		ln k	-0.50	-0.693	-0.23
		R <sup>2</sup>	0.89	0.880	0.86
	H-J	A x10 <sup>-5</sup>	1.29	1.274	1.68
		B	-1.68	-1.534	-1.73
		R <sup>2</sup>	0.63	0.694	0.67
OS	Langmuir	Q <sub>m</sub>	0.02	0.013	0.04
		b	31.3	37.608	29.3
		R <sup>2</sup>	0.87	0.939	0.25
	Freundlich	K <sub>f</sub>	113	676.39	7.37
		n	0.49	0.397	0.78
		R <sup>2</sup>	0.94	0.979	0.79
	Temkin	B <sub>1</sub>	0.03	0.062	0.05
		K <sub>T</sub>	288	111.12	134
		R <sup>2</sup>	0.63	0.803	0.75
	Frumkin	a	1.22	42.945	6.26
		ln k	0.60	-1.893	-0.31
		R <sup>2</sup>	0.74	0.924	0.95

Appendix B: Tables of kinetic and adsorption isotherm parameters

	H-J	A x10 <sup>-5</sup>	2.08	0.972	1.59
		B	-1.73	-1.644	-1.64
		R <sup>2</sup>	0.86	0.740	0.85
HU	Langmuir	Q <sub>m</sub>	0.02	0.014	0.02
		b	28.8	39.087	42.9
		R <sup>2</sup>	0.83	0.858	0.71
	Freundlich	K <sub>f</sub>	1.21	288.86	453
		n	1.02	0.439	0.49
		R <sup>2</sup>	1.00	0.985	0.79
	Temkin	B <sub>1</sub>	0.05	0.059	0.05
		K <sub>T</sub>	178	121.59	146.7
		R <sup>2</sup>	0.74	0.897	0.83
	Frumkin	a	7.55	27.445	4.44
		ln k	-0.26	-1.404	-0.15
		R <sup>2</sup>	0.89	0.870	0.90
	H-J	A x10 <sup>-5</sup>	1.29	1.145	1.79
		B	-17.1	-1.648	-1.65
		R <sup>2</sup>	0.91	0.715	0.85
WA	Langmuir	Q <sub>m</sub>	0.06	0.024	0.03
		b	13.52	26.654	29.90
		R <sup>2</sup>	0.04	0.461	0.22
	Freundlich	K <sub>f</sub>	2.15	9.908	4.54
		n	1.39	0.665	0.83
		R <sup>2</sup>	0.50	0.787	0.69
	Temkin	B <sub>1</sub>	0.03	0.035	0.02
		K <sub>T</sub>	302.2	168.90	592.4
		R <sup>2</sup>	0.50	0.568	0.34
	Frumkin	a	1.07	3.837	1.56
		ln k	0.67	0.617	-0.31
		R <sup>2</sup>	0.77	0.874	0.31
	H-J	A x10 <sup>-5</sup>	2.03	1.512	3.92
		B	-1.70	-1.578	-1.42
		R <sup>2</sup>	0.91	0.968	0.77
BS	Langmuir	Q <sub>m</sub>	0.01	0.014	0.02
		b	43.3	42.181	29.53
		R <sup>2</sup>	0.84	0.786	0.59
	Freundlich	K <sub>f</sub>	1382	518.56	36.52
		n	0.40	0.436	0.56
		R <sup>2</sup>	0.97	0.931	0.85
	Temkin	B <sub>1</sub>	0.02	0.059	0.07
		K <sub>T</sub>	334	152.78	141.1
		R <sup>2</sup>	0.47	0.804	0.87
	Frumkin	a	3.55	32.382	25.34
		ln k	-0.03	-1.327	-0.83
		R <sup>2</sup>	0.93	0.883	0.89

	H-J	A x10 <sup>-5</sup>	1.40	1.108	1.37
		B	-1.65	-1.762	-1.76
		R <sup>2</sup>	0.86	0.847	0.79
MO	Langmuir	Q <sub>m</sub>	0.01	0.014	0.01
		b	31.41	30.81	46.99
		R <sup>2</sup>	0.58	0.622	0.87
	Freundlich	K <sub>f</sub>	353	286.1	6932
		n	0.42	0.431	0.34
		R <sup>2</sup>	0.84	0.882	0.99
	Temkin	B <sub>1</sub>	0.07	0.059	0.06
		K <sub>T</sub>	126	112.1	109
		R <sup>2</sup>	0.89	0.786	0.72
	Frumkin	a	67.26	27.531	12.6
		ln k	-1.27	-1.462	-0.66
		R <sup>2</sup>	0.89	0.851	0.88
HO	H-J	A x10 <sup>-5</sup>	0.94	1.035	1.26
		B	-1.76	-1.626	-1.63
		R <sup>2</sup>	0.72	0.700	0.80
	Langmuir	Q <sub>m</sub>	0.02	0.017	0.08
		b	24.67	26.644	13.3
		R <sup>2</sup>	0.88	0.807	0.05
	Freundlich	K <sub>f</sub>	43.02	86.397	1.81
		n	0.54	0.485	0.97
		R <sup>2</sup>	0.95	0.948	0.71
	Temkin	B <sub>1</sub>	0.02	0.051	0.05
		K <sub>T</sub>	334	114.9	129.9
		R <sup>2</sup>	0.47	0.797	0.79
Frumkin	a	0.79	13.71	3.75	
	ln k	0.80	-0.841	-0.14	
	R <sup>2</sup>	0.75	0.902	0.93	
H-J	A x10 <sup>-5</sup>	2.35	1.203	1.78	
	B	-1.62	-1.572	-1.57	
	R <sup>2</sup>	0.97	0.698	0.78	
CA	Langmuir	Q <sub>m</sub>	0.04	0.027	0.04
		b	16.99	20.35	24.72
		R <sup>2</sup>	0.68	0.843	0.11
	Freundlich	K <sub>f</sub>	176.8	18.437	2.43
		n	0.46	0.588	0.96
		R <sup>2</sup>	0.96	0.956	0.64
	Temkin	B <sub>1</sub>	0.02	0.041	0.04
		K <sub>T</sub>	403	129.4	157.2
		R <sup>2</sup>	0.44	0.762	0.73
	Frumkin	a	0.87	5.786	1.44
		ln k	0.85	-0.020	0.27
		R <sup>2</sup>	0.73	0.952	0.95
H-J	A x10 <sup>-5</sup>	2.35	1.500	2.26	

		B	-1.71	-1.516	-1.52
		R <sup>2</sup>	0.91	0.719	0.87
FO	Langmuir	Q <sub>m</sub>	0.02	0.017	0.01
		b	29.8	28.571	40.17
		R <sup>2</sup>	0.94	0.867	0.84
	Freundlich	K <sub>f</sub>	9.92	74.319	2082
		n	0.94	0.502	0.36
		R <sup>2</sup>	1.00	0.936	0.90
	Temkin	B <sub>1</sub>	0.06	0.048	0.06
		K <sub>T</sub>	111	128.3	114
		R <sup>2</sup>	0.70	0.745	0.79
	Frumkin	a	32.3	11.56	8.09
		ln k	-1.02	-0.588	-0.47
		R <sup>2</sup>	0.92	0.936	0.94
	H-J	A x10 <sup>-5</sup>	0.85	1.205	1.42
		B	-1.69	-1.613	-1.61
		R <sup>2</sup>	0.84	0.878	0.88
HH	Langmuir	Q <sub>m</sub>	0.04	0.021	0.02
		b	21.07	24.551	45.11
		R <sup>2</sup>	0.85	0.932	0.74
	Freundlich	K <sub>f</sub>	14.77	42.97	617
		n	0.64	0.531	0.44
		R <sup>2</sup>	0.95	0.975	0.94
	Temkin	B <sub>1</sub>	0.06	0.046	0.04
		K <sub>T</sub>	163	124.9	156
		R <sup>2</sup>	0.86	0.798	0.75
	Frumkin	a	16.74	9.068	1.91
		ln k	-0.61	-0.419	0.17
		R <sup>2</sup>	0.86	0.947	0.97
	H-J	A x10 <sup>-5</sup>	1.25	1.353	2.09
		B	-1.79	-1.564	-1.57
		R <sup>2</sup>	0.75	0.740	0.89
AR	Langmuir	Q <sub>m</sub>	0.02	0.015	0.03
		b	30.96	33.48	30.17
		R <sup>2</sup>	0.77	0.919	0.25
	Freundlich	K <sub>f</sub>	58.84	149.6	1.82
		n	0.54	0.473	1.26
		R <sup>2</sup>	0.88	0.917	1.00
	Temkin	B <sub>1</sub>	0.03	0.050	0.05
		K <sub>T</sub>	267	136.9	153
		R <sup>2</sup>	0.56	0.677	0.64
	Frumkin	a	1.68	17.53	4.22
		ln k	0.46	-0.910	-0.11
		R <sup>2</sup>	0.78	0.967	0.96
	H-J	A x10 <sup>-5</sup>	1.81	1.123	1.65

		B	-1.76	-1.664	-1.66
		R <sup>2</sup>	0.93	0.877	0.95
WY	Langmuir	Q <sub>m</sub>	0.01	0.013	0.02
		b	88.2	37.09	36.90
		R <sup>2</sup>	0.51	0.871	0.78
	Freundlich	K <sub>f</sub>	12.5	28.75	3.21
		n	0.64	0.557	0.84
		R <sup>2</sup>	0.86	0.904	0.97
	Temkin	B <sub>1</sub>	0.04	0.042	0.04
		K <sub>T</sub>	173	131.1	155
		R <sup>2</sup>	0.70	0.670	0.63
	Frumkin	a	4.78	7.790	1.94
		ln k	-0.10	-0.256	0.17
		R <sup>2</sup>	0.93	0.957	0.94
	H-J	A x10 <sup>-5</sup>	1.37	1.348	1.98
		B	-1.73	-1.554	-1.55
R <sup>2</sup>		0.94	0.762	0.92	
BU	Langmuir	Q <sub>m</sub>	0.02	0.008	0.02
		b	31.1	45.77	40.30
		R <sup>2</sup>	0.69	0.908	0.73
	Freundlich	K <sub>f</sub>	416	767.2	110
		n	0.42	0.384	0.52
		R <sup>2</sup>	0.97	0.968	0.89
	Temkin	B <sub>1</sub>	0.05	0.065	0.07
		K <sub>T</sub>	178	99.02	107
		R <sup>2</sup>	0.72	0.832	0.91
	Frumkin	a	5.62	47.44	15.06
		ln k	-0.15	-2.083	-0.74
		R <sup>2</sup>	0.91	0.894	0.85
	H-J	A x10 <sup>-5</sup>	1.35	0.912	1.5
		B	-1.76	-1.610	-1.60
R <sup>2</sup>		0.92	0.713	0.55	

Q<sub>m</sub> in mg g<sup>-1</sup>, b in L mg<sup>-1</sup>, k<sub>f</sub> in L g<sup>-1</sup>.

**Table B. 7 Constant parameters, adsorption capacity and correlation coefficient for chromium calculated for the five-adsorption models at different pHs.**

Sludge	Model	Parameter	pH2	pH4	pH7
GU	Langmuir	Q <sub>m</sub>	0.11	0.07	0.03
		b	0.87	1.25	3.15
		R <sup>2</sup>	0.93	0.68	0.74
	Freundlich	K <sub>f</sub>	0.23	0.19	0.28
		n	1.79	1.75	1.52
		R <sup>2</sup>	0.99	0.80	0.73
	Temkin	B <sub>1</sub>	0.02	0.01	0.02
		K <sub>T</sub>	671	499	471
		R <sup>2</sup>	0.88	0.68	0.50
	Frumkin	a	-1.34	1.07	1.73
		ln k	4.09	-2.80	2.37
		R <sup>2</sup>	0.59	0.36	0.56
	H-J	A x10 <sup>-5</sup>	7.21	5.24	4.00
		B	-1.07	-1.10	-1.26
		R <sup>2</sup>	0.71	0.80	0.92
WD	Langmuir	Q <sub>m</sub>	0.14	0.10	0.10
		b	0.65	0.87	0.90
		R <sup>2</sup>	1.00	0.99	0.97
	Freundlich	K <sub>f</sub>	0.39	0.21	0.17
		n	1.33	1.43	1.49
		R <sup>2</sup>	0.99	0.96	0.99
	Temkin	B <sub>1</sub>	0.02	0.02	0.02
		K <sub>T</sub>	241	187	171
		R <sup>2</sup>	0.95	0.95	0.93
	Frumkin	a	0.19	0.38	0.82
		ln k	2.40	2.26	2.10
		R <sup>2</sup>	0.85	0.72	0.62
	H-J	A x10 <sup>-5</sup>	5.25	4.53	4.50
		B	-1.07	-0.91	-0.82
		R <sup>2</sup>	0.64	0.70	0.67
OS	Langmuir	Q <sub>m</sub>	0.10	0.08	0.08
		b	0.97	1.10	1.13
		R <sup>2</sup>	0.96	0.94	0.92
	Freundlich	K <sub>f</sub>	0.17	0.13	0.11
		n	1.69	1.83	2.01
		R <sup>2</sup>	0.99	1.00	0.94
	Temkin	B <sub>1</sub>	0.02	0.01	0.01
		K <sub>T</sub>	284	316	406
		R <sup>2</sup>	0.94	0.91	0.84
	Frumkin	a	-1.15	252	0.07
		ln k	3.35	-2.31	3.41
		R <sup>2</sup>	0.65	0.91	0.00

	H-J	A x10 <sup>-5</sup>	6.20	5.86	6.01
		B	-0.90	-0.80	-0.79
		R <sup>2</sup>	0.68	0.73	0.85
HU	Langmuir	Q <sub>m</sub>	0.08	0.09	0.11
		b	1.21	1.06	0.09
		R <sup>2</sup>	0.99	0.99	0.98
	Freundlich	K <sub>f</sub>	0.13	0.21	0.24
		n	2.31	1.60	1.49
		R <sup>2</sup>	0.96	0.95	0.98
	Temkin	B <sub>1</sub>	0.01	0.02	0.02
		K <sub>T</sub>	1210	305	257
		R <sup>2</sup>	0.93	0.96	0.94
	Frumkin	a	-1.25	-0.06	0.26
		ln k	4.78	2.79	2.56
		R <sup>2</sup>	0.42	0.03	0.39
H-J	A x10 <sup>-5</sup>	9.09	5.52	5.01	
	B	-0.86	-0.96	-0.99	
	R <sup>2</sup>	0.65	0.62	0.66	
WA	Langmuir	Q <sub>m</sub>	0.16	0.14	0.12
		b	0.62	0.66	0.75
		R <sup>2</sup>	0.92	0.95	0.99
	Freundlich	K <sub>f</sub>	0.54	0.34	0.33
		n	1.36	1.34	1.39
		R <sup>2</sup>	0.98	0.99	0.99
	Temkin	B <sub>1</sub>	0.02	0.02	0.02
		K <sub>T</sub>	429	239	265
		R <sup>2</sup>	0.90	0.91	0.95
	Frumkin	a	0.21	0.43	0.16
		ln k	2.84	2.37	2.53
		R <sup>2</sup>	0.21	0.60	0.53
H-J	A x10 <sup>-5</sup>	5.46	4.60	4.87	
	B	-1.30	-1.08	-1.08	
	R <sup>2</sup>	0.74	0.71	0.63	
BS	Langmuir	Q <sub>m</sub>	0.10	0.07	0.07
		b	0.93	1.22	1.31
		R <sup>2</sup>	0.88	0.97	0.98
	Freundlich	K <sub>f</sub>	0.17	0.11	0.14
		n	1.86	1.89	1.74
		R <sup>2</sup>	0.98	0.98	0.94
	Temkin	B <sub>1</sub>	0.01	0.01	0.01
		K <sub>T</sub>	496	323	303
		R <sup>2</sup>	0.84	0.91	0.89
	Frumkin	a	-1.12	0.00	0.41
		ln k	4.01	2.84	2.71
		R <sup>2</sup>	0.58	0.00	0.26

	H-J	A x10 <sup>-5</sup>	6.79	5.75	5.30
		B	-0.94	-0.77	-0.87
		R <sup>2</sup>	0.82	0.77	0.71
MO	Langmuir	Q <sub>m</sub>	0.09	0.09	0.09
		b	1.05	1.07	1.08
		R <sup>2</sup>	0.99	0.98	1.00
	Freundlich	K <sub>f</sub>	0.20	0.19	0.21
		n	1.87	1.88	1.77
		R <sup>2</sup>	0.97	0.97	0.96
	Temkin	B <sub>1</sub>	0.02	0.01	0.02
		K <sub>T</sub>	678	721	544
		R <sup>2</sup>	0.95	0.94	0.97
	Frumkin	a	0.52	0.53	-0.29
		ln k	3.46	3.34	3.37
		R <sup>2</sup>	0.10	0.20	0.61
HO	H-J	A x10 <sup>-5</sup>	7.57	6.79	6.39
		B	-1.03	-1.07	-1.05
		R <sup>2</sup>	0.71	0.69	0.61
	Langmuir	Q <sub>m</sub>	0.02	0.02	0.12
		b	4.82	5.04	0.74
		R <sup>2</sup>	0.77	0.71	0.75
	Freundlich	K <sub>f</sub>	2.80	0.45	0.47
		n	1.17	1.53	1.50
		R <sup>2</sup>	0.83	0.96	0.97
	Temkin	B <sub>1</sub>	0.03	0.02	0.02
		K <sub>T</sub>	1085	790	771
		R <sup>2</sup>	0.91	0.96	0.95
Frumkin	a	0.26	-0.45	-0.40	
	ln k	3.10	3.56	3.51	
	R <sup>2</sup>	0.02	0.46	0.44	
H-J	A x10 <sup>-5</sup>	5.97	5.22	5.04	
	B	-1.84	-1.45	-1.47	
	R <sup>2</sup>	0.43	0.68	0.67	
CA	Langmuir	Q <sub>m</sub>	0.11	0.09	0.08
		b	0.85	1.06	1.13
		R <sup>2</sup>	0.98	1.00	1.00
	Freundlich	K <sub>f</sub>	0.31	0.23	0.22
		n	1.67	1.68	1.70
		R <sup>2</sup>	0.99	0.95	0.93
	Temkin	B <sub>1</sub>	0.02	0.02	0.02
		K <sub>T</sub>	654	309	469
		R <sup>2</sup>	0.94	0.96	0.95
	Frumkin	a	-0.03	-0.24	-0.30
		ln k	3.41	3.17	3.17
		R <sup>2</sup>	0.01	0.36	0.24
H-J	A x10 <sup>-5</sup>	6.94	6.09	6.10	

		B	-1.18	-1.06	-1.05
		R <sup>2</sup>	0.68	0.62	0.58
FO	Langmuir	Q <sub>m</sub>	0.11	0.11	0.02
		b	0.81	0.81	5.84
		R <sup>2</sup>	0.86	0.84	0.67
	Freundlich	K <sub>f</sub>	0.18	0.20	0.18
		n	1.70	1.61	1.63
		R <sup>2</sup>	0.97	0.98	0.95
	Temkin	B <sub>1</sub>	0.02	0.02	0.02
		K <sub>T</sub>	333	309	316
		R <sup>2</sup>	0.83	0.84	0.80
	Frumkin	a	-0.88	-0.01	0.73
		ln k	3.59	2.98	2.76
		R <sup>2</sup>	0.40	0.00	0.34
	H-J	A x10 <sup>-5</sup>	5.99	5.28	5.02
		B	-0.92	-0.97	-0.97
R <sup>2</sup>		0.84	0.79	0.86	
HH	Langmuir	Q <sub>m</sub>	0.13	0.13	0.13
		b	0.77	0.78	0.73
		R <sup>2</sup>	0.81	0.97	0.91
	Freundlich	K <sub>f</sub>	0.35	0.48	0.28
		n	1.59	1.52	1.44
		R <sup>2</sup>	0.99	0.98	0.99
	Temkin	B <sub>1</sub>	0.02	0.02	0.02
		K <sub>T</sub>	604	741	623
		R <sup>2</sup>	0.85	0.91	0.89
	Frumkin	a	-0.30	-0.13	0.12
		ln k	3.47	3.41	3.25
		R <sup>2</sup>	0.15	0.07	0.04
	H-J	A x10 <sup>-5</sup>	6.45	5.89	5.63
		B	-1.23	-1.39	-1.33
R <sup>2</sup>		0.78	0.66	0.67	
AR	Langmuir	Q <sub>m</sub>	0.11	0.08	0.06
		b	0.77	0.97	1.48
		R <sup>2</sup>	0.65	0.81	0.93
	Freundlich	K <sub>f</sub>	0.13	0.07	0.06
		n	1.75	1.79	2.13
		R <sup>2</sup>	0.93	0.92	0.99
	Temkin	B <sub>1</sub>	0.01	0.01	0.01
		K <sub>T</sub>	259	144	251
		R <sup>2</sup>	0.77	0.80	0.87
	Frumkin	a	0.93	-0.74	-2.06
		ln k	2.59	2.31	2.18
		R <sup>2</sup>	0.36	0.26	0.70
	H-J	A x10 <sup>-5</sup>	5.84	4.20	5.39

Appendix B: Tables of kinetic and adsorption isotherm parameters

		B	-0.76	-0.54	-0.56
		R <sup>2</sup>	0.81	0.92	0.81
WY	Langmuir	Q <sub>m</sub>	0.11	0.11	0.11
		b	0.82	0.85	0.83
		R <sup>2</sup>	0.87	0.96	0.93
	Freundlich	K <sub>f</sub>	0.19	0.23	4.04
		n	1.78	1.49	1.50
		R <sup>2</sup>	0.97	0.98	0.99
	Temkin	B <sub>1</sub>	0.02	0.02	0.02
		K <sub>T</sub>	478	254	276
		R <sup>2</sup>	0.83	0.92	0.91
	Frumkin	a	0.26	0.56	0.58
		ln k	3.30	2.46	2.51
		R <sup>2</sup>	0.07	0.55	0.39
	H-J	A x10 <sup>-5</sup>	6.42	-4.98	5.20
		B	-0.99	0.97	-1.00
R <sup>2</sup>		0.85	0.70	0.63	
BU	Langmuir	Q <sub>m</sub>	0.10	0.09	0.10
		b	0.89	1.06	0.92
		R <sup>2</sup>	0.92	0.99	0.95
	Freundlich	K <sub>f</sub>	0.17	0.17	4.55
		n	1.65	1.78	1.71
		R <sup>2</sup>	1.00	0.98	0.96
	Temkin	B <sub>1</sub>	0.02	0.01	0.02
		K <sub>T</sub>	265	435	507
		R <sup>2</sup>	0.90	0.94	0.89
	Frumkin	a	-0.12	-0.14	0.22
		ln k	2.89	3.29	3.27
		R <sup>2</sup>	0.05	0.07	0.07
	H-J	A x10 <sup>-5</sup>	5.97	6.01	5.75
		B	-0.85	-0.96	-1.09
R <sup>2</sup>		0.73	0.73	0.76	

Q<sub>m</sub> in mg g<sup>-1</sup>, b in L mg<sup>-1</sup>, k<sub>f</sub> in L g<sup>-1</sup>.

**Table B. 8 Constant parameters, adsorption capacity and correlation coefficient for cadmium calculated for the five-adsorption models at different pHs.**

Sludge	Model	Parameter	pH4	pH7	pH9
GU	Langmuir	Q <sub>m</sub>	0.02	0.06	0.01
		b	1.64	0.77	2.09
		R <sup>2</sup>	0.85	0.42	0.53
	Freundlich	K <sub>f</sub>	1.22	0.74	4.66
		n	0.48	0.56	0.41
		R <sup>2</sup>	0.96	0.96	0.98
	Temkin	B <sub>1</sub>	0.11	0.09	0.15
		K <sub>T</sub>	16.06	15.80	15.7
		R <sup>2</sup>	0.55	0.76	0.67
	Frumkin	a	1.09	0.28	1.71
		ln k	-0.65	-0.32	-0.93
		R <sup>2</sup>	0.96	0.27	0.67
	H-J	A x10 <sup>-5</sup>	0.83	0.34	0.00
		B	-0.52	-0.50	-0.69
		R <sup>2</sup>	0.74	0.55	0.56
WD	Langmuir	Q <sub>m</sub>	0.52	0.66	0.10
		b	0.11	0.09	0.58
		R <sup>2</sup>	0.05	0.01	0.24
	Freundlich	K <sub>f</sub>	0.38	0.16	0.10
		n	0.75	1.08	0.62
		R <sup>2</sup>	0.83	0.50	0.82
	Temkin	B <sub>1</sub>	0.08	0.04	0.12
		K <sub>T</sub>	21.52	40.14	18.9
		R <sup>2</sup>	0.84	0.44	0.89
	Frumkin	a	0.74	0.30	1.10
		ln k	-0.41	-0.05	-0.71
		R <sup>2</sup>	0.76	0.18	0.41
	H-J	A x10 <sup>-5</sup>	0.80	0.54	0.00
		B	-0.41	-0.30	-0.60
		R <sup>2</sup>	0.37	0.36	0.36
OS	Langmuir	Q <sub>m</sub>	0.52	0.32	0.25
		b	0.11	0.15	0.23
		R <sup>2</sup>	0.16	0.05	0.20
	Freundlich	K <sub>f</sub>	0.10	0.25	0.33
		n	1.09	0.74	0.76
		R <sup>2</sup>	0.92	0.83	0.92
	Temkin	B <sub>1</sub>	0.04	0.06	0.08
		K <sub>T</sub>	22.34	17.63	17.5
		R <sup>2</sup>	0.78	0.91	0.89
	Frumkin	a	-0.47	0.85	0.62
		ln k	-0.68	-0.47	-0.46
		R <sup>2</sup>	0.03	0.86	0.69

HU	H-J	A x10 <sup>-5</sup>	1.20	0.20	0.00
		B	-0.13	-0.37	-0.40
		R <sup>2</sup>	0.45	0.36	0.42
	Langmuir	Q <sub>m</sub>	0.02	0.01	0.01
		b	1.89	2.75	3.34
		R <sup>2</sup>	0.84	0.55	0.74
	Freundlich	K <sub>f</sub>	3.08	25.63	0.04
		n	0.45	0.74	0.36
		R <sup>2</sup>	0.97	0.95	0.96
Temkin	B <sub>1</sub>	0.13	0.02	0.17	
	K <sub>T</sub>	18.51	21.93	4.15	
	R <sup>2</sup>	0.62	0.95	0.54	
Frumkin	a	1.13	3.81	2.92	
	ln k	-0.06	-1.26	-1.04	
	R <sup>2</sup>	0.94	0.57	0.71	
WA	H-J	A x10 <sup>-5</sup>	0.67	0.22	0.00
		B	-0.67	-0.78	-0.86
		R <sup>2</sup>	0.63	0.50	0.65
	Langmuir	Q <sub>m</sub>	0.70	0.13	0.19
		b	0.06	0.35	0.23
		R <sup>2</sup>	0.01	0.80	0.15
	Freundlich	K <sub>f</sub>	0.09	0.06	0.08
		n	0.97	1.16	0.98
		R <sup>2</sup>	0.87	0.92	0.92
Temkin	B <sub>1</sub>	0.05	0.17	0.04	
	K <sub>T</sub>	16.41	15.89	14.6	
	R <sup>2</sup>	0.58	0.75	0.53	
Frumkin	a	0.01	0.16	0.09	
	ln k	-0.06	0.02	-0.29	
	R <sup>2</sup>	0.02	0.14	0.29	
H-J	A x10 <sup>-5</sup>	0.88	0.59	0.00	
	B	-0.13	-0.09	-0.13	
	R <sup>2</sup>	0.45	0.40	0.42	
BS	Langmuir	Q <sub>m</sub>	0.07	0.02	0.02
		b	0.81	1.67	1.77
		R <sup>2</sup>	0.49	0.74	0.88
	Freundlich	K <sub>f</sub>	1.08	1.51	1.87
		n	0.57	0.46	0.48
		R <sup>2</sup>	0.93	0.98	0.93
	Temkin	B <sub>1</sub>	0.11	0.11	0.12
		K <sub>T</sub>	19.08	15.11	16.3
		R <sup>2</sup>	0.74	0.59	0.53
	Frumkin	a	0.46	0.33	1.35
		ln k	-0.34	-0.44	-0.67
		R <sup>2</sup>	0.43	0.32	0.98

MO	H-J	A x10 <sup>-5</sup>	0.68	0.11	0.00
		B	-0.57	0.60	-0.66
		R <sup>2</sup>	0.65	0.58	0.65
	Langmuir	Q <sub>m</sub>	0.03	0.06	0.10
		b	1.27	0.58	0.50
		R <sup>2</sup>	0.77	0.22	0.24
	Freundlich	K <sub>f</sub>	1.21	0.26	0.60
		n	0.51	0.65	0.62
		R <sup>2</sup>	0.97	0.88	0.91
Temkin	B <sub>1</sub>	0.11	0.07	0.10	
	K <sub>T</sub>	16.63	14.6	16.0	
	R <sup>2</sup>	0.67	0.68	0.88	
Frumkin	a	0.35	0.24	0.83	
	ln k	-0.38	-0.40	-0.66	
	R <sup>2</sup>	0.37	0.23	0.53	
HO	H-J	A x10 <sup>-5</sup>	0.62	0.76	0.00
		B	-0.56	0.31	-0.47
		R <sup>2</sup>	0.57	0.46	0.40
	Langmuir	Q <sub>m</sub>	0.40	0.29	0.15
		b	0.15	0.19	0.38
		R <sup>2</sup>	0.06	0.06	0.27
	Freundlich	K <sub>f</sub>	1.43	0.39	0.52
		n	1.52	0.75	0.67
		R <sup>2</sup>	0.87	0.76	0.93
Temkin	B <sub>1</sub>	0.08	0.07	0.09	
	K <sub>T</sub>	21.62	21.1	17.2	
	R <sup>2</sup>	0.90	0.91	0.87	
Frumkin	a	0.70	0.72	0.72	
	ln k	-0.36	-0.42	-0.53	
	R <sup>2</sup>	0.78	0.52	0.64	
CA	H-J	A x10 <sup>-5</sup>	0.99	0.58	0.00
		B	-0.40	-0.44	-0.46
		R <sup>2</sup>	0.31	0.39	0.48
	Langmuir	Q <sub>m</sub>	0.17	0.08	0.08
		b	0.36	0.54	0.68
		R <sup>2</sup>	0.12	0.18	0.24
	Freundlich	K <sub>f</sub>	0.74	1.52	1.16
		n	0.68	0.60	0.58
		R <sup>2</sup>	0.87	0.86	0.87
Temkin	B <sub>1</sub>	0.10	0.09	0.12	
	K <sub>T</sub>	23.04	16.7	18.3	
	R <sup>2</sup>	0.88	0.90	0.87	
Frumkin	a	0.78	0.86	1.05	
	ln k	-0.36	-0.54	-0.68	
	R <sup>2</sup>	0.78	0.68	0.51	
H-J	A x10 <sup>-5</sup>	1.04	0.74	0.00	

		B	-0.50	-0.49	-0.61
		R <sup>2</sup>	0.36	0.47	0.46
FO	Langmuir	Q <sub>m</sub>	0.20	0.07	0.05
		b	0.28	0.61	0.95
		R <sup>2</sup>	0.11	0.22	0.28
	Freundlich	K <sub>f</sub>	0.58	0.59	1.62
		n	0.67	0.59	0.53
		R <sup>2</sup>	0.82	0.90	0.89
	Temkin	B <sub>1</sub>	9.20	0.09	0.13
		K <sub>T</sub>	0.73	15.6	17.1
		R <sup>2</sup>	0.84	0.86	0.86
	Frumkin	a	0.84	0.93	1.25
		ln k	-0.52	-0.57	-0.78
		R <sup>2</sup>	0.70	0.79	0.50
	H-J	A x10 <sup>-5</sup>	0.80	0.69	0.00
		B	-0.47	-0.46	-0.62
R <sup>2</sup>		0.38	0.46	0.39	
HH	Langmuir	Q <sub>m</sub>	0.02	0.03	0.02
		b	2.38	1.66	2.20
		R <sup>2</sup>	0.73	0.74	0.65
	Freundlich	K <sub>f</sub>	8.16	1.70	5.20
		n	0.40	0.50	0.43
		R <sup>2</sup>	0.96	0.98	0.97
	Temkin	B <sub>1</sub>	0.15	0.10	0.14
		K <sub>T</sub>	18.52	18.2	18.6
		R <sup>2</sup>	0.66	0.55	0.57
	Frumkin	a	1.57	0.29	1.58
		ln k	-0.80	-0.36	-0.81
		R <sup>2</sup>	0.83	0.29	0.75
	H-J	A x10 <sup>-5</sup>	0.48	0.60	0.00
		B	-0.75	-0.64	-0.74
R <sup>2</sup>		0.67	0.62	0.56	
AR	Langmuir	Q <sub>m</sub>	0.03	0.10	0.02
		b	1.53	0.57	2.20
		R <sup>2</sup>	0.54	0.28	0.65
	Freundlich	K <sub>f</sub>	3.58	0.92	5.2
		n	0.45	0.60	0.43
		R <sup>2</sup>	0.96	0.94	0.97
	Temkin	B <sub>1</sub>	0.14	0.10	0.14
		K <sub>T</sub>	18.31	19.1	18.68
		R <sup>2</sup>	0.76	0.85	0.57
	Frumkin	a	1.21	0.88	1.58
		ln k	-0.68	-0.42	-0.81
		R <sup>2</sup>	0.82	0.86	0.75
	H-J	A x10 <sup>-5</sup>	0.96	0.44	0.00

		B	-0.67	-0.57	-0.74
		R <sup>2</sup>	0.63	0.52	0.56
WY	Langmuir	Q <sub>m</sub>	0.45	0.20	0.01
		b	0.10	0.22	3.44
		R <sup>2</sup>	0.05	0.37	0.81
	Freundlich	K <sub>f</sub>	0.10	0.06	27.03
		n	0.95	1.09	0.37
		R <sup>2</sup>	0.88	0.86	0.92
	Temkin	B <sub>1</sub>	0.05	0.02	0.16
		K <sub>T</sub>	17.75	20.92	23.65
		R <sup>2</sup>	0.59	0.91	0.44
	Frumkin	a	0.00	0.16	2.86
		ln k	-0.02	0.03	-0.94
		R <sup>2</sup>	0.00	0.14	0.78
	H-J	A x10 <sup>-5</sup>	1.09	0.94	0.00
		B	-0.16	-0.07	-0.92
R <sup>2</sup>		0.51	0.42	0.70	
BU	Langmuir	Q <sub>m</sub>	0.28	0.14	0.82
		b	0.16	0.35	0.06
		R <sup>2</sup>	0.15	0.54	0.03
	Freundlich	K <sub>f</sub>	7.54	14.79	0.10
		n	0.87	1.07	0.98
		R <sup>2</sup>	0.92	0.84	0.94
	Temkin	B <sub>1</sub>	0.05	0.02	0.05
		K <sub>T</sub>	16.86	24.06	16.18
		R <sup>2</sup>	0.71	0.85	0.58
	Frumkin	a	0.04	0.62	0.05
		ln k	-0.10	-0.18	-0.14
		R <sup>2</sup>	0.06	0.87	0.11
	H-J	A x10 <sup>-5</sup>	-18604	-26510	-0.17
		B	-1.47	-2.02	-1.54
R <sup>2</sup>		0.13	0.07	0.16	

Q<sub>m</sub> in mg g<sup>-1</sup>, b in L mg<sup>-1</sup>, k<sub>f</sub> in L g<sup>-1</sup>.

**Table B. 9 Constant parameters, adsorption capacity and correlation coefficient for iron calculated for the five-adsorption models at pH 2.**

Sludge	Model	Parameter	pH 2
GU	Langmuir	$Q_m$	-166
		b	0.00
		$R^2$	0.00
	Freundlich	$K_f$	3.35
		n	1.44
		$R^2$	0.80
	Temkin	$B_1$	4.31
		$K_T$	10.19
		$R^2$	0.36
	Frumkin	a	Nd
		$\ln k$	Nd
		$R^2$	Nd
	H-J	$A \times 10^{-5}$	46.9
		B	0.67
		$R^2$	0.85
WD	Langmuir	$Q_m$	-20.7
		b	0.00
		$R^2$	0.26
	Freundlich	$K_f$	2.72
		n	0.91
		$R^2$	0.88
	Temkin	$B_1$	7.35
		$K_T$	3.18
		$R^2$	0.47
	Frumkin	a	Nd
		$\ln k$	Nd
		$R^2$	Nd
	H-J	$A \times 10^{-5}$	0.03
		B	1.08
		$R^2$	0.19
OS	Langmuir	$Q_m$	-30.5
		b	0.00
		$R^2$	0.08
	Freundlich	$K_f$	2.89
		n	1.76
		$R^2$	0.70
	Temkin	$B_1$	3.45
		$K_T$	14.2
		$R^2$	0.32
	Frumkin	a	Nd
		$\ln k$	Nd
		$R^2$	Nd

	H-J	A x10 <sup>-5</sup>	0.44
		B	0.87
		R <sup>2</sup>	0.97
HU	Langmuir	Q <sub>m</sub>	-4.87
		b	-0.02
		R <sup>2</sup>	0.68
	Freundlich	K <sub>f</sub>	3.01
		n	1.67
		R <sup>2</sup>	0.62
	Temkin	B <sub>1</sub>	3.14
		K <sub>T</sub>	22.9
		R <sup>2</sup>	0.19
	Frumkin	a	Nd
		ln k	Nd
		R <sup>2</sup>	Nd
H-J	A x10 <sup>-5</sup>	0.49	
	B	0.79	
	R <sup>2</sup>	0.82	
WA	Langmuir	Q <sub>m</sub>	-52.1
		b	0.00
		R <sup>2</sup>	0.03
	Freundlich	K <sub>f</sub>	2.54
		n	1.14
		R <sup>2</sup>	0.84
	Temkin	B <sub>1</sub>	5.58
		K <sub>T</sub>	4.34
		R <sup>2</sup>	0.41
	Frumkin	a	Nd
		ln k	Nd
		R <sup>2</sup>	Nd
H-J	A x10 <sup>-5</sup>	0.15	
	B	1.06	
	R <sup>2</sup>	0.86	
BS	Langmuir	Q <sub>m</sub>	-0.83
		b	-0.03
		R <sup>2</sup>	0.85
	Freundlich	K <sub>f</sub>	0.28
		n	6.31
		R <sup>2</sup>	0.28
	Temkin	B <sub>1</sub>	0.09
		K <sub>T</sub>	23.3
		R <sup>2</sup>	0.22
	Frumkin	a	Nd
		ln k	Nd
		R <sup>2</sup>	Nd

	H-J	A x10 <sup>-5</sup>	0.54
		B	2.04
		R <sup>2</sup>	0.79
MO	Langmuir	Q <sub>m</sub>	-2.82
		b	-0.02
		R <sup>2</sup>	0.59
	Freundlich	K <sub>f</sub>	0.15
		n	2.16
		R <sup>2</sup>	0.83
	Temkin	B <sub>1</sub>	0.39
		K <sub>T</sub>	3.78
		R <sup>2</sup>	0.32
	Frumkin	a	Nd
		ln k	Nd
		R <sup>2</sup>	Nd
HO	H-J	A x10 <sup>-5</sup>	0.16
		B	2.97
		R <sup>2</sup>	0.24
	Langmuir	Q <sub>m</sub>	-12.2
		b	-0.01
		R <sup>2</sup>	0.21
	Freundlich	K <sub>f</sub>	0.92
		n	1.12
		R <sup>2</sup>	0.76
Temkin	B <sub>1</sub>	5.68	
	K <sub>T</sub>	1.37	
	R <sup>2</sup>	0.41	
Frumkin	a	Nd	
	ln k	Nd	
	R <sup>2</sup>	Nd	
H-J	A x10 <sup>-5</sup>	0.15	
	B	1.56	
	R <sup>2</sup>	0.41	
CA	Langmuir	Q <sub>m</sub>	-0.25
		b	-0.04
		R <sup>2</sup>	0.87
	Freundlich	K <sub>f</sub>	0.16
		n	5.10
		R <sup>2</sup>	0.21
	Temkin	B <sub>1</sub>	0.01
		K <sub>T</sub>	72.2
		R <sup>2</sup>	0.00
	Frumkin	a	Nd
		ln k	Nd
		R <sup>2</sup>	Nd
H-J	A x10 <sup>-5</sup>	0.42	

		B	2.14
		R <sup>2</sup>	0.71
FO	Langmuir	Q <sub>m</sub>	-7.50
		b	0.00
		R <sup>2</sup>	0.20
	Freundlich	K <sub>f</sub>	0.64
		n	5.12
		R <sup>2</sup>	0.44
	Temkin	B <sub>1</sub>	0.31
		K <sub>T</sub>	16.5
		R <sup>2</sup>	0.40
	Frumkin	a	Nd
		ln k	Nd
		R <sup>2</sup>	Nd
	H-J	A x10 <sup>-5</sup>	0.72
		B	1.95
R <sup>2</sup>		0.88	
HH	Langmuir	Q <sub>m</sub>	-13.8
		b	0.00
		R <sup>2</sup>	0.01
	Freundlich	K <sub>f</sub>	Nd
		n	Nd
		R <sup>2</sup>	Nd
	Temkin	B <sub>1</sub>	-0.82
		K <sub>T</sub>	0.19
		R <sup>2</sup>	0.36
	Frumkin	a	Nd
		ln k	Nd
		R <sup>2</sup>	Nd
	H-J	A x10 <sup>-5</sup>	0.49
		B	3.02
R <sup>2</sup>		0.37	
AR	Langmuir	Q <sub>m</sub>	-25.2
		b	0.00
		R <sup>2</sup>	0.96
	Freundlich	K <sub>f</sub>	0.80
		n	1.49
		R <sup>2</sup>	0.95
	Temkin	B <sub>1</sub>	3.53
		K <sub>T</sub>	0.96
		R <sup>2</sup>	0.86
	Frumkin	a	Nd
		ln k	Nd
		R <sup>2</sup>	Nd
	H-J	A x10 <sup>-5</sup>	0.01

		B	2.12
		R <sup>2</sup>	0.12
WY	Langmuir	Q <sub>m</sub>	-1.31
		b	-0.18
		R <sup>2</sup>	0.69
	Freundlich	K <sub>f</sub>	0.21
		n	3.11
		R <sup>2</sup>	0.75
	Temkin	B <sub>1</sub>	0.19
		K <sub>T</sub>	0.66
		R <sup>2</sup>	0.24
	Frumkin	a	Nd
		ln k	Nd
		R <sup>2</sup>	Nd
	H-J	A x10 <sup>-5</sup>	0.49
		B	2.07
R <sup>2</sup>		0.67	
BU	Langmuir	Q <sub>m</sub>	-3.65
		b	-0.02
		R <sup>2</sup>	0.47
	Freundlich	K <sub>f</sub>	0.28
		n	2.73
		R <sup>2</sup>	0.70
	Temkin	B <sub>1</sub>	0.40
		K <sub>T</sub>	0.59
		R <sup>2</sup>	0.33
	Frumkin	a	Nd
		ln k	Nd
		R <sup>2</sup>	Nd
	H-J	A x10 <sup>-5</sup>	0.52
		B	2.03
R <sup>2</sup>		0.76	

Q<sub>m</sub> in mg g<sup>-1</sup>, b in L mg<sup>-1</sup>, k<sub>f</sub> in L g<sup>-1</sup>. Please see the chapter 3 for explanation of negative values for Fe in section 3.3.2.

Nd: not determined.